HAL open science

Blaschke-Santaló diagrams and other shape optimization problems

Ilias Ftouhi

▶ To cite this version:

Ilias Ftouhi. Blaschke-Santaló diagrams and other shape optimization problems. Optimization and Control [math.OC]. Sorbonne Université, 2021. English. NNT : 2021SORUS008 . tel-03253019

HAL Id: tel-03253019

https://theses.hal.science/tel-03253019v1

Submitted on 8 Jun 2021

HAL is a multi-disciplinary open access archive for the deposit and dissemination of scientific research documents, whether they are published or not. The documents may come from teaching and research institutions in France or abroad, or from public or private research centers.

L'archive ouverte pluridisciplinaire **HAL**, est destinée au dépôt et à la diffusion de documents scientifiques de niveau recherche, publiés ou non, émanant des établissements d'enseignement et de recherche français ou étrangers, des laboratoires publics ou privés.

Sorbonne Université

École doctorale Sciences Mathématiques Paris-Centre

Institut de Mathématiques de Jussieu-Paris Rive Gauche

Diagrammes de Blaschke-Santaló et autres problèmes en optimisation de forme.

Par Ilias FTOUHI

Thèse de doctorat en Mathématiques réalisée sous la direction de

Antoine HENROT
École des Mines de Nancy

Jimmy LAMBOLEY
Sorbonne Université

Soutenue publiquement par visioconférence le xx-01-2021 devant un jury composé de

Giuseppe BUTTAZZO (Rapporteur)
Université de Pise

Ilaria FRAGALÀ (Examinatrice)
École Polytechnique de Milan

Richard S. LAUGESEN (Examinateur)
Univesité d'Illinois

Grégoire NADIN (Examinateur)
Sorbonne Université

Édouard OUDET (Rapporteur)
Université Grenoble Alpes

Table of contents

1 Introduction **5**
1.1 Notational conventions and definitions . . . 5
1.2 Structure of the introduction . . . 6
1.3 Presentation of the problems . . . 6
1.3.1 Chapters 2 & 3 and Section 1 of Chapter 4: Blaschke-Santaló diagrams . . . 7
1.3.2 Chapter 4: The Cheeger inequality for convex sets . . . 16
1.3.3 Chapter 5: Numerical study of the convexity constraint and application to Blaschke-Santaló diagrams . . . 18
1.3.4 Chapter 5: Where to place a spherical obstacle so as to maximize the first Steklov eigenvalue ? . . . 22
1.4 Main contributions and methods of the Thesis . . . 24
1.4.1 Contributions of Chapter 1: Blaschke-Santaló diagrams for volume, perimeter and Cheeger constant. . . . 24
1.4.2 Contributions of Chapter 2: Blaschke-Santaló diagram for volume, perimeter and first Dirichlet eigenvalue . . . 30
1.4.3 Contributions of Chapter 4: On the Cheeger inequality for convex sets . . . 35
1.4.4 Contributions of Chapter 5: Numerical study of convexity constraint and application to Blaschke-Santaló diagrams . . . 40
1.4.5 Contributions of Chapter 5: . . . 42
1.5 Open problems & research projects . . . 44
1.5.1 On Blaschke-Santaó diagrams . . . 44
1.5.2 An upper estimate of the area of inner convex sets . . . 46
1.5.3 Shape derivation of functionals defined as infima . . . 47

I Study of some relevant Blaschke-Santaló diagrams **48**

2 Blaschke-Santaló diagrams for the volume, the perimeter and the Cheeger constant. **49**
2.1 Introduction and main results . . . 49
2.2 Classical results and preliminaries . . . 54
2.2.1 Classical results . . . 54
2.2.2 Preliminary lemmas . . . 55
2.3 Proof of the main results . . . 59
2.3.1 Proof of inequality (2.5) . . . 59
2.3.2 Proof of the second assertion of Theorem 5 (convex sets) . . . 60
2.3.3 Proof of the first assertion of Theorem 5 (simply connected sets) . . . 63
2.3.4 Proof of inequality (2.7) . . . 63
2.3.5 Proof of Theorem 6 . . . 64
2.4 Numerical simulations . . . 73
2.4.1 Parameterization of the domains . . . 73

2.4.2 Computation of the gradients . . . 73
2.4.3 Results . . . 74
2.5 Some applications . . . 76
2.5.1 First application . . . 76
2.5.2 Second application: on the stability of the Cheeger constant of polygons . . . 77

3 Blaschke-Santaló diagrams for the volume, the perimeter and the first Dirichlet eigenvalue 78
3.1 Introduction . . . 78
3.2 Proof of Theorem 10 . . . 82
3.3 The case of convex domains . . . 85
3.3.1 Known inequalities and numerical simulations . . . 85
3.3.2 Proof of Theorem 11 . . . 89
3.3.3 Asymptotics of the diagram . . . 107
3.4 Further remarks and Conjectures . . . 112
3.4.1 About $\mathcal{D}_{\mathcal{K}^2}$ . . . 112
3.4.2 About $\mathcal{D}_{\mathcal{K}^d}$ for $d \geq 3$ . . . 113
3.4.3 About $\mathcal{D}_{\mathcal{S}^d}$ where $\mathcal{S}^d$ is the class of simply connected domains . . . 113

4 On the Cheeger inequality for convex sets 115
4.1 Introduction and main results . . . 115
4.2 Sharp estimates for the Cheeger constant: Proof of Theorem 16 . . . 118
4.3 Improving the Cheeger inequality for planar convex sets . . . 120
4.3.1 Proof of Theorem 15 . . . 120
4.3.2 A slight improvement of the result of Theorem 15 . . . 121
4.3.3 Improvements for special classes of shapes . . . 121
4.4 On the existence of a minimizer in higher dimensions . . . 123
4.4.1 Proof of Theorem 17 . . . 123
4.4.2 Discussion of the hypothesis $\beta_n < \beta_{n-1}$ . . . 126
4.5 Appendix: Some applications . . . 128
4.5.1 Some sharp upper bounds for the first Dirichlet eigenvalue . . . 128
4.5.2 A sharp Cheeger-type inequality . . . 131

5 Numerical study of convexity constraint and application to Blaschke-Santaló diagrams 133
5.1 Parametrization of convex sets and numerical setting . . . 133
5.1.1 Support function parametrization . . . 134
5.1.2 Gauge function parametrization . . . 138
5.1.3 Radial function parametrization . . . 140
5.1.4 Polygonal approximation and parametrization via vertices . . . 144
5.1.5 Computations of the functionals and numerical optimization . . . 145
5.2 Application to Blaschke-Santaló diagrams . . . 145
5.2.1 Some theoretical results on the diagrams . . . 145
5.2.2 The purely geometric diagram $(P, |\cdot|, d)$ . . . 146
5.2.3 Diagram $(P, \lambda_1, |\cdot|)$ . . . 152
5.2.4 Diagram $(d, \lambda_1, |\cdot|)$ . . . 154
5.2.5 Conclusion and comments . . . 156
5.3 Appendix 1: Some useful shape derivatives . . . 158
5.3.1 First order shape derivative of the diameter . . . 158
5.3.2 First order shape derivative of the Cheeger constant . . . 160
5.4 Appendix 2: Validation of Parini's conjecture [152] . . . 164

II Optimal placement of an obstacle **165**

6 Where to place a spherical obstacle so as to maximize the first Steklov eigenvalue ? **166**
6.1 Introduction . . . 166
6.1.1 Optimization of the Steklov eigenvalue . . . 166
6.1.2 Perforated domains: state of the art . . . 167
6.1.3 Results of the paper . . . 168
6.2 Proof of Theorem 21 . . . 169
6.2.1 Proof of the first assertion of Proposition 18 . . . 169
6.2.2 Spherical coordinates and preliminary computations . . . 170
6.2.3 Proof of the second assertion of Proposition 18 . . . 171
6.2.4 Proof of the third assertion of Proposition 18 . . . 175
6.3 The Dirichlet-Steklov problem . . . 177
6.3.1 A key Proposition . . . 177
6.3.2 Proof of Theorem 22 . . . 178
6.4 Appendix . . . 178
6.4.1 Computation of the eigenvalues via classical separation of variables technique . . 179
6.4.2 A monotonicity result . . . 181
6.4.3 Proof of Theorem 23 . . . 183

Author's bibliography

Accepted papers

- *Blaschke-Santaló diagram for volume, perimeter and first Dirichlet eigenvalue*, with Jimmy Lamboley. Accepted for publication in *SIAM Journal on Mathematical Analysis*. This work corresponds to Chapter 3 of this manuscript.

Submitted papers

- *Where to place a spherical obstacle so as to maximize the first Steklov eigenvalue.* This work corresponds to Chapter 6 of this manuscript.
- *Complete systems of inequalities relating the perimeter, the area and the Cheeger constant of planar domains.* This work corresponds to Chapter 2 of this manuscript.
- *On the Cheeger inequality for convex sets.* This work corresponds to Chapter 4 of this manuscript.

Papers in preparation

- *Numerical study of convexity constraint and application to Blaschke-Santaló diagrams.* This work corresponds to Chapter 5 of this manuscript.

Chapter 1

Introduction

This thesis is a contribution to the mathematical field of shape optimization which may be seen as a sub-discipline of the calculus of variations. We are interested in the study of isoperimetric estimations relating spectral and geometric shape functionals.

1.1 Notational conventions and definitions

Although the notations used in this manuscript will be properly introduced in due time, we gather here, for the sake of readability, the most common ones used throughout the chapters.

- Sets and classes of sets:
  1. $\mathbb{N}$ is the set of non-negative integers, $\mathbb{N}^*$ is defined as $\mathbb{N}^* = \mathbb{N}\backslash\{0\}$.
  2. $\mathbb{R}$ is the set of real numbers, $\mathbb{R}^*$ is defined as $\mathbb{R}^* := \mathbb{R}\backslash\{0\}$, $\mathbb{R}^+$ (resp. $\mathbb{R}^-$) is the set of non-negative (resp. non-positive) real numbers, $\mathbb{R}^*_+$ (resp. $\mathbb{R}^*_-$) is the set of positive (resp. negative) real numbers.
  3. For any $n \in \mathbb{N}^*$, $\mathbb{R}^n := \{(x_1, \dots, x_n)|\ x_1, \dots, x_n \in \mathbb{R}\}$.
  4. For any $n \in \mathbb{N}^*$, $\mathcal{K}^n$ is the class of convex compact subsets of $\mathbb{R}^n$ and $\mathcal{K}^n_1$ is the class of convex compact subsets of $\mathbb{R}^n$ of unit Lebesgue measure.
  5. For any $n \in \mathbb{N}^*$, $\mathcal{S}^n$ is the class of open bounded simply connected subsets of $\mathbb{R}^n$.
  6. for any $N \geq 3$, $\mathcal{P}_N$ is the class of convex polygons of at most N sides.
- Shape functionals: Let $n \in \mathbb{N}^*$.
  1. The **diameter** of a given set $\Omega \subset \mathbb{R}^n$ is denoted $d(\Omega)$.
  2. The **inradius** of a given set $\Omega \subset \mathbb{R}^n$ (which is the radius largest ball included in Ω) is denoted $r(\Omega)$.
  3. The underlying measure is the Lebesgue measure. For any any Borel set $\Omega \subset \mathbb{R}^n$, $|\Omega|$ is the n-th dimensional Lebesgue measure. It is called **volume** of Ω or more specifically **area** of Ω when $n = 2$.
  4. For any any Borel set $\Omega \subset \mathbb{R}^n$, $P(\Omega)$ denotes the **perimeter** of De Giorgi of Ω in $\mathbb{R}^n$, see for example [140]. We note that there are other definitions for the perimeter and that they all agree for domains with Lipschitz boundary conditions.
  5. Let $\Omega \subset \mathbb{R}^n$ be a bounded Borel set. The **Cheeger constant** of Ω is defined as

$$h(\Omega) := \inf_{\substack{E\subset\Omega \\ E \text{ measurable}}} \frac{P(E)}{|E|}.$$

A set $C_\Omega \subset \Omega$ for which the infimum is attained is called a Cheeger set of Ω.

6. Let $\Omega \subset \mathbb{R}^n$ be an open subset of $\mathbb{R}^n$. The **first eigenvalue of the Laplace operator with Dirichlet boundary conditions** Ω is defined as follows:

$$\lambda_1(\Omega) := \inf_{u \in H_0^1(\Omega)\setminus\{0\}} \frac{\int_\Omega |\nabla u|^2 dx}{\int_\Omega u^2 dx}.$$

1.2 Structure of the introduction

This Introduction is structured as follows:

We present the main problems and questions treated in the present thesis in Section 1.3. We state and comment our main results in Section 1.4 and describe the sketches of proofs and the developed methods. Finally, in Section 1.5, We present some open problems and possible research projects.

Problem	Presentation of the problem and main questions	Main results and methods of proofs	Detailed proofs
Blaschke-Santaló diagrams for $(P, h, \lvert\cdot\rvert)$	Section 1.3.1	Section 1.4.1	Chapter 2
Blaschke-Santaló diagrams for $(P, \lambda_1, \lvert\cdot\rvert)$	Section 1.3.1	Section 1.4.2	Chapter 3
Blaschke-Santaló diagram for $(r, h, \lvert\cdot\rvert)$	Section 1.3.1	Section 1.4.3	Section 1 of Chapter 4
Cheeger's inequality for convex sets	Section 1.3.2	Section 1.4.3	Sections 2 & 3 of Chapter 4
Numerical study of convexity constraint	Section 1.3.3	Section 1.4.4	Chapter 5
Optimal placement of an obstacle	Section 1.3.4	Section 1.4.5	Chapter 6

1.3 Presentation of the problems

Let us first introduce the reader to the subject of shape optimization: let J be a shape functional, that is an application that takes a set $\Omega \subset \mathbb{R}^n$ ($n \in \mathbb{N}^*$) as an input and returns a real value $J(\Omega) \in \mathbb{R}$. We would be interested in problems of the form:

$$\inf_{\Omega \in \mathcal{F}_{\text{ad}}} J(\Omega),$$

where $\mathcal{F}_{\text{ad}}$ is a class of admissible shapes. It encodes the constraints of the problem. This can for example be the class of convex sets or those of unit volume...

Unfortunately, the task of explicitly finding optimal shapes (when they exist) can be very challenging (or even impossible), thus it is natural and classical to ask the following type of questions when working on a shape optimization problem:

- Does the problem admit a solution ?
- Can we prove some qualitative results on the optimal set (regularity, symmetries...)?

- Can we prove that a given shape is a local solution for the problem ? (the term local depends on the choice of topology of the class of domains).
- How can we use numerical simulations to find approximations of the optimal shapes?

We note that each of those questions will be discussed at a certain level in this thesis.

The present thesis is structured in 5 chapters organized in two parts:

Part I: Study of some relevant Blaschke-Santaló diagrams.

- **Chapter 2:** Blaschke-Santaló diagrams for the volume, the perimeter and the Cheeger constant.
- **Chapter 3:** Blaschke-Santaló diagrams for the volume, the perimeter and the first Dirichlet eigenvalue.
- **Chapter 4:** On the Cheeger inequality for convex sets.
- **Chapter 5:** Numerical study of the convexity constraint and application to Blaschke Santaló diagrams.

Part II: Optimal placement of an obstacle.

- **Chapter 6:** Where to place a spherical obstacle so as to maximize the first Steklov eigenvalue ?

1.3.1 Chapters 2 & 3 and Section 1 of Chapter 4: Blaschke-Santaló diagrams

Introduction to Blaschke-Santaló diagrams

In all mathematical fields, it is always interesting and useful to have (sharp) estimates of quantities (for which it could be difficult or impossible to have an explicit expression) via other functionals (easier to handle). This is why inequalities relating given shape functionals were extensively studied in the literature by various mathematical communities.

When studying the inequalities relating some given quantities, a natural question arises:

Can one describe all the possible inequalities relating given shape functionals? in the sense that there would be no other estimate (involving the considered quantities) which improves the latter ones.

The first mathematician who raised interest of such questions was Blaschke [28] in 1915. He considered a compact convex set Ω in $\mathbb{R}^3$, with volume $|\Omega|$, surface area $P(\Omega)$, and integral of the mean curvature $M(\Omega)$. He asked for a characterization of the set of all points in $\mathbb{R}^3$ of the form $(|\Omega|, P(\Omega), M(\Omega))$ as Ω ranges over the family $\mathcal{K}^3$ (where $\mathcal{K}^n$ denotes the class of compact convex sets in $\mathbb{R}^n$ for $n \geq 1$). Due to scaling arguments, the latter problem is equivalent to the characterization of the following set of points:

$$\big\{\big(P(\Omega), M(\Omega)\big) \ \mid \ |\Omega| = 1 \ \text{ and } \ \Omega \in \mathcal{K}^3\big\}.$$

This set of points is known as the *Blaschke diagram.* Then, in 1959, L. A. Santaló proposed a related family of problems involving the following purely geometrical functionals: area $|\cdot|$, perimeter P, diameter d, minimal width w, circumradius R and inradius r for the class $\mathcal{K}^2$. As in [28], the problem is to find complete systems of inequalities for any 3 quantities chosen from the ones listed above (this yields a total of $\binom{6}{3} = 20$ problems). In his work [163], L.A. Santaló completely solved 6 cases, then came a series of recent papers [110, 112, 36, 111, 71], where 8 other diagrams are solved, meanwhile, up to our knowledge the remaining 6 problems remain unsolved. We refer to the introduction of the very recent paper [71] for a detailed state of the art.

Let us now settle the general framework of the so called *Blaschke-Santaló diagrams*: we consider 3 homogeneous shape functionals J_1, J_2 and J_3 defined on a given class $\mathcal{F}_{\text{ad}}$ of subsets of $\mathbb{R}^n$ for

$n \in \mathbb{N}^*$. By homogeneous, we mean that there exists $\alpha_1, \alpha_2, \alpha_3 \in \mathbb{R}$ such that $J_i(t\Omega) = t^{\alpha_i} J_i(\Omega)$ for every $t > 0$ and $\Omega \in \mathcal{F}_{\text{ad}}$ and $i \in \{1, 2, 3\}$. It is possible (due to homogeneity properties) to define the Blaschke-Santaló diagram associated to the triplet (J_1, J_2, J_3) in the class $\mathcal{F}_{\text{ad}}$ as the following set of points:

$$\mathcal{D}_{\mathcal{F}_{\text{ad}}} := \big\{ \big(J_1(\Omega), J_2(\Omega)\big) \ \mid \ J_3(\Omega) = 1 \ \text{ and } \ \Omega \in \mathcal{F}_{\text{ad}} \big\}.$$

The ultimate goal is to provide the explicit description of $\mathcal{D}_{\mathcal{F}_{\text{ad}}}$. In this case, we say that we managed to find a complete system of inequalities relating the three functionals J_1, J_2 and J_3 on the class $\mathcal{F}_{\text{ad}}$. Unfortunately, the task of finding the diagram may be very difficult or even impossible, especially when a spectral quantity is involved, see the discussion of Conjecture 4 for example. Here is a non-exhaustive list of recent works in this framework [11, 13, 22, 23, 24, 44, 49, 60, 92, 138]. Here are some questions that are classically asked when working on Blaschke-Santaló diagrams:

1. **is the diagram closed ? arcwise connected ?**

   In general, both assertions are true when $\mathcal{F}_{\text{ad}}$ is given by the class of convex sets of $\mathbb{R}^n$. The proof of this is quite classical and relies on the continuity of the functionals, compactness of convex sets for the Hausdorff distance (see Blaschke selection Theorem [164]) and the use of Minkowski sums to construct continuous paths relating points of the diagram. We refer for example to [13, Theorem 2.2] and [138, Proposition 3.10].

2. **Does the diagram contain holes ?**

   Even though, this seems in general to be false, this might be quite challenging to prove, see for example [13, Conjecture 1] and [138, Conjecture 2]. In Chapters 2 and 3, we develop a strategy that allows to tackle this question for the studied diagrams in the case of convex sets. This result (of simple connectedness) seems up to our knowledge to be the first of its kind when dealing with diagrams mixing spectral and geometrical quantities on convex sets. In Section 1.4.2, we explain the main difficulties in this framework (in contrary to the purely geometrical one) and present the methods we developed to overpass it.

3. **Is the diagram convex ? or at least vertically or horizontally convex ?**

   A diagram is said to be vertically (resp. horizontally) convex, if the segment relating any couple of points with the same abscissa (resp. ordinate) is included in the diagram.

   We note that proving the convexity of a Blaschke-Santaló diagram is a quite challenging question, see for example [49] where the authors could not establish the convexity of a certain diagram but proved the vertical and horizontal convexity.

4. **Can we give qualitative properties on the boundary of the diagram ?**

   For example one may be interested in properties such as continuity, monotonicity, differentiability or convexity of the curves describing the boundary of the diagram, see for example [49, 138].

   Another classical problem is to find or at least have estimates on the tangent of the boundary at some special points (for example the one corresponding to the ball). We refer for instance to [44] where the authors prove that the boundary of the diagram associated to the triplet $(\lambda_1, \lambda_2, |\cdot|)$ (where λ_1 and λ_2 are the first and second Dirichlet Laplacian eigenvalues) has a horizontal tangent at its lowest point corresponding to the union of two disjoint balls of half measure.

5. **Can we numerically describe the diagram ? and state new conjectures ?**

   Numerical simulations may significantly help to have a better understanding of the diagram. It may be used to state or numerically validate some related conjectures. We refer for example to Chapter 5 for a description of the different methods we used to study some relevant diagrams.

Study of an example: the $(P, |\cdot|, r)$-diagram

For a better understanding, let us discuss the purely geometrical diagram of the triplet $(P, |\cdot|, r)$ in the case of planar convex domains. We recall that this diagram had already been solved by Santaló in [163].

Let us first recall some classical inequalities between the considered quantities. We have for every $\Omega \in \mathcal{K}^2$:

$$\frac{P(\Omega)}{|\Omega|^{1/2}} \geq \frac{P(B)}{|B|^{1/2}} = 2\sqrt{\pi}, \tag{1.1}$$

where $B \subset \mathbb{R}^2$ is the ball of unit volume. This is the famous *isoperimetric inequality*.

Then, there are the following inequalities, which are direct consequences of the inclusion of the inscribed ball in Ω:

$$|\Omega| \geq \pi \times r(\Omega)^2, \tag{1.2}$$

and

$$P(\Omega) \geq 2\pi \times r(\Omega). \tag{1.3}$$

All these inequalities are sharp as equality occurs when Ω is a ball, but, as explained before, the main question is to know if they form a complete system of inequalities: to do so we study the following set of points:

$$\mathcal{D} := \big\{ \big(P(\Omega), |\Omega|\big) \ \mid \ r(\Omega) = 1 \ \text{ and } \ \Omega \in \mathcal{K}^2 \big\}.$$

We note that inequalities (1.1), (1.2) and (1.3) are represented in the diagram as the curves of some functions that delimit a subregion of $\mathbb{R}^2$ which contains the diagram $\mathcal{D}$, indeed:

$$\begin{aligned} (x,y) \in \mathcal{D} \quad &\Rightarrow \quad \exists \Omega \in \mathcal{K}^2 \ \text{ such that } \ r(\Omega) = 1, \ \ x = P(\Omega) \ \text{ and } \ y = |\Omega|, \\ &\Rightarrow \quad y \leq \frac{x^2}{4\pi}, \quad y \geq \pi \quad \text{and} \quad x \geq 2\pi. \end{aligned}$$

Thus, we get the inclusion:

$$\mathcal{D} \subset \left\{ (x,y) \mid y \leq \frac{x^2}{4\pi} \right\} \cap \{(x,y) \mid y \geq \pi\} \cap \{(x,y) \mid x \geq 2\pi\}.$$

Figure 1.1 shows inequalities (1.1),(1.2) and (1.3) and the domain they describe which contains $\mathcal{D}$. We note that thanks to this graphical representation, one can easily see that the isoperimetric inequality (1.1) is stronger than (1.3). This is one of the reasons that make these diagrams useful and very interesting to study.

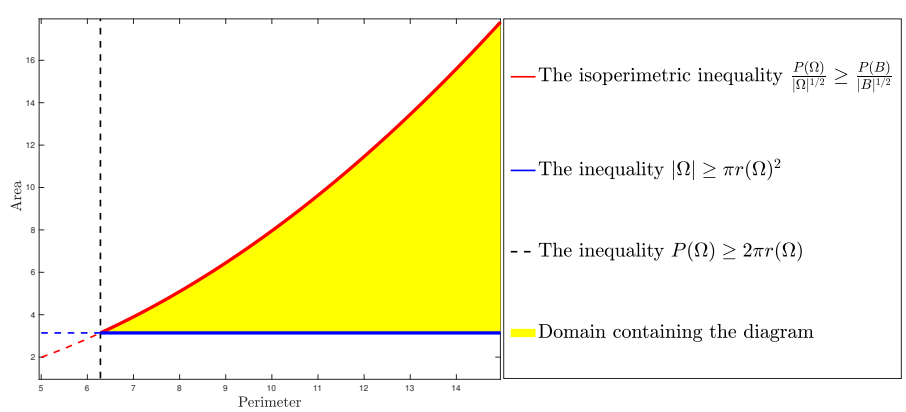

Figure 1.1: A domain containing the Diagram $\mathcal{D}$.

Now that we have a better understanding of the diagram, let us push forward the analysis and give the explicit description of $\mathcal{D}$. This is done in two steps:

Step 1: Finding the (external) boundary of the diagram $\mathcal{D}$

In general to do so, one has to solve the following shape optimization problems:

$$\begin{cases} \inf\{|\Omega| \ \mid \ \Omega \in \mathcal{K}^2,\ r(\Omega) = 1 \ \text{ and } \ P(\Omega) = p_0\}, \\ \sup\{|\Omega| \ \mid \ \Omega \in \mathcal{K}^2,\ r(\Omega) = 1 \ \text{ and } \ P(\Omega) = p_0\}, \\ \inf\{P(\Omega) \ \mid \ \Omega \in \mathcal{K}^2,\ r(\Omega) = 1 \ \text{ and } \ |\Omega| = a_0\}, \\ \sup\{P(\Omega) \ \mid \ \Omega \in \mathcal{K}^2,\ r(\Omega) = 1 \ \text{ and } \ |\Omega| = a_0\}, \end{cases} \tag{1.4}$$

where $p_0 \in [2\pi, +\infty)$ and $a_0 \in [\pi, +\infty)$. As noted by Santaló, these problems are solved in [35]: the first and third are solved by stadiums, while the second and fourth are solved by symmetric 2-cap bodies, namely the convex hull of a disk of radius 1 and two points lined-up with its center. We then have the following inequalities:

$$P(\Omega)r(\Omega) \leq 2|\Omega|, \tag{1.5}$$

and:

$$|\Omega| \leq r(\Omega)\big(P(\Omega) - \pi r(\Omega)\big). \tag{1.6}$$

This shows that the (external) boundary of the diagram $\mathcal{D}$ is given by the curves of the functions:

$$x \in [2\pi, +\infty) \longmapsto \frac{x}{2} \ \text{ and } \ x \in [2\pi, +\infty) \longmapsto x - \pi.$$

Step 2: Filling the diagram (i.e. showing that it contains no holes)

Once the external boundary is found, it remains to prove that the whole region delimited by this boundary is in the diagram. As it is explained above, this step could be rather challenging when dealing with diagrams for which no (or few) information on the extremal sets (those corresponding to the points on the external boundary) is known. Fortunately, this is not the case for the present (P,$|\cdot|$,r) diagram. Indeed, one can use the linearity property of perimeter and inradius for Minkowski sums and the continuity of the functionals for Hausdorff distance in $\mathcal{K}^2$ to construct <u>vertical</u> lines that connect the upper boundary to the lower one. Let us take K_1 and K_2 two convex sets of inradius 1 and perimeter p_0: for every $t \in [0, 1]$, we have $P(tK_1 + (1-t)K_2) = t \times P(K_1) + (1-t) \times P(K_2) = p_0$ and $r(tK_1 + (1-t)K_2) = t \times r(K_1) + (1-t) \times r(K_2) = 1$, thus, the vertical and continuous line $\{p_0\} \times [|K_1|, |K_2|]$ relating the points corresponding to K_1 and K_2 is included in the diagram $\mathcal{D}$.

Finally, we conclude that:

$$\mathcal{D} = \{(x, y) \mid y \leq x - \pi\} \cap \{(x, y) \mid y \geq x/2\},$$

which means that inequalities (1.5) and (1.6) form a complete system of inequalities of the triplet $(P, |\cdot|, r)$, see Figure 1.2.

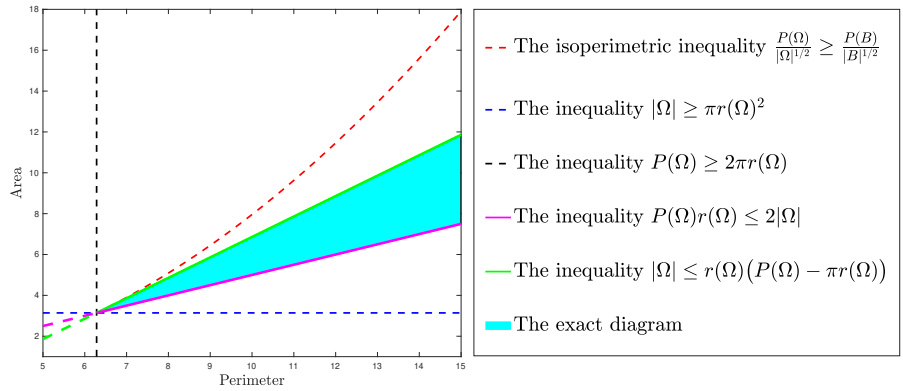

Figure 1.2: The Diagram $\mathcal{D}$ and related inequalities.

Another classical representation of the diagrams

At last, we point out that it is classical to represent Blaschke-Santaló diagrams in the square $[0,1] \times [0,1]$. It is done by looking for 2 inequalities such that each one involves only two functionals. These inequalities allows to define new variables $X, Y \in [0,1]$. In our case, as already mentioned in [163], this may be done by using inequalities:

$$2\pi r(\Omega) \leq P(\Omega) \quad \text{and} \quad \frac{P(\Omega)^2}{|\Omega|} \geq 4\pi,$$

and then considering the following set of points:

$$\left\{ \left(\frac{2\pi r(\Omega)}{P(\Omega)}, \frac{4\pi|\Omega|}{P(\Omega)^2} \right) \;\middle|\; \Omega \in \mathcal{K}^2 \right\} \subset [0,1] \times [0,1].$$

Let us denote $X = \frac{2\pi r(\Omega)}{P(\Omega)}$ and $Y = \frac{4\pi|\Omega|}{P(\Omega)^2}$, where $\Omega \in \mathcal{K}^2$. Inequalities (1.5) and (1.6) are respectively equivalent to:

$$Y \geq X \quad \text{and} \quad Y \leq X(2 - X).$$

The diagram is then given by Figure 1.3.

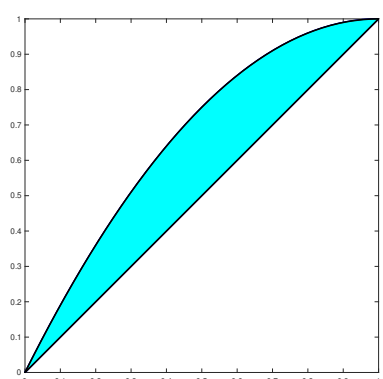

Figure 1.3: The diagram that fits into the unit square $[0,1] \times [0,1]$.

An overview on the main diagrams studied in the present thesis

In the present thesis, we are mainly interested in the study of the following diagrams:

- The diagram of the triplet $(P, h, |\cdot|)$ is studied in Chapter 2.
- The diagram of the triplet $(P, \lambda_1, |\cdot|)$ is studied in Chapter 3.
- The diagram of the triplet $(r, h, |\cdot|)$ is studied in Chapter 4.

Let us give more details on the problems and the questions we are interested in.

The diagram $(P, h, |\cdot|)$

Since the Cheeger constant is defined via the infimum of the ratio between the perimeter and the area, it seems natural to seek for complete systems of inequalities that relates the latter functionals. We are then interested in the study of the following sets of points:

$$\mathcal{D}^h_{\mathcal{C}} := \{\big(P(\Omega), h(\Omega)\big) \mid \Omega \in \mathcal{C} \text{ and } |\Omega| = 1\},$$

where $\mathcal{C}$ is a class of planar measurable sets.

Let us first give some classical and trivial inequalities: if Ω is a measurable subset of $\mathbb{R}^2$ and B a disk of unit area, we have:

- the isoperimetric inequality:
$$\frac{P(\Omega)}{|\Omega|^{1/2}} \geq \frac{P(B)}{|B|^{1/2}} = 2\sqrt{\pi}, \tag{1.7}$$
- a consequence of the definition of the Cheeger constant
$$h(\Omega) = \inf_{E \subset \Omega} \frac{P(E)}{|E|} \leq \frac{P(\Omega)}{|\Omega|}, \tag{1.8}$$
- a Faber-Krahn type inequality:
$$|\Omega|^{1/2} h(\Omega) \geq |B|^{1/2} h(B) = \frac{P(B)}{|B|^{1/2}} = 2\sqrt{\pi}, \tag{1.9}$$

One should note that inequalities (1.8) and (1.9) imply (1.7) and also define a region in the plane that contains the diagram, more precisely:

$$\mathcal{D}^h_{\mathcal{C}} \subset \{(x, y) \mid x \geq h(B),\ y \geq P(B) \text{ and } y \leq x\}.$$

It is then natural to ask the following questions:

Questions 1. *Let $\mathcal{C}$ a given class of measurable planar domains (we investigate simply connected sets, convex sets and convex polygons). Do inequalities* (1.8) *and* (1.9) *form a complete system of inequalities for the class $\mathcal{C}$? If not, Can we find a complete system of inequalities for the triplet $(P, h, |\cdot|)$ in the class $\mathcal{C}$.*

We refer to Section 1.4.1 for the statement of the related results and sketches of proofs and to Chapter 2 for detailed demonstrations.

The diagram $(P, \lambda_1, |\cdot|)$

Another interesting functional is the first eigenvalue of the Laplace operator with Dirichlet boundary condition denoted λ_1. As for the latter example, we are interested in describing sets of points:

$$\mathcal{D}_{\mathcal{C}}^{\lambda_1} := \{\big(P(\Omega), \lambda_1(\Omega)\big) \mid \Omega \in \mathcal{C} \text{ and } |\Omega| = 1\},$$

where $\mathcal{C}$ is a class of open sets.

Again, we are interested in the inequalities that relates the three functionals: P, $|\cdot|$ and λ_1. In addition to the isoperimetric inequality (1.7), there is the classical Faber-Krahn inequality that states that for every open set $\Omega \subset \mathbb{R}^n$ (where $n \geq 2$), one has:

$$|\Omega|^{\frac{2}{n}} \lambda_1(\Omega) \geq |B|^{\frac{2}{n}} \lambda_1(B), \tag{1.10}$$

where B is a ball of unit volume.

The isoperimetric and Faber-Krahn's inequalities (1.7) and (1.10) imply that the diagrams $\mathcal{D}_{\mathcal{C}}^{\lambda_1}$ are included in the quadrant $[P(B), +\infty) \times [\lambda_1(B), +\infty)$. This leads to the following question:

Questions 2. *Do inequalities* (1.7) *and* (1.10) *provide a complete system of inequalities for the triplet* $(P, \lambda_1, |\cdot|)$ *?*

Yet, the answer to the latter question depends on the choice of the class of sets $\mathcal{C}$. If the response is not trivial for general open sets (we refer to the first part of **Theorem of the Thesis 2**), it is not difficult to see that for other classes of domains the answer is no. For example, if $\mathcal{C}$ is given by the class of planar bounded convex domains denoted $\mathcal{K}^2$, there are other inequalities relating the involved functions which are sometimes better than (1.7) and (1.10). Indeed, if we denote $\mathcal{K}^2$ the class of planar convex bodies, we have for any $\Omega \in \mathcal{K}^2$:

1. Polya's inequality [156] (1959)
$$\lambda_1(\Omega) < \frac{\pi^2}{4} \left(\frac{P(\Omega)}{|\Omega|}\right)^2. \tag{1.11}$$

2. Makai's inequality [141] (1960):
$$\lambda_1(\Omega) > \frac{\pi^2}{16} \left(\frac{P(\Omega)}{|\Omega|}\right)^2. \tag{1.12}$$

3. Payne-Weinberger's inequality [154] (1961):
$$|\Omega|\lambda_1(\Omega) - |B|\lambda_1(B) \leq \lambda_1(B) \left(\frac{1}{J_1^2(j_{01})} - 1\right) \left(\frac{P(\Omega)^2}{4\pi|\Omega|} - 1\right), \tag{1.13}$$
where B is a disk of unit area, J_1 is the Bessel function of the first kind of order one and j_{01} is the first zero of the Bessel function of the first kind and of order zero.

These inequalities in addition to (1.10) provide a region in the plane (which is strictly included in the quadrant $[P(B), +\infty) \times [\lambda_1(B), +\infty)$) that contains the diagram $\mathcal{D}_{\mathcal{K}^2}^{\lambda_1}$, see Figure 1.4.

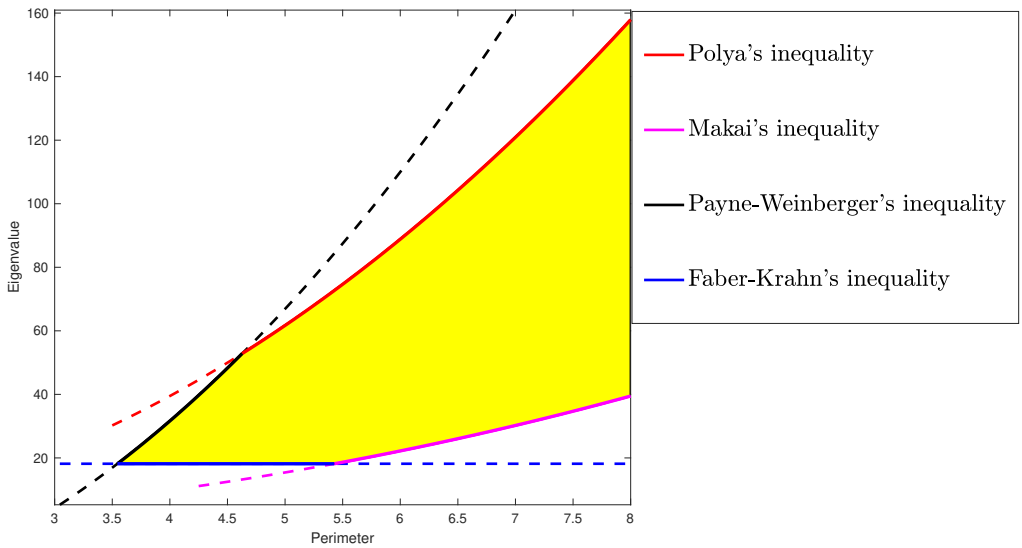

Figure 1.4: The smallest known domain that contains the diagram (in yellow).

Since, there is no explicit formula for the first Dirichlet eigenvalue, giving an explicit description of the diagram $\mathcal{D}^{\lambda_1}_{\mathcal{K}^2}$ does not seem to be possible, this is in general the case for diagrams that involve spectral quantities, this why in this framework one is interested in proving qualitative properties of the diagrams, see for example [13, 24, 44, 49, 138]. Numerical simulations may be very helpful in conjecturing some properties of a Blaschke-Santaló diagram. In a first time, let us give a numerical approximation of $\mathcal{D}^{\lambda_1}_{\mathcal{K}^2}$ by generating 10^5 random convex sets (polygons) of unit area for each we compute the first Dirichlet eigenvalue and the perimeter. We then obtain the following Figure 1.5

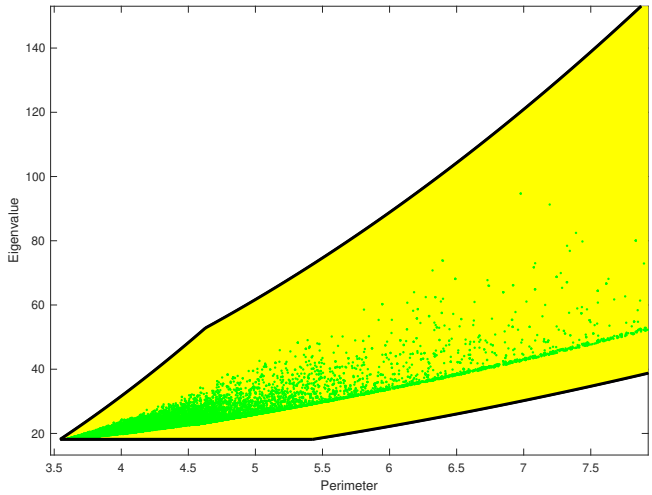

Figure 1.5: Approximation of the Blaschke-Santaló diagram $\mathcal{D}^{\lambda_1}_{\mathcal{K}^2}$ obtained by generating 10^5 random convex polygons.

As one sees in Figure 1.5, the diagram $\mathcal{D}^{\lambda_1}_{\mathcal{K}^2}$ seems to be given by the set of points located between the curves of two continuous and strictly increasing functions. Thus, it is natural to ask the following questions:

Questions 3.
- *Can we prove that $\mathcal{D}^{\lambda_1}_{\mathcal{K}^2}$ is exactly given by the set of points contained between the curves of two continuous and strictly increasing functions? Note that this will in particular prove the vertical and horizontal convexities of $\mathcal{D}^{\lambda_1}_{\mathcal{K}^2}$.*
- *Can we give asymptotic information on the boundary of the diagram ?*

We refer to Section 1.4.2 for the statement of the related results and sketches of proofs and to Chapter 3 for more details.

The diagram $(r, h, |\cdot|)$ for planar convex sets

At last, we are interested in describing the inequalities between the inradius, the Cheeger constant and the area of planar convex sets. Here also, we introduce and study a Blaschke-Santaló diagram:

$$\mathcal{D}^r_{\mathcal{K}^2} := \left\{ \left(\frac{1}{r(\Omega)}, h(\Omega) \right) \mid \Omega \in \mathcal{K}^2 \text{ and } |\Omega| = 1 \right\}.$$

Again, we denote B a ball of unit area. Let us state the trivial and classical inequalities relating the involved functionals:

- the Faber-Krahn type inequality:

$$|\Omega|^{1/2} h(\Omega) \geq |B|^{1/2} h(B) = \frac{P(B)}{|B|^{1/2}} = 2\sqrt{\pi}, \tag{1.14}$$

- an isoperimetric inequality for the inradius:

$$\frac{r(\Omega)}{|\Omega|^{1/2}} \leq \frac{r(B)}{|B|^{1/2}}, \tag{1.15}$$

- a consequence of the inclusion $B_{r(\Omega)} \subset \Omega$ and the definition of the Cheeger constant:

$$h(\Omega) \leq \frac{P(B_{r(\Omega)})}{|B_{r(\Omega)}|} = \frac{2}{r(\Omega)}, \tag{1.16}$$

  where $B_{r(\Omega)}$ is a ball of radius $r(\Omega)$ contained in Ω.

We note that the choice of defining the diagram via $\frac{1}{r}$ instead of r is purely done to have a better readability of the diagram as the quantity $\frac{1}{r}$ appears in different inequalities, this is for example the case for (1.16). It also allows, by inequalities (1.14) and (1.15), to have a diagram included in the quadrant $[1/r(B), +\infty) \times [h(B), +\infty)$.

Here also, it is natural to ask:

Questions 4. *Do inequalities* (1.14) *and* (1.16) *provide a complete system of inequalities of the triplet* $(r, h, |\cdot|)$ *in the class* $\mathcal{K}^2$*? If not, can we find the explicit description of the diagram* $\mathcal{D}^r_{\mathcal{K}^2}$*?*

We refer to Section 1.4.3 for the statement of the related results (see **Theorem of the Thesis 4**) and sketches of proofs and to the first section of Chapter 4 for detailed demonstrations.

1.3.2 Chapter 4: The Cheeger inequality for convex sets

A celebrated inequality proven by Jeff Cheeger in [55] states that, for every bounded domain $\Omega \subset \mathbb{R}^n$, with $n \geq 1$, one has:

$$\lambda_1(\Omega) \geq \frac{1}{4} h(\Omega)^2. \tag{1.17}$$

Recently, Enea Parini remarked in [152] that for planar convex sets the constant 1/4 is not optimal. He took a shape optimization point of view and studied the functional

$$J_n(\Omega) := \frac{\lambda_1(\Omega)}{h(\Omega)^2}$$

It is important to note that the functional J_n is invariant by rigid motions and by dilations (i.e. $J_n(t\Omega) = J_n(\Omega)$ for $t > 0$): this is a consequence of the following homothety properties for the first Dirichlet eigenvalue and the Cheeger constant:

$$\forall t > 0, \quad \lambda_1(t\Omega) = \frac{\lambda_1(\Omega)}{t^2} \quad \text{and} \quad h(t\Omega) = \frac{h(\Omega)}{t}.$$

The planar case: study of the functional J_2

We summarize the main results of [152] in the following Theorem:

Theorem 1. *We have the following bounds:*

$$\forall \Omega \in \mathcal{K}^2, \qquad \frac{\pi^2}{16} < J_2(\Omega) = \frac{\lambda_1(\Omega)}{h(\Omega)^2} < \frac{\pi^2}{4}. \tag{1.18}$$

- *The upper bound is sharp: every sequence (Ω_k) in $\mathcal{K}^2$, such that $|\Omega_k| = V$ for some $V > 0$ and $d(\Omega_k) \underset{k\to+\infty}{\longrightarrow} +\infty$, where $d(\Omega_k)$ is the diameter of Ω_k, satisfies*

$$\lim_{k\to+\infty} J_2(\Omega_k) = \frac{\pi^2}{4}.$$

- *J_2 admits a minimizer in the class $\mathcal{K}^2$. Thus, the lower bound $\frac{\pi^2}{16}$ is not optimal.*

We note that in the original work of E. Parini, the improved Cheeger inequality ($J_2(\Omega) > \frac{\pi^2}{16}$) is stated in a large form. Let us quickly show how one can obtain strict inequality: Parini's proof is based on the definition of the Cheeger constant and the following classical inequality proved by Hersch [115]:

$$\forall \Omega \in \mathcal{K}^2, \qquad \lambda_1(\Omega) \geq \frac{\pi^2}{4r(\Omega)^2}. \tag{1.19}$$

To get the strict inequality, we can use the following Protter's inequality [158], which is an improved version of (1.19):

$$\forall \Omega \in \mathcal{K}^2, \qquad \lambda_1(\Omega) \geq \frac{\pi^2}{4}\left(\frac{1}{r(\Omega)^2} + \frac{1}{d(\Omega)^2}\right). \tag{1.20}$$

For the denominator, E. Parini uses the following upper bound obtained by taking the inscribed ball $B_{r(\Omega)}$ as a test set in the variational definition of the Cheeger constant of Ω:

$$h(\Omega) := \inf_{E\subset\Omega} \frac{P(E)}{|E|} \leq \frac{P(B_{r(\Omega)})}{|B_{r(\Omega)}|} = \frac{2}{r(\Omega)},$$

this inequality is an equality if and only if Ω is a ball.

We then write:

$$J_2(\Omega) = \frac{\lambda_1(\Omega)}{h(\Omega)^2} = \frac{\lambda_1(\Omega) \times r(\Omega)^2}{\big(h(\Omega) \times r(\Omega)\big)^2} \geq \frac{\pi^2}{16}\left(1 + \left(\frac{r(\Omega)}{d(\Omega)}\right)^2\right) > \frac{\pi^2}{16}.$$

We note that even-though the use of Protter's inequality allows to obtain a strict inequality (and even a stronger lower bound in term of the diameter and the inrhadius of Ω), it is not sufficient to improve the constant $\frac{\pi^2}{16}$. Indeed, if we take $\Omega_k := (0,k) \times (0,2)$ for $k \in \mathbb{N}\backslash\{0,1\}$, we have $d(\Omega_k) \geq k$ and $r(\Omega_k) = 1$. In this case, the correcting term goes to 0:

$$0 < \frac{r(\Omega_k)}{d(\Omega_k)} \leq \frac{1}{k} \underset{k\to+\infty}{\longrightarrow} 0.$$

Thus, we cannot expect to obtain a better constant than $\frac{\pi^2}{16}$ with these estimates.

It is natural to try to find (or at least conjecture) the optimal lower bound $\min\limits_{\Omega\in\mathcal{K}^2} J_2(\Omega)$ or have more information on the minimizer Ω^* (i.e. any set $\Omega^* \in \mathcal{K}^2$ such that $\min\limits_{\Omega\in\mathcal{K}^2} J_2(\Omega) = J_2(\Omega^*)$).

In [152], the author gives some optimality conditions that a set should satisfy to be a minimizer and conjectures that it is given by squares (we recall that J is scaling invariant). In this case, the optimal lower bound would be:

$$J_2\big((0,1)^2\big) = \frac{2\pi^2}{(2+\sqrt{\pi})^2} \approx 1.387...$$

As far as we know, this conjecture was supported by the fact that the square (numerically) seems to realise the lowest value of J_2 between all regular polygons, it also the best between rectangles. It is then natural to ask the following question which is studied in Chapter 5:

Questions 5. *Can we provide more numerical evidence to validate Parini's conjecture that states that the squares manimize the functional J_2 between planar convex sets ?*

We note that it is quite unusual for the minimizer to be "singular" in shape optimization, which seems to be the case for the problem of minimizing J over planar convex domains as the minimizer seems to be a square. The phenomena of apparition of singular optimal sets (more precisely polygons) when imposing convexity constraint was observed in quite different fields [62, 129]. Then came a series of works by A. Novruzi, J. Lamboley and M. Pierre who extensively studied the convexity constraint and determined some "concavity" conditions on the functionals, which, once satisfied, ensure that the optimal set would be polygonal, we refer to [131, 134] (see also the work of C. Bianchini and A. Henrot [25] for the complete resolution of a purely geometrical shape optimization problem under convexity constraint).

Before getting back to the Cheeger inequality and stating the related questions theoretically studied in this thesis, let us give a beautiful and quite eloquent analogy that would help us heuristically understand why polygons may appear when imposing convexity constraint: in finite dimension optimization, it is quite common to minimize a given convex function on a compact subset (constraints) of $\mathbb{R}^n$, where $n \geq 1$, but what happens if we assume the function to be concave? It is clear that in this case the solution of the minimization problem will be on the boundary of the compact subset and thus saturates the constraints. In the same spirit, if we assume our shape depending functional to be "concave" in a certain sense and minimize it under convexity constraint (over the set of convex domains) the solution should logically "saturate" the convexity constraint in the sense that its boundary tends to have flat parts.

Questions 6. *Can we find a better lower bound for $\inf\limits_{\Omega\in\mathcal{K}^2} J_2(\Omega)$ than the $\frac{\pi^2}{16}$ obtained in Theorem 1 ?*

We refer to Section 1.4.3 for the statement of the related results (see **Theorem of the Thesis 3**) and sketches of proofs and Section 4.3 of Chapter 4 for detailed demonstrations.

On higher dimensions

It is natural to seek for generalizations of Theorem 1 in higher dimensions. We distinguish two main reseach directions:

1. **Finding upper and lower bounds for the functional J_n.**

   A natural and first strategy to attack the first point is to look for generalizations of the arguments used by Parini in the planar case. By doing so, L. Brasco recently remarked that the upper bound holds for any dimensions [40, Remark 1.1.]. Similarly, for the lower bound, we remark that Hersch's inequality (1.19) holds for higher dimensions (see [158, Theorem 2]). We then use the same strategy of Parini (detailed in the last paragraph) and obtain the following lower bound:

   $$\forall \Omega \in \mathcal{K}^n, \quad J_n(\Omega) > \frac{\pi^2}{4n^2},$$

   which improves the original constant $\frac{1}{4}$ given by J. Cheeger only for $n \in \{2, 3\}$. In this case, we have:

   $$\forall \Omega \in \mathcal{K}^2, \quad J_2(\Omega) > \frac{\pi^2}{16} \approx 0.616... \quad \text{and} \quad \forall \Omega \in \mathcal{K}^3, \quad J_3(\Omega) > \frac{\pi^2}{36} \approx 0.274...$$

2. **Proving the existence of a minimizer of J_n in the class $\mathcal{K}^n$.**

   The proof of [152] for the planar case follows the classical method of calculus of variations: the author proves that any minimizing sequence (Ω_k) of planar convex sets cannot collapse to a segment: indeed, if it was the case the author proves that $(J_2(\Omega_k)$ converges to $\frac{\pi^2}{4}$ which is strictly higher than $J_2\big((0,1)^2\big)$ and thus cannot be a minimizing sequence. In his paper [152], the author used explicit values of the Cheeger constant of triangles and noted (see [152, Section 6]) that such results are lacking in higher dimensions which makes the problem more challenging in this case.

   In the present thesis, we study the following question:

   Questions 7. *Can we prove the existence of a minimizer of J_n in the class $\mathcal{K}^n$?*

   We refer to Section 1.4.3 for the statement of the related results (see **Theorem of the Thesis 5**) and to Section 4.4 of Chapter 4 for detailed demonstrations.

In Subsection 1.4.3, we state the related results, explain the main challenges behind the latter questions and present the ideas and methods developed in order to overcome these difficulties. The details of the proofs may be found in Chapter 4.

1.3.3 Chapter 5: Numerical study of the convexity constraint and application to Blaschke-Santaló diagrams

Parametrization of shape optimization problems

As highlighted in the beginning of Section 1.3, the task of theoretically finding an optimal shape (when it exists) may be very challenging or even impossible, this motivates to develop numerical methods of shape optimization. This numerical framework is very interesting as it has various applications in

different fields, see for example [4, 5] for industrial examples and [31, 34] for more theoretical ones. In the present thesis, we focus on numerical simulations related to spectral geometry.

When aiming to numerically solve a shape optimization problem, the first step is to understand the situation and the related constraints in order to choose a suitable parametrization of the considered shapes so as to reduce the optimization problem to a finite dimensional one in order to be able to use common methods and software developed for finite dimensional optimization: this is known as parametric shape optimization.

Mathematically, if we want to solve the following shape optimization problem:

$$\inf_{\Omega \in \mathcal{F}_{\mathrm{ad}}} J(\Omega), \tag{1.21}$$

where $J : \Omega \in \mathcal{F}_{\mathrm{ad}} \longmapsto J(\Omega) \in \mathbb{R}$ is a given shape functional and $\mathcal{F}_{\mathrm{ad}}$ is a class of sets in $\mathbb{R}^2$ or $\mathbb{R}^3$ defining the constraints or the problem (for example $\mathcal{F}_{\mathrm{ad}}$ could be the class of planar convex sets of unit area). The idea is to choose an efficient (approximated) description of the set Ω via a finite number of parameters $(p_1, ..., p_N)$. We then consider the function

$$j : (p_1, ..., p_N) \in \mathbb{R}^N \longmapsto j(p_1, ..., p_N) := J(\Omega).$$

The constraints encoded in $\mathcal{F}_{\mathrm{ad}}$ would be given by inequalities and/or equalities on $(p_1, ..., p_N)$. Problem (1.21) is then approximated by the following finite dimensional optimization problem:

$$\begin{cases} \inf\limits_{p_1,...,p_N} j(p_1, ..., p_N), \\ \forall k \in [\![1, L]\!], \quad C_k(p_1, ..., p_N) \leq 0, \\ \forall k \in [\![1, L^{\mathrm{eq}}]\!], \quad C_k^{\mathrm{eq}}(p_1, ..., p_N) = 0, \end{cases}$$

where C_k and C_k^{eq} are real functions associated to the constraints.

An example: the isoperimetric inequality for triangles

For a better understanding, let us develop an example. Assume that we want to solve the isoperimetric problem for triangles, which is to look for the triangle that minimizes the perimeter between triangles of the same area V_0 ? (The answer is well known: as expected, it is the regular one). Our problem could be written as in (1.21):

$$\inf_{\Omega \in \mathcal{T}_{V_0}} P(\Omega),$$

where $\mathcal{T}_{V_0}$ is the class of triangles of area V_0. A natural parametrization of this problem would be via the coordinates of the vertices of the triangles, then each triangle $\Omega := A_1A_2A_3$ will be corresponding to the parameters $(x_1, x_2, x_3, y_1, y_2, y_3)$, where $(x_i, y_i)_{i\in\{1,2,3\}}$ are the coordinates of A_i. The problem is then equivalent to the following one:

$$\begin{cases} \inf\limits_{(x_1,...,y_3)\in\mathbb{R}^6} \sqrt{(x_1 - x_2)^2 + (y_1 - y_2)^2} + \sqrt{(x_2 - x_3)^2 + (y_2 - y_3)^2} + \sqrt{(x_3 - x_1)^2 + (y_3 - y_1)^2}, \\ \frac{1}{2} \left|(x_1y_2 - x_2y_1) + (x_2y_3 - x_3y_2) + (x_3y_1 - x_3y_1)\right| = V_0. \end{cases}$$

This problem can then be solved by any optimization solver and one will obtain the coordinates of a regular triangle.

An important tool: shape derivation

We note that to have accurate results it is highly recommended (if not to say mandatory) to have good approximations of the gradients of the objective function and the constraints. Being time-consuming

and less efficient, the finite difference approximation is in general not suitable in the framework of shape optimization, especially when dealing with functionals depending on solutions of PDEs. This is one of the motivations behind the extensive study of the so called *shape derivation*, which is a notion of differentiation of a given shape depending functional. We recall that the term shape derivative usually refers either to Eulerian semiderivatives, using the speed method to define domain perturbations, see for example [67, Chapter 9], or to Fréchet derivatives, obtained using the method of perturbation of identity, see for example [108, Chapter 5]. It is well-known that they yield the same expression for the first order derivative, but different expressions for second order derivatives.

Throughout the following thesis the term directional shape derivative will correspond to the following notion:

Definition 1. *let us take a shape depending functional $J : \Omega \subset \mathbb{R}^n \longrightarrow \mathbb{R}$, where $n \geq 2$, and let $V : \mathbb{R}^n \to \mathbb{R}^n$ a perturbation vector field. Let $\Omega \subset \mathbb{R}^n$, we denote $\Omega_t := (I + tV)(\Omega)$ where $I : x \in \mathbb{R}^n \longmapsto x$ is the identity map and t a sufficiently small positive number. We say that the functional J admits a directional shape derivative at Ω in the direction V if the following limit $\lim\limits_{t\to 0^+} \frac{J(\Omega_t)-J(\Omega)}{t}$ exists. In this case we denote:*

$$J'(\Omega, V) := \lim_{t\to 0^+} \frac{J(\Omega_t) - J(\Omega)}{t}.$$

The importance given to the study of shape derivatives comes from the variety of their applications, we state for instance:

- Showing that a certain shape is a critical point for a shape optimization problem by proving that the first order shape derivative vanishes. In this case one could go further and study the coercivity of the second order shape derivative in order to prove that the latter critical shape is a local minimum of maximum of the functional, see for example [33, 159].
- Showing some quantitative inequalities and stability results, see for example [63, 41, 143].
- Numerical simulation of optimal shapes. Indeed, having an explicit formula of the shape derivative allows to get an efficient estimate of the shape gradient with less numerical costs.

When dealing with shape derivatives, two natural and main questions arise:

1. **Do shape derivatives of a given functional exist ? If yes, then how can we compute it ?**

   A classical tool to show differentiability is the implicit functions Theorem, but it does not give a formula of the derivative, for example as explained in [106, Chapter 5] one may show without assuming any regularity assumption on the shape that the perimeter is differentiable (as a shape functional) at any order, but cannot write down formulae of the derivatives (unless more regularity is assumed).

   If we want to sum up, there are up to our knowledge 3 ways of computing shape derivatives:

   (a) by direct differentiation if we have an explicit formula of the functional, which is the case of the volume for example, as one can see in the example developed below.

   (b) By differentiating a variational formulation as it is classically done to compute shape derivatives of Dirichlet energy or first Dirichlet eigenvalue λ_1 (see for example [106, Chapter 5]).

   (c) By using classical techniques developed for differentiation of functions defined as infima, namely Danskin's Theorem [65] which allows to show the existence and compute first order directional derivatives of such functions. This allows to prove that a functional defined as *infimum* (or *supremum*) of a certain quantity over some given space admits a first order directional shape derivative and also to derive a formula. For examples, we refer to [139] where the authors use similar approach for first Dirichlet eigenvalue of p-Laplace operator and [153] for the Cheeger constant.

2. **Are there different expressions for shape derivatives ?**

   It is common to express shape derivatives as integrals on the domain or (if possible) its boundary. Indeed, it is natural to expect that the variation of the functional could be quantified by the variation of the boundary of the domain along its normal directions. These type of results are called *"Structure theorems for shape derivatives"*, they have been studied in detail for smooth domains, see for example [146], and are challenging in non-smooth settings, see for example [86, 85, 87, 135].

The main purpose behind the introduction of shape derivatives in this thesis is to apply them in numerical shape optimization. We ask the following question:

Questions 8. *How can we compute the directional shape derivatives of the diameter and the Cheeger constant and use them in numerical simulations?*

We refer to Theorems 19 and 20 of Chapter 5 for the corresponding results.

Convexity constraint

Let us now talk about the principal geometrical constraint treated in in this thesis: it is the convexity constraint. As explained above in the beginning of Section 1.3, the convexity constraint allows in general to have the existence of a solution of shape optimization problems and also may be very captivating since the optimal domain could be singular (polygonal for example, see [134]), which is not very common in shape optimization and seems to be very challenging to study from a numerical point of view, see Chapter 5.

One classical problem in spectral geometry is to find the domain that minimizes (or maximizes) a certain eigenvalue of a differential operator, for example the Laplacian, which was extensively studied in the last century and continues nowadays to interest various communities. One early result in this direction was (independently) obtained by Faber [78] and Krahn [126], who show that the set minimizing the first Dirichlet eigenvalue λ_1 among domains of given volume is the ball. As for the second one it was proved that the minimum is attained by the union of any two disjoint balls of half volume, see [155, 117, 126].

In 1973, Troesch performed some numerical simulations and remarked that if one add convexity constraint to the problem of minimizing λ_2 among planar sets of given area, the solution seems to be a stadium (ie. the convex hull of two balls). This conjecture was refuted in 2002 by A. Henrot and E. Oudet [107] who proved that the boundary of the optimal domains cannot contain circular arcs, which excludes stadiums, but proved that it contains two segments as supported by numerical evidence.

At last, here is a non-exhaustive list of works where authors obtain numerical results of shape optimization problems under convexity constraint:

- Maximizing Steklov eigenvalues under area constraint [32].
- Minimization of Dirichlet eigenvalues with constant width constraint [33].
- Numerical approximation of optimal convex shapes [19].
- Using the support function to parametrize convex sets [20, 128]

The questions we are interested in in the present thesis are the following

Questions 9.
- *How is the convexity constraint classically handled in the literature? can we provide some original methods?*
- *What are the advantages and disadvantages of each method ?*
- *How to use numerical simulations to have a quite optimal and satisfying numerical description of Blaschke-Santaló diagrams involving the first Dirichlet eigenvalue, the perimeter, the area and the diameter?*

In Subsection 1.4.4, we describe the different numerical approaches used in this thesis and present some numerical results. For more information and numerical results, we refer to Chapter 5.

1.3.4 Chapter 5: Where to place a spherical obstacle so as to maximize the first Steklov eigenvalue ?

Up to this point a major interest was given to the study of shape optimization among convex sets. In the last part of the thesis, we study different kind of problems: we look for the sets that optimize certain functionals between multiply-connected domains (that contain holes) or in particular doubly-connected sets (that contain one simply connected hole). One can consider several extremum problems, letting the boundary conditions vary on the outer boundary and/or the hole. Most of the known results were obtained in the sixties by Payne, Weinberger and Hersch, see [114, 154]. Let us recall some classical results.

Maximizing the first Dirichlet-Neumann eigenvalue

Let $\mathcal{O}_{L_0,A}$ be the class of doubly-connected planar domains Ω of area $A > 0$ with outer boundary Γ_0 of length $L_0 > 0$ and inner boundary γ. We denote by Λ_1^{pw} the first eigenvalue of the following mixed problem:

$$\begin{cases} -\Delta u = \Lambda_1^{\mathrm{pw}}(\Omega) u & \text{on } \Omega, \\ u = 0 & \text{on } \Gamma_0, \\ \frac{\partial u}{\partial n} = 0 & \text{on } \gamma. \end{cases}$$

Theorem 2. *(Payne-Weinberger [154])*
The annular ring (with concentric circles) maximizes Λ_1^{pw} in the class $\mathcal{O}^2_{L_0,A}$.

The proof relies on the construction of relevant test functions that one can plug into the variational characterization of the eigenvalue, we refer to [106, Section 3.5] for a survey on the topic and some detailed proofs. The latter idea is then adapted to other situations: for example if one denotes $\mathcal{O}_{A,L_1}$ the class of doubly-connected planar domains Ω of area $A > 0$ with inner boundary Γ_1 of length $L_1 > 0$ and outer boundary γ, Hersch proved in [114] that here also the annular ring (with concentric circles) maximizes Λ_1^{h} the first eigenvalue of the following mixed problem:

$$\begin{cases} -\Delta u = \Lambda_1^{\mathrm{h}}(\Omega) u & \text{on } \Omega, \\ \frac{\partial u}{\partial n} = 0 & \text{on } \gamma, \\ u = 0 & \text{on } \Gamma_1. \end{cases}$$

For similar results for several holes, we refer to [150] for some recent generalisations to the case of the $p-$Laplace operator. As far as we know the latter problems are still open in higher dimensions.

On the pure Dirichlet boundary condition

One interesting case that has been widely studied is when we take Dirichlet boundary condition on both the outer and inner boundaries. A first result in this framework was obtained by Hersch, it is stated as follows:

Theorem 3. *(Hersch [114])*
Let $\mathcal{O}^2$ be the class of doubly-connected planar domains Ω of area A satisfying:

- *the outer boundary has length $L_0 > 0$,*
- *the inner boundary has length $L_1 > 0$,*
- $L_0^2 - L_1^2 = 4\pi A$.

Then, the annular ring (with concentric circles) maximizes the first Dirichlet eigenvalue λ_1 in the class $\mathcal{O}^2$.

The proof relies on a result of H. Weinberger [173], that states that we can find a closed curve γ "between" Γ_0 and Γ_1 such that the first eigenfunction u_1 of Ω satisfies:

$$\frac{\partial u_1}{\partial n} = 0 \quad \text{on } \gamma.$$

Then, the author considers the doubly connected sets Ω_0 and Ω_1 respectively delimited by Γ_0 and γ one hand and by γ and Γ_1 on the other, he remarks that $\lambda_1(\Omega) = \lambda_1^{\mathrm{pw}}(\Omega_0) = \lambda_1^{\mathrm{h}}(\Omega_1)$ and then applies the latter results to write:

$$\lambda_1(\Omega) \leq \min(\lambda_1^{\mathrm{pw}}(R_0), \lambda_1^{\mathrm{h}}(R_1)),$$

where R_0 (resp. R_1) is the annular ring whose inner (resp. external) boundary's length is equal to L_0 (resp. L_1) and such that $|R_0| = |\Omega_0|$ and $|R_1| = |\Omega_1|$. This brings the problem to the comparison of eigenvalues of annular rings (for which one has explicit expressions).

The case of spherical obstacles

Theorem 3 implies, in particular, that for doubly connected domains of the form $B_1 \backslash B_2$ where B_1 and B_2 are two disks such that $B_2 \subset B_1$, the first Dirichlet eigenvalue is maximal when the disks are concentric. Later, this result was simultaneously extended to higher dimensions by M. Ashbaugh and T. Chatelain in a private communication, E. Harrell, P. Kroger and K. Kurata in [105] and R. Kesavan in [123]. Actually, the generalization of [105] is given in the following way:

Theorem 4. *Let Ω be a convex domain in $\mathbb{R}^n$ $(n \geq 2)$ and B a ball contained in Ω. Assume that Ω is symmetric with respect to some hyperplane H. We are interested in the position of B which maximizes or minimizes the first Dirichlet eigenvalue $\lambda_1(\Omega \backslash B)$. Then:*

- *at the minimizing position B touches the boundary of Ω,*
- *at the maximizing position B is centered on H.*

The proof relies on the judicious use of shape derivative, reflection arguments and the maximum principle that allow to prove a certain monotonicity result which is mainly that the eigenvalue decreases as the spherical obstacle approaches the boundary of Ω.

After, came a series of works treating the case of spherical obstacles for different boundary conditions, we cite for example [8, 57, 73, 75, 172].

Steklov boundary condition

Very recently, there has been a grown interest for the so-called *Steklov* boundary condition which denotes a situation where the eigenvalue is defined in the equation on the boundary: let $\Omega \subset \mathbb{R}^n$, be a bounded, open set with Lipschitz boundary. The Steklov eigenvalue problem for the Laplace operator corresponds to the following system:

$$\begin{cases} \Delta u = 0 & \text{in } \Omega, \\ \frac{\partial u}{\partial n} = \sigma u & \text{on } \partial\Omega. \end{cases} \tag{1.22}$$

It is well-know that the Steklov spectrum is discrete as long as the trace operator $H^1(\Omega) \to L^2(\partial\Omega)$ is compact, which is the case when the domain has Lipschitz boundary; in other words, in our framework the values of σ for which the problem (6.1) admits non-trivial solutions form an increasing sequence of eigenvalues $0 = \sigma_0(\Omega) < \sigma_1(\Omega) \leq \sigma_2(\Omega) \leq \cdots \nearrow +\infty$, known as the Steklov spectrum of Ω.

Up to our knowledge, problems of optimal placement of obstacles in the framework of pure Steklov boundary conditions have not been extensively studied (at least as it was the case for other boundary conditions problems) and yet much problems remain unsolved.

Finally, before stating the main question tackled in this thesis, let us point out some recent results in the case of mixed Dirichlet-Steklov boundary conditions: we are interested in the first eigenvalue of the problem:

$$\begin{cases} \Delta u = 0 & \text{in } \Omega\backslash\overline{K}, \\ u = 0 & \text{on } \partial K, \\ \frac{\partial u}{\partial n} = \tau u & \text{on } \partial\Omega, \end{cases} \tag{1.23}$$

where $\Omega \subset \mathbb{R}^n$ and K is a simply connected open set contained in Ω.

Up to our knowledge, this specific problem was considered for the first time by Hersch and Payne in 1968 [116], where the authors use conformal mapping to provide an upper estimate of the first eigenvalue of problem (1.23) in the case of planar doubly connected domains. Recently, S. Verma and G. Santhanam [172] proved that in the particular case when both Ω and K are balls, the eigenvalue τ_1 is maximal when in the concentric case (this result was proved for dimensions $n \geq 3$ and is extended to the planar case ($n = 2$) in the present thesis, see Theorem 22). This result was then extended from Euclidean spaces to two-point homogeneous spaces by D.H. Seo [165]. Furthermore, in their very recent paper [149], G. Paoli, R. Piscitelli, and R. Sannipoli proved that the spherical shell locally maximizes the first eigenvalue among nearly spherical sets when both the internal ball and the volume are fixed.

To the best of our knowledge, results as those stated above have not been proven yet for the pure Steklov case which also seems very challenging as classical techniques (as the maximum principle and reflection arguments) cannot be used, we also note that the eigenfunctions corresponding to the first non-trivial eigenvalue of the spherical shell (the case of concentric balls) are not radial functions which complicates the computations and make it difficult to use them to construct suitable test functions.

In this thesis we provide an answer to the following questions:

Questions 10.
- *Where to place a spherical obstacle inside a given ball so as to maximize its first non-trivial (pure) Steklov eigenvalue ?*
- *Can we provide an alternative proof of [172, Theorem 1] that does not rely on MATHEMATICA ? and can we extend the result to the planar case ?*

In Subsection 1.4.3, we state the related results and describe the ideas and methods used in the proofs, we note that our approach allows to give an alternative and simpler proof to [172, Theorem 1]. For more information and detailed demonstrations, we refer to Chapter 6.

1.4 Main contributions and methods of the Thesis

1.4.1 Contributions of Chapter 1: Blaschke-Santaló diagrams for volume, perimeter and Cheeger constant.

Main results

As explained in Paragraph 1.3.1, we are interested in describing all possible inequalities relating the perimeter, the area and the Cheeger constant for different classes of planar sets: we mainly consider the class $\mathcal{S}^2$ of simply connected sets, the class $\mathcal{K}^2$ of convex sets and the class $\mathcal{P}_N$ of convex polygons of at most N sides.

All in all, in **Theorem of the Thesis 1**, we provide complete descriptions of the diagrams:

$$\mathcal{D}^h_{\mathcal{S}^2} := \big\{\big(P(\Omega), h(\Omega)\big) \mid \Omega \in \mathcal{S}^2 \text{ and } |\Omega| = 1\big\}, \quad \mathcal{D}^h_{\mathcal{K}^2} := \big\{\big(P(\Omega), h(\Omega)\big) \mid \Omega \in \mathcal{K}^2 \text{ and } |\Omega| = 1\big\}$$

and

$$\mathcal{D}^h_N := \big\{\big(P(\Omega), h(\Omega)\big) \mid \Omega \in \mathcal{P}_N \text{ and } |\Omega| = 1\big\},$$

when $N \in \{3\} \cup \{2k \mid k \geq 2\}$ and provide an advanced description of the boundary of $\mathcal{D}^h_N$ when $N \geq 5$ is odd.

Theorem of the Thesis 1. *$(P, h, |\cdot|)$-diagrams.*
We denote by B a ball of unit area in $\mathbb{R}^2$ and R_N the regular polygon of N sides and unit area.

1. *We denote by $\mathcal{D}^h_{\mathcal{S}^2}$ the diagram in the case of simply connected sets of $\mathbb{R}^2$, we have:*

$$\mathcal{D}^h_{\mathcal{S}^2} = \{(P(B), P(B))\} \cup \{(x, y) \ \mid \ x \geq P(B) \quad \text{and} \quad P(B) < y \leq x\}.$$

2. *We denote by $\mathcal{D}^h_{\mathcal{K}^2}$ the diagram in the case of convex domains of $\mathbb{R}^2$, we have:*

$$\mathcal{D}^h_{\mathcal{K}^2} = \left\{(x, y) \ \mid \ x \geq P(B) \quad \text{and} \quad \frac{1}{2}x + \sqrt{\pi} \leq y \leq x\right\}.$$

3. *Let us now state results on Blaschke-Santaló diagrams for $\mathcal{P}_N$: we distinguish the following cases:*

   (a) *if $N = 3$, we have*

$$\mathcal{D}_3 = \{(x, x/2 + \sqrt{\pi}) | \ \ x \geq P(R_3)\}$$

   (b) *if N is even, then*

$$\mathcal{D}^h_N = \big\{(x, y) \mid x \geq P(R_N) \ \ \text{and} \ \ x/2 + \sqrt{\pi} \leq y \leq f_N(x)\big\},$$

   where $f_N : x \in [P(R_N), +\infty) \longmapsto \frac{x + \sqrt{x^2 + 4(\pi - N \tan \frac{\pi}{N})}}{2}$.

   (c) *if $N \geq 5$ is odd, we provide a qualitative description of the boundary of the diagram $\mathcal{D}_N$:*

   - *The lower boundary is given by the half line:*

$$\{(x, y) \mid x \geq P(R_N) \ \text{and} \ y = x/2 + \sqrt{\pi}\},$$

     which is included in the diagram $\mathcal{D}_N$.
   - *The upper boundary is given by the curve:*

$$\{(x, y) \mid x \geq P(R_N) \ \text{and} \ y = g_N(x)\},$$

     which is also included in the diagram $\mathcal{D}_N$, where g_N is a continuous and strictly increasing function such that $g_N \leq f_N$ on $\big[P(R_N), +\infty\big)$. Moreover, there exists $c_N \geq b_N > P(R_N)$ such that $g_N = f_N$ on $[P(R_N), b_N]$ and $g_N < f_N$ on $\big[c_N, +\infty\big)$.

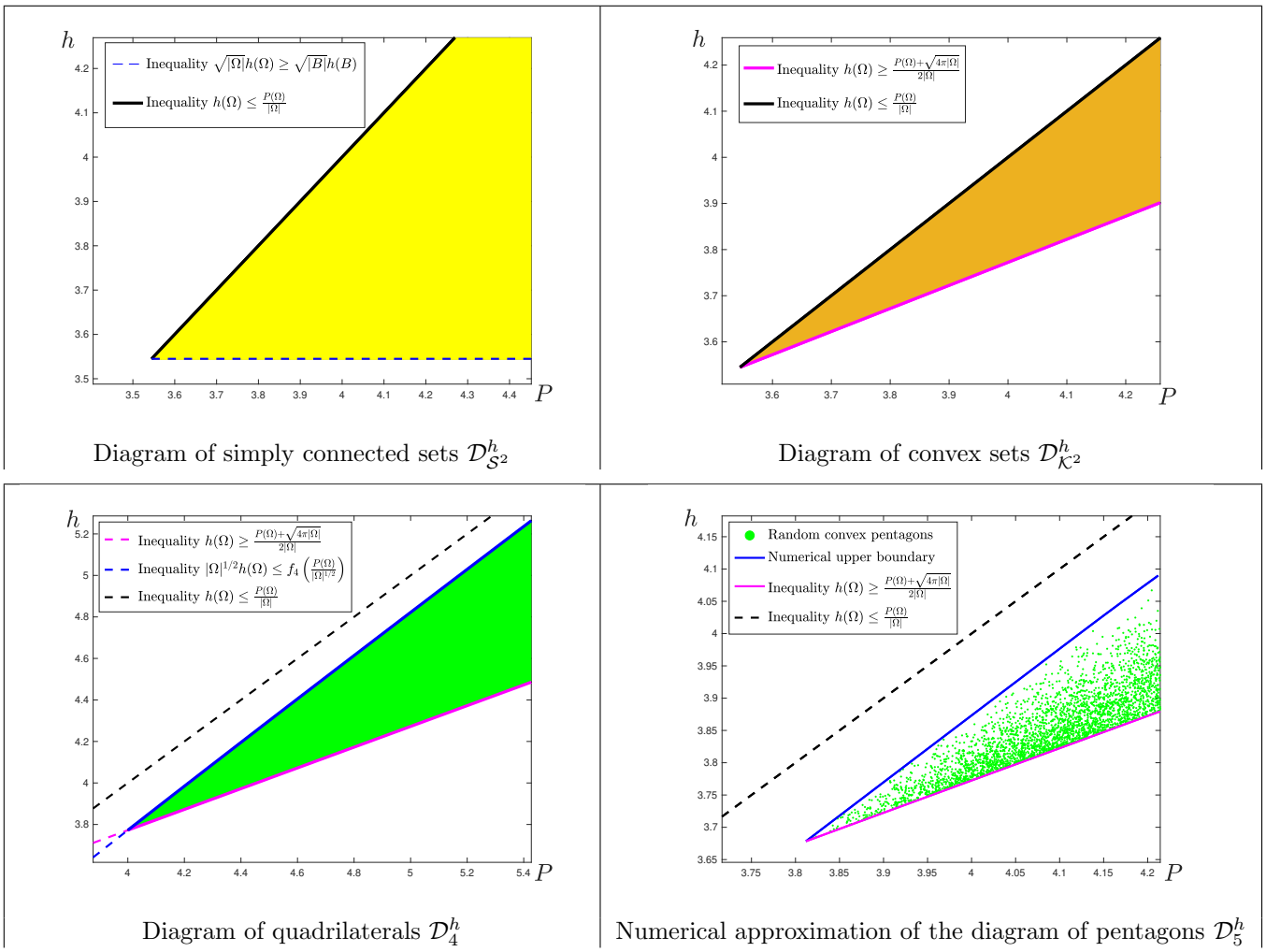

Figure 1.6: Illustrations of the diagrams studied in **Theorem of the Thesis 1**

Some comments on the results of Theorem of the Thesis 1

- In the first assertion of **Theorem of the Thesis 1**, we prove that inequalities (1.8) and (1.9) provide a complete system of inequalities for the class $\mathcal{S}^2$. Meanwhile, we show in the second assertion that this is no longer the case for convex sets for which inequalities (1.8) and the following new one:

$$\forall \Omega \in \mathcal{K}^2, \qquad h(\Omega) \geq \frac{P(\Omega) + \sqrt{4\pi|\Omega|}}{2|\Omega|}, \tag{1.24}$$

  are shown to realise a complete system of inequalities. We note (as explained in Chapter 2 (see Section 2.3.1) and also in [50, Remark 32]) that inequality (1.24) was already known for Cheeger regular polygons (those whose all sides touch their Cheeger set), but as far as we know the result was not known for arbitrary planar convex sets (neither general convex polygons).

- We note that in the proof of the case of simply connected sets relies on the characterization of the diagram of convex sets given in the second assertion, but we chose to present the result in this order for a more coherent presentation.

- In the case of convex polygons, we prove and use an improved version of inequality (1.8) in the class $\mathcal{P}_N$:

$$\forall \Omega \in \mathcal{P}_N, \qquad h(\Omega) \leq \frac{P(\Omega) + \sqrt{P(\Omega)^2 + 4\big(\pi - N\tan\frac{\pi}{N}\big)|\Omega|}}{2|\Omega|}, \tag{1.25}$$

  which, in addition to (1.24), provide a complete system of inequalities for the class $\mathcal{P}_N$ only when $N \geq 4$ is even. Indeed, when N is odd, we prove that the curve

$$\left\{(x,y) \mid x \geq P(R_N) \text{ and } y = \frac{x + \sqrt{x^2 + 4(\pi - N\tan\frac{\pi}{N})}}{2}\right\},$$

  which corresponds to inequality (1.25), does not match with the upper boundary of the diagram $\mathcal{D}_N$.

- As it is explained in the sketches of proofs, the method used to treat the cases of convex sets (diagram $\mathcal{D}^h_{\mathcal{S}^2}$) and convex N-gons (diagrams $\mathcal{D}_N$), when N is even, tightly relies on the fact that we are able (in the present cases) to find explicit extremal domains (that corresponds to the points on the boundary). Unfortunately, when $N \geq 5$ is odd, the problem of finding the upper domains seems to be very challenging as we do not have uniqueness of the solutions and we do not dispose of an explicit formula of the Cheeger constant when the polygons are not Cheeger regular: we note that numerical simulations suggest that for higher values of p_0, solutions of problems

$$\max\{h(\Omega) \mid \Omega \in \mathcal{P}_N, \quad P(\Omega) = p_0 \quad \text{and} \quad |\Omega| = 1\}$$

  are not Cheeger regular.

Sketches of proofs and methods

As stated in the comments above, the proof of the first assertion relies on the second one, we then begin by giving the elements of proof for the class of convex sets then we explain how to solve the case of simply connected sets, the case of convex polygons is developed in the last part.

The second assertion: the case of convex sets

We first give the sketch of proof of inequality (1.24), then we present the strategy used to give the description of $\mathcal{D}^h_{\mathcal{K}^2}$.

Sketch of proof of inequality (1.24):

The proof is done in three steps:

1. As mentioned in [50, Remark 32], in the case of Cheeger regular polygons (those whose all sides touch their Cheeger set), the inequality is a direct consequence of the explicit formula of the Cheeger constant given in [122] and the isoperimetric inequality on polygons (see [147] for example).

2. For general polygons, we prove that if a polygon Ω is not Cheeger regular, one can judiciously move its sides in such a way to obtain a Cheeger regular polygon $\tilde{\Omega}$ satisfying

$$h(\Omega) = h(\tilde{\Omega}), \quad P(\tilde{\Omega}) \geq P(\Omega) \quad \text{and} \quad |\Omega| \leq |\tilde{\Omega}|.$$

   We then conclude as follows:

$$h(\Omega) = h\big(\tilde{\Omega}\big) \geq \frac{P\left(\tilde{\Omega}\right) + \sqrt{4\pi\left|\tilde{\Omega}\right|}}{2\left|\tilde{\Omega}\right|} = \frac{P\big(\tilde{\Omega}\big)}{2\left|\tilde{\Omega}\right|} + \frac{\pi}{\sqrt{\left|\tilde{\Omega}\right|}} \geq \frac{P(\Omega)}{2|\Omega|} + \frac{\pi}{\sqrt{|\Omega|}} = \frac{P(\Omega) + \sqrt{4\pi|\Omega|}}{2|\Omega|}.$$

3. Once proven for polygons, one easily extend inequality (1.24) to arbitrary convex sets by density of polygons in the class of convex sets and continuity of the involved functionals functionals for Hausdorff distance.

Characterization of the diagram $\mathcal{D}^h_{\mathcal{K}^2}$:

The proof is done in 3 steps schematized in Figure 1.8:

- **Step 1:** By inequalities (1.24) and $h(\Omega) \leq \frac{P(\Omega)}{|\Omega|}$, we have the following inclusion:

$$\mathcal{D}^h_{\mathcal{K}^2} \subset \left\{ (x,y) \ \mid \ x \geq P(B) \quad \text{and} \quad \frac{1}{2}x + \sqrt{\pi} \leq y \leq x \right\}.$$

- **Step 2:** We then prove that the half lines $\{(x,x) \mid x \geq P(B)\}$ and $\{(x, x/2 + \sqrt{\pi}) \mid x \geq P(B)\}$ are included in the diagram $\mathcal{D}^h_{\mathcal{K}^2}$, as they respectively could be filled by continuous families of stadiums and tear shaped sets that are domains given by convex hulls of the ball B and a point outside it which continuously moves away from it, see Figure 1.7.

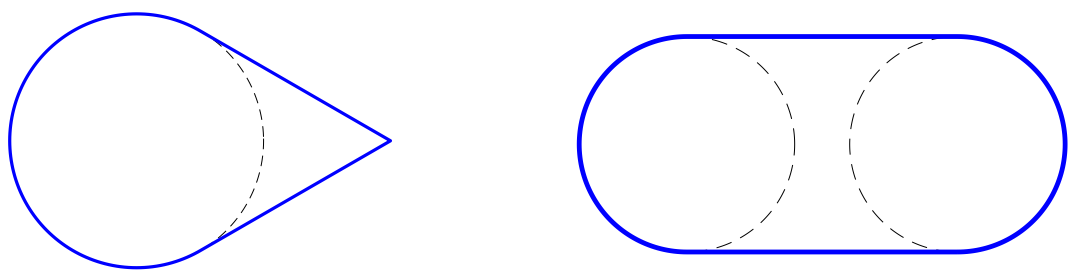

Figure 1.7: Tear shaped domain and stadium.

- **Step 3:** The last step is to fill the diagram. We want to do as for the diagram of $(P, r, |\cdot|)$ developed in Section 1.3.1, by introducing continuous paths (defined via Minkowski sums) that connect the upper boundary to the lower one. Unfortunately, in our case the paths are not given by straight lines and we do not have explicit description of them, but we do know that the domains in the extremities of those paths continuously vary, this allows to show a certain "uniform continuity" of the paths which permits to use the continuity of the index (winding number) of closed curves to show that we fill the whole zone located between the upper and lower boundaries.

The first assertion: the case of simply connected sets

We denote

$$\mathcal{D}' := \{(P(B), P(B))\} \cup \{(x,y) \mid x \geq P(B) \text{ and } P(B) < y \leq x\}.$$

We want to prove that $\mathcal{D}^h_{\mathcal{K}^2} = \mathcal{D}'$. By using inequalities (1.8) and (1.9) and the fact that $\mathcal{K}^2 \subset \mathcal{S}^2$, we have the following inclusions:

$$\mathcal{D}^h_{\mathcal{K}^2} \subset \mathcal{D}^h_{\mathcal{S}^2} \subset \mathcal{D}'.$$

It remains to prove the inclusion $\mathcal{D}' \backslash \mathcal{D}^h_{\mathcal{K}^2} \subset \mathcal{D}^h_{\mathcal{S}^2}$, which means to prove that for every $(x,y) \in \mathcal{D}' \backslash \mathcal{D}^h_{\mathcal{K}^2}$, we are able to find $\Omega \in \mathcal{S}^2$ of unit area such that $x = P(\Omega)$ and $y = h(\Omega)$. This is done by considering a "tailed" version L' (see Figure 1.9) of the tear shaped set L of unit area that corresponds to the point $(2(y - \sqrt{\pi}), y)$ (which lays on the lower boundary of $\mathcal{D}^h_{\mathcal{K}^2}$). Indeed, for such domains the Cheeger constant is constant while the perimeter continuously grows to infinity as the tail is elongated.

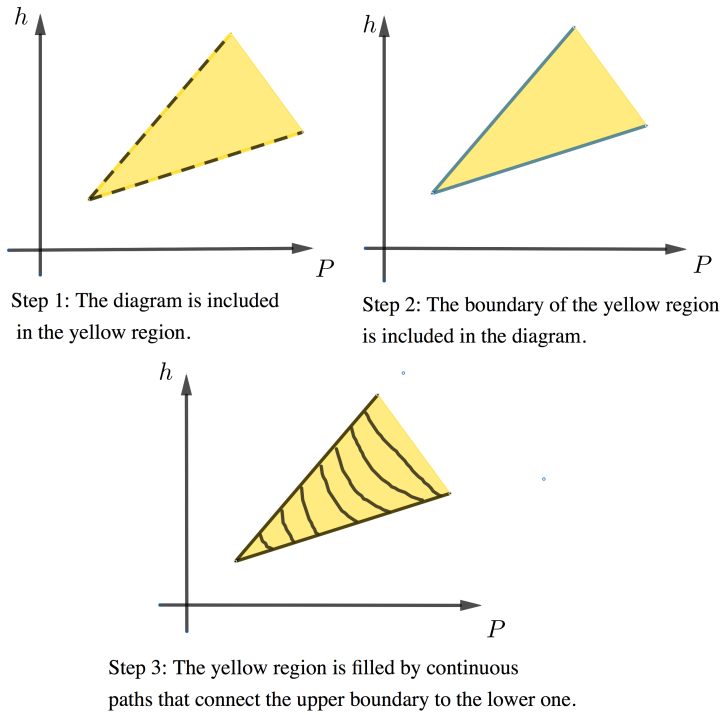

Figure 1.8: Illustration of the steps of proof in the convex case.

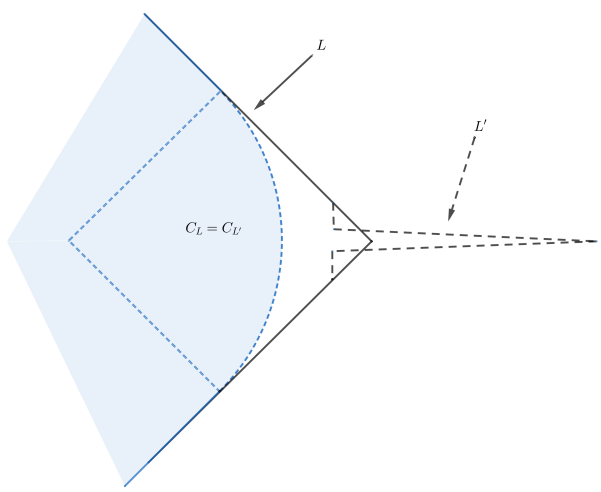

Figure 1.9: Tailed domain.

The third assertion: the case of convex polygons

The case $N = 3$ follows from the fact that if Ω is a triangle, then: $h(\Omega) = \frac{P(\Omega)+\sqrt{4\pi|\Omega|}}{2|\Omega|}$.

From now on we take $N \geq 4$. We first give the sketch of proof of inequality (1.25) which improves inequality $h(\Omega) \leq \frac{P(\Omega)}{|\Omega|}$ for convex N-gons, then present the ideas of demonstrations of the stated results on the diagrams $\mathcal{D}_N$.

Sketch of proof of inequality (1.25):

The proof is done in two steps:

1. first, we recall (see [122, Proposition 4]) that if a polygon Ω is Cheeger regular, then its Cheeger constant is given by
$$h(\Omega) = \frac{P(\Omega) + \sqrt{P(\Omega)^2 - 4\big(T(\Omega) - \pi\big)|\Omega|}}{2|\Omega|},$$
where $T(\Omega) := \sum_i \frac{1}{\tan\frac{\alpha_i}{2}}$ and α_i are the inner angles of the polygon Ω.

   It is natural to wonder about what happens if we drop the assumption of Cheeger regularity: we are able to prove that in this case one has only an inequality:
$$h(\Omega) \leq \frac{P(\Omega) + \sqrt{P(\Omega)^2 - 4\big(T(\Omega) - \pi\big)|\Omega|}}{2|\Omega|}, \tag{1.26}$$
with equality if and only if Ω is Cheeger regular. The proof is based on a nice idea consisting of using an estimate of the areas of the inner sets $\Omega_{-t} := \{x \in \Omega \mid d(x, \partial\Omega) > t\}$ to have an upper or lower bound of the Cheeger constant $h(\Omega)$ which is the inverse of the solution of the equation $|\Omega_{-t}| = \pi t^2$ on the interval $\big[0, r(\Omega)\big)$.

2. Then we conclude by using the following inequality which holds for convex N-gons:
$$N \tan\frac{\pi}{N} \leq T(\Omega),$$
where equality occurs if and only if the polygon Ω has N sides and its angles are equal.

When N is even:

In this case, we are able to find continuous families of N-gons that fill the upper and lower boundaries of $\mathcal{D}_N$ (respectively corresponding to the curves $\{\big(x, f_N(x)\big) \mid x \geq P(R_N)\}$ and $\{(x, x/2 + \sqrt{\pi}) \mid x \geq P(R_N)\}$). We then fill the diagram as for the case of convex sets by constructing continuous paths connecting the upper domains to the lower ones. We should note that one could no longer use Minkowski sums as they increase the number of sides, we construct the continuous paths by moving the vertices.

When N in odd:

The techniques used to prove that the upper bound is given by the curve of a continuous and strictly increasing function are quite similar to those used in the study of the boundary of the diagram $\mathcal{D}^{\lambda_1}_{\mathcal{K}^2}$, we then refer to Section 1.4.2 for more details and to Chapter 2 for the proofs.

1.4.2 Contributions of Chapter 2: Blaschke-Santaló diagram for volume, perimeter and first Dirichlet eigenvalue

As explained in Paragraph 1.3.1, we are interested in describing all possible inequalities relating the perimeter, the area and the first Dirichlet eigenvalue for the class of open subsets of $\mathbb{R}^n$, where $n \geq 2$, and the class of planar convex sets. This leads to the study of the following Blaschke-Santaló diagrams:

$$\mathcal{D}^{\lambda_1}_{\mathcal{O}^n} := \big\{\big(P(\Omega), \lambda_1(\Omega)\big) \mid \Omega \in \mathcal{O}^n \text{ and } |\Omega| = 1\big\} \quad \text{and} \quad \mathcal{D}^{\lambda_1}_{\mathcal{K}^2} := \big\{\big(P(\Omega), h(\Omega)\big) \mid \Omega \in \mathcal{K}^2 \text{ and } |\Omega| = 1\big\}$$

In **Theorem of the Thesis 2**, we give a complete description of the diagram for open sets in any dimension, and provide an advanced description in the case of planar convex sets.

Let us note that in the planar convex case, contrary to the triplet $(P, h, |\cdot|)$ treated in Chapter 2, we do not expect to give a complete description of the extremal domains (those laying on the boundary):

indeed, by numerical simulations we conjecture that the regular polygons are located on the lower boundary of the diagram. We show in Chapter 3 (see the discussion of the Conjecture 4 of Chapter 3) that the latter assertion is stronger (in the case of convex polygons) than a famous and open Conjecture due to Polya which states that the regular polygon minimizes the first Dirichlet eigenvalue between polygons with given measure and number of sides. Thus, the latter strategy of using the extremal domains to construct continuous paths that connect the upper and lower boundaries cannot be used. Fortunately, we managed to give a quite advanced description of the diagram and its boundary by only using few information on the involved functionals. We also note that the methods developed in this framework could be applied for other functionals and thus allow to give similar qualitative results for other diagrams (see Chapter 5).

Theorem of the Thesis 2. $(P, \lambda_1, |\cdot|)$***-diagrams.***

1. *Let $\mathcal{O}^n$ be the class of C^∞ open sets in $\mathbb{R}^n$, with $n \geq 2$, we have:*

$$\mathcal{D}^{\lambda_1}_{\mathcal{O}^n} = \Big(\big(P(B), +\infty\big) \times \big(\lambda_1(B), +\infty\big)\Big) \cup \big\{\big(P(B), \lambda_1(B)\big)\big\}$$

where B is a ball of volume 1. This shows that in the case of C^∞ open sets, the only inequalities relating the three quantities P, λ_1 and $|\cdot|$ are the isoperimetric $\frac{P(\Omega)}{|\Omega|^{\frac{n-1}{n}}} \geq \frac{P(B)}{|B|^{\frac{n-1}{n}}}$ and Faber-Krahn's $|\Omega|^{n/2}\lambda_1(\Omega) \geq |B|^{n/2}\lambda_1(B)$ inequalities.

2. *As for planar convex sets, we show that there exist two functions $f : [x_0, +\infty) \to \mathbb{R}$ and $g : [x_0, +\infty) \to \mathbb{R}$ (where $x_0 := P(B)$), such that*

   (a) *the diagram $\mathcal{D}^{\lambda_1}_{\mathcal{K}^2}$ is made of all points in $\mathbb{R}^2$ lying between the graphs of f and g, more precisely:*

$$\mathcal{D}^{\lambda_1}_{\mathcal{K}^2} = \Big\{(x, y) \in \mathbb{R}^2,\ x \geq x_0 \quad \text{and} \quad f(x) \leq y \leq g(x)\Big\}, \tag{1.27}$$

   (b) *functions f and g are continuous and strictly increasing, this, combined with the (3.3) imply that the diagram $\mathcal{D}^{\lambda_1}_{\mathcal{K}^2}$ is horizontally and vertically convex.*

   (c) *For every $x > x_0$, let $\Omega \in \mathcal{K}^2$ such that $|\Omega| = 1$ and $\lambda_1(\Omega) = x$, then*
   - *if $P(\Omega) = g(x)$, then Ω is $C^{1,1}$,*
   - *if $P(\Omega) = f(x)$, then Ω is a polygon.*

   (d) $f'(x_0) = 0$ *and* $\limsup_{x \to x_0} \frac{g(x) - g(x_0)}{x - x_0} \geq \frac{\lambda_1(B)}{3\sqrt{\pi}} \left(\frac{\lambda_1(B)}{\pi} - 2\right)$.

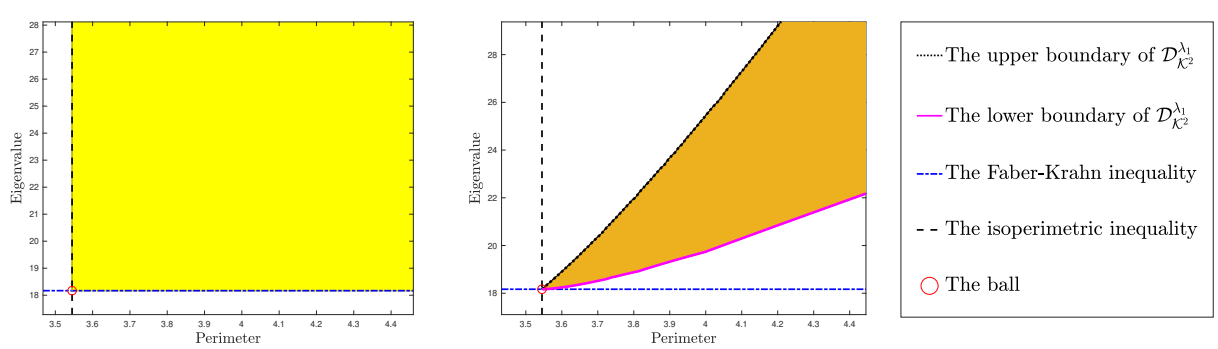

Figure 1.10: The diagram of open sets on the left and the diagram of convex sets on the right.

Sketches of proofs and methods

Let us now give the sketches of proofs of the two cases treated in **Theorem of the Thesis 1**.

1. It is easy to see that the diagram is included in the quadrant $[P(B), +\infty) \times [\lambda_1(B), +\infty)$ as it is a direct consequence of the isoperimetric and Faber-Krahn inequalities:

$$P(\Omega) \geq P(B) \quad \text{and} \quad \lambda_1(\Omega) \geq \lambda_1(B),$$

   where Ω is a smooth subset of $\mathbb{R}^n$ with unit volume.

   Now, we want to fill the quadrant, which means showing that for any $(x_0, y_0) \in (P(B), +\infty) \times (\lambda_1(B), +\infty)$, one is able to construct an open smooth set Ω of unit volume such that $P(\Omega) = x_0$ and $\lambda_1(\Omega) = y_0$. Heuristically, filling the upper part of the quadrant means to increase the eigenvalue of a set while controlling its perimeter, to do so we use perforated domains and classical results on homogenization (see [58]). As for the lower part of the diagram, the idea this time is to use sets given as union of a domain and a cylinder of high perimeter, by this process we keep the eigenvalue constant while increasing the perimeter.

2. The description of the diagram is done in 3 steps: first, we focus on the study of its boundary and prove that it is given by the union of the curves of two strictly increasing functions. Then, we show that the diagram contains no holes and thus exactly corresponds to the set of points located between the two curves. Finally, some information on the slopes near the vertex corresponding to the ball are given in addition to some asymptotics of the infinite branches of the boundary.

   1) Study of the boundary of the diagram

   We define the functions f and g as follows:

$$\begin{array}{rccl} f: & [P(B), +\infty) & \longrightarrow & \mathbb{R} \\ & p & \longmapsto & \min\left\{\lambda_1(\Omega), \Omega \in \mathcal{K}^2, |\Omega| = 1 \text{ and } P(\Omega) = p\right\}, \end{array}$$

$$\begin{array}{rccl} g: & [P(B), +\infty) & \longrightarrow & \mathbb{R} \\ & p & \longmapsto & \max\left\{\lambda_1(\Omega),\ \Omega \in \mathcal{K}^2, |\Omega| = 1 \text{ and } P(\Omega) = p\right\}, \end{array}$$

   where B is a ball of unit volume.

   - Continuity of the functions f and g:
     Since f and g are defined as infimum and supremum, a natural strategy to prove their continuity is to show inequalities on their inferior and superior limits. To do so we had to prove a certain perturbation lemma for the perimeter of convex sets: we show that one can continuously deform a planar convex set so as to **strictly** increase or decrease (when different from the ball) its perimeter while preserving the area and the convexity. The lemma is stated as follows:

     Lemma 1. *(Perturbation Lemma for the perimeter)*
     We recall that $\mathcal{K}_1^2 := \{\Omega \in \mathcal{K}^2 |\ |\Omega| = 1\}$, we have:
     1. The ball is the only local minimizer of the perimeter in the class $\mathcal{K}_1^2$ for the Hausdorff distance.
     2. There is no local maximizer of the perimeter in the class $\mathcal{K}_1^2$ for the Hausdorff distance.

     If decreasing the perimeter can be easily done by continuous Steiner symmetrization which preserves the volume and the convexity in any dimension, this is unfortunately not the case when trying to increase the perimeter where it seems difficult to preserve the convexity especially in higher dimensions: this is why the perturbation Lemma is only stated for planar sets as it relies on results of [132] which are up to our knowledge only known for the planar case.

- Monotonicity of the functions f and g

  As for the monotonicty of the functions, we argue by contradiction by assuming that the function f (resp. g) is not strictly increasing, this yields in particular to the existence of a convex set of unit area denoted Ω_f (resp. Ω_g) (different from the ball) that is a local minimizer (resp. maximizer) of λ_1 under area and convexity constraints, then we use the following perturbation lemma for the first Dirichlet eigenvalue λ_1 to find a contradiction, see Figure 1.11.

  Lemma 2. *(Perturbation Lemma for λ_1)*
  We recall that $\mathcal{K}_1^2 := \{\Omega \in \mathcal{K}^2 |\ |\Omega| = 1\}$, we have:
  1. The ball is the only local minimizer of λ_1 in the class $\mathcal{K}_1^2$ for the Hausdorff distance.
  2. A $C^{1,1}$ convex domain cannot be a local maximizer of λ_1 in $\mathcal{K}_1^2$ for the Hausdorff distance.

  As for the perimeter, decreasing λ_1 could be easily done by continuous Steiner symmetrization but increasing it under convexity and volume constraints is a rather challenging task: to do so we use an upcoming result of J. Lamboley and A. Novruzi [130] that states that in the planar case, a local maximizer of λ_1 under convexity and area constraints is a polygon and thus cannot be $C^{1,1}$, it will then remain to prove that there exists Ω_g which is $C^{1,1}$ and corresponds to a local maximum of the function g: this is done by remarking that one can choose to work with a domain Ω_g which is a solution of a certain minimization problem:

  $$\min\{P(\Omega) \mid \Omega \in \mathcal{K}^2,\ |\Omega| = 1 \text{ and } \lambda_1(\Omega) = \lambda^*\},$$

  where $\lambda^* > \lambda_1(B)$, see Figure 1.11. We then want to apply the result of [134, Theorem 2.6] with the constraint $m : \Omega \longmapsto \big(|\Omega|, \lambda_1(\Omega)\big)$, to do so one have first to check that the first order shape derivatives of the constraints are linearly independent; we are then tempted to use the classical Serrin's Theorem [166], but this is unfortunately not possible since we do not have any regularity as the sets are only assumed to be convex. We then extend Serrin's result [166] to convex sets (in arbitrary dimensions):

  Lemma 3. *Let Ω be an open and bounded convex set in $\mathbb{R}^n$ ($n \geq 2$), and u a first eigenfunction of the Dirichlet-Laplacian in Ω. We also assume that there exists constant $c \geq 0$ such that*

  $$|\nabla u| = c \qquad \text{on } \partial\Omega.$$

  Then Ω is a ball and $c > 0$.

  This result is interesting for itself and is obtained by adapting the regularity theory of free boundaries problems by taking advantage of the convexity of Ω.

2) The diagram contains no holes

Once we proved that the diagram is contained between the curves of two continuous functions (which are also included in the diagram), it remains to prove that we can fill all the points between the latter curves. As explained in Chapter 3, the explicit description of the extremal sets seems to be difficult and challenging (we refer to the discussion of Conjecture 4 of Chapter 3), thus we cannot use similar strategy as for the diagram $(P, h, |\cdot|)$, this is why we propose an approach based only on the construction of relevant continuous paths included in the diagram via Minkowski sums, the perturbation results of the perimeter of convex sets and Blaschke's selection Theorem [164, Theorem 1.8.6].

The proof is done by contradiction: by assuming that there exists a point $A(x_A, y_A) \in \{(x, y) \mid x > P(B) \text{ and } f(x) < y < g(x)\}$ which is not included in the diagram. The idea of is to study the "position" of the curves (obtained by Minkowski sums) relating domains (of unit area) having the same perimeter $p \in [P(B), +\infty)$: when p is close to x_A we are able to prove that there exist curves which are located "on the left of A" (the notion of being on the left or the right of the point A is rigorously defined in Chapter 3 via the index, also called winding number, of a closed

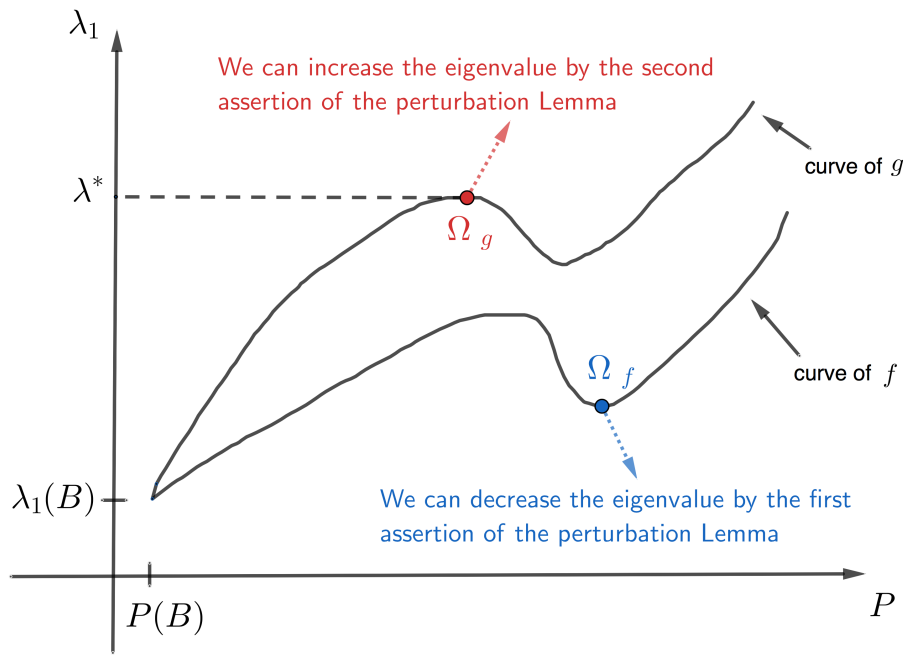

Figure 1.11: Using the perturbation Lemma 2 to prove the monotonicity of f and g.

curve around a point), meanwhile for sufficiently higher values of p we show that <u>all</u> the curves are this time "on the right of A". We then introduce the value p_0 such that:

(a) for every $p < p_0$, <u>there exists</u> a couple convex sets of unit area and of perimeter p who are related by a continuous path which is located "on the left of A".

(b) For every $p > p_0$, <u>all</u> couples of convex sets of unit area and perimeter p are related by continuous paths which are located "on the right of A".

We then analyse two case: if p_0 corresponds to the **case (a)** or to the **case (b)**. By using continuity properties of the index, the perturbation Lemma for the perimeter of planar convex sets and the Blaschke selection Theorem (see [164]), we are able to prove that both cases are impossible, which provides the desired contradiction.

<u>3) Study of the slopes of the boundary at the vertex corresponding to the ball</u>

Since the ball is a critical point for the perimeter and Dirichlet eigenvalue under volume constraint, the study of the slopes of the diagram near the vertex $(P(B), \lambda_1(B))$ involves second order shape derivatives. In Section 3.3.3, we study (for arbitrary dimensions) some stability results and quantitative (Faber-Krahn and isoperimetric) inequalities that are then applied to develop a better understanding of the asymptotics of the boundary of the diagram in the neighborhood of the vertex $(P(B), \lambda_1(B))$.

If the theoretical study (done in arbitrary dimensions) of Section 3.3.3 (see also [145, 64]) supports that the upper boundary (the curve of g) admits an oblique tangent at $(P(B), \lambda_1(B))$ which is equivalent to the existence of a constant b_n (depending only on the dimension n and for which we are able to give a lower estimate, see Corollary 5) such that

$$g(x) - g(x_0) \underset{x \to x_0}{\sim} b_n \times (x - x_0),$$

where we recall that $x_0 := P(B)$ where $B \subset \mathbb{R}^n$ is a ball of unit volume, the behaviour of the lower boundary (the curve of f) is much interesting to study as it is tightly related to new quantitative Faber-Krahn's inequalities. Our theoretical study supports the following conjecture:

Conjecture 1. *There exist $c_n, h_n > 0$ depending only on the dimension n such that for every $\forall \Omega \in \mathcal{K}^n$ close to B in the sense that $d^H(\Omega, B) \leq h_n$, we have:*

$$|\Omega|^{2/n}\lambda_1(\Omega) - |B|^{2/n}\lambda_1(B) \geq c_n \left(\frac{P(\Omega)}{|\Omega|^{1-\frac{1}{n}}} - \frac{P(B)}{|B|^{1-\frac{1}{n}}} \right)^{\frac{3}{2}}. \tag{1.28}$$

Let us give some comments:

- The exponent 3/2 may seem unexpected in first sight as it mainly appears because of the convexity assumption. Indeed, inequalities of the type:

$$|\Omega|^{2/n}\lambda_1(\Omega) - |B|^{2/n}\lambda_1(B) \geq c_n \left(\frac{P(\Omega)}{|\Omega|^{1-\frac{1}{n}}} - \frac{P(B)}{|B|^{1-\frac{1}{n}}} \right)^{\alpha},$$

  where α is a positive constant, fails for general open sets.
- Conjecture 1 is tightly related to the asymptotic study of the lower boundary (that corresponds to the curve of the function f) in the neighborhood of the vertex $\big(P(B), \lambda_1(B)\big) = \big(x_0, \lambda_1(B)\big)$ as it implies the following result:

$$\forall x \in [x_0, x_0 + h), \qquad f(x) - f(x_0) \geq c_n (x - x_0)^{\frac{3}{2}}.$$

- Theoretical and numerical evidences support the fact the exponent 3/2 is optimal. We note that it is retrieved in the planar case by two different ways (by studying exponents α such that the ball B is a local minimizer for the functional $\lambda_1 - \big(P - P(B)\big)^{\alpha}$, see Theorem 14 and by studying the regular polygons which numerically seem to be on the lower boundary, see Proposition 8).
- We should finally note that one could use the quantitative inequalities of [102] to obtain quit similar estimates as (1.28) but with non-optimal exponents (larger than the expected 3/2).

1.4.3 Contributions of Chapter 4: On the Cheeger inequality for convex sets

Main results

Now that we introduced the Cheeger inequality and E. Parini's results for the case of convex planar sets, let us describe the contributions of the present thesis and give some comments on the proofs. As one sees in Questions 7, there are two directions we want to explore: the first one is to improve the lower bound $\frac{\pi^2}{16} \approx 0.616...$ (which we recall to be significantly lower than the conjectured one given by $\frac{2\pi^2}{(2+\sqrt{\pi})^2} \approx 1.383...$), the second one is to generalize and develop a better understanding of the problem in higher dimensions.

In the following Theorem, we improve the lower bound $\frac{\pi^2}{16}$:

Theorem of the Thesis 3. *We have:*

$$\forall \Omega \in \mathcal{K}^2, \qquad J_2(\Omega) := \frac{\lambda_1(\Omega)}{h(\Omega)^2} \geq \left(\frac{\pi j_{01}}{2j_{01} + \pi} \right)^2 \approx 0.902...$$

where j_{01} denotes the first zero of the first Bessel function.

The proof uses a new sharp upper bound of the Cheeger constant via the inradius and the area in the case of planar convex sets which was found while working on the Blaschke-Santaló diagram relating the latter quantities. The results are stated as follows:

Theorem of the Thesis 4. *We have:*

$$\forall \Omega \in \mathcal{K}^2, \qquad \frac{1}{r(\Omega)} + \frac{\pi r(\Omega)}{|\Omega|} \leq h(\Omega) \leq \frac{1}{r(\Omega)} + \sqrt{\frac{\pi}{|\Omega|}}, \tag{1.29}$$

where $r(\Omega)$ denotes the inradius of Ω. These inequalities are sharp as equalities are obtained for stadiums in the lower estimate and for domains that are homothetical to their form bodies in the upper one.
Moreover, we have the following explicit description of the Blaschke-Santaló diagram:

$$\left\{ \left(\frac{1}{r(\Omega)}, h(\Omega) \right) \mid \Omega \in \mathcal{K}^2 \text{ and } |\Omega| = 1 \right\} = \left\{ (x, y) \;\middle|\; x \geq \frac{1}{r(B)} = \sqrt{\pi} \text{ and } x + \frac{\pi}{x} \leq y \leq x + \sqrt{\pi} \right\},$$

where $B \subset \mathbb{R}^2$ is a ball of unit area.

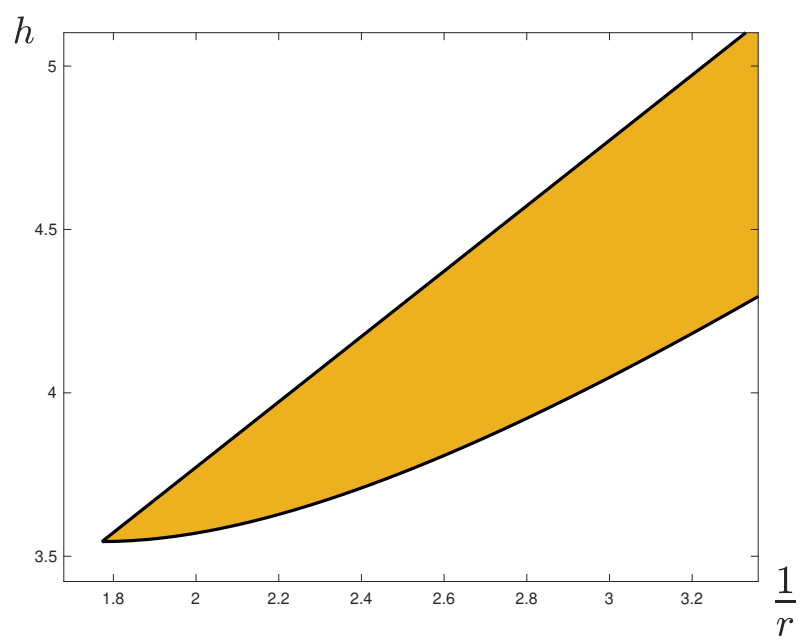

Figure 1.12: The diagram of the triplet $(r, h, |\cdot|)$.

At last, we provide an existence theorem of optimal shape that minimizes the functional $J_n : \Omega \longmapsto \frac{\lambda_1(\Omega)}{h(\Omega)^2}$ in the class $\mathcal{K}^n$ of convex shapes.

Theorem of the Thesis 5. *Let us define the real sequence $(\beta_n)_n$ as follows:*

$$\forall n \in \mathbb{N}^*, \qquad \beta_n := \inf_{\Omega \in \mathcal{K}^n} J_n(\Omega),$$

where $J_n : \Omega \in \mathcal{K}^n \longmapsto \frac{\lambda_1(\Omega)}{h(\Omega)^2}$. We have:

1. *$(\beta_n)_n$ is a decreasing sequence.*
2. *$\lim\limits_{n \to +\infty} \beta_n = \frac{1}{4}$.*
3. *For $n \geq 2$, if the <u>strict</u> inequality $\beta_n < \beta_{n-1}$ holds, we have the following existence result:*

$$\exists \Omega_n^* \in \mathcal{K}^n, \quad J_n(\Omega_n^*) = \inf_{\Omega \in \mathcal{K}^n} J_n(\Omega).$$

Some comments on the results of Theorems of the Thesis 3, 4 & 5

Before presenting the sketches of proofs, let us give some relevant comments on the latter results:

- In **Theorem of the Thesis 3** we obtain an improved lower bound of the functional $J_2 : \Omega \longmapsto \frac{\lambda_1(\Omega)}{h(\Omega)^2}$ for planar convex sets, we note that this result is improved for special classes of convex sets namely triangles, rhombi and stadiums, see Proposition 9.
- In **Theorem of the Thesis 4**, the choice of working with $\frac{1}{r}$ instead of the inradius is purely esthetical: indeed, in this setting the upper boundary of the corresponding Blaschke-Santaló diagram is given by the curves of the linear function $x \longmapsto x + \sqrt{\pi}$, meanwhile, the lower boundary is given by the curve of a continuous and strictly increasing function. This, in our humble opinion, makes the diagram more easy to read.
- It is interesting to note that by combining the upper bound of inequality (1.29) with the reverse Cheeger inequality [152]:

$$\forall \Omega \in \mathcal{K}^2, \quad J_2(\Omega) = \frac{\lambda_1(\Omega)}{h(\Omega)^2} < \frac{\pi^2}{4},$$

  we obtain a new sharp upper bound of the first Dirichlet eigenvalue of planar convex set Ω:

$$\Omega \in \mathcal{K}^2, \quad \lambda(\Omega) \leq \frac{\pi^2}{4} \left(\frac{1}{r(\Omega)} + \sqrt{\frac{\pi}{|\Omega|}} \right)^2,$$

  where equality asymptotically holds for any family of thin collapsing domains, see Prposition 10 of Chapter 4. This inequality, is often better than the one obtained by using the inclusion $B_{r(\Omega)} \subset \Omega$ (where $B_{r(\Omega)}$ is a ball of radius $r(\Omega)$ included in Ω) and the monotonicity of λ_1:

$$\lambda_1(\Omega) \leq \lambda_1\big(B_{r(\Omega)}\big) = \frac{j_{01}^2}{r(\Omega)^2},$$

  where equality holds when Ω is a ball.
- The convergence result $\lim\limits_{n \to +\infty} \beta_n = \frac{1}{4}$ of **Theorem of the Thesis 5** shows that the constant $\frac{1}{4}$ given in the original Cheeger inequality [55] is optimal in the sense that there exists no constant $C > \frac{1}{4}$ such that:

$$\forall n \geq 1, \forall \Omega \in \mathcal{K}^n, \quad \frac{\lambda_1(\Omega)}{h(\Omega)^2} \geq C.$$

- We believe that the assertion $\beta_n < \beta_{n-1}$ is true for any $n \geq 2$. This conjecture is motivated by the discussion of Section 4.4.2.

  In particular:

  - when $n = 2$, we have:
  $$\beta_2 < \frac{\pi^2}{4} = \beta_1,$$
  thus we retrieve Parini's result of existence in the class of planar sets without using the explicit formulae of Cheeger constants of planar convex sets.

  - When $n = 3$, it is interesting to note that if one manages to improve the lower bound of J_2 up to a certain value, this will imply the existence of the optimal shape in dimension 3. Indeed, by using the explicit value of the Cheeger constant of the tube $T = (0,1) \times D$ recently obtained in [29] (where $D \subset \mathbb{R}^2$ is disk of unit radius), we have:
  $$\beta_3 = \inf_{\Omega \in \mathcal{K}^3} J_3(\Omega) \leq J_3(T) = \frac{\lambda_1(T)}{h(T)^2} = \frac{\lambda_1(D) + \frac{\pi^2}{1^2}}{h(T)^2} < 1.043.$$
  Thus, if one manages to show the following estimate:
  $$\forall \Omega \in \mathcal{K}^2, \qquad J_2(\Omega) \geq 1.043,$$
  which is weaker than Parini's conjecture [152] (that states that the square minimizes J_2 among planar convex sets), he will be able to prove that $\beta_2 > 1.043 > \beta_3$ and thus apply the latter Theorem to prove the existence of an optimal shape in dimension 3.

  Unfortunately, even if the result of Theorem of the Thesis 3 provides a significant improvement of the lower bound $\frac{\pi^2}{16}$ of J_2 (given in [152]), it is still not sufficient to prove the assertion $\beta_3 < \beta_2$.

Sketches of proofs and methods

Since **Theorem of the Thesis 3** is a consequence of the upper bound of (1.29), we first discuss the ideas of proof of **Theorem of the Thesis 4**.

Theorem of the Thesis 4: study of the $(r, h, |\cdot|)-$diagram

Let us first give the sketches of proofs of inequalities (1.29):

- The lower estimate is a consequence of two arguments: the first is the classical Bonnesen's [35] inequality:
$$\forall \Omega \in \mathcal{K}^2, \qquad P(\Omega) \geq \pi r(\Omega) + \frac{|\Omega|}{r(\Omega)},$$
where equality occurs if Ω is a stadium, and the second is to remark that the set Ω and its Cheeger set have the same inradius.

- The upper estimate is more tricky as its demonstration is inspired from an idea of proof of inequality (1.26): since the Cheeger constant of a planar convex set Ω is given by the inverse of the solution of the equation
$$|\Omega_{-t}| = \pi t^2, \quad \text{for } t \in \big[0, r(\Omega)\big),$$
where $\Omega_{-t} := \{x \in \Omega \mid d(x, \partial\Omega) > t\}$ (called an inner set of Ω), if one can bound the area of the inner sets by a function $g : t \in \big[0, r(\Omega)\big) \longmapsto g(t)$, this will provide an estimation of the Cheeger constant $h(\Omega)$ via the first solution of the equation $g(t) = \pi t^2$ on the interval $\big[0, r(\Omega)\big)$.

In the present case we use a classical inequality found in [142, Theorem 2]:

$$\forall t \in \big(0, r(\Omega)\big), \qquad |\Omega_{-t}| \geq |\Omega| \left(1 - \frac{t}{r(\Omega)}\right)^2,$$

where equality holds if and only if Ω is homothetical to its form body[1].

The latter inequalities define the upper and lower boundaries and we are able (as it is the case for the diagram $(P, h, |\cdot|)$) to explicit two families of convex sets which are continuous for Hausdorff distance and that respectively fill the upper and lower boundaries of the diagram (stadiums for the lower boundary and symmetrical two cups for the upper one). Thus, by reproducing the same steps as in Chapter 2 (Section 1.4.1) we can fill all the region between these curves.

Theorem of the Thesis 3: improving the Cheeger inequality for planar convex sets

This Theorem is a consequence of the upper bound given in (1.29), Faber-Krahn's inequality [78, 126] $|\Omega|\lambda_1(\Omega) \geq |B|\lambda_1(B)$ (where $B \subset \mathbb{R}^2$ is a ball) and Hersch's inequality [115] $\lambda_1(\Omega) \geq \frac{\pi^2}{4r(\Omega)^2}$.

Theorem of the Thesis 5: on the existence of a minimizer in higher dimensions

Let us discuss the proofs of the 3 assertion of **Theorem of the Thesis 5**.

1. Let $n \geq 2$. In order to prove inequality $\beta_{n-1} \geq \beta_n$, we studied the Cheeger constant of cylinders of the form $\omega \times (0, d)$ when d tends to infinity, where $\Omega \in \mathcal{K}^{n-1}$. We are able to prove that:

$$\lim_{d \to +\infty} J_n\big(\omega \times (0, d)\big) = J_{n-1}(\omega),$$

and finally conclude as follows:

$$\beta_n = \inf_{\Omega \subset \mathcal{K}^n} J_n(\Omega) \leq \inf\{J_n\big(\omega \times (0, d)\big) \mid \omega \in \mathcal{K}^{n-1} \text{ and } d > 0\} \leq \inf_{\omega \subset \mathcal{K}^{n-1}} J_{n-1}(\omega) = \beta_{n-1}.$$

2. To compute the limit of (β_n), we use the explicit known values of the Cheeger constant and Dirichlet eigenvalue of balls $B_{\subset}\mathbb{R}^n$. We write:

$$\frac{1}{4} \leq \beta_n \leq J_n(B_n) = \frac{\lambda_1(B_n)}{h(B_n)^2} \underset{n \to +\infty}{\longrightarrow} \frac{1}{4}.$$

3. Let us finally give the idea of proof of the existence result. Let $n \geq 2$, we assume that $\beta_n < \beta_{n-1}$. We prove that if (Ω_k) is a minimizing sequence such that $|\Omega_k| = 1$ for every $k \in \mathbb{N}$, then the sequence $\big(d(\Omega_k)\big)$ of diameters is bounded. Indeed, if it was not the case (that is to say that $d(\Omega_k) \underset{k \to +\infty}{\longrightarrow} +\infty$ up to a subsequence), we prove that:

$$\liminf_{k \to +\infty} J_n(\Omega_k) \geq \underbrace{\beta_{n-1} > \beta_n.}_{\text{by the hypothesis of the Theorem.}}$$

We note that the proof of inequality $\liminf_{k \to +\infty} J_n(\Omega_k) \geq \beta_{n-1}$ follows from the use of relevant test sets in the variational characterization of the Cheeger constant (which provides a bound from above of the Cheeger constant) and a lower bound (found in the proof of [41, Lemma 6.11]) of λ_1 via the eigenvalue of $(n-1)$ dimensional sections.

[1] We refer to [136, Section 1.1] for the definition of form bodies and to [164] for more details.

1.4.4 Contributions of Chapter 5: Numerical study of convexity constraint and application to Blaschke-Santaló diagrams

In this section, we give a brief description of the methods used and the main results of Chapter 5.

Parametrizing the convexity constraint

One originality of the numerical study of the present thesis is that we do not limit ourselves to numerically find optimal shapes but present and discuss different (classical and original) parametrizations that allow to handle the convexity constraint. As expected, the efficiency of a method mainly depends on the regularity of the optimal shape. The results presented in Chapter 5 correspond to a work in progress: in a first time, we only perform qualitative comparison between the different methods, in the upcoming work [89] we will present a deeper analysis.

We briefly list and comment the 4 methods used in this thesis, for more details and definitions we refer to Chapter 5.

- Method 1: Approximating the support function by Fourier series

  This method is quite classical now. It was up to our knowledge used for the first time in [20] for purely geometrical functionals in the planar case and then successfully used by other authors for other problems (in dimension 3 and also for problems involving spectral quantities), see [20, 33, 15]. This method often allows to obtain good approximations of the optimal shapes (especially when it contains no flat parts because those ones correspond to Dirac measures in the radius of curvature which corresponds to sum of the support function and its second order derivative), allows to handle the convexity and diameter constraints quite easily (they are parametrized as linear constraints), but is not very adapted when the expected shape is polygonal.

- Method 2: Approximating the gauge function by Fourier series

  This method is quite similar to the last one, as the convexity constraint is handled in a similar way (linear constraints), it was already stated in [20, Remark 6.], but we did not find a work where it has been used. The advantage compared to the previous one is that it can easily detect flat parts (as they correspond this time to a null curvature, which is proportional to the sum of the gauge function and its second order derivative). As for disadvantages, this method is not suitable when the expected optimal shape has corners (as they correspond to Dirac measures in the curvature), which is of course the case for polygons and other relevant shapes as Reuleaux triangles. At last, this setting is not quite adapted to handle the the diameter constraint.

- Method 3: Using the radial function

  This method consists on assuming that the set contains the origin and using a polygonal approximation of its boundary, we then show that the convexity constraint can be parametrized in an elegant way (by means of quadratic inequalities): up to our knowledge this method is original. In addition to the easy formulation of the convexity constraint, this method allows to handle the diameter constraints and provides quite satisfying results (even when the optimal shapes are polygonal). Nevertheless, it is less suitable than the latter methods when the optimal shape is smooth: which is expected as here the sets are approached by polygons in contrary to before where the support and gauge functions are approached by truncated ones corresponding to smooth shapes. It may also be more time consuming.

- Method 4: Optimizing the coordinates of the vertices

  Here, the convexity constraint is equivalent to the condition that all the inner angles should be less than π, this also leads to quadratic inequalities on the coordinates of the vertices. This last method is quite efficient when the optimal shapes are polygons (with a reasonable number of sides), unfortunately, it fails when we consider a large number of vertices as the sides quickly overlap as soon as the process of optimization is launched.

Application to Blaschke-Santaló diagrams

The complete description of Blaschke-Santaló diagrams seems in general to be very challenging (if not to say impossible), especially when they involve spectral quantities. It is then natural to use numerical simulations in order to have an approximation of these diagrams and conjecture some of their properties and new inequalities.

One first idea is to randomly generate a large number of convex sets for which we compute the values of the functionals and then plot the obtained points. This was for example done in [11, 13] where the authors randomly generate polygons of at most 8 sides. In the present thesis we use an algorithm based on a work of P. Valtr [171] in order to generate convex polygons with large number of sides (we use polygons of at most 30 sides), we refer to [162] for a nice description and implementation of the latter algorithm. Although, considering polygons with large number of sides provides a slight improved versions of the diagrams, it is still not satisfying as it is quite difficult to describe the boundary (especially when the optimal sets are expected to be smooth).

The main novelty of the present thesis is that we combine the theoretical results of simple connectedness (more precisely vertical convexity) of the diagrams (see Theorem 23) with the numerical description of the boundary of the diagram, which is done by (numerically) solving some shape optimization problems under convexity constraint (similar to (1.4)) to provide a quite satisfying description of the diagrams and thus to state some interesting conjectures.

In this thesis, a special attention is given to the investigation of the relations between the first Dirichlet eigenvalue λ_1 (spectral functional), the perimeter P, the area $|\cdot|$ and the diameter d (geometrical functionals) of planar convex sets. This gives us 4 diagrams to study: $(P, \lambda_1, |\cdot|)$, $(d, \lambda_1, |\cdot|)$, (P, λ_1, d) and the purely geometrical $(P, d, |\cdot|)$-diagram. We also briefly discuss other diagrams involving other relevant functionals as the Cheeger constant and the inradius (for which we propose a quite efficient method of computation based on Matlab's toolbox "Clipper").

An example: $(P, \lambda_1, |\cdot|)$-Diagram

For a better understanding let us develop the example of triplet $(P, \lambda_1, |\cdot|)$ studied in Chapter 3: to describe the boundaries of the corresponding diagram we (numerically) solve the following problems:

$$\min / \max\{\lambda_1(\Omega) \mid \Omega \in \mathcal{K}^2 \;\; P(\Omega) = p_0 \;\text{ and }\; |\Omega| = 1\},$$

where $p_0 \geq P(B) = 2\sqrt{\pi}$. As shown in **Theorem of the Thesis 2**, the upper domains (solutions of the maximization problem) are smooth ($C^{1,1}$), meanwhile the lower ones are singular (polygons). This is why we had to use different approaches for each case (methods 1,2 and 3 give satisfying results for the upper domains, while one we use method 4 for the lower), see Chapter 5 for more details.

In Figure 1.13, we give the optimal shapes obtained for different values of p_0 and in Figure 1.14, we plot the improved description of the diagram obtained by filling all the region between the curves of the upper and lower boundaries and compare it to the one obtained by random generation of polygons.

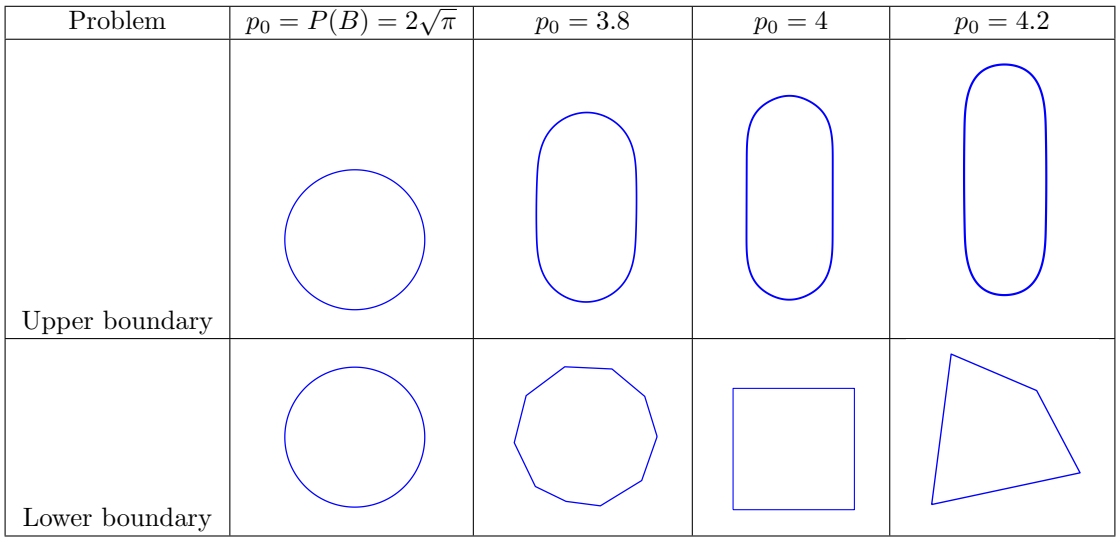

Figure 1.13: Numerically obtained optimal shapes corresponding to different values of p_0.

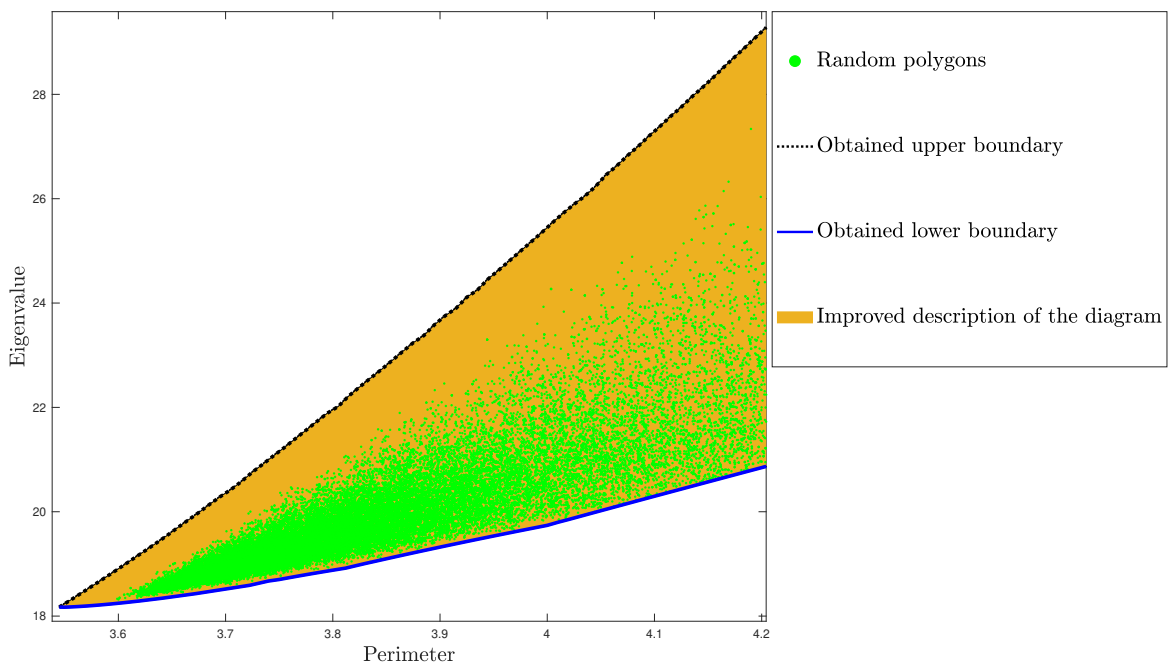

Figure 1.14: Improved $(P, \lambda_1, |\cdot|)$-diagram.

1.4.5 Contributions of Chapter 5:

Main results

In Chapter 6, we are interested in finding the optimal placement of a spherical obstacle in a given ball in order to optimize a certain quantity. In this thesis, we consider the first Steklov eigenvalue of the Laplacian introduced and defined in Section 1.3.4. We prove that the optimal situation (that maximizes the eigenvalue) is when the balls are concentric. In [172], the authors consider a mixed

Steklov-Dirichlet eigenvalue problem. They prove that the first non-trivial eigenvalue is maximal when the balls are concentric in dimensions larger or equal than 3 (see [172, Theorem 1]) and note that the planar case remains open (cf. Remark 2). We show that the ideas developed for the latter case provide an alternative and simpler proof of Theorem 1 [172]. Then, we extend this result to the planar case, see Theorem 22 of Chapter 6.

Our main result in the pure Steklov setting is stated as follows:

Theorem of the Thesis 6. *Among all doubly connected domains of $\mathbb{R}^n$ $(n \geq 2)$ of the form $B_1 \backslash \overline{B_2}$, where B_1 and B_2 are open balls of fixed radii such that $\overline{B_2} \subset B_1$. The first non-trivial Steklov eigenvalue achieves its maximal value uniquely when the balls are concentric.*

Sketches of proofs and methods

One classical method in spectral geometry when trying to prove an upper estimate of a quantity defined via a Rayleigh quotient (as it is the case for Laplace eigenvalues) is to use suitable test functions. Let us enlighten this idea by developing the example of the pure Steklov boundary conditions: we recall that the first non trivial Steklov eigenvalue of a Lipschitz set Ω is given by

$$\sigma_1(\Omega) = \inf \left\{ \frac{\int_\Omega |\nabla u|^2 dx}{\int_{\partial\Omega} u^2 d\sigma} \;\middle|\; u \in H^1(\Omega)\backslash\{0\} \text{ such that } \int_{\partial\Omega} u d\sigma = 0 \right\},$$

thus, for every function $u \in H^1(\Omega)\backslash\{0\}$ satisfying $\int_{\partial\Omega} u d\sigma = 0$, we have the following inequality

$$\sigma_1(\Omega) \leq \frac{\int_\Omega |\nabla u|^2 dx}{\int_{\partial\Omega} u^2 d\sigma}.$$

Any upper bound of the quotient $\frac{\int_\Omega |\nabla u|^2 dx}{\int_{\partial\Omega} u^2 d\sigma}$ will give an estimate from above of the eigenvalue $\sigma_1(\Omega)$. Of course, the choice of a suitable test function is not an easy task. In both cases of Theorem of the Thesis 6, we chose the eigenfunctions corresponding to the spherical shell (for which the external and internal balls are concentric) as test functions.

We take Ω a doubly connected domain of $\mathbb{R}^n$ (where $n \geq 2$) of the form $B_1 \backslash \overline{B_2}$, where B_1 and B_2 are open balls of fixed radii such that $\overline{B_2} \subset B_1$ and denote $\Omega_0 := \overline{B_2'} \subset B_1$ the spherical shell such that B'_2 is the ball with same radius as B_2 and same center as B_1. We denote by f an eigenfunction corresponding to $\sigma_1(\Omega_0)$: the first Steklov eigenvalue of concentric spherical shells and the corresponding eigenfunctions are computed in Theorem 6.6. We remark by symmetry arguments that $\int_{\partial\Omega} f d\sigma = 0$, thus f can be used as a test function in the Rayleigh quotient corresponding to the eigenvalue $\sigma_1(\Omega)$:

$$\sigma_1(\Omega) \leq \frac{\int_\Omega |\nabla f|^2 dx}{\int_{\partial\Omega} f^2 d\sigma}.$$

Since $\sigma_1(\Omega_0) = \frac{\int_{\Omega_0} |\nabla f|^2 dx}{\int_{\partial\Omega_0} f^2 d\sigma}$, the problem would be solved if one manages to prove that

$$\frac{\int_\Omega |\nabla f|^2 dx}{\int_{\partial\Omega} f^2 d\sigma} \leq \frac{\int_{\Omega_0} |\nabla f|^2 dx}{\int_{\partial\Omega_0} f^2 d\sigma}.$$

Surprisingly, in both considered cases, the numerator and denominator both behave in the ad hoc way, in the sense that one could prove the following inequalities:

$$\int_\Omega |\nabla f|^2 dx \leq \int_{\Omega_0} |\nabla f|^2 dx \quad \text{and} \quad \int_{\partial\Omega} f^2 d\sigma \geq \int_{\partial\Omega_0} f^2 d\sigma. \tag{1.30}$$

At last, it is interesting to note that the constant term is treated with an elegant way that allows to avoid complicated computations: the idea is to interpret it as a geometrical quantity (perimeter or volume of a translated ball in our case) and use its invariance by translations, see the proofs of Lemmas 9 and 10.

1.5 Open problems & research projects

We finally present possible research projects.

1.5.1 On Blaschke-Santaó diagrams

An interesting diagram

In the present thesis we present theoretical and numerical studies of some relevant diagrams. We note that there are still other diagrams that are very interesting and worth to explore. Let us develop an example.

In Chapter 5, we numerically study diagrams involving the first Dirichlet eigenvalue and other geometric functionals, we numerically find the extremal domains which are in some cases quite simple to describe (like symmetrical lens, symmetrical 2-cap bodies and symmetrical slices). Unfortunately, theoretical demonstrations of these observations seem to be very challenging. Nevertheless, there is one interesting take away idea that we would like to highlight:

"If you do not manage to prove a conjecture involving the first Dirichlet eigenvalue, then try first to prove it for the Cheeger constant."

Indeed, the Cheeger constant corresponds to the first eigenvalue of the 1-Laplace operator, see [121] for more details. It is then quite natural to expect some similar behaviours with λ_1. The advantage of working with the Cheeger constant is that in addition to being a bit easier to handle (as it involves the perimeter and the volume), there are various works that provide a better understanding of this constant, the most complete one is the classical paper [122] of T. Lachand Robert and B. Kawohl that provides a characterization of the Cheeger constant of planar convex sets. In this spirit, we cite the work [50] of D. Bucur and I. Fragala who proved that among polygons with the same number of sides and same area, the Cheeger constant is minimized by the regular one. This result is a variant of a classical and very difficult conjecture stated in the sixties by G. Polya for the first Dirichlet eigenvalue.

Let us now give an example of a relevant diagram for which an explicit description is expected. It is the diagram relating the Cheeger constant, the diameter and the area of planar convex sets: more precisely, we are interested studying the following set of points:

$$\mathcal{D} := \big\{ \big(d(\Omega), h(\Omega)\big) \mid \Omega \in \mathcal{K}^2 \text{ and } |\Omega| = 1 \big\}.$$

By combining the inequality

$$\forall \Omega \in \mathcal{K}^2, \quad h(\Omega) \leq \frac{1}{r(\Omega)} + \sqrt{\frac{\pi}{|\Omega|}},$$

which is an equality for shapes that are homothetic to their form bodies[2] (this result is stated in **Theorem of the thesis 4**, and proved in the first section of Chapter 4) and results on the diagram $(|\cdot|, d, r)$ obtained in [110] (see also [71]), we are able to explicitly describe the lower boundary. Indeed, we have the following proposition:

Proposition 1. *Let $d_0 \geq d(B) = \frac{2}{\sqrt{\pi}}$. The solution of the problem*

$$\min\{h(\Omega) |\ |\Omega| = 1,\ d(\Omega) = d_0 \text{ and } \Omega \in \mathcal{K}^2\}$$

is given by the symmetrical 2-cap body of unit area and diameter d_0.

[2] We refer to [136, Section 1.1] for the definition of form bodies and to [164] for more details.

Proof. Let $d_0 \geq d(B) = \frac{2}{\sqrt{\pi}}$. We denote C_{1,d_0} the symmetrical 2-cap body of unit area and diameter d_0. We have:

$$\begin{aligned}
\min\{h(\Omega) \mid |\Omega| = 1,\ d(\Omega) = d_0 \text{ and } \Omega \in \mathcal{K}^2\} &\leq \min\left\{\frac{1}{r(\Omega)} + \sqrt{\frac{\pi}{|\Omega|}} \;\middle|\; |\Omega| = 1,\ d(\Omega) = d_0 \text{ and } \Omega \in \mathcal{K}^2\right\} \\
&= \min\left\{\frac{1}{r(\Omega)} \;\middle|\; |\Omega| = 1,\ d(\Omega) = d_0 \text{ and } \Omega \in \mathcal{K}^2\right\} + \sqrt{\pi} \\
&= \frac{1}{r(C_{1,d_0})} + \sqrt{\frac{\pi}{|C_{1,d_0}|}} \qquad \text{(by the results of [110])} \\
&= h(C_{1,d_d}) \qquad \text{(because } C_{1,d_0} \text{ is homothetic to its form body)} \\
&\leq \min\{h(\Omega) \mid |\Omega| = 1,\ d(\Omega) = d_0 \text{ and } \Omega \in \mathcal{K}^2\}.
\end{aligned}$$

Thus we have the equality

$$\min\{h(\Omega) \mid |\Omega| = 1,\ d(\Omega) = d_0 \text{ and } \Omega \in \mathcal{K}^2\} = h(C_{1,d_d}).$$

□

In Figure 1.16, we provide a numerical approximation of the diagram $\mathcal{D}$ by generating 10^5 random convex polygon. We also plot the curves corresponding to the lower domains given by symmetrical 2-cap bodies and the expected upper domains, which are given by symmetrical slices and smoothed nonagons (introduced for the first time in [71]), see Figure 1.15.

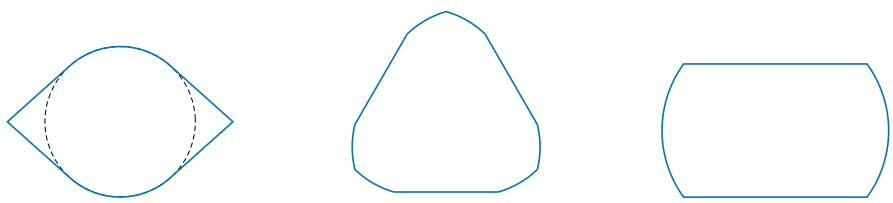

Figure 1.15: From left to right: a symmetrical 2-cap body, a smoothed nonagon and a symmetrical slice.

Numerical simulations support the following conjecture:

Conjecture 2. *Let $d \geq d(B) = \frac{2}{\sqrt{\pi}}$ and $d^* = \frac{2}{3^{1/4}}$ be the diameter of the regular triangle of unit area, we have:*

- *if $d_0 \in (d(B), d^*)$, the problem*

$$\max\{h(\Omega) \mid |\Omega| = 1,\ d(\Omega) = d_0 \text{ and } \Omega \in \mathcal{K}^2\}$$

  is solved by a smoothed nonagon.

- *If $d_0 \geq d^*$, the problem is solved by the symmetrical slice.*

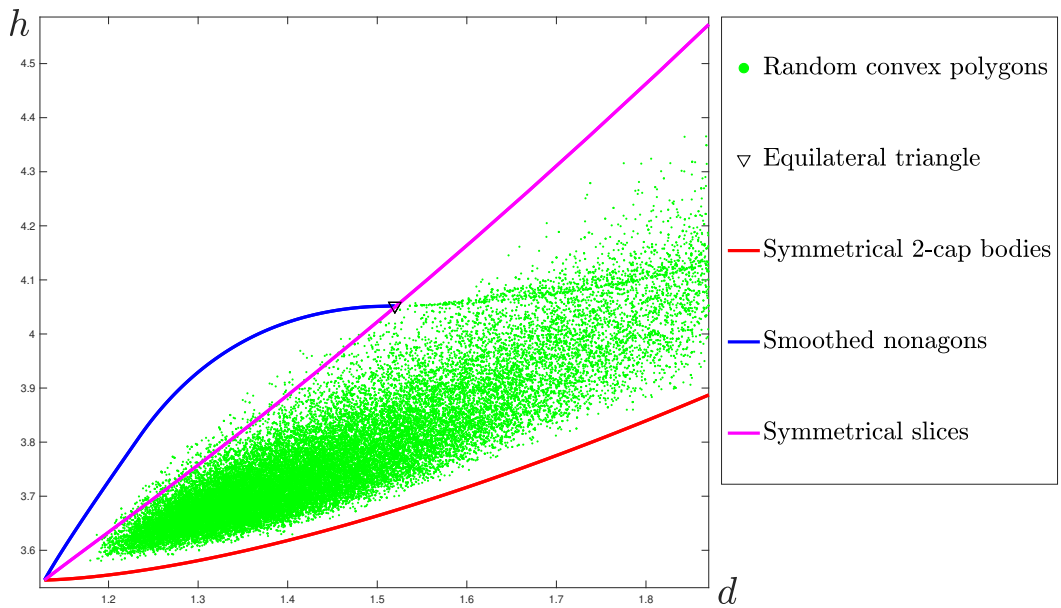

Figure 1.16: The diagram of the triplet $(d, h, |\cdot|)$.

Generalizing the approach used for the study of the $(P, \lambda_1, |\cdot|)$-diagram

It is interesting to note that the methods developed for the qualitative study of the $(P, \lambda_1, |\cdot|)$-diagram seem to apply for other functionals. It is then natural to seek for a general theorem such that once some conditions are satisfied by 3 given functionals J_1, J_2 and J_3, one is able to give qualitative properties on the diagram such as the continuity and monotonicity of the upper and lower curves and the non-existence of holes.

What about other classes of sets?

In this thesis, we mainly focus on Blaschke-Santaló diagrams of convex sets. Nevertheless, it is interesting to develop a better understanding of what happens for other relevant classes of shapes, for example the star-shaped ones or the simply connected ones.

1.5.2 An upper estimate of the area of inner convex sets

Let $\Omega \in \mathcal{K}^2$, for $t \in \big[0, r(\Omega)\big)$, we define $\Omega_{-t} := \{x \in \Omega \mid d(x, \partial\Omega) > t\}$. As explained in Section 1.4.1, finding estimates of the area of inner sets is very linked to the study of inequalities involving the Cheeger constant. We wanted to apply this strategy to prove inequality:

$$\forall \Omega \in \mathcal{K}^2, \qquad h(\Omega) \geq \frac{P(\Omega) + \sqrt{4\pi|\Omega|}}{2|\Omega|}. \tag{1.31}$$

Surprisingly, we did not find in the literature an upper estimate of $|\Omega_{-t}|$ that can be used. We then conjecture the following result which seems to be true and which can be used to give an alternative proof of inequality 1.31 and characterize the case of equality:

Conjecture 3. *Let $\Omega \in \mathcal{K}^2$, we have for every $t \in \big(0, r(\Omega)\big)$:*

$$|\Omega_{-t}| \leq |\Omega| - P(\Omega)t + \frac{P(\Omega)^2}{4|\Omega|}t^2, \tag{1.32}$$

with equality if and only if Ω is homothetic to its form body.

Remark 1. *We are thankful to Simon Larson for proposing an idea to prove the following weaker version of* (1.32)*:*

$$\forall t \in \big(0, r(\Omega)\big), \qquad |\Omega_{-t}| \leq |\Omega| - P(\Omega)t + \frac{P(\Omega)^2}{2|\Omega|}t^2.$$

The proof uses the result of [136, Theorem 1.2] (which is demonstrated in arbitrary dimensions), where it is proved that:

$$\forall t \in \big(0, r(\Omega)\big), \qquad P(\Omega_{-t}) \geq \left(1 - \frac{t}{r(\Omega)}\right) P(\Omega),$$

where equality holds if and only if Ω is homothetic to its form body. By integrating the latter inequality on $(0, t)$, we obtain:

$$\forall t \in \big(0, r(\Omega)\big), \qquad |\Omega_{-t}| \leq |\Omega| - P(\Omega)t + \frac{P(\Omega)^2}{2r(\Omega)}t^2,$$

which is an equality if and only if Ω is homothetic to its form body. At last, we use the bound $r(\Omega)P(\Omega) \geq |\Omega|$ to get rid of the inradius and finally obtain the announced inequality.

1.5.3 Shape derivation of functionals defined as infima

Many shape functionals are defined as an infimum (or supremum) of a certain quantity, this is for example the case for the diameter, the Cheeger constant and the first Dirichlet eigenvalue. there are various works in the literature where the first order shape derivatives of such functionals are computed, we refer for example to:

- [153] for the Cheeger constant, see also our revised version in Theorem 20.
- [67, Chapter 10] for the Dirichlet energy.
- [139] for the first eigenvalue of the p-Laplace operator with Dirichlet boundary condition.
- Theorem 19 of the present thesis for the diameter.

All this results are proven by following a classical strategy introduced by Danskin [65]. Unfortunately, the hypothesises of Danskin's Theorem are not straightforward to check (especially in the shape derivation framework, see for example [67, Chapter 10]). It is then very interesting to look for a specific shape optimization theorem with more straightforward assumptions.

Part I

Study of some relevant Blaschke-Santaló diagrams

Chapter 2

Blaschke-Santaló diagrams for the volume, the perimeter and the Cheeger constant.

This chapter is a reprint of the submitted paper ***Complete systems of inequalities relating the perimeter, the area and the Cheeger constant of planar domains*** *[88].*

Abstract

We are interested in finding complete systems of inequalities between the perimeter P, the area $|\cdot|$ and the Cheeger constant h of planar sets. To do so, we study the so called Blaschke-Santaló diagram of the triplet $(P, |\cdot|, h)$ for different classes of domains: simply connected sets, convex sets and convex polygons with at most N sides. We are able to completely determine the diagram in the latter cases except for the class of convex N-gons when $N \geq 5$ is odd: therein, we show that the external boundary of the diagram is given by the curves of two continuous and strictly increasing functions, we give an explicit formula of the lower one and provide a numerical method to obtain the upper one. We finally give some applications of the results and methods developed in the present paper.

2.1 Introduction and main results

Let Ω be a bounded subset of $\mathbb{R}^n$ (where $n \geq 2$). The Cheeger problem consists of studying the following minimization problem:

$$h(\Omega) := \inf \left\{ \frac{P(E)}{|E|} \;\middle|\; E \text{ measurable and } E \subset \Omega \right\}, \tag{2.1}$$

where $P(E)$ is the distributional perimeter of E measured with respect to $\mathbb{R}^n$ (see for example [151] for definitions) and $|E|$ is the n-dimensional Lebesgue measure of E. The quantity $h(\Omega)$ is called *the Cheeger constant of* Ω and any set $C_\Omega \subset \Omega$ for which the infimum is attained is called a *Cheeger set of* Ω.

Since the early work of Jeff Cheeger [55], the study of the Cheeger problem has interested various authors, we refer to [151] for an introductory survey on the subject. We recall that every bounded domain Ω with Lipschitz boundary admits at least one Cheeger set C_Ω, see for example [151, Proposition 3.1]. In [6], the authors prove uniqueness of the Cheeger set when $\Omega \subset \mathbb{R}^n$ is convex, but as far as we know there is no complete characterization of C_Ω in the case of higher dimensions $n \geq 3$ (even

when convexity is assumed), in contrary with the planar case which was treated by Bernd Kawohl and Thomas Lachand-Robert in [122] where a complete description of the Cheeger sets of planar convex domains is given in addition to an algorithm to compute the Cheeger constant of convex polygons.

In this paper we are interested in describing all possible geometrical inequalities involving the perimeter, the volume and the Cheeger constant of a given planar shape. This is equivalent to study a so called Blaschke-Santaló diagram of the triplet $(P, |\cdot|, h)$.

A Blaschke-Santaló diagram is a tool that allows to visualize all possible inequalities between three quantities depending on the shape of a set: it was named as a reference to [163, 28], where the authors were looking for the description of inequalities involving three geometrical quantities for a given convex set. Afterward, this diagrams have been extensively studied especially for the class of planar convex sets. We refer to [110] for more details and various examples.

For more precision, let us define the Blaschke-Santaló diagrams we are interested in in this paper: given $\mathcal{F}$ a class of measurable sets of $\mathbb{R}^2$, we define

$$\begin{aligned}\mathcal{D}_{\mathcal{F}} &:= \Big\{(x,y)\in\mathbb{R}^2,\ \exists\ \Omega\in\mathcal{F} \text{ such that } |\Omega|=1, P(\Omega)=x,\ h(\Omega)=y\Big\}\\ &:= \Big\{\ \big(P(\Omega),h(\Omega)\big),\ \Omega\in\mathcal{F},\ |\Omega|=1\ \Big\}.\end{aligned}$$

We note that thanks to the following homothety properties

$$\forall t>0,\quad h(t\Omega)=\frac{h(\Omega)}{t},\qquad |t\Omega|=t^2|\Omega|\qquad\text{and}\qquad P(t\Omega)=tP(\Omega),$$

one can give a scaling invariant formulation of the diagram:

$$\begin{aligned}\mathcal{D}_{\mathcal{F}} &= \Big\{(x,y)\in\mathbb{R}^2,\ \exists\Omega\in\mathcal{F} \text{ such that } P(\Omega)/|\Omega|^{1/2}=x,\ \ |\Omega|^{1/2}\lambda_1(\Omega)=y\Big\}\\ &= \Big\{\ \Big(\frac{P(\Omega)}{|\Omega|^{1/2}},|\Omega|^{1/2}h(\Omega)\Big),\ \ \Omega\in\mathcal{F}\Big\}\end{aligned}$$

In the whole paper, we denote:

- $\mathcal{K}^2$ the set of planar non-empty convex sets,
- $\mathcal{P}_N$ the set of convex polygons of at most N sides,
- B the disk of unit area,
- R_N a regular polygon of N sides and unit area,
- d^H the Hausdorff distance, see for example [108, Chapter 2] for definition and more details.
- $d(\Omega)$ and $r(\Omega)$ respectively the diameter and inradius of the set $\Omega\subset\mathbb{R}^2$.

We are aiming at describing all possible inequalities relating P, $|\cdot|$ and h in different classes of planar sets and then describing the associated Blaschke-Santaló diagrams. Let us first state the inequalities we already know; if Ω is measurable, we have :

- the isoperimetric inequality:
$$\frac{P(\Omega)}{|\Omega|^{1/2}}\geq\frac{P(B)}{|B|^{1/2}}=2\sqrt{\pi}, \tag{2.2}$$
- a consequence of the definition of the Cheeger constant
$$h(\Omega)=\inf_{E\subset\Omega}\frac{P(E)}{|E|}\leq\frac{P(\Omega)}{|\Omega|}, \tag{2.3}$$

- a Faber-Krahn type inequality:

$$|\Omega|^{1/2}h(\Omega) \geq |B|^{1/2}h(B) = \frac{P(B)}{|B|^{1/2}} = 2\sqrt{\pi}, \tag{2.4}$$

this inequality readily follows from definition (4.1) and the isoperimetric inequality. Indeed:

$$|\Omega|^{1/2}h(\Omega) = h(\Omega') = \frac{P(C_{\Omega'})}{|C_{\Omega'}|} \geq \frac{P(C^*_{\Omega'})}{|C^*_{\Omega'}|} \geq h(B) = P(B) = 2\sqrt{\pi},$$

where $\Omega' := |\Omega|^{-1/2}\Omega$ and $C^*_{\Omega'}$ is a ball with the same volume as $C_{\Omega'}$.

Note that each inequality may be visualised in the Blaschke-Santaló diagram as the curve of a given function, see Figure 2.1, and that the first inequality may be obtained by combining the second and third ones.

It is natural to wonder if there are other inequalities, we prove that this is not the case for general sets, indeed, in Theorem 5 we give the explicit description of the Blaschke-Santaló diagram in the case of simply connected domains (see also Figure 2.1). One could wonder why we chose to work with the class of simply connected domains: the main reason is that for any subclass of measurable domains that contains the simply connected ones, the diagram is the same.

Now, let us provide complete descriptions of the Blaschke-Santaló diagram of the triplet $(P, h, |\cdot|)$ for both the classes $\mathcal{S}^2$ of planar simply connected sets and $\mathcal{K}^2$ of planar convex sets.

Theorem 5. *Denote $x_0 = P(B) = 2\sqrt{\pi}$.*

1. *The diagram of the class $\mathcal{S}$ of planar simply connected domains is given by:*

$$\mathcal{D}_{\mathcal{S}^2} = \{(x_0, x_0)\} \cup \{(x, y) \ \mid \ x \geq x_0 \quad \textit{and} \quad x_0 < y \leq x\}.$$

2. *The diagram of the class $\mathcal{K}$ of planar convex domains is given by:*

$$\mathcal{D}_{\mathcal{K}^2} = \left\{(x, y) \ \middle| \ x \geq x_0 \quad \textit{and} \quad \frac{x}{2} + \sqrt{\pi} \leq y \leq x\right\}.$$

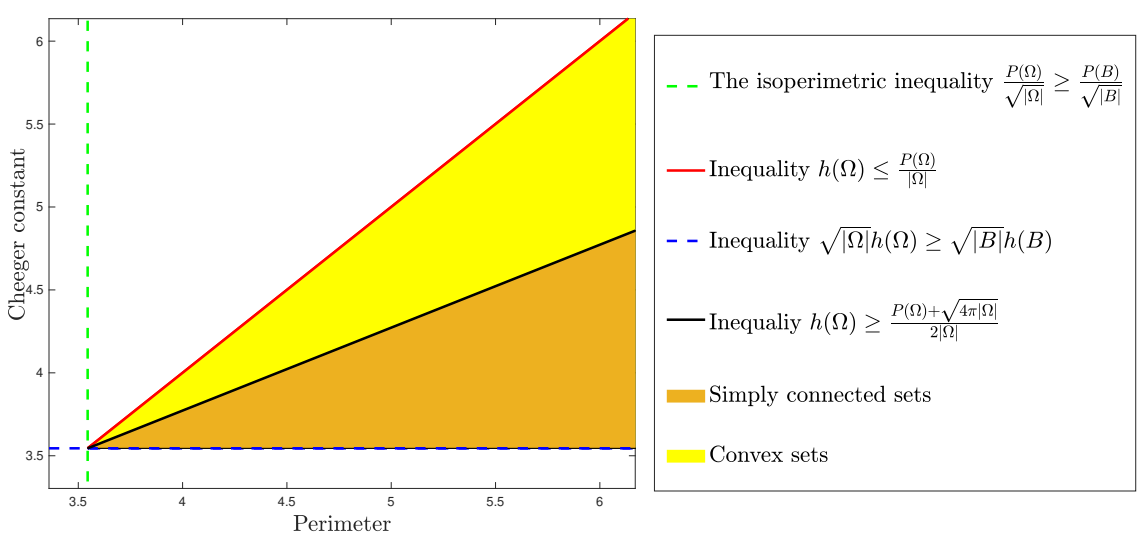

Figure 2.1: Blaschke-Santaló diagrams for the classes of simply connected sets and convex sets.

We note that by taking advantage of inequalities (2.2) and (2.4), it is also classical to represent Blaschke-Santaló diagram as subset of $[0,1]^2$, in our situation, this means to consider sets:

$$\mathcal{D}'_{\mathcal{F}} := \left\{ (X,Y) \ \mid \exists \Omega \in \mathcal{F} \text{ such as } |\Omega| = 1 \text{ and } (X,Y) = \left(\frac{P(B)}{P(\Omega)}, \frac{h(B)}{h(\Omega)} \right) \right\} \subset [0,1]^2,$$

where $\mathcal{F}$ is a given class of planar sets. With this parametrization, Blaschke-Santaló diagrams for the classes $\mathcal{S}$ and $\mathcal{K}^2$ are given by the following sets:

$$\begin{cases} \mathcal{D}'_{\mathcal{S}^2} &= \{(1,1)\} \cup \{(X,Y) \mid X \in (0,1) \text{ and } X \leq Y < 1\}, \\ \mathcal{D}'_{\mathcal{K}^2} &= \{(X,Y) \mid X \in (0,1] \text{ and } X \leq Y \leq \frac{2X}{1+X}\}, \end{cases}$$

which are represented in Figure 2.2.

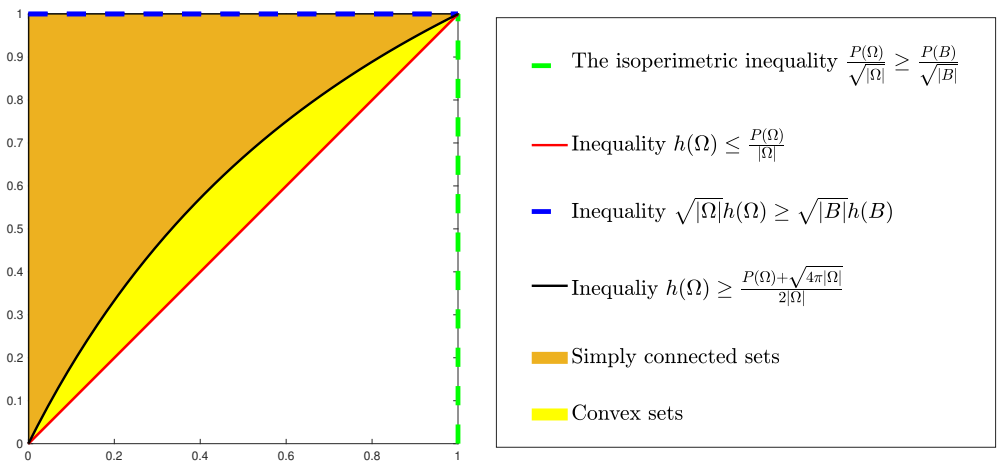

Figure 2.2: Blaschke-Santaló diagrams for the classes of simply connected sets and convex sets represented in $[0,1]^2$.

Let us give some comments on the latter results:

- One major step in the study of the diagram of convex sets is to prove the following sharp inequality:

$$\forall \Omega \in \mathcal{K}^2, \qquad h(\Omega) \geq \frac{P(\Omega) + \sqrt{4\pi|\Omega|}}{2|\Omega|}, \tag{2.5}$$

  where equality occurs for example for circumscribed polygons (ie. those whose sides touch their incircles) and more generally for sets which are homothetical to their form bodies[1].

- Inequality (2.5) is rather easy to prove when the convex Ω is a Cheeger-regular polygon (that is, its Cheeger set touches all of its sides), see [50, Remark 32], but much difficult to prove for general convex sets as shown in the present paper. We also note that this inequality may be seen as a quantitative isoperimetric inequality for the Cheeger constant of convex planar sets: indeed, it could be written in the following form

$$\forall \Omega \in \mathcal{K}^2, \qquad |\Omega|^{1/2} h(\Omega) - |B|^{1/2} h(B) \geq \frac{1}{2} \left(\frac{P(\Omega)}{|\Omega|^{1/2}} - \frac{P(B)}{|B|^{1/2}} \right) \geq 0.$$

[1] We refer to [164, Page 386] for the definition of form bodies.

At last, we note in Section 2.5.1 that inequality (2.5) is stronger than a classical result [48, Theorem 3] due to R. Brooks and P. Waksman. It also improves in the planar case a more recent estimate given in [39, Corollary 5.2], that states that for any open bounded convex set $\Omega \subset \mathbb{R}^n$, where $n \geq 2$, one has:

$$h(\Omega) \geq \frac{1}{n} \times \frac{P(\Omega)}{|\Omega|}.$$

- We note that the first statement of Theorem 5 asserts that (2.3) and (2.4) form a complete system of inequalities of the triplet $(P, h, |\cdot|)$ in any class of sets that contains the class $\mathcal{S}$. Meanwhile, the second one asserts that this is no longer the case for the class $\mathcal{K}^2$ of planar convex sets, where estimates (2.3) and (2.5) are then shown to be forming a complete system of inequalities of the triplet $(P, h, |\cdot|)$.
- We finally note that due to technical convenience, we first show the second assertion (diagram of convex sets) and then use it to prove the first one (diagram of simply connected sets).

Now, let us focus on the class of convex polygons. We give an improvement of inequality (2.3) in the class $\mathcal{P}_N$ of convex polygons of at most N sides, where $N \geq 3$. We recall that since triangles are inscribed polygons, one has:

$$\forall \Omega \in \mathcal{P}_3, \quad h(\Omega) = \frac{P(\Omega) + \sqrt{4\pi|\Omega|}}{2|\Omega|}. \tag{2.6}$$

As for the case $N \geq 4$, we prove the following sharp upper bound for the Cheeger constant of convex N-gons:

$$\forall \Omega \in \mathcal{P}_N, \qquad h(\Omega) \leq \frac{P(\Omega) + \sqrt{P(\Omega)^2 + 4\big(\pi - N\tan\frac{\pi}{N}\big)|\Omega|}}{2|\Omega|}, \tag{2.7}$$

with equality if and only if Ω is Cheeger-regular and all of its angles are equal (to $(N-2)\pi/N$). Equality is also attained asymptotically by the following family $\big((0,1)\times(0,d)\big)_{d\geq 1}$ of rectangles when $d \longrightarrow +\infty$.

It is interesting to note that inequalities (2.5) and (2.7) form a complete system of inequalities of the triplet $(P, |\cdot|, h)$ in the class $\mathcal{P}_N$ if and only if N is even. In the following Theorem 6, we give an explicit description of the diagram of convex polygons when N is even or equal to 3, give the explicit description of the lower boundary and provide some qualitative results on the upper one when N is odd. In Section 2.4, we perform some numerical simulations in order to numerically find the extremal upper domains and thus give a numerical description of the upper boundary.

Theorem 6. *Take $N \geq 3$, we recall that R_N denotes a regular polygon of N sides and unit area.*

We denote

$$\mathcal{D}_N := \left\{ \left(\frac{P(\Omega)}{|\Omega|^{1/2}}, |\Omega|^{1/2} h(\Omega) \right) \;\middle|\; \Omega \in \mathcal{P}_N \right\}.$$

We distinguish the following cases:

- *if $N = 3$, we have*

$$\mathcal{D}_3 = \left\{ \left(x, \frac{x}{2} + \sqrt{\pi} \right) \;\middle|\; x \geq P(R_3) \right\}$$

- *if N is even, then*

$$\mathcal{D}_N = \left\{ (x,y) \mid x \geq P(R_N) \;\; \textit{and} \;\; \frac{x}{2} + \sqrt{\pi} \leq y \leq f_N(x) \right\},$$

where $f_N : x \in [P(R_N), +\infty) \longmapsto \frac{x + \sqrt{x^2 + 4(\pi - N\tan\frac{\pi}{N})}}{2}$.

- *if $N \geq 5$ is odd, we provide a qualitative description of the boundary of the diagram $\mathcal{D}_N$:*
  - *The lower boundary is given by the half line:*
  $$\{(x,y) \mid x \geq P(R_N) \text{ and } y = x/2 + \sqrt{\pi}\},$$
  which is included in the diagram $\mathcal{D}_N$.
  - *The upper boundary is given by the curve:*
  $$\{(x,y) \mid x \geq P(R_N) \text{ and } y = g_N(x)\},$$
  which is also included in the diagram $\mathcal{D}_N$, where g_N is a continuous and strictly increasing function such that $g_N \leq f_N$ on $\big[P(R_N), +\infty\big)$. Moreover, there exists $c_N \geq b_N > P(R_N)$ such that $g_N = f_N$ on $[P(R_N), b_N]$ and $g_N < f_N$ on $\big[c_N, +\infty\big)$.

The paper is organized as follows: Section 2.2 contains two subsections, in the first one we recall some classical results needed for the proofs, in the second one we state and prove some preliminary lemmas which are also interesting for themselves. The proofs of the main results are given in Section 2.3. Then, we provide some numerical results on the diagrams $\mathcal{D}_N$ in Section 2.4. Finally, we give some applications of the results and ideas of the present paper in Section 2.5.

2.2 Classical results and preliminaries

2.2.1 Classical results

In this subsection, we recall some classical results that are used throughout the whole paper.

Theorem 7. *[61, Th.2 and Remark 3]*
Take $N \geq 3$ and $\Omega \subset \mathbb{R}^2$ a convex polygon of N sides. We define:
$$T(\Omega) := \sum_{i=1}^{N} \frac{1}{\tan \frac{\alpha_i}{2}},$$
where $\alpha_i \in (0, \pi]$ are the inner angles of Ω. We have the following estimates:
$$N \tan \frac{\pi}{N} \leq T(\Omega) \leq \frac{P(\Omega)^2}{4|\Omega|}. \tag{2.8}$$
The lower bound is attained if and only if all the angles α_i are equal (to $\frac{N-2}{2N}\pi$), meanwhile the upper one is an equality if and only the polygon Ω is circumscribed.

Remark 2. *The lower bound is a simple application of Jensen's inequality to the function cotan which is strictly convex on $(0, \pi/2)$. On the other hand, since $N \tan \frac{\pi}{N} > \pi$, the upper estimate may be seen as an improvement of the isoperimetric inequality for convex polygons. We refer to [61] for a detailed proof of Theorem 7.*

Let us now recall some classical and important results on the Cheeger problem for planar convex sets.

Theorem 8. *[122, Th. 1] There exists a unique value $t = t^* > 0$ such that $|\Omega_{-t}| = \pi t^2$. Then $h(\Omega) = 1/t^*$ and the Cheeger set of Ω is $C_\Omega = \Omega_{-t^*} + t^* B_1$, with B_1 denoting the unit disk.*

Theorem 9. *[122, Th. 3] If Ω is a Cheeger-regular polygon (that is, its Cheeger set touches every side of Ω), then:*
$$h(\Omega) = \frac{P(\Omega) + \sqrt{P(\Omega)^2 - 4\big(T(\Omega) - \pi\big)|\Omega|}}{2|\Omega|}.$$

It is natural to wonder if equality holds also for some Cheeger irregular polygons: in Lemma 4, we prove that there is only an inequality and that the equality case occurs only when the polygon is Cheeger regular.

2.2.2 Preliminary lemmas

In this section we prove some important Lemmas that we use in Section 2.3 for the proofs of the main results.

The following Lemma shows that the equality of Theorem 8 which is valid for Cheeger regular polygons becomes an inequality for general polygons and thus gives an upper bound of the Cheeger constant of polygons that we use to prove inequality (2.7).

Lemma 4. *If Ω is a polygon, one has:*

$$h(\Omega) \leq \frac{P(\Omega) + \sqrt{P(\Omega)^2 - 4\big(T(\Omega) - \pi\big)|\Omega|}}{2|\Omega|},$$

with equality if and only if Ω is Cheeger-regular.

Proof. Let us denote:

$$F(\Omega) := \frac{P(\Omega) + \sqrt{P(\Omega)^2 - 4\big(T(\Omega) - \pi\big)|\Omega|}}{2|\Omega|}.$$

The key of the proof is to understand the graphical interpretation of $h(\Omega)$ and $F(\Omega)$. Indeed:

- $1/h(\Omega)$ is the (unique) solution of the equation $g(t) := |\Omega_{-t}| - \pi t^2$ in $[0, r(\Omega)]$,
- $1/F(\Omega)$ is the smallest solution of the equation $f(t) := |\Omega| - P(\Omega)t + T(\Omega)t^2 - \pi t^2$ in $[0, r(\Omega)]$,

where $r(\Omega)$ is the inradius of Ω.

The number of sides of the inner sets Ω_t of a polygon is decreasing with respect to $t \geq 0$. Actually, the function $t \in [0, r_\Omega] \longmapsto n(t)$ (where $n(t)$ is the number of sides of Ω_{-t}) is a piece-wise constant decreasing function. We introduce the sequence $0 = t_0 < t_1 < ... < t_N = r(\Omega)$, where $N \in \mathbb{N}^*$, such that:

$$\forall k \in [\![0, N-1]\!], \forall t \in [t_k, t_{k+1}) \qquad n(t) = n(0) - k.$$

Let us take $t \in [0, r(\Omega)]$ and a $k \in [\![1, N]\!]$. We have:

$$\begin{aligned}
|\Omega_{t_k}| - (t - t_k)P(\Omega_{-t_k}) + (t - t_k)^2 T(\Omega_{-t_k}) &= |\Omega_{-t_{k-1}}| - (t_k - t_{k-1})P(\Omega_{-t_{k-1}}) + (t_k - t_{k-1})^2 T(\Omega_{-t_k}) \\
&\quad - (t - t_k)\big(P(\Omega_{-t_{k-1}}) - 2(t_k - t_{k-1})T(\Omega_{-t_{k-1}})\big) + (t - t_k)^2 T(\Omega_{-t_k}) \\
&> |\Omega_{-t_{k-1}}| - (t - t_{k-1})P(\Omega_{-t_{k-1}}) + (t - t_{k-1})^2 T(\Omega_{-t_{k-1}}),
\end{aligned}$$

where we used Steiner formulas for inner convex polygons for the first equality and the fact that $T(\Omega_{-t_{k-1}}) < T(\Omega_{-t_k})$ for the inequality (see [122, Section 5.]). By straightforward induction we show that for every $k \in [\![1, N]\!]$, one has:

$$\forall t \in [0, r(\Omega)], \qquad |\Omega_{t_k}| - (t - t_k)P(\Omega_{-t_k}) + (t - t_k)^2 T(\Omega_{-t_k}) \geq |\Omega| - tP(\Omega) + t^2 T(\Omega). \tag{2.9}$$

Now, let us take $k \in [\![0, N]\!]$ and $t \in [t_k, t_{k+1})$. We have:

$$\begin{aligned}
g(t) := |\Omega_{-t}| - \pi t^2 = |(\Omega_{-t_k})_{-(t-t_k)}| - \pi t^2 &= |\Omega_{t_k}| - (t - t_k)P(\Omega_{-t_k}) + (t - t_k)^2 T(\Omega_{-t_k}) - \pi t^2 \\
&\geq |\Omega| - tP(\Omega) + t^2 T(\Omega) - \pi t^2 =: f(t),
\end{aligned}$$

where equality $g(t) = f(t)$ holds only on $[0, t_1]$.

Finally

$$\begin{cases} \forall t \in [0, t_1], & g(t) = f(t), \\ \forall t \in \big(t_1, r(\Omega)\big), & g(t) > f(t) \end{cases}$$

where equality holds only on $[0, t_1]$. This tells us that $1/h(\Omega)$, the first zero of g on $[0, r(\Omega)]$, is actually larger than $1/F(\Omega)$, the first zero of f, with equality if and only if the first zero of g is in $[0, t_1]$, which is the case if and only when the polygon Ω is Cheeger-regular (see [122, Theorem 3.]). This ends the proof. $\square$

Since inequality (2.5) is quite easy to obtain for Cheeger regular polygons (because in this case we have an explicit formula for the Cheeger constant in terms of the perimeter, the area and the inner angles), it is natural when dealing with general polygons to try to come back the latter case of Cheeger regular ones. The following Lemma shows how to deform a given polygon to a Cheeger regular with while preserving its Cheeger constant, increasing its perimeter and decreasing its area, this allows as shown in **Step 2** of Section 2.3.1 to prove inequality (2.5) for the case of general polygons.

Lemma 5. *Let Ω be a polygon. There exists a Cheeger-regular polygon $\widetilde{\Omega}$ such that: $|\Omega| \geq |\widetilde{\Omega}|$, $P(\Omega) \leq P(\widetilde{\Omega})$ and $h(\Omega) = h(\widetilde{\Omega})$.*

Proof. If Ω is Cheeger regular we take $\widetilde{\Omega} = \Omega$. Let Ω be a Cheeger irregular polygon. We give an algorithm of deforming Ω into a Cheeger regular polygon with the same Cheeger set (thus also the same Cheeger value), larger perimeter and smaller area.

Since Ω is Cheeger irregular, there exists three consecutive vertices that we denote X, Y and Z such that at least one (may be both) of the sides XY and YZ does not touch the Cheeger set C_Ω.

First step: using parallel chord movements

We begin by the case where both the sides XY and YZ does not touch C_Ω. We use a parallel chord movement. More precisely, we move Y along the line passing through Y and being parallel to the line (XZ). This way, the volume is preserved, and the perimeter must increase when moving Y away from the perpendicular bisector of $[XZ]$ (which is possible at least in one direction). We assume without loss of generality that the direction which increases the perimeter is from Z to X (see Figure 2.3). We then move Y until one the following cases occurs:

1. (XY) becomes colinear to the other side of extremity X.
2. $[YZ]$ touches the boundary of C_Ω.

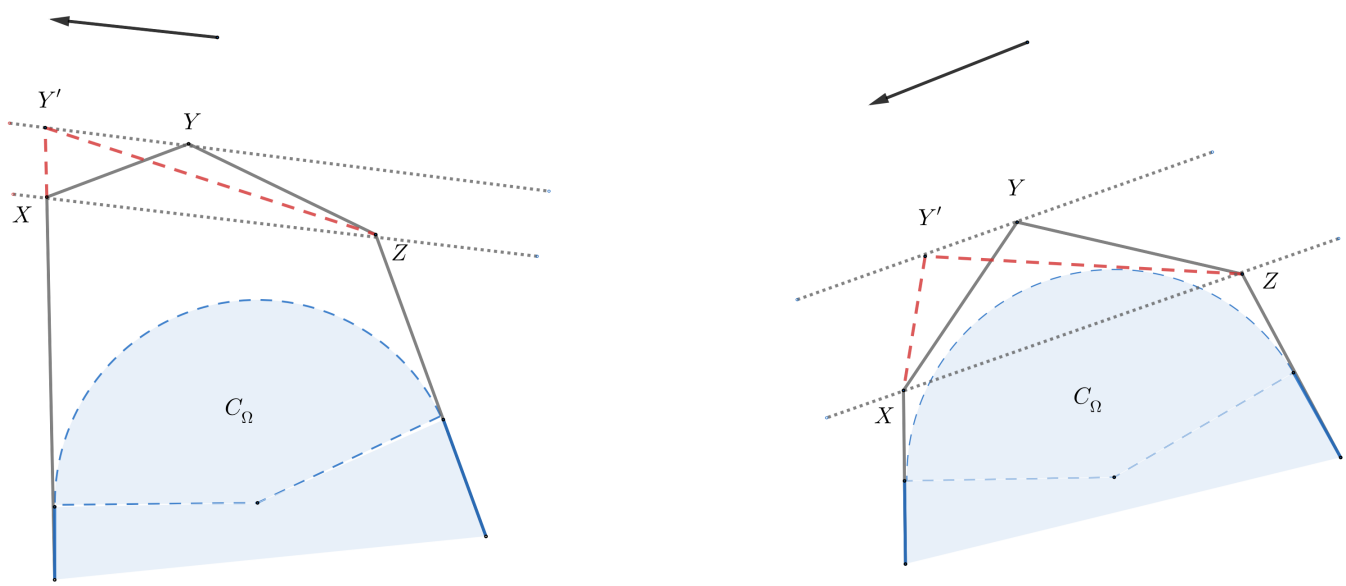

Figure 2.3: Case 1 on the left and case 2 on the right.

In both cases, the number of sides that do not touch ∂C_Ω is diminished by one, while the area and the Cheeger constant are conserved and the perimeter is increased.

We iterate the latter process for all vertices which are extremities of two sides that do not touch ∂C_Ω, since the number of vertices is finite, in a finite number of steps we obtain a polygon where there are no consecutive sides that do not touch ∂C_Ω.

Second step: rotating the remaining sides

The second step is to "rotate" the remaining sides that do not touch ∂C_Ω in such a way to make them touch it (see Figure 2.4), in order to get a Cheeger-regular polygon with the same Cheeger constant, larger perimeter and smaller area. This kind of deformations was inspired from the work of D. Bucur and I. Fragala [50].

We denote by α_1,$\alpha_2 \in (0, \pi)$ the inner angles of the polygon Ω respectively associated to the vertices X and Y, O the mid-point of the side $[XY]$, t the angle of our "rotation" and X_t and Y_t the vertices of the obtained polygon Ω_t (see Figure 2.4).

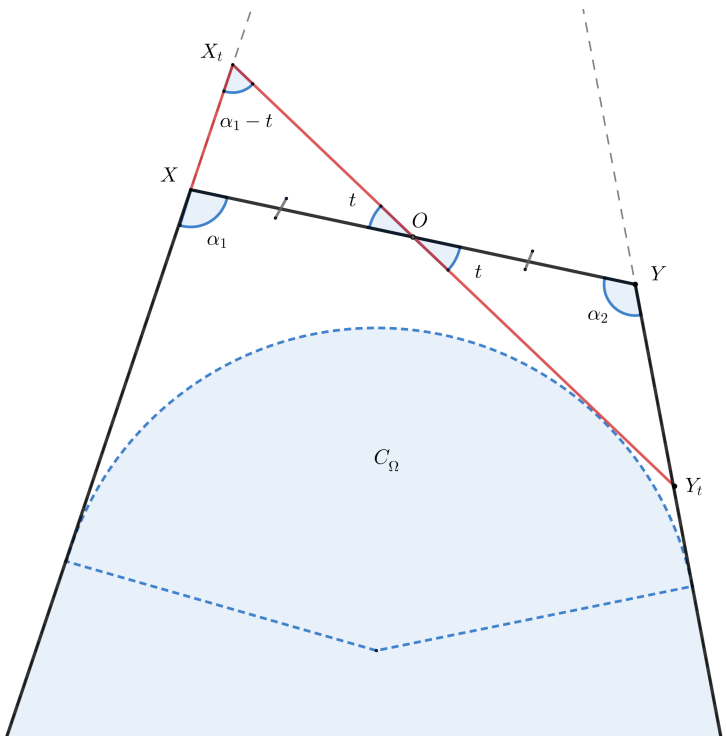

Figure 2.4: Rotation of the free side along its midpoint.

Without loss of generality, we assume that $\alpha_2 \geq \alpha_1$ and $t \geq 0$. It is classical that Ω and Ω_t have the same Cheeger constant, moreover if the side $[XY]$ is not touching ∂C_Ω then $\alpha_1 + \alpha_2 \geq \pi$ (see [122, Section 5]).

By using the sinus formula on triangles OXX_t and OYY_t, we have:

$$\begin{cases} AX_t = a\frac{\sin t}{\sin(\alpha_1 - t)} & \text{and} \qquad OX_t = a\frac{\sin \alpha_1}{\sin(\alpha_1 - t)} \\ BY_t = a\frac{\sin t}{\sin(\alpha_2 + t)} & \text{and} \qquad OY_t = a\frac{\sin \alpha_2}{\sin(\alpha_2 + t)} \end{cases}$$

where $a := OX = XY/2$.

Moreover, if we denote by $\mathcal{S}_{OXX_t}$ and $\mathcal{S}_{OYY_t}$ the areas of the triangles OXX_t and OYY_t, we have:

$$\begin{aligned}
|\Omega_t| - |\Omega| &= \mathcal{S}_{OXX_t} - \mathcal{S}_{OYY_t} \\
&= \frac{1}{2} OX \times OX_t \sin t - \frac{1}{2} OY \times OY_t \sin t \\
&= \frac{a^2}{2} \left(\frac{\sin \alpha_1}{\sin(\alpha_1 - t)} - \frac{\sin \alpha_2}{\sin(\alpha_2 + t)} \right) \sin t \\
&= \frac{a^2 \sin^2 t \sin(\alpha_1 + \alpha_2)}{2 \sin(\alpha_1 - t) \sin(\alpha_2 + t)} \leq 0
\end{aligned}$$

because $t \geq 0$, $\alpha_1 - t, \alpha_2 + t \in [0, \pi]$ and $\alpha_1 + \alpha_2 \in [\pi, 2\pi]$, because Ω is a convex polygon and the side $[XY]$ does not touch ∂C_Ω (see [122, Section 5]).

For the perimeters, we have:

$$\begin{aligned}
P(\Omega_t) - P(\Omega) &= XX_t + OX_t + OY_t - XY - YY_t \\
&= a \left(\frac{\sin t}{\sin(\alpha_1 - t)} + \frac{\sin \alpha_1}{\sin(\alpha_1 - t)} + \frac{\sin \alpha_2}{\sin(\alpha_2 + t)} - 2 - \frac{\sin t}{\sin(\alpha_2 + t)} \right) \\
&= a \left(\frac{\sin t + \sin \alpha_1}{\sin(\alpha_1 - t)} + \frac{\sin \alpha_2 - \sin t}{\sin(\alpha_2 + t)} - 2 \right) \\
&= a \left(\frac{2 \sin\left(\frac{\alpha_1 + t}{2}\right) \cos\left(\frac{\alpha_1 - t}{2}\right)}{2 \sin\left(\frac{\alpha_1 - t}{2}\right) \cos\left(\frac{\alpha_1 - t}{2}\right)} + \frac{2 \sin\left(\frac{\alpha_2 - t}{2}\right) \cos\left(\frac{\alpha_2 + t}{2}\right)}{2 \sin\left(\frac{\alpha_2 + t}{2}\right) \cos\left(\frac{\alpha_2 + t}{2}\right)} - 2 \right) \\
&= a \left(\sqrt{\frac{\sin\left(\frac{\alpha_1 + t}{2}\right)}{\sin\left(\frac{\alpha_1 - t}{2}\right)}} - \sqrt{\frac{\sin\left(\frac{\alpha_1 - t}{2}\right)}{\sin\left(\frac{\alpha_1 + t}{2}\right)}} \right)^2 \geq 0.
\end{aligned}$$

Finally, in a finite number of steps, we get a Cheeger-regular polygon $\tilde{\Omega}$ such that: $|\Omega| \geq |\widetilde{\Omega}|$, $P(\Omega) \leq P(\widetilde{\Omega})$ and $h(\Omega) = h(\widetilde{\Omega})$.

□

Let us now recall the definition of a radial function: let Ω be a starlike planar domain that contains the origin O. We define the radial function $f_\Omega : \mathbb{R} \longrightarrow \mathbb{R}$ of Ω as follows:

$$\forall \theta \in \mathbb{R}, \quad f_\Omega(\theta) = \sup \left\{ t > 0 \mid t \begin{pmatrix} \cos \theta \\ \sin \theta \end{pmatrix} \in \Omega \right\}.$$

In the following Lemma we give some quantitative estimates for the Cheeger constant and area via radial functions, that will be used in the fourth step of Section 2.3.2.

Lemma 6. *Take Ω_1 and Ω_2 two starlike planar domains with radial functions f_1 and f_2 such that $f_1, f_2 \geq r_0$, where $r_0 > 0$.*

We have:

1. $|h(\Omega_1) - h(\Omega_2)| \leq \frac{2}{r_0^2} \times \|f_1 - f_2\|_\infty$.
2. $\big||\Omega_1| - |\Omega_2|\big| \leq \pi \times \max(\|f_1\|_\infty, \|f_2\|_\infty) \times \|f_1 - f_2\|_\infty$

Proof. 1. The proof of this assertion inspired from [59, Proposition 1].

We denote $d = \|f_1 - f_2\|_\infty$, we have $(1 + d/r_0) f_1 \geq (f_2 - d) + d = f_2$, thus:

$$h(\Omega_1) \leq h\left(\frac{1}{1 + d/r_0} \Omega_2 \right) = \left(1 + \frac{d}{r_0} \right) h(\Omega_2) \leq h(\Omega_2) + \frac{d}{r_0} h(B_{r_0}) = h(\Omega_2) + \frac{2d}{r_0^2},$$

where B_{r_0} is the disk of radius r_0.

By similar arguments we obtain:

$$h(\Omega_2) \leq h(\Omega_1) + \frac{2d}{r_0^2},$$

which proves the announced inequality.

2. We have

$$\begin{aligned}\big||\Omega_1| - |\Omega_2|\big| &= \frac{1}{2} \times \left| \int_0^{2\pi} (f_1^2(\theta) - f_2^2(\theta)) d\theta \right| \\ &\leq \frac{1}{2} \int_0^{2\pi} (|f_1(\theta)| + |f_2(\theta)|) \times |f_1(\theta) - f_2(\theta)| d\theta \\ &\leq \pi \times \max(\|f_1\|_\infty, \|f_2\|_\infty) \times \|f_1 - f_2\|_\infty\end{aligned}$$

□

2.3 Proof of the main results

2.3.1 Proof of inequality (2.5)

The proof is done in four steps:

Step 1: Cheeger-regular polygons

Even-though the inequality was already known in this case, we briefly recall the proof for sake of completeness.

Since Ω is a Cheeger-regular polygon, by Theorem 9, we dispose of an explicit formula of its Cheeger constant, we then just have to use Theorem 7 to conclude.

We write:

$$h(\Omega) = \frac{P(\Omega) + \sqrt{P(\Omega)^2 - 4\big(T(\Omega) - \pi\big)|\Omega|}}{2|\Omega|} \geq \frac{P(\Omega) + \sqrt{P(\Omega)^2 - 4\left(\frac{P(\Omega)^2}{4|\Omega|} - \pi\right)|\Omega|}}{2|\Omega|} = \frac{P(\Omega) + \sqrt{4\pi|\Omega|}}{2|\Omega|}.$$

Step 2: General polygons

By Lemma 5, there exists $\tilde{\Omega}$ a Cheeger-regular polygon such that: $|\Omega| \leq |\widetilde{\Omega}|$, $P(\Omega) = P\big(\widetilde{\Omega}\big)$ and $h(\Omega) = h\big(\widetilde{\Omega}\big)$.

Then, we get:

$$h(\Omega) = h\big(\widetilde{\Omega}\big) \geq \frac{P\left(\widetilde{\Omega}\right) + \sqrt{4\pi\left|\widetilde{\Omega}\right|}}{2\left|\widetilde{\Omega}\right|} = \frac{P\big(\widetilde{\Omega}\big)}{2\left|\widetilde{\Omega}\right|} + \frac{\pi}{\sqrt{\left|\widetilde{\Omega}\right|}} \geq \frac{P(\Omega)}{2|\Omega|} + \frac{\pi}{\sqrt{|\Omega|}} = \frac{P(\Omega) + \sqrt{4\pi|\Omega|}}{2|\Omega|}.$$

Step 3: General convex sets

By density of the polygons in $\mathcal{K}^2$ and the continuity of the area, perimeter and Cheeger constant for the Hausdorff distance, we show that the inequality holds for general convex sets.

Step 4: Equality for sets that are homothetical to their form bodies

If Ω is homothetical to its form body (which is in the case of circumscribed polygons), we have by using [164, (7.168)] and equality $\frac{1}{2}r(\Omega)P(\Omega) = |\Omega|$:

$$\forall t \in [0, r(\Omega)], \quad |\Omega_{-t}| = \left(1 - \frac{t}{r(\Omega)}\right)^2 |\Omega| = |\Omega| - P(\Omega)t + \frac{P(\Omega)^2}{4|\Omega|}.$$

Thus, by using Theorem 8 we obtain the equality:

$$h(\Omega) = \frac{P(\Omega) + \sqrt{4\pi|\Omega|}}{2|\Omega|}. \tag{2.10}$$

2.3.2 Proof of the second assertion of Theorem 5 (convex sets)

As explained in the introduction, inequalities (2.3) and (2.5) imply that

$$\mathcal{D}_{\mathcal{K}} \subset \left\{ (x,y) \ \mid \ x \geq x_0 \quad \text{and} \quad \frac{1}{2}x + \sqrt{\pi} \leq y \leq x \right\}.$$

It remains to prove the reverse inclusion. The proof follows the following steps:

1. We explicit a continuous family $(S_p)_{p \geq P(B)}$ of convex bodies which fill the upper boundary of the diagram.
2. We explicit a continuous family $(L_p)_{p \geq P(B)}$ of convex bodies which fill the lower boundary of the diagram.
3. We use the latter domains to construct (via Minkowski sums) a family of continuous paths $(\Gamma_p)_{p \geq P(B)}$ which relate upper domains to lower ones. By continuously increasing the perimeter, we show that we are able to cover all the area between the upper and lower boundaries.

Step 1: The upper boundary of the diagram:

The upper boundary corresponds to domains which are Cheeger of themselves, which means that $C_\Omega = \Omega$. It is shown in [122, Theorem 2] that stadiums (i.e. the convex hull of two identical disks) are Cheeger of themselves, we then use them to fill the upper boundary $\{(x,x) \mid x \geq P(B)\}$.

Let us consider the family of stadiums $(Q_t)_{t \geq 0}$ given by convex hulls of the balls of unit radius centred in $O(0,0)$ and $O_t(0,t)$ rescaled so as $|Q_t| = 1$. The function $t \in [0,+\infty) \longmapsto P(Q_t) = \frac{2(\pi+t)}{\sqrt{\pi+2t}}$ is continuous and strictly increasing. Thus, we have by the intermediate values Theorem:

$$\big\{ \big(P(Q_t), h(Q_t)\big) \mid t \geq 0 \big\} = \big\{ \big(P(Q_t), P(Q_t)\big) \mid t \geq 0 \big\} = \{(x,x) \mid x \geq P(B)\}.$$

Step 2: The lower boundary of the diagram:

Since equality (2.10) holds for sets that are homothetical to their form bodies, we use such domains to fill the lower boundary.

Let us consider the family $(C_d)_{d \geq 2}$ of the so-called symmetrical cup-bodies, which are given by convex hulls of the unit ball (centred in $O(0,0)$ of radius 1) and the points of coordinates $(-d/2, 0)$ and $(d/2, 0)$ rescaled so as $|C_d| = 1$. By using formulae (7) and (8) of [113], we have for every $d \geq 2$:

$$P(C_d) = 2\sqrt{\sqrt{d^2-1} + 2\arcsin\frac{2}{d}}.$$

The function $d \in [2,+\infty) \longmapsto P(C_d) = 2\sqrt{\sqrt{d^2-1} + 2\arcsin\frac{2}{d}}$ is continuous and strictly increasing, this shows by the intermediate values Theorem that:

$$\big\{ \big(P(C_d), h(C_d)\big) \mid d \geq 2 \big\} = \big\{ \big(P(C_t), P(C_t)/2 + \sqrt{\pi}\big) \mid d \geq 2 \big\} = \{(x, x/2 + \sqrt{\pi}) \mid x \geq P(B)\}.$$

Step 3: Continuous paths:

Since the functions $t \in [0,+\infty) \longmapsto P(Q_t) = \frac{2(\pi+t)}{\sqrt{\pi+2t}}$ and $d \in [2,+\infty) \longmapsto P(C_d) = 2\sqrt{\sqrt{d^2-1} + 2\arcsin\frac{2}{d}}$ are continuous and strictly increasing, we have that for every $p \geq P(B)$ there exists a unique

$(t_p, d_p) \in [0,+\infty) \times [2,+\infty)$ such that $P(Q_{t_p}) = P(C_{d_p}) = p$: from now on we denote $S_p := Q_{t_p}$ and $L_p := C_{d_p}$.

For every $p \geq P(B)$, we introduce the closed and continuous path Γ_p :

$$\begin{array}{rcl} \Gamma_p \ : \ [0,3] & \longrightarrow & \mathbb{R}^2 \\ t & \longmapsto & \begin{cases} \big(P(K_p^t), h(K_p^t)\big) & \text{if } t \in [0,1], \\ \big((t-1)P(B) + (2-t)p, (t-1)P(B) + (2-t)(p/2+\sqrt{\pi})\big) & \text{if } t \in [1,2], \\ \big((t-2)P(B) + (3-t)p,\ (t-2)P(B) + (3-t)p)\big) & \text{if } t \in [2,3], \end{cases} \end{array}$$

where

$$K_p^t := \frac{tS_p + (1-t)L_p}{\sqrt{|tS_p + (1-t)L_p|}} \in \mathcal{K}_1^2.$$

The application $t \in [0,1] \longmapsto tS_p + (1-t)L_p \in (\mathcal{K}^2, d^H)$ is continuous and since the measure is continuous for the Hausdorff distance, we deduce that $t \in [0,1] \longmapsto K_p^t \in (\mathcal{K}_1^2, d^H)$ is continuous, thus by continuity of the perimeter and the Cheeger constant for the Hausdorff distance, the path $t \in [0,3] \longmapsto \Gamma_p(t) \in \mathbb{R}^2$ is a continuous curve.

Since the diameters of L_p and S_p are colinear, we can use the results of steps 1. and 3. of the proof of [**ftouhi**], thus we have

$$\forall t \in [0,1], \qquad \frac{p}{2} \leq P(K_p^t) \leq p. \tag{2.11}$$

Step 4: Stability of the paths:

Now, we prove a continuity result on the paths $\big(\Gamma_p\big)_{p \geq P(B)}$: let us take $p_0 \geq P(B)$ and $\varepsilon > 0$, we show that:

$$\exists\ \alpha_\varepsilon > 0, \forall p \in (p_0 - \alpha_\varepsilon, p_0 + \alpha_\varepsilon) \cap [P(B), +\infty), \qquad \sup_{t \in [0,3]} \parallel \Gamma_p(t) - \Gamma_{p_0}(t) \parallel \leq \varepsilon. \tag{2.12}$$

Let us take $p \in [P(B), p_0 + 1]$, with straightforward computations we have that for every $t \in [1,3]$:

$$\|\Gamma_p(t) - \Gamma_{p_0}(t)\| \leq 2|p - p_0| \underset{p \to p_0}{\longrightarrow} 0.$$

The remaining case ($t \in [0,1]$) requires more computations. For every $t \in [0,1]$, we have

$$\|\Gamma_p(t) - \Gamma_{p_0}(t)\| \leq |P(K_p^t) - P(K_{p_0}^t)| + |h(K_p^t) - h(K_{p_0}^t)| \leq \underbrace{\left(2\pi + \frac{(p_0+1)^6}{2}\right)}_{C_{p_0} > 0} d^H(K_p^t, K_{p_0}^t).$$

Indeed, we used:

- for the term with perimeters

$$|P(K_p^t) - P(K_{p_0}^t)| = \left| \int_0^{2\pi} h_{K_p^t} - \int_0^{2\pi} h_{K_{p_0}^t} \right| \leq 2\pi \times \left\| h_{K_p^t} - h_{K_{p_0}^t} \right\|_\infty = 2\pi \times d^H(K_p^t, K_{p_0}^t),$$

- the first assertion of Lemma 6 for the term with the Cheeger constants, with the sets K_p^t and $K_{p_0}^t$ that we assume to contain the origin O and whose radial functions are denoted $f_{p,t}, f_{p_0,t}$.

$$\begin{aligned} |h(K_p^t) - h(K_{p_0}^t)| &\leq \frac{2}{\min\big(r(K_p^t), r(K_p^t)\big)^2} \times \|f_{p,t} - f_{p_0,t}\|_\infty \quad \text{(by Lemma 6)} \\ &\leq \frac{2}{\min\big(r(K_p^t), r(K_p^t)\big)^2} \times \frac{\|f_{p,t}\|_\infty \|f_{p_0,t}\|_\infty}{\min\big(r(K_p^t), r(K_p^t)\big)^2} \times d^H(K_p^t, K_{p_0}^t) \quad \text{(by [37, Proposition 2])} \\ &\leq \frac{(p_0+1)^6}{2} d^H(K_p^t, K_{p_0}^t) \quad \text{(we used } r(\Omega) \geq \frac{|\Omega|}{P(\Omega)} \text{ (see [40]) and } \|f\|_\infty \leq d(\Omega) \leq \frac{P(\Omega)}{2}). \end{aligned}$$

Moreover, we have:

$$
\begin{aligned}
d^H(K_p^t, K_{p_0}^t) &= \left\| h_{K_p^t} - h_{K_{p_0}^t} \right\|_\infty \\
&= \left\| \frac{(1-t)h_{L_{p_0}} + t h_{S_{p_0}}}{\sqrt{|(1-t)L_{p_0} + tS_{p_0}|}} - \frac{(1-t)h_{L_p} + t h_{S_p}}{\sqrt{|(1-t)L_p + tS_p|}} \right\|_\infty \\
&\leq (1-t) \left\| \frac{h_{L_{p_0}}}{\sqrt{|(1-t)L_{p_0} + tS_{p_0}|}} - \frac{h_{L_p}}{\sqrt{|(1-t)L_p + tS_p|}} \right\|_\infty \\
&\quad + t \left\| \frac{h_{S_{p_0}}}{\sqrt{|(1-t)L_{p_0} + tS_{p_0}|}} - \frac{h_{S_p}}{\sqrt{|(1-t)L_p + tS_p|}} \right\|_\infty \\
&\leq \frac{1}{\sqrt{|(1-t)L_p + tS_p|}} \left(\left\| h_{S_{p_0}} - h_{S_p} \right\|_\infty + \left\| h_{L_{p_0}} - h_{L_p} \right\|_\infty \right) \\
&\quad + \left(\left\| h_{S_{p_0}} \right\|_\infty + \left\| h_{L_{p_0}} \right\|_\infty \right) \left| \frac{1}{\sqrt{|(1-t)L_p + tS_p|}} - \frac{1}{\sqrt{|(1-t)L_{p_0} + tS_{p_0}|}} \right| \\
&\leq \left(d^H(S_{p_0}, S_p) + d^H(L_{p_0}, L_p) \right) \\
&\quad + \left(\left\| h_{S_{p_0}} \right\|_\infty + \left\| h_{L_{p_0}} \right\|_\infty \right) \times \Big| \, |(1-t)L_p + tS_p| - |(1-t)L_{p_0} + tS_{p_0}| \, \Big| \\
&\leq \underbrace{\left(d^H(S_{p_0}, S_p) + d^H(L_{p_0}, L_p) \right) + \left(\left\| h_{S_{p_0}} \right\|_\infty + \left\| h_{L_{p_0}} \right\|_\infty \right) \times \sum_{k=0}^{2} |W_k(L_p, S_p) - W_k(L_{p_0}, S_{p_0})|}_{G(p,p_0) \underset{p \to p_0}{\longrightarrow} 0} .
\end{aligned}
$$

Finally, we deduce that $\lim_{p \to p_0} \sup_{t \in [0,3]} \| \Gamma_p(t) - \Gamma_{p_0}(t) \| = 0$, which proves (2.12).

Step 5: Conclusion:

Now that we proved that the boundaries $\{(x,x) \mid x \geq P(B)\}$ and $\{(x, x/2 + \sqrt{\pi}) \mid x \geq P(B)\}$ are included in the diagram $\mathcal{D}_{\mathcal{K}^2}$, it remains to show that it is also the case for the set of points contained between them. We argue by contradiction, assuming that there exists $A(x_A, y_A) \in \{(x,y) \mid x > x_0 \quad \text{and} \quad x/2 + \sqrt{\pi} < y < x\}$, such that $A \notin \mathcal{D}_{\mathcal{K}^2}$.

We consider the function $\phi_A : p \in [P(B), +\infty) \longmapsto \text{ind}(\Gamma_p, A)$, where $\text{ind}(\Gamma_p, A)$ is the index of A with respect to Γ_p (also called the winding number of the closed curve Γ_p around the point A).

- By Step 3 and continuity of the index, the function ϕ_A is constant on $[P(B), +\infty)$.
- By the first inequality of (2.11), for every $p \leq x_A$ the point A is in the exterior of Γ_p, thus $\phi_A(p) = 0$.
- On the other hand, By the second inequality of (2.11), for every $p \geq 2x_A$, the point A is in the exterior of Γ_p, thus $\phi_A(p) \neq 0$.

By the last three points we get a contradiction, thus $A \in \mathcal{D}_{\mathcal{K}^2}$. Finally, we get the equality

$$
\mathcal{D}_{\mathcal{K}^2} = \left\{ (x,y) \mid x \geq x_0 \quad \text{and} \quad \frac{1}{2}x + \sqrt{\pi} \leq y \leq x \right\}.
$$

2.3.3 Proof of the first assertion of Theorem 5 (simply connected sets)

By inequalities (2.3) and (2.4) we have

$$\mathcal{D}_{\mathcal{S}^2} \subset \{(x_0, x_0)\} \cup \{(x, y) \ \mid \ x \geq x_0 \quad \text{and} \quad 0 < y \leq x\}.$$

We have $(x_0, x_0) = \big(P(B), h(B)\big) \in \mathcal{S}^2$. Take $(p, \ell) \in \{(x, y) \ \mid \ x > x_0 \quad \text{and} \quad 0 < y \leq x\}$, let us prove that there exists a simply connected domain $\Omega \subset \mathbb{R}^2$ of unit area such that $P(\Omega) = p$ and $h(\Omega) = \ell$.

If $\ell \geq p/2 + \sqrt{\pi}$, then by the second assertion of Theorem 5 there exists a convex (thus simply connected) domain satisfying the latter properties. Now, let us assume $\ell < p/2 + \sqrt{\pi}$: we take L_p as in the proof of the second assertion of Theorem 5 to be the convex hull of a disk and a point outside it such that $h(L_p) = \ell$ and $|L_p| = 1$. As shown in Figure 2.5, it is possible to continuously deform L_p in such a way to increase its perimeter while keeping constant its area and its Cheeger constant, thus there exists a simply connected set L'_p such that $|L'_p| = 1$, $P(L'_p) = p$ and $h(L'_p) = \ell$, which means that $(p, \ell) \in \mathcal{D}_{\mathcal{S}}$.

Finally, we obtain the equality

$$\mathcal{D}_{\mathcal{S}^2} = \{(x_0, x_0)\} \cup \{(x, y) \ \mid \ x \geq x_0 \quad \text{and} \quad 0 < y \leq x\}.$$

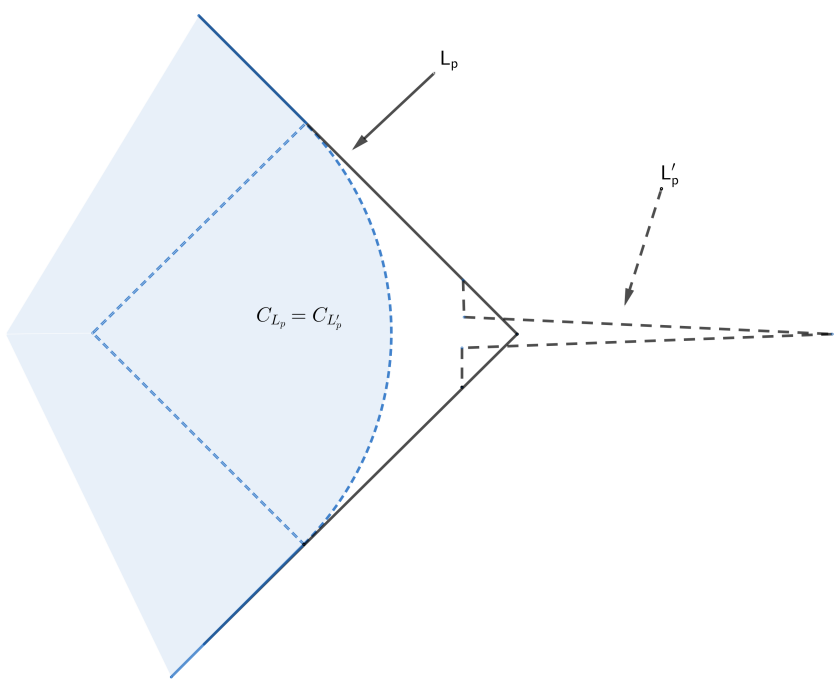

Figure 2.5: Tailed domain L'_p with the same area and Cheeger set and higher perimeter.

2.3.4 Proof of inequality (2.7)

This is a quite direct application of Lemma 4 and the inequality $T(\Omega) \geq N \tan \frac{\pi}{N}$ (see Theorem 7). Indeed, for any $\Omega \in \mathcal{P}_N$, one has:

$$h(\Omega) \leq F(\Omega) = \frac{P(\Omega) + \sqrt{P(\Omega)^2 - 4\big(T(\Omega) - \pi\big)|\Omega|}}{2|\Omega|} \leq \frac{P(\Omega) + \sqrt{P(\Omega)^2 + 4\big(\pi - N \tan \frac{\pi}{N}\big)|\Omega|}}{2|\Omega|}.$$

The first inequality is an equality if and only if Ω is Cheeger-regular and the second one is an equality if and only if $T(\Omega) = N \tan \frac{\pi}{N}$, which is equivalent to $\alpha_1 = ... = \alpha_N = \frac{N-2}{2N}\pi$.

2.3.5 Proof of Theorem 6

If $N = 3$

We have by (2.6):

$$\forall \Omega \in \mathcal{P}_3, \qquad \sqrt{|\Omega|}h(\Omega) = \frac{P(\Omega)}{2\sqrt{|\Omega|}} + \sqrt{\pi},$$

thus we have the inclusion:

$$\mathcal{D}_3 \subset \left\{ \left(x, \frac{x}{2} + \sqrt{\pi} \right) \Big| \ x \geq P(R_3) \right\}.$$

The reverse inclusion is shown by considering for example the family $(T_d)_{d\geq 1}$ of isosceles triangles of vertices $X_d\left(0, \frac{\sqrt{3}}{2}\right)$, $Y_d\left(\frac{d}{2}, 0\right)$ and $Z_d\left(-\frac{d}{2}, 0\right)$.

We have for every $d \geq 1$:

$$\begin{cases} P(R_3) = x_1 \leq x_d := \frac{P(T_d)}{\sqrt{|T_d|}} = \frac{d+\sqrt{d^2+3}}{\frac{3^{1/4}}{2}\sqrt{d}} \underset{d\to+\infty}{\longrightarrow} +\infty \\ h(R_3) = y_1 \leq y_d := \frac{P(T_d)}{2\sqrt{|T_d|}} + \sqrt{\pi} = \frac{d+\sqrt{d^2+3}}{3^{1/4}\sqrt{d}} + \sqrt{\pi} \underset{d\to+\infty}{\longrightarrow} +\infty, \end{cases}$$

where inequalities $x_1 \leq x_d$ and $y_1 \leq y_d$ are consequences of the isoperimetric inequality for triangles.

This shows by using the intermediate value Theorem, that:

$$\left\{ \left(\frac{P(T_d)}{|T_d|^{1/2}}, |T_d|^{1/2}h(T_d) \right) \mid d \geq 1 \right\} = \{(x_d, y_d) \mid d \geq 1\} = \left\{ \left(x, \frac{x}{2} + \sqrt{\pi} \right) \Big| \ x \geq P(R_3) \right\} \subset \mathcal{D}_3,$$

thus, we obtain the equality

$$\mathcal{D}_3 = \left\{ \left(x, \frac{x}{2} + \sqrt{\pi} \right) \Big| \ x \geq P(R_3) \right\}.$$

If N is even

We have by inequalities (2.5) and (2.7):

$$\mathcal{D}_N \subset \left\{ (x, y) \mid x \geq P(R_N) \ \text{ and } \ \frac{x}{2} + \sqrt{\pi} \leq y \leq f_N(x) \right\},$$

where $f_N : x \in [P(R_N), +\infty) \longmapsto \frac{x+\sqrt{x^2+4(\pi - N\tan\frac{\pi}{N})}}{2}$.

It remains to prove the reverse inclusion: we are able to provide explicit families of elements of $\mathcal{P}_N$ that respectively fill the upper and lower boundaries of $\mathcal{D}_N$ and then use those domains to construct continuous paths that fill the diagram.

Step 1: The upper boundary:

We recall that inequality (2.7) is an equality if and only if Ω is Cheeger-regular and all its angles are equal to $(N-2)\pi/N$. A natural family of N-gons that satisfy those two properties is the one obtained by elongating two parallel sides of R_N (the regular N-gon of unit area). Note that the existence of two parallel sides is due to the fact that N is even. We parameterize this family via the diameters of its elements and denote it $(U_\delta)_{\delta \geq d(R_N)}$.

Since the map $\delta \in [P(R_N), +\infty) \longmapsto U_\delta \in (\mathcal{P}_N, d^H)$ is continuous, the perimeter and area are continuous for the Hausdorff distance d^H, $P(U_{d(R_N)}) = P(R_N)$ and

$$\frac{P(U_\delta)}{|U_\delta|^{1/2}} \geq \frac{P(U_\delta)}{\delta^{1/2} \times d(R_N)^{1/2}} \geq \frac{2\delta}{\delta^{1/2} \times d(R_N)^{1/2}} = \frac{2}{d(R_N)^{1/2}} \times \delta^{1/2} \underset{\delta\to+\infty}{\longrightarrow} +\infty, \tag{2.13}$$

we deduce by the intermediate values Theorem that

$$\forall\ p \geq P(R_N), \exists\ \delta_p \geq d(R_N), \qquad \frac{P(U_{\delta_p})}{|U_{\delta_p}|^{1/2}} = p.$$

Moreover, the sets (U_δ) are Cheeger-regular and have all angles equal to $(N-2)\pi/N$, thus they all realise equality in (2.7) :

$$|U_\delta|^{1/2} h(U_\delta) = \frac{P(U_\delta) + \sqrt{P(U_\delta)^2 + 4\big(\pi - N\tan\frac{\pi}{N}\big)|U_\delta|}}{2|U_\delta|^{1/2}} = f_N\left(\frac{P(U_\delta)}{\sqrt{|U_\delta|}}\right).$$

Finally, we deduce that the upper boundary of $\mathcal{D}_N$ is given by the set of points $\big\{\big(x, f_N(x)\big) \ \mid\ x \geq P(R_N)\big\}$.

Step 2: The lower boundary:

As for the upper boundary's case we construct a continuous family of N-gons $(V_\delta)_{\delta \geq d(R_N)}$, such that $V_{d(R_N)} = R_N$ and $d(V_\delta) = \delta$ for every $\delta \geq d(R_N)$. We assume that the diameter of R_N is given by $[OA]$, where $O = (0,0)$ and $A = (d(R_N), 0)$ and denote B_N its incircle (see Figure 2.6) and $M_1, ..., M_N$ its vertices.

Take $\delta \geq d(R_N)$, we denote $A_\delta = (\delta, 0)$ and $(\Delta_\delta), (\Delta'_\delta)$ the lines passing through A_δ which are tangent to B_N. The line (Δ_δ) (resp. (Δ_δ)) cuts the boundary of R_N in two points: we denote $M^\delta_{k_\delta}$ (resp. $M^\delta_{N-k_\delta+1}$) the farthest one from A_δ (see Figure 2.6), where $k_\delta \in [\![1, N/2]\!]$ such that $2k_\delta - 2$ is the number of vertices of R_N that are in the region given by the convex cone delimited by (Δ_δ) and (Δ'_δ). We then define V_δ as the (convex) polygon whose vertices are given by:

$$\begin{cases} M^\delta_1 = M_1 = O, \\ M^\delta_i = M_i, \quad \text{for all } k \in [\![2, k_\delta - 1]\!] \\ M^\delta_{k_\delta} = ... = M^\delta_{\frac{N}{2}} \\ M^\delta_{\frac{N}{2}+1} = A_\delta \\ M^\delta_{\frac{N}{2}+1} = ... = M^\delta_{N+2-k_\delta} \\ M^\delta_i = M_i \quad \text{for all } k \in [\![\frac{N}{2} + 2, N-1]\!] \end{cases}$$

Note that V_δ has at most N sides and that it is a circumscribed polygon which means that it lays on the lower boundary of the diagram $\mathcal{D}_N$. We also, note that the applications $\delta \in [P(R_N), +\infty) \longmapsto M^\delta_k \in \mathbb{R}^2$ are continuous and thus it is also the case for $\delta \in [P(R_N), +\infty) \longmapsto V_\delta \in (\mathcal{P}_N, d^H)$. Then, by similar estimates than (2.13) we get that $\lim\limits_{\delta \to +\infty} \frac{P(V_\delta)}{|V_\delta|^{1/2}} = +\infty$, thus the lower boundary of $\mathcal{D}_N$ is given by the set of points $\big\{\big(x, x/2 + \sqrt{\pi}\big) \ \mid\ x \geq P(R_N)\big\}$.

Step 3: Continuous paths:

Now that we have two families (U_δ) and (V_δ) of extremal shapes, it remains to define continuous paths that relates the upper domains to the lower ones and fill the whole diagram. Unfortunately, unlike for the case of the class $\mathcal{K}^2$, one cannot use Minkowski sums as they increase the number of sides and thus could give polygons that are not in the class $\mathcal{P}_N$, we will then construct the paths paths by continuously mapping the lower and upper polygons vertices.

We assume without loss of generality that as for V_δ the diameter of U_δ is given by OA_δ. We denote by $O = L^\delta_1, L^\delta_2, ..., L^\delta_{N/2-1} = A_\delta, L^\delta_{N/2}, ..., L^\delta_N$ the vertices of U_δ. For $t \in [0,1]$, we define Ω^δ_t as the polygon of vertices $((1-t)M^\delta_k + tL^\delta_k)_{k \in [\![1;N]\!]}$. The polygon Ω^δ_t is convex and included in the rectangle

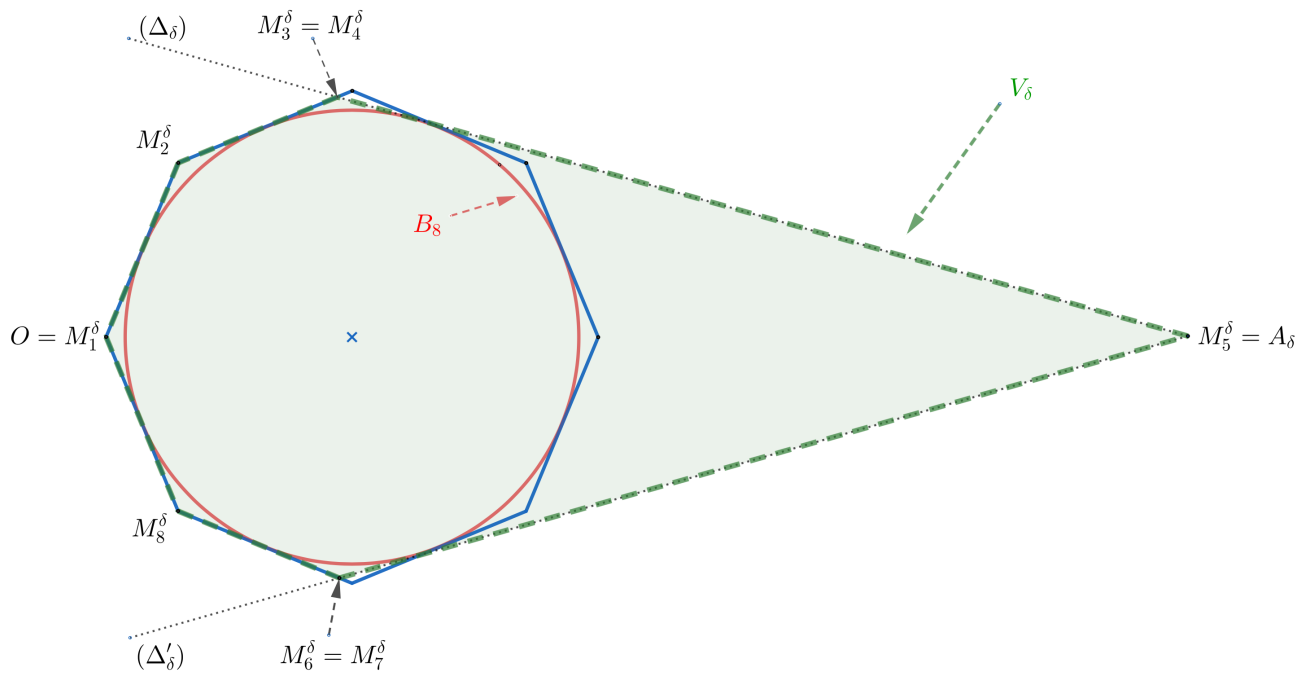

Figure 2.6: Construction of the circumscribed polygons V_δ for $N = 8$.

$(0;\delta) \times \big(0; d(R_N)\big)$, thus we have the following inequality :

$$\forall t \in [0,1], \qquad \frac{P(\Omega_t^\delta)}{|\Omega_t^\delta|^{1/2}} \geq \frac{2\delta}{\delta^{1/2} \times d(R_N)^{1/2}} = \frac{2}{d(R_N)^{1/2}} \times \delta^{1/2}. \tag{2.14}$$

For every $\delta \geq d(R_N)$, we introduce the closed and continuous path γ_δ :

$$\begin{array}{rcl} \gamma_\delta \quad : \quad [0,3] & \longrightarrow & \mathbb{R}^2 \\ t & \longmapsto & \begin{cases} \left(\frac{P(\Omega_t^\delta)}{|\Omega_t^\delta|^{1/2}}, |\Omega_t^\delta|^{1/2} h(\Omega_t^\delta)\right) & \text{if } t \in [0,1], \\ \left((t-1)P(R_N) + (2-t)\frac{P(V_\delta)}{|V_\delta|^{1/2}}\ ,\ (t-1)P(R_N) + (2-t)\frac{P(V_\delta)}{2|V_\delta|^{1/2}} + \sqrt{\pi}\right) & \text{if } t \in [1,2], \\ \left((t-2)P(R_N) + (3-t)\frac{P(U_\delta)}{|U_\delta|^{1/2}}\ ,\ (t-2)P(R_N) + (3-t)\frac{P(U_\delta)}{|U_\delta|^{1/2}}\right) & \text{if } t \in [2,3], \end{cases} \end{array}$$

Step 4: Stability of the paths:

Take $\delta_0 \geq d(R_N)$ and $\varepsilon > 0$, let us show that

$$\exists\ \alpha_\varepsilon > 0, \forall \delta \in (\delta_0 - \alpha_\varepsilon, \delta_0 + \alpha_\varepsilon) \cap [P(R_N), +\infty), \qquad \sup_{t\in[0,3]} \parallel \gamma_\delta(t) - \gamma_{\delta_0}(t) \parallel \leq \varepsilon. \tag{2.15}$$

Let us take $\delta \in [d(R_N), \delta_0 + 1]$, with straightforward computations we have that for every $t \in [1,3]$:

$$\|\gamma_\delta(t) - \gamma_{\delta_0}(t)\| \leq 2 \min\left(\left|\frac{P(U_\delta)}{|U_\delta|^{1/2}} - \frac{P(U_{\delta_0})}{|U_{\delta_0}|^{1/2}}\right|, \left|\frac{P(V_\delta)}{|V_\delta|^{1/2}} - \frac{P(V_{\delta_0})}{|V_{\delta_0}|^{1/2}}\right|\right) \underset{\delta\to\delta_0}{\longrightarrow} 0.$$

Moreover, by the quantitative estimates of Section 2.2, there exist constants $C(\delta_0), C'(\delta_0) > 0$ depending only on δ_0 such that for all $\delta \in [d(R_N), \delta_0 + 1]$ and all $t \in [0,1]$

$$\begin{aligned}
\|\gamma_\delta(t) - \gamma_{\delta_0}(t)\| &\leq \left| \frac{P(\Omega_t^\delta)}{|\Omega_t^\delta|^{1/2}} - \frac{P(\Omega_t^{\delta_0})}{|\Omega_t^{\delta_0}|^{1/2}} \right| + \left| |\Omega_t^\delta|^{1/2} h(\Omega_t^\delta) - |\Omega_t^{\delta_0}|^{1/2} h(\Omega_t^{\delta_0}) \right| \\
&\leq C(\delta_0) \times \Big(|P(\Omega_t^\delta) - P(\Omega_t^{\delta_0})| + \Big| |\Omega_t^\delta| - |\Omega_t^{\delta_0}| \Big| + |h(\Omega_t^\delta) - h(\Omega_t^{\delta_0})| \Big) \\
&\leq C'(\delta_0) \times \max_{i \in [\![1,N]\!]} \|(1-t)M_i^\delta + tL_i^\delta - (1-t)M_i^{\delta_0} - tL_i^{\delta_0}\| \\
&\leq C'(\delta_0) \times \max_{i \in [\![1,N]\!]} (\|M_i^\delta - M_i^{\delta_0}\| + \|L_i^\delta - L_i^{\delta_0}\|) \underset{\delta \to \delta_0}{\longrightarrow} 0.
\end{aligned}$$

Finally, we deduce that $\lim_{\delta \to \delta_0} \sup_{t \in [0,3]} \| \gamma_\delta(t) - \gamma_{\delta_0}(t)\| = 0$, which proves (2.15).

Step 5: Conclusion:

As for the case of convex sets, once we proved that the boundaries $\{\big(x, f_N(x)\big) \ \mid \ x \geq P(R_N)\}$ and $\{(x, x/2 + \sqrt{\pi}) \ \mid \ x \geq P(R_N)\}$ are included in the diagram $\mathcal{D}_N$, it remains to show that it is also the case for the zone between them. We argue by contradiction, assuming that there exists $A(x_A, y_A) \in \{(x,y) \ \mid \ x > P(R_N) \quad \text{and} \quad x/2 + \sqrt{\pi} < y < x\}$, such that $A \notin \mathcal{D}_N$.

We consider the function $\psi_A : \delta \in [d(R_N), +\infty) \longmapsto \text{ind}(\gamma_\delta, A)$, where $\text{ind}(\gamma_p, A)$ is the index of A with respect to γ_δ (also called the winding number pf the closed curve γ_δ around the point A).

- By Step 4 and the continuity of the index, the function ψ_A is constant on $[P(R_N), +\infty)$.
- By the estimates above (step 4), for δ sufficiently close to δ_0 the point A is in the interior of γ_δ, thus $\psi_A(\delta) = 0$.
- On the other hand, by inequality (2.14), the point A is in the interior of γ_δ for sufficiently high values of δ, thus $\psi_A(\delta) \neq 0$.

By the last three points we get a contradiction, thus $A \in \mathcal{D}_N$. Finally, we get the equality

$$\mathcal{D}_N = \left\{ (x,y) \ \mid \ x \geq P(R_N) \quad \text{and} \quad \frac{1}{2}x + \sqrt{\pi} \leq y \leq f_N(x) \right\}.$$

If N is odd

By inequalities (2.5) and (2.7), we have:

$$\mathcal{D}_N \subset \{(x,y) \mid x \geq P(R_N) \text{ and } x/2 + \sqrt{\pi} \leq y \leq f_N(x)\}.$$

Let us study the upper and lower boundaries of the diagram $\mathcal{D}_N$.

Lower boundary:

Since $N-1$ is even, we have by Section 2.3.5 that:

$$\{(x, x/2 + \sqrt{\pi}) \mid x \geq P(R_{N-1})\} \subset \mathcal{P}_{N-1} \subset \mathcal{P}_N.$$

It remains to prove that $\{(x, x/2 + \sqrt{\pi}) \mid x \in [P(R(N), P(R_{N-1})]\} \subset \mathcal{P}_N$. To do so, we continuously move two consecutive sides of the polygon R_N so as to align them while keeping the polygon circumscribed, this gives us a continuous (for the Hausdorff distance) family $(W_t)_{t \in [0,1]}$ of convex inscribed polygons such that $W_0 = R_N$ and W_1 is an element of $\mathcal{P}_{N-1}$, see Figure 2.7.

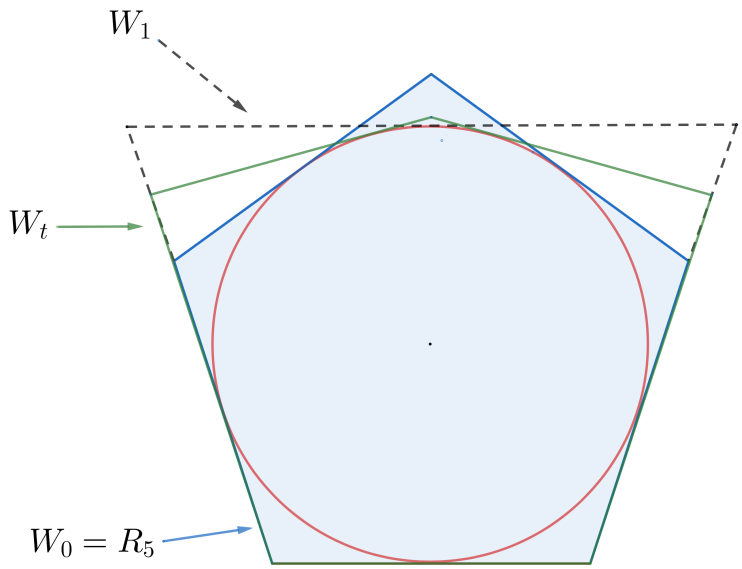

Figure 2.7: Construction of the circumscribed polygons W_t.

Since the map $t \in [0,1] \longmapsto W_t \in (\mathcal{K}^2, d^H)$ is continuous, the functionals perimeter, area and Cheeger constant are continuous on $(\mathcal{K}^2, d^H)$ and $\frac{P(W_1)}{\sqrt{|W_1|}} \geq P(R_{N-1})$ (because of the polygonal isoperimetric inequality in $\mathcal{P}_{N-1}$), we have by the intermediate values Theorem:

$$\{(x, x/2 + \sqrt{\pi}) \mid x \in [P(R_N), P(R_{N-1})]\} \subset \left\{ \left(\frac{P(W_t)}{\sqrt{|W_t|}}, \sqrt{|W_t|} h(W_t) \right) \;\middle|\; t \in [0,1] \right\} \subset \mathcal{D}_N.$$

We finally have:

$$\{(x, x/2 + \sqrt{\pi}) \mid x \in [P(R(N), +\infty)\} \subset \mathcal{P}_N.$$

Upper boundary:

Let us now study the upper boundary. We introduce the function

$$\begin{array}{rccl} g_N : & [P(R_N), +\infty) & \longrightarrow & \mathbb{R} \\ & p & \longmapsto & \sup\{h(\Omega) \mid \Omega \in \mathcal{P}_N, \quad |\Omega| = 1 \text{ and } P(\Omega) = p\} \end{array} \tag{2.16}$$

First, let us prove that the problem $\sup\{h(\Omega) \mid \Omega \in \mathcal{P}_N, \quad |\Omega| = 1 \text{ and } P(\Omega) = p\}$ admits a solution, that we denote $\Omega_p \in \mathcal{P}_N$.

Take $(\Omega_p^n)_{n\in\mathbb{N}}$ sequence of elements of $\mathcal{P}_N$ such that $|\Omega_p^n| = 1$ and $P(\Omega_p^n) = p$ for every $n \in \mathbb{N}$ which satisfies

$$\lim_{n\to+\infty} h(\Omega_p^n) = \sup\{h(\Omega) \mid \Omega \in \mathcal{P}_N, \quad |\Omega| = 1 \text{ and } P(\Omega) = p\}.$$

Since the diameters of the sets (Ω_p^n) are all bounded by p and the involved functionals are invariant by translations, we may assume without loss of generality that there exist a fixed ball $D \subset \mathbb{R}^2$ that contains all the polygons Ω_p^n. Let us denote $A_1^n, ..., A_N^n$ the vertices of Ω_p^n, the sequences $(A_1^n), ..., (A_N^n)$ are bounded in $\mathbb{R}^2$, thus, by Bolzano-Weirstrass Theorem, there exist $\sigma : \mathbb{N} \longrightarrow \mathbb{N}$ strictly increasing

and $A_1, ..., A_N \in \mathbb{R}^2$ such that $\lim_{n\to+\infty} A_k^{\sigma(n)} = A_k$. By elementary arguments of convex geometry one shows that the points $A_1, ..., A_N$ are the vertices of a convex polygon Ω_p which is also the limit of $(\Omega_p^{\sigma(n)})_n$ for Hausdorff distance. By the continuity of the perimeter, the volume and the Cheeger constant for the Hausdorff distance among convex sets, we have:

$$\begin{cases} |\Omega_p| = \lim_{n\to+\infty} |\Omega_p^{\sigma(n)}| = 1 \\ P(\Omega_p) = \lim_{n\to+\infty} P\big(\Omega_p^{\sigma(n)}\big) = p \\ h(\Omega_p) = \lim_{n\to+\infty} h\big(\Omega_p^{\sigma(n)}\big) = \sup\left\{h(\Omega) \mid \Omega \in \mathcal{P}_N, \quad |\Omega| = 1 \text{ and } P(\Omega) = p\right\}. \end{cases}$$

Finally, we conclude that $\Omega_p \in \mathcal{P}_N$ is a solution of the problem $\sup\left\{h(\Omega) \mid \Omega \in \mathcal{P}_N, \quad |\Omega| = 1 \text{ and } P(\Omega) = p\right\}$.

Next, let us prove the stated properties of the function g_N.

1) The function g_N is continuous

Let $p_0 \in [P(R_N), +\infty)$

- We first show an **superior limit inequality**. Let $(p_n)_{n\geq 1}$ real sequence converging to p_0 such that

$$\limsup_{p\to p_0} h(\Omega_p) = \lim_{n\to+\infty} h(\Omega_{p_n}).$$

  As the perimeter of $(\Omega_{p_n})_{n\in\mathbb{N}^*}$ is uniformly bounded, one may assume that the domains $(\Omega_{p_n})_{n\in\mathbb{N}^*}$ are included in a fixed ball: then by similar arguments than above, (Ω_{p_n}) converges to a convex polygon $\Omega^* \in \mathcal{P}_N$ for the Hausdorff distance, up to a subsequence that we also denote p_n for simplicity.

  Again, by the continuity of the perimeter, the volume and the Cheeger constant for the Hausdorff distance among convex sets, we have:

$$\begin{cases} |\Omega^*| = \lim_{n\to+\infty} |\Omega_{p_n}| = 1 \\ P(\Omega^*) = \lim_{n\to+\infty} P(\Omega_{p_n}) = \lim_{n\to+\infty} p_n = p_0 \\ h(\Omega^*) = \lim_{n\to+\infty} h(\Omega_{p_n}) = \limsup_{p\to p_0} h(\Omega_p) \end{cases}$$

  Then by definition of g_N (since $\Omega^* \in \mathcal{P}_N$, $|\Omega^*| = 1$ and $P(\Omega^*) = p_0$), we obtain:

$$g_N(p_0) \geq \ h(\Omega^*) = \lim_{n\to+\infty} h(\Omega_{p_n}) = \limsup_{p\to p_0} h(\Omega_p) = \limsup_{p\to p_0} g_N(p).$$

- It remains to prove **an inferior limit inequality**. Let $(p_n)_{n\geq 1}$ be a real sequence converging to p_0 such that:

$$\liminf_{p\to p_0} g_N(p) = \lim_{n\to+\infty} g_N(p_n).$$

  By using parallel chord movements (see the proof of Lemma 5), we can construct a sequence of unit area polygons $(K_n)_{n\geq 1}$ with at most N sides, converging to Ω_{p_0} for Hausdorff distance such that $P(K_n) = p_n$ for sufficiently high values of $n \in \mathbb{N}^*$.

  By using the definition of g_N one can write

$$\forall n \in \mathbb{N}^*, \qquad g_N(p_n) \geq h(K_n).$$

  Passing to the limit, we get:

$$\liminf_{p\to p_0} g_N(p) = \lim_{n\to+\infty} g_N(p_n) \geq \lim_{n\to+\infty} h(K_n) = h(\Omega_{p_0}) = g_N(p_0).$$

As a consequence we finally get $\lim_{p\to p_0} g_N(p) = g_N(p_0)$, so g_N is continuous on $[P(R_N), +\infty)$.

2) The function g_N is strictly increasing

Let us assume by contradiction that g_N is not strictly increasing, then there exist $p_2 > p_1 \geq P(R_N)$ such that $g_N(p_2) < g_N(p_1)$, and from the equality case in the polygonal isoperimetric inequality, we necessarily have $p_1 > P(R_N)$. Since g is continuous, it reaches its maximum on $[P(R_N), p_2]$ at a point $p^* \in (P(R_N), p_2)$, that is to say

$$\forall \Omega \in \mathcal{P}_N \text{ such that } |\Omega| = 1 \text{ and } P(\Omega) \in [P(R_N), p_2], \;\; h(\Omega_{p^*}) = g_N(p^*) \geq h(\Omega). \tag{2.17}$$

We note that $g_N(p^*) > p^*/2 + \sqrt{\pi}$, indeed if it is not the case (i.e $g_N(p^*) = p^*/2 + \sqrt{\pi}$) we have for $h > 0$:

$$g_N(p^* + h) \geq (p^* + h)/2 + \sqrt{\pi} > p^*/2 + \sqrt{\pi} = g_N(p^*),$$

this contradicts the fact that g_N admits a local maximum at p^*.

(3.17) shows that Ω_{p^*} is a local maximizer of the Cheeger constant between convex N-gons of unit area. On the other hand, the fact that $h(\Omega_{p^*}) = g_N(p^*) > \frac{P(\Omega_{p^*}) + \sqrt{4\pi|\Omega_{p^*}|}}{2|\Omega_{p^*}|}$ implies that Ω_{p^*} is not a circumscribed polygon. Let us now show that any non-circumscribed polygon Ω (ie. $T(\Omega) < \frac{P(\Omega)^2}{4|\Omega|}$) could be perturbed (while preserving the number of sides) in such a way to increase $|\Omega|^{1/2}h(\Omega)$.

We denote $(\ell_i)_{i\in[\![1;N]\!]}$ the lengths of the sides of the polygon Ω and $(\alpha_i)_{i\in[\![1;N]\!]}$ its inner angles and denote

$$r_0 := \min_{1\leq i\leq N} \frac{\ell_i}{\tan\left(\frac{\pi}{2} - \frac{\alpha_i}{2}\right) + \tan\left(\frac{\pi}{2} - \frac{\alpha_{i-1}}{2}\right)}$$

We distinguish two cases:

- If $|\Omega| - r_0 P(\Omega) + r_0^2(T(\Omega) - \pi) \geq 0$, this means by [122, Theorem 3] that there exists a side of Ω that does not touch the Cheeger set C_Ω or touch it in one point. We consider a parallel displacement of this side as shown in Figure 2.8. For $\varepsilon > 0$ sufficiently small, the polygons Ω and Ω_ε have the same Cheeger set, thus we have $|\Omega_\varepsilon|^{1/2}h(\Omega_\varepsilon) > |\Omega|^{1/2}h(\Omega)$.

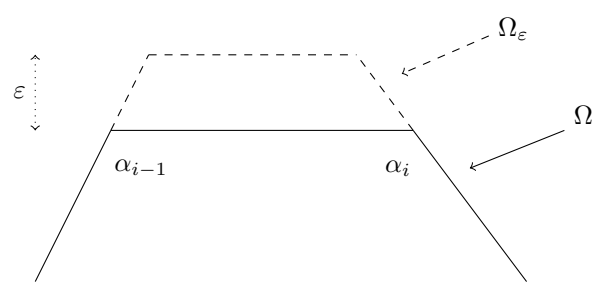

Figure 2.8: Parallel displacement of one side.

- On the other hand if $|\Omega| - r_0 P(\Omega) + r_0^2(T(\Omega) - \pi) < 0$, then by [122, Theorem 3], the polygons Ω and Ω_ε (for $|\varepsilon|$ sufficiently small) are Cheeger-regular and thus we have an explicit expression of their Cheeger constants.

  We have for $|\varepsilon|$ sufficiently small

$$|\Omega_\varepsilon|^{1/2}h(\Omega_\varepsilon) = \frac{P(\Omega_\varepsilon) + \sqrt{P(\Omega_\varepsilon)^2 - 4(T(\Omega_\varepsilon) - \pi)|\Omega_\varepsilon|}}{\sqrt{|\Omega_\varepsilon|}} = \frac{P(\Omega_\varepsilon)}{\sqrt{|\Omega_\varepsilon|}} + \sqrt{\frac{P(\Omega_\varepsilon)^2}{|\Omega_\varepsilon|} - 4(T(\Omega) - \pi)}, \tag{2.18}$$

where we used $T(\Omega) = T(\Omega_\varepsilon)$ for the last equality.

As stated in the proof of [50, Lemma 23] through elementary geometric arguments, we have

$$\begin{cases} P(\Omega_\varepsilon) &= P(\Omega) + \left(\frac{1}{\tan\alpha_{i-1}} + \frac{1}{\tan\alpha_i} + \frac{1}{\sin\alpha_{i-1}} + \frac{1}{\sin\alpha_i}\right) \times \varepsilon, \\ |\Omega_\varepsilon| &= |\Omega| + \ell_i \times \varepsilon + \frac{1}{2}\left(\frac{1}{\tan\alpha_{i-1}} + \frac{1}{\tan\alpha_i}\right) \times \varepsilon^2. \end{cases}$$

Thus :

$$\begin{aligned} \frac{P(\Omega_\varepsilon)^2}{|\Omega_\varepsilon|} &= \frac{\left(P(\Omega) + \left(\frac{1}{\tan\alpha_{i-1}} + \frac{1}{\tan\alpha_i} + \frac{1}{\sin\alpha_{i-1}} + \frac{1}{\sin\alpha_i}\right) \times \varepsilon\right)^2}{|\Omega| + \ell_i \times \varepsilon + \frac{1}{2}\left(\frac{1}{\tan\alpha_1} + \frac{1}{\tan\alpha_2}\right) \times \varepsilon^2} \\ &= \frac{P(\Omega)^2}{|\Omega|} + P(\Omega) \underbrace{\left(2\left(\frac{1}{\tan\alpha_{i-1}} + \frac{1}{\tan\alpha_i} + \frac{1}{\sin\alpha_{i-1}} + \frac{1}{\sin\alpha_i}\right) - \frac{P(\Omega)}{|\Omega|}\ell_i\right)}_{\Psi_i} \times \varepsilon + \underset{\varepsilon\to 0}{o}(\varepsilon). \end{aligned}$$

Let us show that there exists $i \in [\![1; N]\!]$ such that $\Psi_i \neq 0$. We assume by contradiction that $\Psi_i = 0$ for every $i \in [\![1; N]\!]$, we then have

$$\sum_{i=1}^{N} \Psi_i = 0,$$

which is equivalent to

$$P(\Omega) = \frac{4|\Omega|}{P(\Omega)} \times \sum_{i=1}^{N}\left(\frac{1}{\tan\alpha_i} + \frac{1}{\sin\alpha_i}\right) = \frac{4|\Omega|}{P(\Omega)} \times \sum_{i=1}^{N} \frac{1}{\tan\frac{\alpha_i}{2}} = \frac{4|\Omega|}{P(\Omega)} \times T(\Omega).$$

As stated in Theorem 7, this equality holds if and only if Ω is a circumscribed polygon, which is not the case as assumed above. Thus, there exists $i \in [\![1; N]\!]$ such that $\Psi_i \neq 0$, then by performing a parallel displacement (in the suitable sense) of the ith side, one is able to strictly increase $P(\Omega)/|\Omega|^{1/2}$ which by (2.18) increases $|\Omega|^{1/2}h(\Omega)$.

3) Comparison between g_N and f_N and asymptotic

- It is immediate by the inclusion $\mathcal{P}_{N-1} \subset \mathcal{P}_N$ and inequality (2.7) that $f_{N-1} \leq g_N \leq f_N$ on $[P(R_N), +\infty)$.
- If we perform parallel displacement of one of the sides of the regular polygon R_N we obtain a continuous (for Hausdorff distance) family of Cheeger regular polygons $(\Omega_\varepsilon)_{\varepsilon\in[0,\varepsilon_0)}$ with the same angles as R_N such that $P(\Omega_\varepsilon)|\Omega_\varepsilon|^{1/2} > P(\Omega)|\Omega|^{1/2}$ for every $\varepsilon \in (0, \varepsilon_0)$, this proves that there exists $b_N \geq P(\Omega_{\varepsilon_0})/|\Omega_{\varepsilon_0}|^{1/2} > P(R_N)$ such that for every $p \in [P(R_N), b_N]$ we have $g_N(p) = \frac{p+\sqrt{p^2+4(\pi - N\tan\frac{\pi}{N})}}{2} = f_N(p)$.
- Let us prove that if Ω is a unit area polygon of N sides whose angles are all equal (to $\beta_N := \frac{N-2}{2N}\pi$), one has
$$P(\Omega) \leq \frac{2N}{\sqrt{\tan\frac{\beta_N}{2}}} \tag{2.19}$$
Let us assume that $\Omega \subset \{y \geq 0\}$ and its longest side is given by the segment $[OA]$ where $A(\ell, 0)$ and $\ell > 0$. Since N is odd and all the angles of Ω are equal, we deduce that there exists a unique vertex $B(x_B, \eta)$ which is strictly higher (ie. has the largest ordinate) than all other vertices. We can assume without loss of generality that $x_B \geq \ell/2$. As shown in Figure 2.9, by convexity of Ω, the line obtained by extending the left side of extremity B intersects the axis of abscissa in a point $C(x_C, 0)$ such that $x_C \leq 0$.

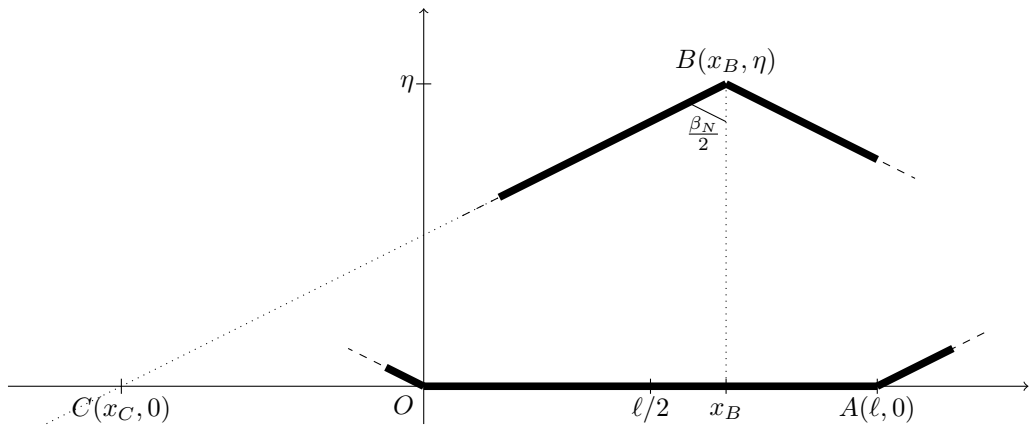

Figure 2.9: An N-gon with all angles equal to β_N.

We have

$$\frac{1}{\tan\frac{\beta_N}{2}} = \operatorname{cotan}\frac{\beta_N}{2} = \frac{\eta}{x_B - x_C} = 2\frac{\frac{1}{2}\ell\eta}{\ell(x_B - x_C)} = 2\frac{\mathcal{S}_{OAB}}{\ell(x_B - x_C)} \leq \frac{4}{\ell^2},$$

where the last inequality is a consequence of $\mathcal{S}_{OAB} \leq 1$ (because $OAB \subset \Omega$) and $x_B - x_C \geq x_B \geq \ell/2$.

Thus, we have the result

$$P(\Omega) \leq N\ell \leq \frac{2N}{\sqrt{\tan\frac{\beta_N}{2}}}.$$

This proves that there is no polygon of unit area, N sides and perimeter larger than $\frac{2N}{\sqrt{\tan\frac{\beta_N}{2}}}$ whose inner angles are all equal (to β_N).

Thus for every $\Omega \in \mathcal{P}_N$ such that $|\Omega| = 1$ and $P(\Omega) \geq \frac{2N}{\sqrt{\tan\frac{\beta_N}{2}}}$, we have

$$h(\Omega) \leq \frac{P(\Omega) + \sqrt{P(\Omega)^2 - 4\big(T(\Omega) - \pi\big)|\Omega|}}{2|\Omega|} < \frac{P(\Omega) + \sqrt{P(\Omega)^2 + 4\big(\pi - N\tan\frac{\pi}{N}\big)|\Omega|}}{2|\Omega|} = f_N\big(P(\Omega)\big),$$

where the first inequality is (2.7) and the second (strict) one is a consequence of Theorem 7.

We finally have that:

$$\forall p > \frac{2N}{\sqrt{\tan\frac{\beta_N}{2}}}, \qquad g_N(p) < f_N(p).$$

- Since $N \geq 4$, we have

$$\forall x \geq P(R_{N-1}), \qquad \frac{x + \sqrt{x^2 + 4(\pi - (N-1)\tan\frac{\pi}{N-1})}}{2} = f_{N-1}(x) \leq g_N(x) \leq f_N(x).$$

Thus

$$g_N(x) \underset{x\to+\infty}{\sim} x.$$

2.4 Numerical simulations

Since it does not seem to be easy to explicitly find the upper boundary of the diagram $\mathcal{D}_N$ when N is odd, we perform some simulations in order to have an approximation of the function g_N; we numerically solve the following problems:

$$\max\left\{h(\Omega) \mid \Omega \in \mathcal{P}_N, \quad |\Omega| = 1 \text{ and } P(\Omega) = p_0\right\}, \tag{2.20}$$

where $p_0 \in [P(R_N), +\infty)$.

2.4.1 Parameterization of the domains

we parameterize a polygon Ω via its vertices' coordinates $A_1(x_1, y_1), ..., A_N(x_N, y_N)$.

- Let us first express the constraint of convexity in terms of the coordinates of the vertices of Ω. It is classical that Ω is convex if and only if all the interior angles are less than or equal to π. By using the cross product (see [19] for example), this, is equivalent to the constraints

  $$C_k(x_1, ..., x_N, y_1, ..., y_N) := (x_{k-1} - x_k)(y_{k+1} - y_k) - (y_{k-1} - y_k)(x_{k+1} - x_k) \leq 0,$$

  for $k = 1, ..., N$, where we used the conventions $A_0 = A_N$ and $A_{N+1} = A_1$.

- The volume and the perimeter of Ω are given by the following formulae

  $$\begin{cases} f(x_1, ..., x_N, y_1, ..., y_N) & := \quad P(\Omega) \ = \sum_{k=1}^{N} \sqrt{(x_{k+1} - x_k)^2 + (y_{k+1} - y_k)^2}, \\ g(x_1, ..., x_N, y_1, ..., y_N) & := |\Omega| \ = \ \frac{1}{2}\left|\sum_{k=1}^{N}(x_k y_{k+1} - x_{k+1} y_k)\right| \end{cases}$$

- Finally, we introduce the function

  $$\phi : (x_1, ..., x_N, y_1, ..., y_N) \longmapsto \begin{cases} h(\Omega) & \text{if the polygon } \Omega \text{ does not have overlapping sides} \\ -1 & \text{if the polygon } \Omega \text{ does have overlapping sides} \end{cases}$$

  where Ω is the polygon of vertices $A_1(x_1, y_1), ..., A_N(x_N, y_N)$. The Cheeger constant is computed by using an open source code of Beniamin Bogosel [30] based on the results of [122].

We are now able to write the Problem (2.20) in the following form

$$\begin{cases} \sup\limits_{(x_1,...,y_N)\in\mathbb{R}^{2N}} \phi(x_1, ..., y_N), \\ \forall k \in [\![1, N]\!], \quad C_k(x_1, ..., x_N, y_1, ..., y_N) \leq 0, \\ f(x_1, ..., x_N, y_1, ..., y_N) = p_0 \\ g(x_1, ..., x_N, y_1, ..., y_N) = 1. \end{cases}$$

2.4.2 Computation of the gradients

We want to use Matlab's routine `fmincon` to solve the last problem, to do so we should compute the gradients of the constraints C_k, f, g and the objective function ϕ.

C_k, f, g are explicitly expressed via usual functions of $(x_1, ..., y_N)$, we then have by easy computations explicit formulae for the gradients. This is not the case for the objective function ϕ. We use the following shape derivative formula of the Cheeger constant proved in [153]:

$$h'(\Omega, V) := \lim_{t\to 0} \frac{h(\Omega_t) - h(\Omega)}{t} = \frac{1}{|C_\Omega|} \int_{\partial C_\Omega \cap \partial\Omega} \big(-h(\Omega)\big)\langle V, n\rangle d\mathcal{H}^1,$$

where $V \in \mathbb{R}^2 \longrightarrow \mathbb{R}^2$ is a smooth perturbation, $\Omega_t = (Id + tV)(\Omega)$, $n(x)$ is the normal to $\partial\Omega$ at the point x and is the curvature of $\partial\Omega$ at the point x.

Since Ω is a convex polygon and C_Ω is $C^{1,1}$, we have $\mathcal{K}^2 appa = 0$ on $\partial C_\Omega \cap \partial\Omega$. Thus, if we denote V_{x_k} and V_{y_k} the perturbations respectively associated to the variables x_k and y_k, where $k \in [\![1, N]\!]$, we have :

$$\begin{cases} \frac{\partial \phi}{\partial x_k}(x_1, ..., x_N, y_1, ..., y_N) &= -\frac{h(\Omega)}{|C_\Omega|} \int_{\partial C_\Omega \cap \partial\Omega} \langle V_{x_k}, n \rangle d\mathcal{H}^1, \\ \frac{\partial \phi}{\partial y_k}(x_1, ..., x_N, y_1, ..., y_N) &= -\frac{h(\Omega)}{|C_\Omega|} \int_{\partial C_\Omega \cap \partial\Omega} \langle V_{y_k}, n \rangle d\mathcal{H}^1 \end{cases}$$

2.4.3 Results

In Figure 2.10, we plot the points corresponding to 1000 random convex pentagons and the points corresponding to the optimal pentagons obtained for $p_0 \in \{P(R_5) + 0.02 \times k \mid k \in [\![1, 100]\!]\}$, in addition to the curves representing Inequalities (2.3) and (2.7). We note (as proved in Theorem 6) that for small values of p_0, the points corresponding to the optimal domains are exactly located on the curve of the function f_5 (that represents inequality (2.7)) which is no longuer the case for those corresponding to larger values of p_0.

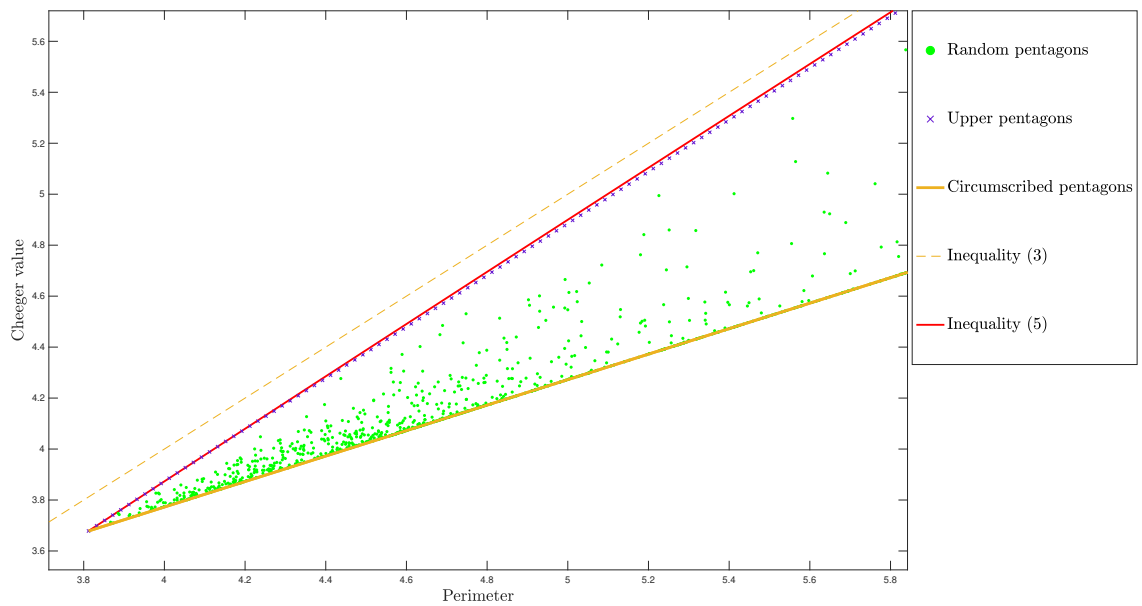

Figure 2.10: Blaschke-Santaló diagram of convex pentagons.

We give in the Figure 2.11 a zoom on the upper boundary, where one notes that the points corresponding to the upper pentagons are at first exactly located on the red curve corresponding to inequality (2.7) and then come off and become strictly lower than it. We numerically note that the abscissa b_5 introduced in the statement of Theorem 6 is indeed (as proven in the present paper) bounded from above by $\frac{10}{\sqrt{\tan\frac{3\pi}{20}}}$.

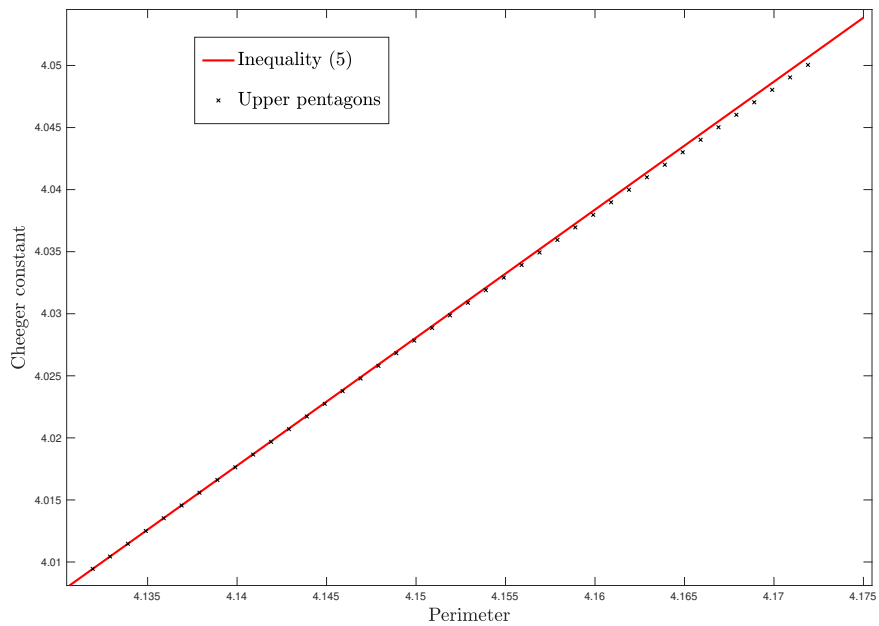

Figure 2.11: A zoom on the upper boundary.

Finally, we give the obtained optimal shapes for $p_0 \in \{3.86, 4, 5\}$. We note that for larger values of p_0 the maximizers seem not to be Cheeger-regular.

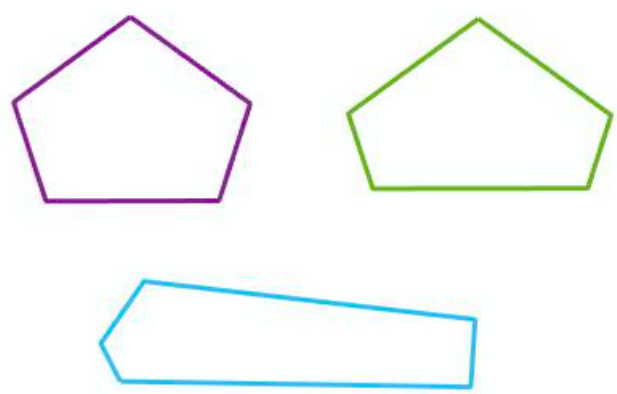

Figure 2.12: Optimal pentagons obtained for $p_0 \in \{3.86, 4, 5\}$.

Remark 3. *Our numerical approach is validated by testing it on the cases for which we have a theoretical description our the boundary, namely:*

- *The lower boundary of the diagrams $\mathcal{D}_N$, where $N \geq 3$, which is given as stated in Theorem 6 by:*
$$\{(x, x/2 + \sqrt{\pi}) \mid x \geq P(R_N)\}.$$
- *The upper boundary of the diagrams $\mathcal{D}_N$, where N is even, which is given as stated in Theorem 6 by:*
$$\left\{ \left(x, \frac{x + \sqrt{x^2 + 4(\pi - N \tan \frac{\pi}{N})}}{2} \right) \;\middle|\; x \geq P(R_N) \right\}.$$

In both cases, satisfying results were obtained.

2.5 Some applications

We give some applications of the results and ideas developed in this paper.

2.5.1 First application

One early result in the spirit of inequality (2.5) is due to R. Brooks and P. Waksman, see Theorem 2 below. It gives a lower estimate of the Cheeger constant of convex polygons, which we show to be a consequence inequality (2.5).

Proposition 2. *[48, Th 3.] If Ω is a convex polygon, we denote Ω^* the (unique up to rigid motions) circumscribed polygon which has the same area as Ω and whose angles are the same as those of Ω, then*

$$h(\Omega) \geq h(\Omega^*) = \frac{\sqrt{T(\Omega)} + \sqrt{\pi}}{\sqrt{|\Omega|}}, \tag{2.21}$$

with equality if and only if $\Omega = \Omega^*$ (up to rigid motions).

Proof. We show inequality (2.5) gives an alternative proof.

$$h(\Omega) \geq \frac{P(\Omega) + \sqrt{4\pi|\Omega|}}{2|\Omega|} \geq \frac{2\sqrt{|\Omega|}\sqrt{T(\Omega)} + \sqrt{4\pi|\Omega|}}{2|\Omega|} = \frac{\sqrt{T(\Omega)} + \sqrt{\pi}}{\sqrt{|\Omega|}} = \frac{\sqrt{T(\Omega^*)} + \sqrt{\pi}}{\sqrt{|\Omega^*|}},$$

where we respectively used (2.5) and (2.8) for the first and second inequalities and the fact that Ω^* has the same area and angles as Ω for the last equality. By Theorem 7 the second inequality is an equality if and only if Ω is circumscribed, in this case the first inequality becomes also an equality.

On the other hand, since Ω^* is an inscribed polygon, we have $T(\Omega^*) = P(\Omega^*)^2/(4|\Omega^*|)$ (by Theorem 7) and $h(\Omega^*) = \frac{P(\Omega^*)+\sqrt{4|\Omega^*|}}{2|\Omega^*|}$.

Thus:

$$\frac{\sqrt{T(\Omega^*)} + \sqrt{\pi}}{\sqrt{|\Omega^*|}} = h(\Omega^*).$$

This ends the proof. □

2.5.2 Second application: on the stability of the Cheeger constant of polygons

We use inequality (2.5) and [52, Proposition 2.1] to give a quantitative version of the Faber-Krahn type inequality for convex polygons:

Proposition 3. *Take $N \geq 3$. There exists a positive constant C_N such that for every convex unit area N-gon Ω there exists a rigid motion ρ of $\mathbb{R}^2$ such that*

$$h(\Omega)^2 - h(\Omega_N)^2 \geq C_N d^H\big(\Omega, \rho(\Omega_N)\big)^2. \tag{2.22}$$

Proof. Take $N \geq 3$ and a N-gon Ω, we have by inequality (2.5)

$$P(\Omega) \leq 2(h(\Omega) - \sqrt{\pi}) \qquad \text{and} \qquad P(\Omega_N) = 2(h(\Omega_N) - \sqrt{\pi}),$$

thus

$$\begin{aligned} P(\Omega)^2 - P(\Omega_N)^2 \quad &\leq \quad 4(h(\Omega) - \sqrt{\pi})^2 - 4(h(\Omega_N) - \sqrt{\pi})^2 \\ &= \quad 4\big(h(\Omega)^2 - h(\Omega_N)^2 - 2\sqrt{\pi}\big(h(\Omega) - h(\Omega_N)\big)\big) \\ &\leq \quad 4\big(h(\Omega)^2 - h(\Omega_N)^2\big), \end{aligned}$$

where the last inequality is a consequence of the polygonal Faber-Krahn type inequality $h(\Omega) \geq h(\Omega_N)$.

On the other hand, it is proved in [52, Proposition 2.1], that there exists $C_N > 0$ depending only on N such that

$$P(\Omega)^2 - P(\Omega_N)^2 \geq 4C_N d^H\big(\Omega, \rho(\Omega_N)\big)^2,$$

combining with the latest inequality we get the announced result. □

Remark 4. *The quantitative inequality* (2.22) *shows in particular the stability of the Cheeger constant in the neighborhood of regular polygons between convex polygons with the same number of sides, in the sense that if the Cheeger constant of a convex polygon is close to the one of the unit area regular polygon with the same number of sides, then the polygon looks (up to rigid motions) like the latter one. A similar result can be obtained for non convex N-gons, see [53].*

Chapter 3

Blaschke-Santaló diagrams for the volume, the perimeter and the first Dirichlet eigenvalue

This chapter is a reprint of the paper ***Blaschke-Santaló diagram for volume, perimeter and first Dirichlet eigenvalue*** *[92], in collaboration with Jimmy Lamboley, accepted for publication in SIAM Journal on Mathematical Analysis.*

Abstract

We are interested in the study of Blaschke-Santaló diagrams describing the possible inequalities involving the first Dirichlet eigenvalue, the perimeter and the volume, for different classes of sets. We give a complete description of the diagram for the class of open sets in $\mathbb{R}^d$, basically showing that the isoperimetric and Faber-Krahn inequalities form a complete system of inequalities for these three quantities. We also give some qualitative results for the Blaschke-Santaló diagram for the class of planar convex domains: we prove that in this case the diagram can be described as the set of points contained between the graphs of two continuous and increasing functions. This shows in particular that the diagram is simply connected, and even horizontally and vertically convex. We also prove that the shapes that fill the upper part of the boundary of the diagram are smooth ($C^{1,1}$), while those on the lower one are polygons (except for the ball). Finally, we perform some numerical simulations in order to have an idea on the shape of the diagram; we deduce both from theoretical and numerical results some new conjectures about geometrical inequalities involving the functionals under study in this paper.

3.1 Introduction

In this paper, we are interested in describing all possible geometrical inequalities that are invariant under homotheties and involving the three following quantities: the volume, the perimeter, and the first Dirichlet eigenvalue of a given shape.

A Blaschke-Santaló diagram is a tool that allows to visualize all possible inequalities between three quantities depending on the shape of a set: it was named as a reference to [28] and [163], where the authors were looking for the description of inequalities involving three geometrical quantities for a given convex set. Usually in convex geometry, Blaschke-Santaló diagrams are studied for purely geometrical fuctionals. We refer to [110] for more details and to [26, 70, 71] for some recent results in this purely geometrical setting.

More recently, some interest has grown for geometrical inequalities involving the spectral quantities of a given shape $\Omega \subset \mathbb{R}^d$, like the eigenvalues of the Laplacian on the set Ω with Dirichlet boundary conditions on $\partial\Omega$: therefore, the approach by Blaschke-Santaló diagrams has been applied in this context, see for example [49] and [13], see also [24, 138].

In the present paper, we propose to study an example mixing geometric and spectral quantities. In order to be more precise, let us define the Blaschke-Santaló diagrams we are interested in in this paper: given $\mathcal{C}$ a class of open sets of $\mathbb{R}^d$, we define

$$\begin{aligned}\mathcal{D}_{\mathcal{C}} &= \Big\{(x,y)\in\mathbb{R}^2,\ \ \exists\Omega\in\mathcal{C} \text{ such that } |\Omega|=1, P(\Omega)=x, \lambda_1(\Omega)=y\Big\}\\ &:= \Big\{\ \big(P(\Omega),\lambda_1(\Omega)\big),\ \Omega\in\mathcal{C},\ |\Omega|=1\ \Big\},\end{aligned}$$

where $|\Omega|$ denotes the volume of the set Ω, $P(\Omega)=\mathcal{H}^{d-1}(\partial\Omega)$ is its perimeter, and $\lambda_1(\Omega)$ is its first Dirichlet eigenvalue, which can be quickly defined with the following variational formulation:

$$\lambda_1(\Omega) := \min\left\{\frac{\displaystyle\int_\Omega |\nabla u|^2 dx}{\displaystyle\int_\Omega u^2 dx},\ u\in H^1_0(\Omega)\setminus\{0\}\right\}, \tag{3.1}$$

where $H^1_0(\Omega)$ denotes the completion for the H^1-norm of the space $C^\infty_c(\Omega)$ of infinitely differentiable functions of compact support in Ω. We recall the following behavior with respect to homothety:

$$\forall t>0,\quad \lambda_1(t\Omega)=\frac{\lambda_1(\Omega)}{t^2},\qquad |t\Omega|=t^d|\Omega| \qquad\text{and}\qquad P(t\Omega)=t^{d-1}P(\Omega).$$

This allows us to give a scaling invariant formulation of the diagram: if $\mathcal{C}$ is a class of nonempty and bounded open sets in $\mathbb{R}^d$, then

$$\begin{aligned}\mathcal{D}_{\mathcal{C}} &= \Big\{(x,y)\in\mathbb{R}^2,\ \ \exists\Omega\in\mathcal{C} \text{ such that } P(\Omega)/|\Omega|^{\frac{d-1}{d}}=x,\ \ |\Omega|^{\frac{2}{d}}\lambda_1(\Omega)=y\Big\}\\ &:= \left\{\left(\frac{P(\Omega)}{|\Omega|^{\frac{d-1}{d}}}, |\Omega|^{\frac{2}{d}}\lambda_1(\Omega)\right),\ \ \Omega\in\mathcal{C}\right\}.\end{aligned}$$

We are now in position to state the first main result in this paper:

Theorem 10. *Let $\mathcal{O}$ be the class of C^∞ open sets in $\mathbb{R}^d$, we have:*

$$\mathcal{D}_{\mathcal{O}} = \Big(\big(P(B),+\infty\big)\times\big(\lambda_1(B),+\infty\big)\Big)\cup\big\{\big(P(B),\lambda_1(B)\big)\big\},$$

where B is a ball of volume 1.

Let us give a few comments on this result:

- the most famous inequalities in this framework are the isoperimetric and the Faber-Krahn inequalities, stating that

$$\forall\Omega\in\mathcal{O} \text{ such that } |\Omega|=1,\quad P(\Omega)\geq P(B)\qquad\text{and}\qquad \lambda_1(\Omega)\geq\lambda_1(B). \tag{3.2}$$

  In terms of the diagram, it says that $\mathcal{D}_{\mathcal{O}}$ is included in the "up-right" quadrant defined by the point $(P(B),\lambda_1(B))$. Theorem 10 asserts that the diagram is in fact exactly this quadrant (see the next point for a discussion about whether the boundary of the quadrant should be included or not in the diagram); in other words, inequalities given in (3.2) are exhaustive in the sense that any other inequality that is invariant with homotheties and only involves the three quantities $(P,\lambda_1,|\cdot|)$ are already taken into account in (3.2); we say that this is a complete system of inequalities in the class $\mathcal{O}$.

- one could wonder why we chose to work with C^∞ domains: the main reason is that there are several definitions of perimeter, that all agree for smooth enough sets (say Lipschitz sets) but may disagree for nonsmooth sets. In the smooth framework, the equality cases in (3.2), up to translations, occurs if and only if Ω is the ball B (see for example [147, Section 2] and [120, Example 2.11] respectively for the first and second inequalities). It explains why the boundary of the quadrant (except the point $(P(B), \lambda_1(B))$) is not included in the diagram. Also, it shows that Theorem 11 is the strongest statement in the sense that for any subclass of Lipschitz domains that contains C^∞-domains, the diagram is the same.

  However, when working with nonsmooth domains, equality in (3.2) may happen for sets different from a ball. If we choose to work with the De Giorgi's perimeter for example, one has $P(B) = P(B\backslash K)$, for any Borel set K with zero Lebesgue measure. On the other hand, for the Faber-Krahn inequality, we have $\lambda_1(B) = \lambda_1(B\backslash K)$ as soon as K is a set of zero capacity, see for example [106, Remark 3.2.2]. In remark 5 we deduce from Theorem 10 a full description of the diagram for the class of non necessarily smooth sets when P is the perimeter of De Giorgi: this description could be different for another definition of the perimeter, but as shown by Theorem 10, this can only affect the boundary of the diagram.

It is now natural to restrict the class of sets, so that the corresponding Blaschke-Santaló diagram becomes more challenging to understand: a natural class that has been extensively studied in the purely geometrical context is the class of planar convex sets. The Blaschke-Santaló diagram of $(P, \lambda_1, |\cdot|)$ in this specific case has been first numerically studied by P. Antunes and P. Freitas in [12]. We would like to give a theoretical description of the diagram, in the same spirit of [49, 26] . We obtain the following main result:

Theorem 11. *Let $\mathcal{K}^2$ be the class of convex planar open sets:*

$$\mathcal{K}^2 = \Big\{\Omega \subset \mathbb{R}^2,\ \ \Omega \text{ is convex and open}\Big\}.$$

We denote $x_0 = P(B) = 2\sqrt{\pi}$, where B is a disk of area 1. Then there exist two functions $f : [x_0, +\infty) \to \mathbb{R}$ and $g : [x_0, +\infty) \to \mathbb{R}$ such that

1. *the diagram $\mathcal{D}_{\mathcal{K}^2}$ is made of all points in $\mathbb{R}^2$ lying between the graphs of f and g, more precisely:*

$$\mathcal{D}_{\mathcal{K}^2} = \Big\{(x, y) \in \mathbb{R}^2,\ x \geq x_0 \quad \text{and} \quad f(x) \leq y \leq g(x)\Big\}, \tag{3.3}$$

2. *the functions f and g are continuous and strictly increasing,*

3. *for every $x > x_0$, let $\Omega \in \mathcal{K}^2$ such that $|\Omega| = 1$ and $\lambda_1(\Omega) = x$, then*

   - *if $P(\Omega) = g(x)$, then Ω is $C^{1,1}$,*
   - *if $P(\Omega) = f(x)$, then Ω is a polygon.*

4. $f(x) \underset{x\to\infty}{\sim} \frac{\pi^2}{16}x^2, \qquad g(x) \underset{x\to\infty}{\sim} \frac{\pi^2}{4}x^2, \qquad f'(x_0) = 0 \quad \text{and} \quad \limsup_{x\to x_0} \frac{g(x)-g(x_0)}{x-x_0} \geq \frac{\lambda_1(B)}{3\sqrt{\pi}}\left(\frac{\lambda_1(B)}{\pi} - 2\right).$

Let us comment about this result and its proof:

- this result gives a good understanding of the shape of the diagram $\mathcal{D}_{\mathcal{K}^2}$: it says in particular that it is simply connected, and even horizontally and vertically convex.

- in other words, the knowledge of f and g is enough to describe all possible (scaling invariant) inequalities involving the three quantities $(P, \lambda_1, |\cdot|)$, in the class of convex sets of $\mathbb{R}^2$: these functions quantify in which way one can improve inequalities (3.2) if one knows that the shape Ω is convex, and not only just an open set.

- of course, it is not expected to have an explicit formula for functions f and g. Up to our knowledge, Theorem 11 is one of the first qualitative and complete description of a Blaschke-Santaló diagram while we do not have a good knowledge of the shapes that achieve the boundary of the diagram. Compare with [24, 138] where it is still an open problem whether the Blaschke-Santaló diagram for the triplet $(\lambda_1, T, |\cdot|)$ where T denotes the torsional rigidity, is simply connected (or horizontally and vertically convex, which is a stronger statement), both for the class of open domains (see [24, Problem 3]) and for the class of convex domains ([138, Conjecture 2]).

- the proof of the first two points in Theorem 11 is therefore the most involved part of this paper (see also Section 3.3.2); it relies in particular on a perturbation lemma (see Lemma 7) among convex sets and involving functionals P, λ_1 and $|\cdot|$, which states that if we denote $\mathcal{K}_1^2$ the set of planar convex domains with unit area endowed with the Hausdorff distance d^H, then

  1. the ball is the only local minimizer of the perimeter, as well as the only local minimizer of λ_1, in $(\mathcal{K}_1^2, d^H)$
  2. however, there is no local maximizer of the perimeter in $(\mathcal{K}_1^2, d^H)$, and no local maximizer of λ_1 that is $C^{1,1}$.

  We believe this Lemma is interesting in itself; its second part is not easy to prove at all. It uses the tools and results of shape optimization under convexity constraints studied in [132, 134, 133]. It mainly explains the restriction to dimension 2. Up to our knowledge, the results given in Theorem 11 or in Lemma 7 are open in dimension 3 or higher. We also denote $\mathcal{K}^d$ the set of convex open subsets of $\mathbb{R}^d$ when $d \geq 3$, and $\mathcal{D}_{\mathcal{K}^d}$ denotes the associated Blaschke-Santaló diagram. Notice that some results from Section 3.3.2 are stated and proved in arbitrary dimensions (see Propositions 4 and 6). In Section 3.4.2, we discuss the case of higher dimensions and conjecture that as for the planar case, $\mathcal{D}_{\mathcal{K}^d}$ is given by the set of points contained between two continuous and increasing curves, see Conjecture 5.

- the third assertion provides some regularity (or non-regularity) properties for domains lying on the boundary of the diagram. If follows from results of [134], see Corollary 3. We note that to be able to apply [134], we have to prove a Serrin's type lemma on convex sets, where no regularity assumption is made: see Lemma 8, which is given for arbitrary dimensions and is rather interesting in itself. The $C^{1,1}$ regularity of the upper optimal domains allows us to restrict the fourth assertion of the perturbation Lemma 7 to the case of smooth domains, which is easier to prove, see also [130].

- though it is not expected to compute explicitly f and g, the last point in Theorem 11 provides some results about the asymptotic behavior of f and g near $+\infty$ and near $x_0 = P(B)$, see Proposition 6, Corollary 5 (which are stated and proved in arbitrary dimensions), and Corollary 7 (which is proved only in dimension 2). We actually provide an improvement to the result $f'(x_0) = 0$, which is the main novelty about these asymptotics: more precisely, investigating the lower part of the diagram for x close to $P(B)$ is related to the following question: for what exponent α may we expect that there is an inequality of the form

  $$\lambda_1(\Omega) - \lambda_1(B) \geq c\,(P(\Omega) - P(B))^\alpha$$

  for $\Omega \in \mathcal{K}_1^2$ close to the ball and for some $c > 0$ independent of Ω. We show in the second part of Theorem 14 that α must necessarily be greater or equal to $3/2$ for such an inequality to be valid, and we show evidence that such an inequality is likely to be true with $\alpha = 3/2$ (see the first part of Theorem 14 and Proposition 8) even though we are not yet in position to prove it, see Section 3.4.1. Finally, we compare the conjectured inequality (with the exponent $3/2$) with the sharp quantitative Faber-Krahn inequality proved in [42], see Remark 11.

In the following section, we give a proof of Theorem 10. In Section 3.3, we focus on the case of convex planar domains: we first recall theoretical information that was known about the diagram, and provide numerical simulations. We then prove the main lemma about perturbation results in the class of convex sets in $\mathbb{R}^2$ (Lemma 7), and then deduce that the boundary of the diagram is made of the graph of two increasing and continuous functions (see Theorem 12), and furthermore that the diagram is simply connected (see Theorem 13). This eventually leads to the proof of Theorem 11. We also describe the asymptotics of f and g near $+\infty$ and x_0, see Proposition 6 and Section 3.3.3. In the last Section, we discuss related problems and new possible conjectures.

3.2 Proof of Theorem 10

As explained below the statement of Theorem 10, the inclusion

$$\mathcal{D}_{\mathcal{O}} \subset \Big(\big(P(B),+\infty\big) \times \big(\lambda_1(B),+\infty\big)\Big) \cup \big\{\big(P(B),\lambda_1(B)\big)\big\}$$

is due to the isoperimetric and Faber-Krahn inequalities with equality cases, see for example [147, Section 2] and [120, Example 2.11]. It remains to show the reverse inclusion.

Step 1: we first show, using a homogenization strategy, that for any $\mu \in (0,+\infty)$, there exists a sequence $(\Omega_n)_{n\in\mathbb{N}}$ of C^∞ open sets with unit area such that:

$$P(\Omega_n) \underset{n\to+\infty}{\longrightarrow} P(B) \tag{3.4}$$

and

$$\lambda_1(\Omega_n) \underset{n\to+\infty}{\longrightarrow} \lambda_1(B)+\mu. \tag{3.5}$$

Let $n \in \mathbb{N}^*$, we cover $\mathbb{R}^d$ by cubes $(P_i^n)_{i\in\mathbb{N}}$ of size $2/n$. From each cube P_i^n such that $P_i^n \subset B$ we remove the ball T_i^n of radius $a_{d,n}$ centered at the center of the cube, where:

$$a_{d,n} = \begin{cases} C_d n^{-d/(d-2)} & \text{if } d \geq 3, \\ \exp\big(-C_2 n^2\big) & \text{if } d = 2 \end{cases} \qquad \text{and} \qquad C_d = \begin{cases} \left(\frac{2^d \mu}{d(d-2)\omega_d}\right)^{\frac{1}{d-2}} & \text{if } d \geq 3, \\ 2\mu/\pi & \text{if } d = 2, \end{cases}$$

with ω_d classically denoting the volume of the unit ball.

We consider n sufficiently big so that $a_{d,n} < \frac{1}{n}$. Let us define $\Lambda_n := B \setminus \bigcup_{i\in I_n} T_i^n$, Where $I_n := \{i \in \mathbb{N} \mid P_i^n \subset B\}$.

In order to preserve the total measure, we use the sets $\Omega_n = \Lambda_n \cup \bigcup_{i\in I_n} (v_d + T_i^n)$ which are smooth and with unit volume, where $v_d \in \mathbb{R}^d$ is chosen such that $B \cap \bigcup_{i\in I_n} (v_d + T_i^n) = \emptyset$ (see Figure 3.1).

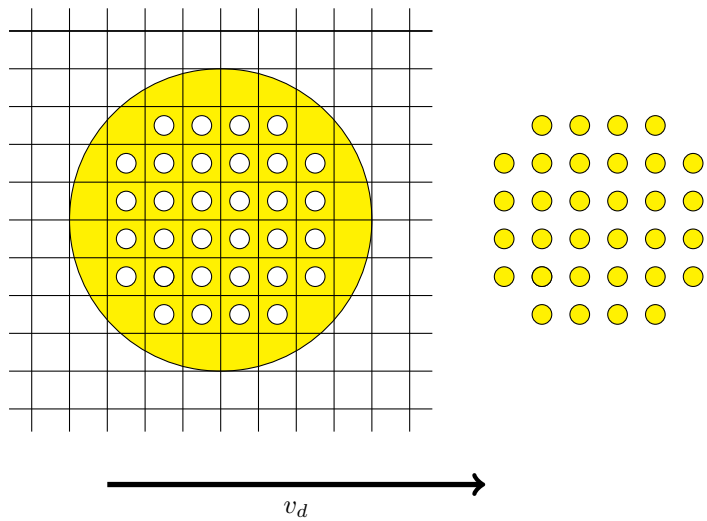

Figure 3.1: The domains Ω_n

We have:

$$P(\Omega_n) = P(B) + 2 \times \mathrm{Card}(I_n) P(T_1^n) \leq P(B) + M_d n^d a_{d,n}^{d-1} \underset{n\to\infty}{\longrightarrow} P(B),$$

where M_d dimensional constant.

Let $A_n : L^2(B) \to L^2(B)$ be the resolvent operator of the Dirichlet Laplacian on Λ_n, which associates to $f \in L^2(B)$ the unique solution $u \in H_0^1(\Lambda_n)$ to $-\Delta u = f$, extended by zero outside Λ_n.

[58, Theorem 1.2] shows that, for every $f \in L^2(B)$, $A_n(f)$ strongly converges to $A(f)$ in $L^2(B)$, where A is the resolvent operator of $-\Delta + \mu$ in $H^1(B)$ with Dirichlet boundary conditions on ∂B. In particular, in view of [106, Theorem 2.3.2], the eigenvalues of A_n converge to the corresponding eigenvalue of A; as a consequence, we have $\lim\limits_{n\to+\infty} \lambda_1(\Lambda_n) = \lambda_1(B) + \mu$. This implies $\lim\limits_{n\to+\infty} \lambda_1(\Omega_n) = \lim\limits_{n\to+\infty} \lambda_1(\Lambda_n) = \lambda_1(B) + \mu$.

Step 2: In this step, we analyze the effect on the perimeter and the first Dirichlet eigenvalue of adding a flat ellipsoid to a given open set, rescaled so that the total volume remains 1.

Given Ω a smooth open set of volume 1, as well as $\varepsilon \in (0,1)$ and $\alpha \in (-\infty, 1]$, we consider $\Omega^{\varepsilon,\alpha} := \left[\left(1-\varepsilon^d\right)^{\frac{1}{d}} \Omega\right] \cup E^{\varepsilon,\alpha}$, where $E^{\varepsilon,\alpha}$ is a translated and rescaled version of

$$\left\{ (x_1, ..., x_d) \in \mathbb{R}^d \quad | \quad \frac{x_1^2}{\varepsilon^{2(1-\alpha)d+2\alpha}} + \frac{1}{\varepsilon^{2\alpha}} \sum_{k=2}^{d} x_k^2 < 1 \right\}$$

so that $\left[\left(1-\varepsilon^d\right)^{\frac{1}{d}} \Omega\right] \cap E^{\varepsilon,\alpha} = \emptyset$ and $|E^{\varepsilon,\alpha}| = \varepsilon^d$. Note first that $|\Omega^{\varepsilon,\alpha}| = (1-\varepsilon^d) + \varepsilon^d = 1$.
Then for every $\alpha \leq 1$ and $\varepsilon \in (0,1)$ we have by Faber-Krahn inequality:

$$\lambda_1(E^{\varepsilon,\alpha}) \geq \lambda_1\left(\varepsilon \frac{B_1}{|B_1|^{1/d}}\right) = |B_1|^{2/d} \lambda_1(B_1) \times \frac{1}{\varepsilon^2},$$

where B_1 is a ball of unit radius.

Since $\left[\left(1-\varepsilon^d\right)^{\frac{1}{d}} \Omega\right] \cap E^{\varepsilon,\alpha} = \emptyset$, we have that $\lambda_1(\Omega^{\varepsilon,\alpha}) = \min\left(\lambda_1\left((1-\varepsilon^d)^{\frac{1}{d}}\Omega\right), \lambda_1(E^{\varepsilon,\alpha})\right)$, which leads to the following fact:

$$\text{if } \varepsilon \text{ is such that } \frac{\lambda_1(\Omega)}{(1-\varepsilon^d)^{\frac{2}{d}}} \leq |B_1|^{2/d} \lambda_1(B_1) \times \frac{1}{\varepsilon^2}, \text{ then } \lambda_1(\Omega^{\varepsilon,\alpha}) = \lambda_1\left((1-\varepsilon^d)^{\frac{1}{d}}\Omega\right) = \frac{\lambda_1(\Omega)}{(1-\varepsilon^d)^{2/d}}. \tag{3.6}$$

On the other hand, given $\varepsilon \in (0,1)$, it is clear that the function $\alpha \in (-\infty, 1] \mapsto P(\Omega^{\varepsilon,\alpha})$ is continuous, and we have

$$P(\Omega^{\varepsilon,1}) = P((1-\varepsilon^d)^{1/d}\Omega) + P(E^{\varepsilon,1}) = (1-\varepsilon^d)^{1-1/d}P(\Omega) + \gamma_d \varepsilon^{d-1} \qquad \text{and} \qquad P(\Omega^{\varepsilon,\alpha}) \underset{\alpha\to-\infty}{\longrightarrow} +\infty, \tag{3.7}$$

where γ_d is the perimeter of the unit ball.

Conclusion: let $x > P(B)$ and $y > \lambda_1(B)$. We want to prove that there exists Ω a smooth open set of unit volume such that $P(\Omega) = x$ and $\lambda_1(\Omega) = y$. To that end, we use the previous steps, and will adjust the parameters $\mu \in (0,+\infty)$, $n \in \mathbb{N}$, $\varepsilon \in (0,1)$, $\alpha \in (-\infty, 1]$.

- First, we use step 1 above that leads to the existence of a sequence of open sets $(\Omega_n)_{n\in\mathbb{N}}$ of unit volume and such that $P(\Omega_n)$ converges to $P(B)$ and $\lambda_1(\Omega_n)$ converges to $\lambda_1(B)+\mu$ where μ will be chosen later.

- For each $n \in \mathbb{N}$, we then use the second step to obtain $\Omega_n^{\varepsilon,\alpha}$ for $\varepsilon \in (0,1)$ and $\alpha \in (-\infty, 1]$. We notice now that

  $$\text{if } \lambda_1(\Omega_n) < y \text{ then one can find } \varepsilon_n = \varepsilon_n(y) \in (0,1) \text{ such that } y = \frac{\lambda_1(\Omega_n)}{(1-\varepsilon_n^d)^{2/d}}.$$

  We therefore assume from now on that $\mu < y - \lambda_1(B)$ and n is large enough so that $\lambda_1(\Omega_n) < y$. By assuming also that μ is close to $y - \lambda_1(B)$, we have $\lambda_1(\Omega_n)$ as close to y as we want for n large enough, and then clearly ε_n is close to 0.

  In particular this implies $\frac{\lambda_1(\Omega_n)}{(1-\varepsilon_n^d)^{\frac{2}{d}}} \le \frac{|B_1|^{2/d}\lambda_1(B_1)}{\varepsilon_n^2}$, so using (3.6), this leads to

  $$\lambda_1(\Omega_n^{\varepsilon_n,\alpha}) = y,$$

  independently of $\alpha \in (-\infty, 1]$.

- Finally, as we just noticed that one can assume ε_n as small as we want, and as $P(\Omega_n)$ is close to $P(B)$ if n is large, the first formula in (3.7) shows that $P(\Omega_n^{\varepsilon_n,1}) \le x$, and therefore by continuity of $\alpha \in (-\infty, 1] \mapsto P(\Omega^{\varepsilon_n,\alpha})$ and using the second part of (3.7), we deduce that there exists α such that $P(\Omega_n^{\varepsilon_n,\alpha}) = x$.

This concludes the proof.

Remark 5. *As explained in the introduction (comments on Theorem 10), if $\mathcal{O}'$ is a class of open domains that may contain nonsmooth sets, say for example the class of open subsets of $\mathbb{R}^d$, the diagram $\mathcal{D}_{\mathcal{O}'}$ depends on the choice of the perimeter. For example, if we consider the distributional (De Giorgi's) perimeter, we are able to prove*

$$\mathcal{D}_{\mathcal{O}'} = \Big(\big[P(B),+\infty\big) \times \big(\lambda_1(B),+\infty\big)\Big) \cup \big\{\big(P(B),\lambda_1(B)\big)\big\},$$

which differs from $\mathcal{D}_{\mathcal{O}}$ as it contains the vertical half-line $\{(P(B),\ell), \quad \ell > \lambda_1(B)\}$.

- *if we take $\Omega \in \mathcal{O}'$ such that $\lambda_1(\Omega) = \lambda_1(B)$, then the H^1-capacity of the symmetrical difference $\Omega\Delta B$ is equal to zero, which also implies that its d-dimensional Lebesgue measure is also equal to zero. Thus since the distributional perimeter doesn't detect sets with zero d-dimensional Lebesgue measure we have $P(\Omega) = P(B)$, and thus the horizontal half line $(P(B),+\infty) \times \{\lambda_1(B)\}$ is not in the diagram.*

- *On the other hand, if we take $\ell > \lambda_1(B)$, we are able to construct a set $K_\ell \in \mathcal{O}'$ with unit measure such that $P(K_\ell) = P(B)$ and $\lambda_1(K_\ell) = \ell$. Let us introduce $r_0, r_1 > 0$, such that:*

– r_1 *is the radius of the ball* $B \subset \mathbb{R}^d$ *of unit measure.*

– r_0 *is chosen such that* $\lambda_1\big(\{x \in \mathbb{R}^d, \quad \|x\| < r_0\}\big) = \ell$*, so in particular* $r_0 < r_1$*.*

One can then choose $N_\ell \in \mathbb{N}^*$ *large enough so that*

– $\forall k \in [\![0, N_\ell - 1]\!], \qquad \lambda_1\left(\left\{x \in \mathbb{R}^d, \quad r_0 + \frac{k(r_1-r_0)}{N_\ell} < \|x\| < r_0 + \frac{(k+1)(r_1-r_0)}{N_\ell}\right\}\right) > \ell.$

We take

$$K_\ell := B \setminus \bigcup_{k=0}^{N_\ell - 1} \left\{x \in \mathbb{R}^d, \quad \|x\| = r_0 + \frac{k(r_1 - r_0)}{N_\ell}\right\}.$$

We have $\lambda_1(K_\ell) = \lambda_1\big(\{x \in \mathbb{R}^d, \quad \|x\| < r_0\}\big) = \ell$ *and* $P(K_\ell) = P(B)$*, because the d-dimensional Hausdorff measure of* $\bigcup_{k=0}^{N_\ell-1} \{x \in \mathbb{R}^d, \quad \|x\| = r_0 + k \times (r_1 - r_0)/N_\ell\}$ *is equal to zero and thus not detected by the De Giorgi's perimeter.*

3.3 The case of convex domains

Finding estimates of λ_1 via geometric quantities is a question that has interested various communities. If Theorem 10 shows that Faber-Krahn and isoperimetric inequalities form a complete system of inequalities in the case of open sets, this is no longer the case if one restricts the class of domains to convex or simply connected ones. We focus in this section on the case of convex sets, see Section 3.4.3 for some comments on the case of simply connected sets.

3.3.1 Known inequalities and numerical simulations

Let us recall the well-known inequalities providing estimates of λ_1 in terms of perimeter and volume:

1. One early result in this direction is due to G. Polya who proved in [156] (1959) that for any convex planar domain Ω one has:

$$\lambda_1(\Omega) < \frac{\pi^2}{4}\left(\frac{P(\Omega)}{|\Omega|}\right)^2. \tag{3.8}$$

This inequality actually holds for simply connected planar sets, see [154]. It is also sharp, as equality is attained asymptotically by a family of vanishing thin rectangles. It is noticed in [119] that Polya's proof of inequality (3.8) holds for convex sets in higher dimensions, and the authors extend it to a larger class of sets. Recently, a generalization for $p \in (1, +\infty)$ in the case of the first p-Laplacian eigenvalue was obtained, see [69, 40].

2. Another classical result is proven by E. Makai in [141] (1960): it gives a lower estimate of the fundamental frequency of a planar convex set Ω:

$$\lambda_1(\Omega) > \frac{\pi^2}{16}\left(\frac{P(\Omega)}{|\Omega|}\right)^2. \tag{3.9}$$

The inequality is sharp, as equality is attained asymptotically by a family of vanishing thin triangles. This result was recently extended to higher dimensions by L. Brasco [39, Corollary 5.1.]: for $d \geq 2$, he proves:

$$\forall \Omega \in \mathcal{K}^d, \qquad \lambda_1(\Omega) \geq \left(\frac{\pi}{2d}\right)^2 \left(\frac{P(\Omega)}{|\Omega|}\right)^2, \tag{3.10}$$

which is also sharp, as equality is attained asymptotically by a certain family of "collapsing pyramids". Note that [39] also generalizes such an inequality for the first p-Laplacian eigenvalue, where $p \in (1, +\infty)$.

3. The Payne-Weinberger's inequality [154] states that for every planar, open and simply connected set Ω, one has:

$$\lambda_1(\Omega) - \lambda_1(B) \leq \lambda_1(B) \left(\frac{1}{J_1^2(j_{01})} - 1 \right) \left(\frac{P(\Omega)^2}{4\pi|\Omega|} - 1 \right), \tag{3.11}$$

where B is the disk of same measure as Ω and J_1 is the Bessel function of the first kind of order one and j_{01} is the first zero of the Bessel function of the first kind and of order zero. Moreover, equality is achieved only when Ω is a disk. For large values of $P(\Omega)$, this inequality is weaker than (3.8). But for values of $P(\Omega)$ close to $P(B)$, (3.11) provides a quantitative estimate of the Faber-Krahn deficit $\lambda_1(\Omega) - \lambda_1(B)$ by the isoperimetric deficit. It shows in particular that when the perimeter of Ω is close to the perimeter of the ball with the same measure, then the eigenvalues are also close to each other. One can find results in the same spirit for convex domains in arbitrary dimensions in [38, 69].

The stated inequalities give an explicit region in $\mathbb{R}^2$ which contains $\mathcal{D}_{\mathcal{K}^2}$ and is, up to our knowledge, the smallest known set containing $\mathcal{D}_{\mathcal{K}^2}$, see Figure 3.2.

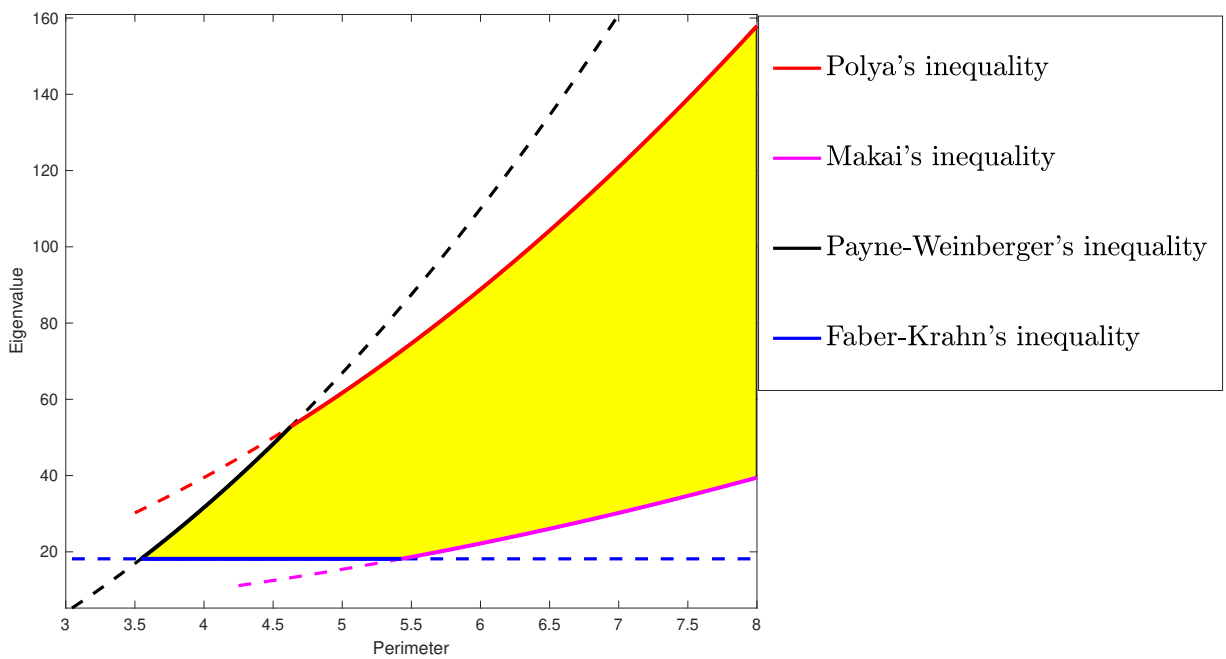

Figure 3.2: The smallest known domain that contains the diagram (in yellow).

In order to have an idea on the shape of $\mathcal{D}_{\mathcal{K}^2}$, P. Antunes and P. Freitas [12] generated random convex polygons of unit area and whose number of sides is between 3 and 8. In this paper, we first get a slight improvement of the numerical diagram by generating 10^5 polygons whose numbers of sides are between 3 and 30, see Figure 3.3. Note that the problem of generating convex polygons is rather interesting in itself: in [162], one can find a brief introduction and an efficient method of generating random convex polygons, the algorithm is based on a work of P. Valtr [171]. We notice that with these random polygons we get a quite good description of the lower boundary of the diagram, in contrast with the upper part of the diagram part which seems more "sparse". This may be explained by the fact that the domains which lay on the lower boundary are polygons while those on the upper one are smooth (see Corollary 3). We also notice:

- on one hand, that regular polygons lay on the lower boundary of the diagram as well as superequilateral triangles (that is, an isosceles triangle whose aperture (angle between its two equal sides)

is greater that $\pi/3$).

- on the other hand, that we expect thin stadiums (domains obtained by adding two half disks to the extremities of a rectangle) to be a good approximation of domains describing the upper part of the diagram: it is easy to prove that they realize asymptotically equality in (3.8), and they are better candidates that any random polygons or shapes we have tested.

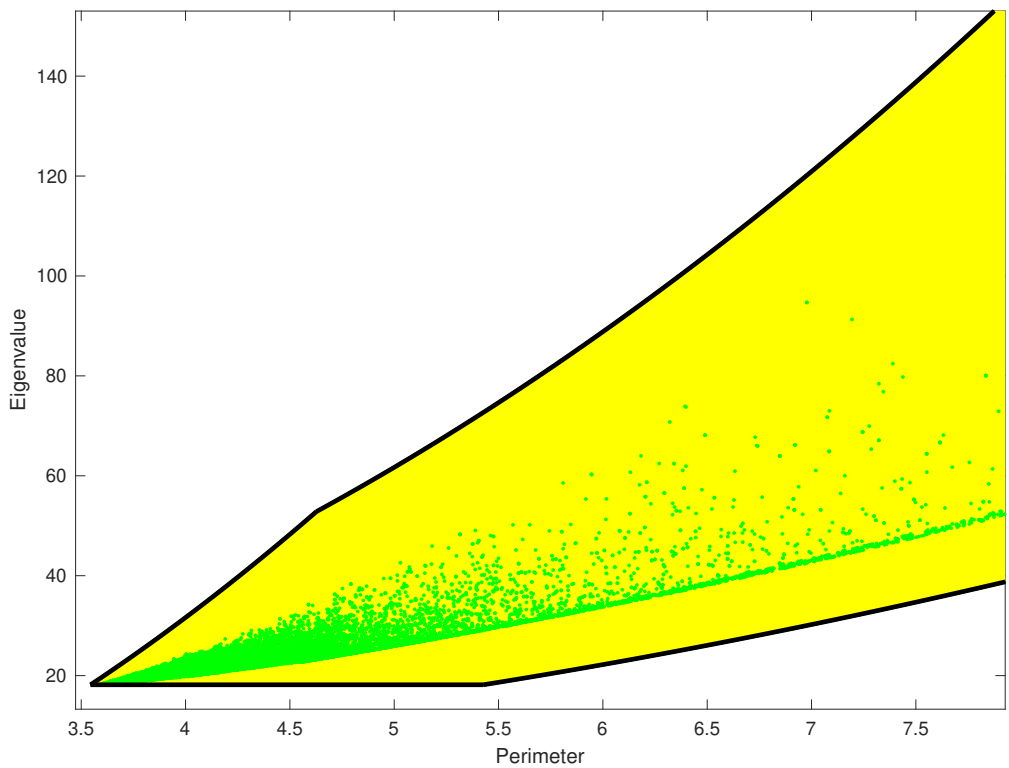

Figure 3.3: Blaschke-Santaló diagram obtained by generating 10^5 random convex polygons with at most 30 edges.

By adding the latter special shapes to the diagram, one can obtain an improved version of $\mathcal{D}_{\mathcal{K}^2}$, see Figure 3.4: indeed we note that thanks to Theorem 13, we can say that it contains the surface lying between the lowest points of the diagram (given by random polygons) and the one given by the stadiums: this zone provides an improved numerical estimation of the diagram, see Figure 3.4.

Actually, since the problem of theoretically finding the extremal shapes (those on the boundary of the diagram) is most certainly challenging (see Section 3.4.1) and actually likely unreachable, it is interesting to try to provide numerical computation of optimal shapes. Then, once a precise description of the upper and lower boundaries is obtained, from Theorem 11 this implies a precise description of the diagram. As mentioned before, we prove in Corollary 3 that the domains realizing the lower boundary of the diagram are polygons while those realizing the upper one are quite smooth ($C^{1,1}$): this suggests that we should use two different shape optimization approaches. We refer to [89] for a more detailed numerical study of the optimal shapes describing the boundary of $\mathcal{D}_{\mathcal{K}^2}$ and also a numerical study of other Blaschke-Santaló diagrams.

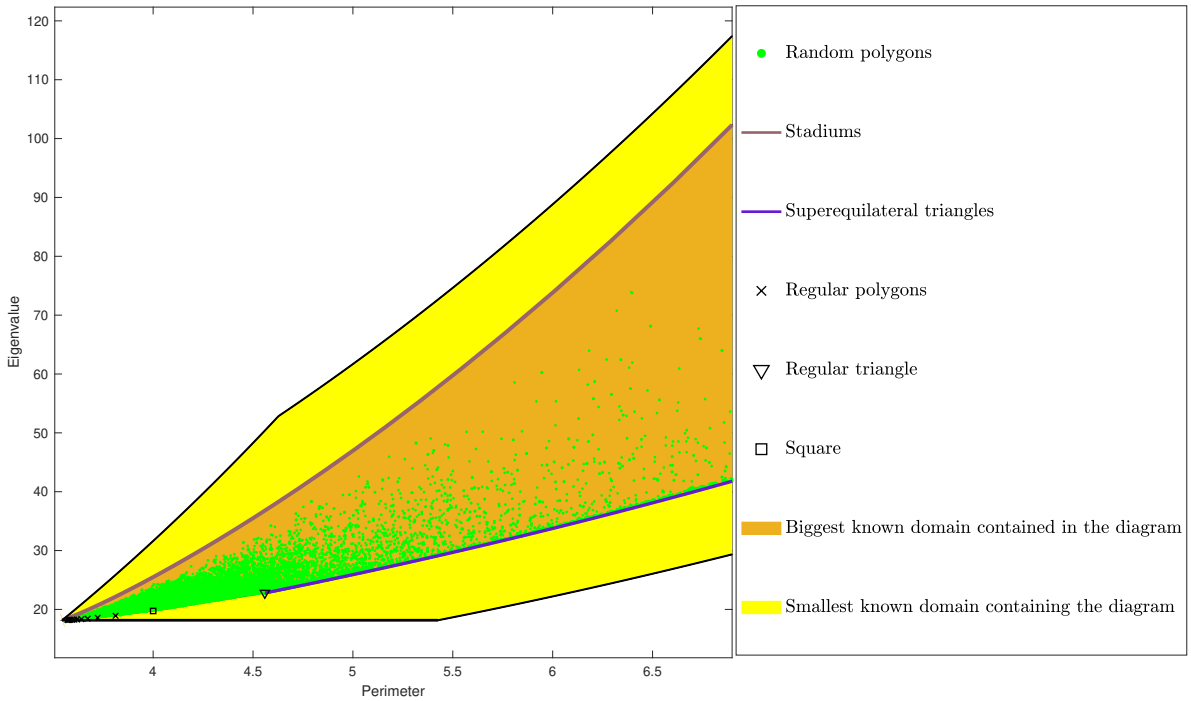

Figure 3.4: An improved description of the diagram.

We note that by taking advantage of (3.2), it is also classical to represent Blaschke-Santaló diagram as subset of $[0,1]^2$, in our situation, this means to consider the set $\left\{\left(P(B)/P(\Omega), \lambda_1(B)/\lambda_1(\Omega)\right) \mid \quad \Omega \in \mathcal{K}_1^2\right\}$, see Figure 3.5 below.

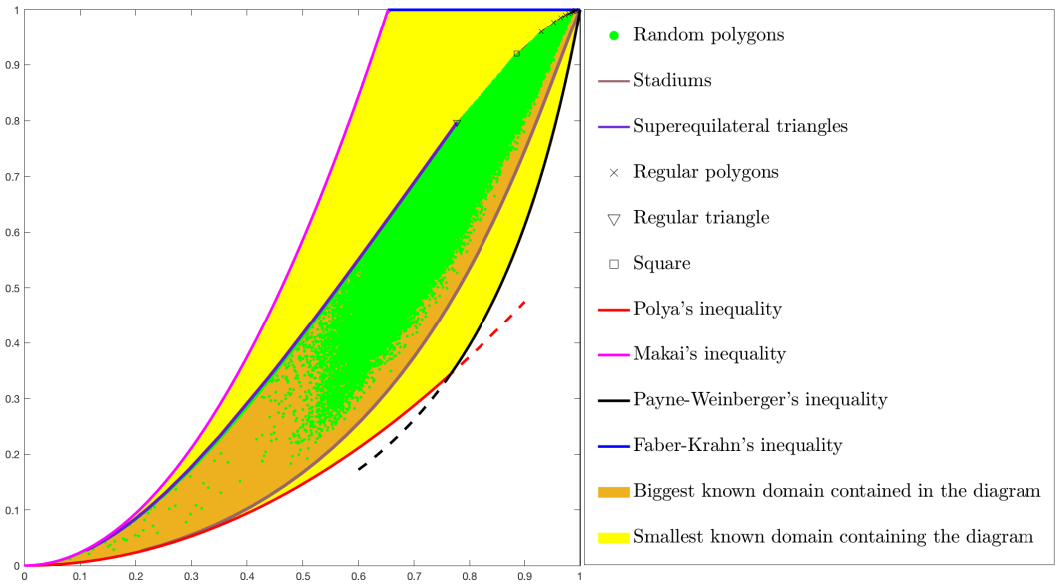

Figure 3.5: Blaschke-Santaló diagram represented in $[0,1]^2$.

3.3.2 Proof of Theorem 11

As the proof of Theorem 11 is quite involved, we proceed in several paragraphs: we first prove that the diagram is closed and path-connected, which rely on the use of Hausdorff convergence and classical results, see Proposition 4. Then in Section 3.3.2 we state and prove the main perturbation lemma (Lemma 7). With these preliminaries, we are in position to prove the four assertions of Theorem 11:

1. see Theorem 13,
2. see Theorem 12,
3. see Corollary 3,
4. see Proposition 6 and Corollaries 5 and 6,

where the proofs of Theorems 12 and 13 are both using Lemma 7. Finally, we note that, as their proofs do not rely on the perturbation lemma, Propositions 4 and 6 and Corollary 5 are stated and proved for arbitrary dimension $d \geq 2$.

Strategy of proof of the first and second assertions of Theorem 11

Before detailing the proofs, let us first give a few comments on the strategy of proof of the first two assertions of Theorem 11, which are consequences of Lemma 7. We decompose the proof into two main steps (both steps use Lemma 7): in Theorem 12 we define f and g as the lower and upper parts of the diagram (see (3.14) and (3.15)), and show that these functions are continuous and strictly increasing. Then in Theorem 13 we show (3.3) which implies that $\mathcal{D}_{\mathcal{K}^2}$ is simply connected: as already mentioned in the introduction the simple connectedness property of a Blaschke-Santaló diagram may be rather complicated to prove. If we were able to find explicitly the extremal domains (those who are on the upper and lower boundaries of the diagram) then we could use them to construct continuous paths via Minkowski sums, relating the upper boundary to the lower one, and prove that this process fills all the surface between the upper and lower curves (in fact it is because one can observe that these explicit optimal sets have a continuous dependence in the abscissa x: this seems to be a difficult statement to achieve without knowing explicitly these optimal shapes). In our situation, finding the explicit extremal domains is at least very challenging (see Conjecture 4 for example) and very likely impossible. Nevertheless, we manage to overpass this difficulty and give a proof of the simple-connectedness of the diagram without knowing the extremal sets (see the proof of Theorem 13): the proof is also based on the construction of suitable Minkowski paths and the use of the perturbation Lemma 7. We believe that our approach can be generalized and applied to other diagrams, in the sense that once a similar perturbation lemma is achieved for a triplet of functionals (instead of $(P, \lambda_1, |\cdot|)$), a similar strategy can be used to obtain qualitative results for its Blaschke-Santaló diagram.

The diagram is closed

We recall the following definition:

Definition 2. *The Minkowski sum of two subsets X and Y of $\mathbb{R}^d$ is the set $X + Y := \{x + y,\ (x, y) \in X \times Y\}$.*

Proposition 4. *Take $d \geq 2$, the diagram $\mathcal{D}_{\mathcal{K}^d}$ is a closed and connected by arcs subset of $\mathbb{R}^2$.*

Proof.

- Let $(x_n, y_n)_n$ a sequence of elements of $\mathcal{D}_{\mathcal{K}^d}$ converging to (x, y) in $\mathbb{R}^2$. Let us show that $(x, y) \in \mathcal{D}_{\mathcal{K}^d}$.

  We have, by definition, the existence of a sequence $(\Omega_n)_n$ of convex open sets such that

  $$\forall n \in \mathbb{N}, |\Omega_n| = 1, \quad P(\Omega_n) = x_n \quad \text{and} \quad \lambda_1(\Omega_n) = y_n.$$

  We recall that for any $\Omega \in \mathcal{K}^d$, one has the following inequality:

  $$d(\Omega) < C_d \frac{P(\Omega)^{d-1}}{|\Omega|^{d-2}}, \tag{3.12}$$

where $d(\Omega)$ denotes the diameter of Ω and C_d is a dimensional constant, see [77, Lemma 4.1].

In particular, the sequence $(P(\Omega_n))_n$ is bounded (because it is convergent), since the sets $(\Omega_n)_n$ are in $\mathcal{K}_1^d$, by (3.12), $(d(\Omega_n))_n$ is also bounded, and given that the considered functionals are invariant by translation, we can assume that the domains $(\Omega_n)_n$ are contained in a bounded box. Then by Blaschke selection Theorem (see for example [164, Th. 1.8.7]), there exists a convex domain Ω^* such that (Ω_n) converges up to a subsequence (for which we keep the notation (Ω_n)) for the Hausdorff distance to Ω^*.

It is well known that the involved functionals (perimeter, volume and λ_1) are continuous for the Hausdorff distance among convex bodies, see for example [164] and [108, Theorem 2.3.17]. So we can write:

$$\begin{cases} |\Omega^*| &= \lim\limits_{n\to+\infty} |\Omega_n| = 1 \\ P(\Omega^*) &= \lim\limits_{n\to+\infty} P(\Omega_n) = x \\ \lambda_1(\Omega^*) &= \lim\limits_{n\to+\infty} \lambda_1(\Omega_n) = y \end{cases}$$

and this concludes the proof.

- Take $\Omega_0, \Omega_1 \in \mathcal{K}_1^d$, we denote $\Omega_t := \frac{(1-t)\Omega_0+t\Omega_1}{|(1-t)\Omega_0+t\Omega_1|^{1/d}}$, since $t \in [0,1] \longmapsto (1-t)\Omega_0+t\Omega_1 \in (\mathcal{K}^d, d^H)$ and the functionals $(|\cdot|, P, \lambda_1)$ are continuous for the Hausdorff distance, we have by composition that $t \in [0,1] \longmapsto \big(P(\Omega_t), \lambda_1(\Omega_t)\big) \in \mathcal{D}_{\mathcal{K}^d} \subset \mathbb{R}^2$ is also continuous and relates Ω_0 to Ω_1.

□

Corollary 1. *Take $d \geq 2$, for every $p \geq P(B)$ and $l \geq \lambda_1(B)$, the optimization problems*

$$\inf/\sup\big\{\lambda_1(\Omega)\ /\ \Omega \in \mathcal{K}^d, |\Omega| = 1 \text{ and } P(\Omega) = p\big\} \quad \text{and} \quad \inf/\sup\big\{P(\Omega)\ /\ \Omega \in \mathcal{K}^d, |\Omega| = 1 \text{ and } \lambda_1(\Omega) = l\big\}$$

have solutions.

Proof. Take $p \geq P(B)$, by inequalities (3.8) and (3.10) and the positivity of λ_1 and the perimeter, we have:

$$\forall y \in \mathbb{R} \text{ such that } (p,y) \in \mathcal{D}_{\mathcal{K}^d}, \qquad 0 \leq y \leq \frac{\pi^2}{4}p^2,$$

$$\forall x \in \mathbb{R} \text{ such that } (x,l) \in \mathcal{D}_{\mathcal{K}^d}, \qquad 0 \leq x \leq \frac{2d}{\pi}l,$$

this implies that the supremum and infimum of $\{y\ /\ (p,y) \in \mathcal{D}_{\mathcal{K}^d}\}$ (resp. $\{x\ /\ (x,l) \in \mathcal{D}_{\mathcal{K}^d}\}$) are finite. If $(y_n)_n$ (resp. (x_n)) is a minimizing or maximizing sequence (i.e. such that $\lim\limits_{n\to+\infty} y_n = \inf/\sup\{y\ /\ (p,y) \in \mathcal{D}_{\mathcal{K}^d}\}$ and $\lim\limits_{n\to+\infty} x_n = \inf/\sup\{x\ /\ (x,l) \in \mathcal{D}_{\mathcal{K}^d}\}$), then the sequence $(p,y_n)_n$ (resp. $(x_n,l)_n$) converges in $\mathbb{R}^2$ and thus by Proposition 4 the limit is in the closed set $\mathcal{D}_{\mathcal{K}^d}$, thus the existence of solutions of the problems in $\mathcal{K}^d$.

□

Main lemma

In the following, we will denote

$$\mathcal{K}_1^d := \{\Omega \in \mathcal{K}^d,\ |\Omega| = 1\}, \qquad \text{and} \qquad \mathcal{K}_{1,p}^d := \{\Omega \in \mathcal{K}^d,\ |\Omega| = 1, P(\Omega) = p\},$$

for $d \geq 2$ and $p \geq P(B)$ with B being the ball of $\mathbb{R}^d$ of volume 1.

Before stating the perturbation lemma, we recall useful classical result on the volume of the Minkowski sum of convex sets. For more details on the Brunn-Minkowski theory, we refer for example to [164].

Proposition 5. *There exist $d+1$ bilinear (for Minkowski sum and dilatation) forms $W_k : \mathcal{K}^d \times \mathcal{K}^d \longrightarrow \mathbb{R}$, for $k \in [\![0; d]\!]$, named Minkowski mixed volumes, such that for every $K_1, K_2 \in \mathcal{K}^d$ and $t_1, t_2 \in \mathbb{R}^+$, we have:*

$$|t_1 K_1 + t_2 K_2| = \sum_{k=0}^{d} \binom{d}{k} t_1^{d-k} t_2^k W_k(K_1, K_2). \tag{3.13}$$

Moreover, the W_k are continuous for the Hausdorff distance, in the sense that if two sequences of convex bodies $(K_1^n)_n$ and $(K_2^n)_n$ converge to some convex bodies K_1 and K_2 both for the Hausdorff distance, one has:

$$\lim_{n \to +\infty} W_k(K_1^n, K_2^n) = W_k(K_1, K_2).$$

Now, we state the perturbation Lemma.

Lemma 7. *(Perturbation Lemma) We endow the space of convex bodies with the Hausdorff distance. We have:*

1. *the ball is the only local minimizer of the perimeter in $\mathcal{K}_1^2$;*
2. *the ball is the only local minimizer of λ_1 in $\mathcal{K}_1^d$, where $d \geq 2$;*
3. *there is no local maximizer of the perimeter in $\mathcal{K}_1^2$;*
4. *a $C^{1,1}$ convex domain cannot be a local maximizer of λ_1 in $\mathcal{K}_1^2$.*

Notice that one of the main difficulties for this lemma is to show that one can perturb a given convex domain in order to increase or decrease its perimeter or its eigenvalue, and still remain convex. Of course, if the domain is smooth and uniformly convex, such perturbations are easy to build. But it is a difficult task, in general, to build any perturbation of a general convex domain, see for example [132]. This mainly explains why the first, third and fourth points are only given when $d = 2$. Note that we trust that the first point could easily be obtained for the perimeter, using the same strategy as the for the second point: as we will use this result only in dimension 2, we chose to show a more elementary proof for the first point, that works well in dimension two but does not seem easy to adapt to higher dimension.

Proof. We prove each assertion:

1. Let $\Omega \in \mathcal{K}_1^2 \backslash \{B\}$. We use the Minkowski sum to build a perturbation of Ω that decreases the perimeter. We denote B_1 the ball of radius 1 (which is not the same as B whose volume is 1); then, given $s > 0$ sufficiently small, Steiner formulas give:

$$|\Omega + sB1| = |\Omega| + P(\Omega)s + |B_1|s^2, \qquad \text{and} \qquad P(\Omega + sB_1) = P(\Omega) + sP(B_1),$$

so considering

$$\Omega_s := \frac{(\Omega + sB_1)}{\sqrt{|\Omega + sB_1|}} \in \mathcal{K}_1^2,$$

where $s > 0$, we obtain

$$P(\Omega_s) = \frac{P(\Omega + sB_1)}{\sqrt{|\Omega + sB_1|}} = \frac{P(\Omega) + sP(B_1)}{\sqrt{|\Omega| + P(\Omega)s + |B_1|s^2}}.$$

By denoting $f : s \in [0, +\infty) \mapsto P(\Omega_s)$, a simple computation shows

$$f'(0) = \frac{P(B_1) - \frac{P(\Omega)^2}{2|\Omega|}}{\sqrt{|\Omega|}}$$

which is such that $f'(0) < 0$ by isoperimetric inequality $\frac{P^2(\Omega)}{|\Omega|} \geq 4\pi = 2P(B_1)$.

So for $s > 0$ small enough, we have $P(\Omega_s) < P(\Omega_0) = P(\Omega)$. Since $\Omega + sB$ converges to Ω when $s \to 0$ and the measure is continuous, both for the Hausdorff distance in $\mathcal{K}^2$, we have that $\Omega_s \underset{s\to 0}{\longrightarrow} \Omega$ for the Hausdorff distance. This shows that Ω is not a local minimizer of the perimeter in $\mathcal{K}_1^2$.

2. Let $\Omega \in \mathcal{K}_1^d \backslash \{B\}$. We now build a perturbation that decreases λ_1: as Ω is not a ball, there exists a hyperplane H such that Ω is not symmetric with respect to H. We choose coordinates so that $H = \{(x, y) \in \mathbb{R}^{d-1} \times \mathbb{R}, y = 0\}$. We introduce the sets:

$$I_\Omega := \left\{x \in \mathbb{R}^{d-1} \ / \quad \exists y \in \mathbb{R}, \quad (x, y) \in \Omega\right\} \quad \text{and} \quad J_\Omega^x := \{y \in \mathbb{R} \ / \quad (x, y) \in \Omega\} \quad \text{where } x \in I_\Omega.$$

Since Ω is convex and of volume 1, it is bounded and non-empty, thus the sets I_Ω and J_Ω^x (where $x \in I_\Omega$) are also convex, bounded and non-empty. We can then introduce $y_1, y_2 : I_\Omega \to \mathbb{R}$ such that:

$$\forall x \in I_\Omega, \qquad y_1(x) = \inf J_\Omega^x \quad \text{and} \quad y_2(x) = \sup J_\Omega^x.$$

By convexity of Ω, we can write:

$$\Omega = \{(x, y) \in \mathbb{R}^{d-1} \times \mathbb{R}, \ \ x \in I_\Omega \ \text{ and } \ y_1(x) < y < y_2(x)\},$$

with y_1 convex and y_2 concave.

Now, we define a displacement field $V : \mathbb{R}^d \longrightarrow \mathbb{R}^d$ by:

$$V(x, y) = \Big(0, -\frac{1}{2}\big(y_1(x) + y_2(x)\big)\Big).$$

Let $\Omega_t := (Id + tV)(\Omega)$, for $0 \leq t \leq 1$, where $Id : x \in \mathbb{R}^d \longmapsto x \in \mathbb{R}^d$ is the identity map. The process of deforming $\Omega = \Omega_0$ to the symmetric set Ω_1 through the path $t \longmapsto \Omega_t$ is a variant of the so called continuous Steiner symmetrization (see [47] for example). It is well known that the volume is preserved throughout this continuous process; moreover, we can show that convexity of domains is also preserved. Indeed, for every $t \in [0, 1]$:

$$\Omega_t = \left\{(x, y) \in \mathbb{R}^2, \ \ x \in I \ \text{ and } \ \left(1 - \frac{t}{2}\right) y_1(x) - \frac{t}{2} y_2(x) < y < -\frac{t}{2} y_1(x) + \left(1 - \frac{t}{2}\right) y_2(x)\right\}.$$

Yet, the facts that I_Ω is convex, the function $-\frac{t}{2} y_1 + \left(1 - \frac{t}{2}\right) y_2$ is concave and the function $\left(1 - \frac{t}{2}\right) y_1 - \frac{t}{2} y_2$ is convex yield that Ω_t is convex.

Moreover, we have that $\Omega_t \underset{t\to 0^+}{\longrightarrow} \Omega$ for the Hausdorff distance. Indeed

$$\begin{aligned} d^H(\Omega_t, \Omega) &= d^H(\partial\Omega_t, \partial\Omega) \\ &:= \max\Big(\sup_{a\in\partial\Omega_t} \inf_{a'\in\partial\Omega} \|a - a'\|, \sup_{b\in\partial\Omega} \inf_{b'\in\partial\Omega_t} \|b - b'\|\Big) \\ &\leq \frac{t}{2} \sup_{x\in I} |y_1(x) + y_2(x)| \underset{t\to 0^+}{\longrightarrow} 0. \end{aligned}$$

Finally, as Ω is not symmetric with respect to H, it was proven in [54, Lemma 3.1] that the continuous symmetrization strictly decreases the first eigenvalue, and since $\Omega_t \underset{t\to 0^+}{\longrightarrow} \Omega$ for the Hausdorff distance, we conclude that Ω is not a local minimizer of λ_1 is $\mathcal{K}_1^d$.

3. On one hand, from [132, Theorem 2.1, Remark 2.2], we deduce that any local maximizer of the perimeter under volume and convexity constraints must be a polygon (more precisely, in [132] they consider local minimum where the word local in understood for the $W^{1,\infty}$-norm on the so-called gauge function of the set ; but this is in particular the case if we consider local minimum for the Hausdorff distance).

   On the other hand, no polygon can be a local maximizer of the perimeter in $\mathcal{K}_1^2$: to prove this, we use a parallel chord movement. More precisely if Ω is a polygon, one can consider A, B, C three consecutive corners so that ABC forms a triangle. One can move B along the line passing through B and being parallel to the line (AC). This way, the volume is preserved, and the perimeter must increase when moving B away from the perpendicular bisector of $[A, C]$ (which is possible at least in one direction).

   From the two previous remarks, we deduce that there is no local maximizer of the perimeter under convexity and volume constraints.

4. In [130], the authors show that a local maximum of λ_1 in $\mathcal{K}_1^2$ is a polygon, this proves that any smooth (in particular $C^{1,1}$) domain is not a local maximizer of λ_1 in $\mathcal{K}_1^2$.

□

One can deduce the following result which gives a refinement of Lemma 7 concerning the perimeter functional:

Corollary 2. *Let $\Omega \in \mathcal{K}_1^2$. Then for any sequence (p_n) converging to $P(\Omega)$ such that $p_n \geq P(B)$ for all $n \in \mathbb{N}$, there exists a sequence (Ω_n) of elements of $\mathcal{K}_1^2$ converging to Ω for the Hausdorff distance, and such that $P(\Omega_n) = p_n$ for all $n \in \mathbb{N}$.*

Proof. If $\Omega \neq B$, by Lemma 7, we can build a sequence $(K_n)_n$ of elements of $\mathcal{K}_1^2$ converging to Ω for the Hausdorff distance, and such that $P(K_{2n}) < P(\Omega) < P(K_{2n+1})$ for every $n \in \mathbb{N}$ and since (p_n) is bounded, we can also assume K_0 and K_1 such that $p_n \in [P(K_0), P(K_1)]$ for all $n \in \mathbb{N}$. We will use this sequence (K_n) to build (Ω_n) : for $n \in \mathbb{N}$,

- if $p_n = P(\Omega)$, we take $\Omega_n = \Omega$ and define $\sigma(n) = n$.
- if $p_n > P(\Omega)$, then as $P(K_{2k+1})$ converges to $P(\Omega)$ from above and $p_n \leq P(K_1)$, we can define $\sigma(n) := \max\{2k+1 \ / \ P(K_{2k+1}) \geq p_n\}$and consider the function:

$$\phi_n : t \longmapsto P\left(\frac{tK_{\sigma(n)} + (1-t)\Omega}{\sqrt{\left|tK_{\sigma(n)} + (1-t)\Omega\right|}}\right).$$

  This function ϕ_n is continuous and since $p_n \in [\phi_n(0), \phi_n(1)] = [P(\Omega), P(K_{\sigma(n)})]$, by the intermediate value Theorem there exists $t_n \in [0, 1]$ such that $\phi_n(t_n) = p_n$, we then take:

$$\Omega_n := \frac{t_n K_{\sigma(n)} + (1-t_n)\Omega}{\sqrt{\left|t_n K_{\sigma(n)} + (1-t_n)\Omega\right|}} \in \mathcal{K}_{1,p_n}^2.$$

- if $p_n < P(\Omega)$, we set $\sigma(n) := \max\{2k \ | \ P(K_{2k}) \leq p_n\}$ and choose Ω_n as in the previous case.

It remains to show that the sequence (Ω_n) converges to Ω for the Hausdorff distance. If the set $I := \{n \in \mathbb{N} \ / \ p_n \neq P(\Omega)\}$ is finite, then the sequence (Ω_n) is equal to Ω for n large enough. If on the other hand I is infinite, the fact that $P(K_n) \underset{n\to+\infty}{\longrightarrow} P(\Omega)$ implies that $\lim\limits_{n\to+\infty} \sigma(n) = +\infty$, which gives

$\lim_{n\to+\infty} K_{\sigma(n)} = \Omega$, thus $(t_n K_{\sigma(n)} + (1-t_n)\Omega) \underset{n\to+\infty}{\longrightarrow} \Omega$ for the Hausdorff distance, then by continuity of the measure, we get that $\Omega_n \underset{n\to+\infty}{\longrightarrow} \Omega$ for the Hausdorff distance.

If $\Omega = B$, one may reproduce the same strategy as above by considering a sequence $(K_n)_n$ of elements of $\mathcal{K}_1^2$ converging to B for the Hausdorff distance such that $P(B) < P(K_n)$ for every $n \in \mathbb{N}$ (second assertion of Lemma 7) and then use Minkowski sums and intermediate value Theorem to construct the sets (Ω_n).

□

Study of the boundary of the diagram

We define functions f and g by:

$$\begin{array}{rccl} f: & [P(B),+\infty) & \longrightarrow & \mathbb{R} \\ & p & \longmapsto & \min\left\{\lambda_1(\Omega)\,, \Omega \in \mathcal{K}^d, |\Omega| = 1 \text{ and } P(\Omega) = p\right\} \end{array} \tag{3.14}$$

$$\begin{array}{rccl} g: & [P(B),+\infty) & \longrightarrow & \mathbb{R} \\ & p & \longmapsto & \max\left\{\lambda_1(\Omega)\,,\ \Omega \in \mathcal{K}^d, |\Omega| = 1 \text{ and } P(\Omega) = p\right\} \end{array} \tag{3.15}$$

and we recall that these optimization problems admit solutions, see Corollary 1. By definition (and by the isoperimetric inequality), we have

$$\mathcal{D}_{\mathcal{K}^d} \subset \Big\{(x,y) \in \mathbb{R}^2 \mid x \geq P(B) \text{ and } f(x) \leq y \leq g(x)\Big\}. \tag{3.16}$$

In this section, we will first give the asymptotics of f and g near $+\infty$ for arbitrary dimension $d \geq 2$, then we prove the second part of Theorem 11, which is stated again below in Theorem 12. To obtain the first part of Theorem 11, we need to show the reverse inclusion of (3.16), which will be obtained with Theorem 13.

Proposition 6. *Take $d \geq 2$, we have*

$$g(x) \underset{x\to\infty}{\sim} \frac{\pi^2}{4}x^2 \quad \textit{and} \quad f(x) \underset{x\to\infty}{\sim} \frac{\pi^2}{4d^2}x^2.$$

Proof. By inequalities (3.10) and (3.8), one has:

$$\forall K \in \mathcal{K}_1^d, \quad \frac{\pi^2}{4d^2}P(K)^2 \leq \lambda_1(K) < \frac{\pi^2}{4}P(K)^2.$$

Then:

$$\forall x \geq P(B), \quad \frac{\pi^2}{4d^2}x^2 \leq f(x) \leq g(x) < \frac{\pi^2}{4}x^2.$$

However, since the right- and left-hand-side inequalities are respectively attained in the limiting case of flat collapsing cuboids and collapsing pyramids (see [39, Corollary 5.1.]), we have the stated equivalences.

□

Remark 6. *In this paper, all the study is done for shapes of volume 1. It is interesting to wonder about what would happen if one removes such constraint: we believe that in this case the diagram would be given by:*

$$\{\big(P(\Omega), \lambda_1(\Omega)\big) \mid \Omega \in \mathcal{K}^d\} = \left\{(x,y) \mid x > 0 \textit{ and } y \geq \frac{\lambda_1(B)P(B)^{\frac{2}{d-1}}}{x^{\frac{2}{d-1}}}\right\},$$

where the boundary corresponds to balls. We note that the idea of "relaxing" the volume constraint has been successfully used in [138] to give some qualitative properties of the boundary of the diagram involving the first Dirichlet eigenvalue, the torsion and the volume.

Theorem 12. *Assume $d = 2$. Then functions f and g are continuous and strictly increasing.*

Remark 7. *Some of the properties of f and g come with minor efforts, namely the lower semicontinuity of f (or upper one of g). But to prove the full continuity and monotonicity, we use Lemma 7, and this explains why Theorem 12 is restricted to dimension 2. Compare to [138, Theorem 1.1] where the authors could not prove that the upper part of the diagram is the graph of a continuous and increasing function.*

Proof. We start by proving the continuity of f. Let $p_0 \in [P(B), +\infty[$.

For every $p \in [P(B), +\infty[$, by Corollary 1, there exists Ω_p a solution of the following minimization problem:

$$\min \left\{ \lambda_1(\Omega) \mid \Omega \in \mathcal{K}_1^2 \text{ and } P(\Omega) = p \right\}.$$

- We first show an **inferior limit inequality**. Let $(p_n)_{n\geq 1}$ real sequence converging to p_0 such that

  $$\liminf_{p\to p_0} \lambda_1(\Omega_p) = \lim_{n\to+\infty} \lambda_1(\Omega_{p_n}).$$

  Up to translations, as the perimeter of $(\Omega_{p_n})_{n\in\mathbb{N}^*}$ is uniformly bounded, one may assume that the domains $(\Omega_{p_n})_{n\in\mathbb{N}^*}$ are included in a fixed ball: then by Blaschke selection Theorem, (Ω_{p_n}) converges to a convex set Ω^* for the Hausdorff distance, up to a subsequence that we denote p_n again for simplicity.

  By the continuity of the perimeter, the volume and λ_1 for the Hausdorff distance among convex sets, we have:

  $$\begin{cases} |\Omega^*| = \lim\limits_{n\to+\infty} |\Omega_{p_n}| = 1, \\ P(\Omega^*) = \lim\limits_{n\to+\infty} P(\Omega_{p_n}) = \lim\limits_{n\to+\infty} p_n = p_0, \\ \lambda_1(\Omega^*) = \lim\limits_{n\to+\infty} \lambda_1(\Omega_{p_n}) = \liminf\limits_{p\to p_0} \lambda_1(\Omega_p). \end{cases}$$

  Then by definition of f (since $\Omega^* \in \mathcal{K}_1^2$ and $P(\Omega^*) = p_0$), we obtain:

  $$f(p_0) \leq \lambda_1(\Omega^*) = \lim_{n\to+\infty} \lambda_1(\Omega_{p_n}) = \liminf_{p\to p_0} \lambda_1(\Omega_p) = \liminf_{p\to p_0} f(p).$$

- It remains to prove **a superior limit inequality**. Let $(p_n)_{n\geq 1}$ be a real sequence converging to p_0 such that:

  $$\limsup_{p\to p_0} f(p) = \lim_{n\to+\infty} f(p_n).$$

  By Corollary 2, there exists a sequence $(K_n)_{n\geq 1}$ of $\mathcal{K}_1^2$ converging to Ω_{p_0} for the Hausdorff distance, and such that $P(K_n) = p_n$ for every $n \in \mathbb{N}^*$.

  Using the definition of f one can write

  $$\forall n \in \mathbb{N}^*, \quad f(p_n) \leq \lambda_1(K_n).$$

  Passing to the limit, we get:

  $$\limsup_{p\to p_0} f(p) = \lim_{n\to+\infty} f(p_n) \leq \lim_{n\to+\infty} \lambda_1(K_n) = \lambda_1(\Omega_{p_0}) = f(p_0).$$

As a consequence we finally get $\lim\limits_{p\to p_0} f(p) = f(p_0)$, so f is continuous on $[P(B), +\infty[$. The same method can be applied to prove the continuity of g.

- We now prove that f **is strictly increasing**. Let us assume by contradiction that it is not the case: then by continuity of f and the fact that $\lim_{+\infty} f = +\infty$ (see Proposition 6), we deduce the existence of a local minimum of f at a point $p_0 > P(B)$. Using Corollary 1, this means there exists $\Omega^* \in \mathcal{K}_1^2$ and $\varepsilon > 0$ such that

$$P(\Omega^*) = p_0 \quad \text{and} \quad \forall p \in (p_0 - \varepsilon, p_0 + \varepsilon), \;\; \lambda_1(\Omega^*) = f(p_0) \leq f(p),$$

which implies

$$\forall \Omega \in \mathcal{K}_1^2 \text{ such that } P(\Omega) \in (p_0 - \varepsilon, p_0 + \varepsilon), \;\; \lambda_1(\Omega^*) \leq \lambda_1(\Omega).$$

Because of the continuity of the perimeter in $\mathcal{K}_1^2$, this would imply that Ω^* is a local minimum (for the Hausdorff distance) of λ_1 in $\mathcal{K}_1^2$, which, from the first point in Lemma 7 implies that Ω^* must be a ball, which in turn contradicts $P(\Omega^*) > P(B)$.

- We finally prove that g **is strictly increasing**. Assuming by contradiction that this is not the case, then there exist $p_2 > p_1 \geq P(B)$ such that $g(p_2) < g(p_1)$, and from the equality case in the isoperimetric inequality, we necessarily have $p_1 > P(B)$. Since g is continuous, it reaches its maximum on $[P(B), p_2]$ at a point $p^* \in (P(B), p_2)$, that is to say

$$\forall \Omega \in \mathcal{K}_1^2 \text{ such that } [P(B), p_2], \;\; g(p^*) \geq \lambda_1(\Omega). \tag{3.17}$$

Using Corollary 1 again, one knows that the problem

$$\min\{P(\Omega), \;\; \Omega \in \mathcal{K}_1^2 \quad \text{and} \quad \lambda_1(\Omega) = g(p^*)\} \tag{3.18}$$

admits a solution $K^* \in \mathcal{K}_1^2$.

On one hand, (3.17) implies that K^* is a local maximum (for the Hausdorff distance) of λ_1 in $\mathcal{K}_1^2$. From Lemma 7 we deduce that K^* cannot be $C^{1,1}$.

On the other hand, K^* is also a solution of (3.18). We want to apply the regularity result [134, Theorem 2] which shows that K^* is $C^{1,1}$, which is a contradiction. This theorem applies as, denoting $m(\Omega) = (\lambda_1(\Omega), |\Omega|) \in \mathbb{R}^2$ (which are the constraints in (3.18) besides the convexity constraint, the latter being dealt with by its own infinitely dimensional Lagrange multiplier, see the proof of [134, Theorem 2]), it is well known that the first order shape derivative (see for example [108] for definitions) writes:

$$\forall \xi \in C^\infty(\mathbb{R}^2, \mathbb{R}^2), \quad m'(K^*).\xi = \left(-\int_{\partial K^*} |\nabla u_1|^2 \xi \cdot n_{\partial K^*} d\sigma, \; \int_{\partial K^*} \xi \cdot n_{\partial K^*} d\sigma \right),$$

where u_1 is the first normalized Dirichlet eigenfunction on K^*: the convexity of K^* is used here to provide enough smoothness so that this formula is valid (indeed it is well-known that $u_1 \in H^2(\Omega)$ so its gradient has a trace on ∂K^*, see also [106, Theorem 2.5.1]). Therefore this shape derivative at K^* is in $L^\infty(\partial K^*)^2$ (see [134, Section 3.3] for the link between shape derivatives and derivatives in term of the gauge function as considered in [134, Theorem 2]), and also that it is onto: indeed, if it was not, we would have the existence of $c \geq 0$ such that $|\nabla u_1| = c$ on ∂K^*. With Lemma 8 proven just below, this would imply that K^* is a ball, which is again impossible. We conclude that g is strictly increasing, which ends the proof.

□

In the previous proof, we used the following lemma:[1]

[1] We thank Bozhidar Velichkov for helping us with the proof of this lemma.

Lemma 8. *Let Ω be an open and bounded convex set in $\mathbb{R}^d$, and u_1 solution of* (3.1)*, that is to say a first eigenfunction of the Dirichlet-Laplacian in Ω. We also assume that there exists $c \geq 0$ a constant such that*

$$|\nabla u_1| = c \text{ on } \partial\Omega. \tag{3.19}$$

Then Ω is a ball and $c > 0$.

Remark 8. *The result in Lemma 8 deals with a well-known problem that goes back to the famous result by J. Serrin [166]. The main difficulty here is that we do not assume regularity for Ω or u_1, except the one given by the convexity of Ω. There is an extensive literature on extensions of [166], some of which weakening these regularity assumptions, but we did not find a direct answer to the question raised in Lemma 8: the closest result we could find was [137, Theorem 1 and Remark (2) in Section 5]. Therefore, we adapt the regularity theory of free boundary problems by taking advantage of the convexity of Ω, which makes the context favorable.*

Proof. First note that from regularity theory, $u_1 \in H^2(\Omega) \cap W^{1,\infty}(\Omega)$ (see for example [100]), so ∇u_1 has a trace on $\partial\Omega$, which shows that (3.19) has a meaning in the sense of traces. Also $u_1 \in C^0(\overline{\Omega})$ can be extended by 0 outside Ω, and then $u_1 \in C^0(\mathbb{R}^d)$.

- Let us first exclude the case $c = 0$. Assuming to the contrary that the hypotheses of the lemma are satisfied with $c = 0$, we have

  $$\forall \varphi \in H^1(\Omega), \quad \int_\Omega \nabla u_1 \cdot \nabla \varphi dx = \lambda_1(\Omega) \int_\Omega u_1 \varphi dx + \int_{\partial\Omega} (\partial_n u_1) \varphi d\sigma.$$

  As $\partial_n u_1 = 0$ on $\partial\Omega$ and applying this property with $\varphi \equiv 1$, we obtain $\lambda_1(\Omega) \int_\Omega u_1 dx = 0$, which is a contradiction as $u_1 > 0$ in Ω.

- Assume $c > 0$. In order to apply [166], we aim at proving that (3.19) implies regularity of the domain Ω. To that end, we use the theory of regularity for free boundaries: in our context, we want to apply [66, Theorem 1.2] with $f := \lambda_1(\Omega) u_1 \in C^0(\mathbb{R}^d) \cap L^\infty(\mathbb{R}^d)$, which says that as Ω is a Lipschitz domain, if one can prove that (3.19) is valid in the sense of viscosity, then Ω must actually be $C^{1,\alpha}$ for some $\alpha > 0$. From there it is very classical with [124] that Ω is actually C^∞, which implies that $u_1 \in C^\infty(\overline{\Omega})$ and so [166] applies and provides the conclusion.

  Therefore, let us prove that $|\nabla u_1| = c$ in the sense of viscosity: this means that for every $x_0 \in \overline{\Omega}$ and every $\varphi \in C_c^2(\mathbb{R}^d)$,

  1. if $x_0 \in \Omega$, $\varphi(x_0) = u_1(x_0)$ and $\varphi \leq u_1$ (resp. $\varphi \geq u_1$), then $\Delta\varphi(x_0) \leq f(x_0)$ (resp. $\Delta\varphi(x_0) \geq f(x_0)$),
  2. if $x_0 \in \partial\Omega$, $\varphi(x_0) = u_1(x_0)$ and $\varphi_+ \leq u_1$ (resp. $\varphi_+ \geq u_1$), then $|\nabla\varphi(x_0)| \leq c$ (resp. $|\nabla\varphi(x_0)| \geq c$), where $\varphi_+ : x \in \mathbb{R}^d \longmapsto \max(\varphi(x), 0)$.

  For the first point, this follows from the regularity of u_1 inside Ω, namely $u_1 \in C^2(\Omega)$. Let us focus on the second point and take $x_0 \in \partial\Omega$ and $\varphi \in C_c^2(\mathbb{R}^d)$. In order to simplify the computations, we choose x_0 as the origin which allows to consider $x_0 = 0$: we will do a blow-up at x_0, so we denote

  $$\Omega_r = \frac{\Omega}{r}, \qquad \text{and} \qquad \forall x \in \mathbb{R}^d, \ u_r(x) = \frac{u_1(rx)}{r}, \quad \varphi_r(x) = \frac{\varphi(rx)}{r}.$$

  We then claim:

  1. $(\Omega_r)_{r>0}$ is increasing and one can define

     $$\Omega_0 := \bigcup_{r>0} \Omega_r$$

     which is a cone (it is the (interior of the) usual tangent of Ω at x_0 in the context of convex geometry). We also have that $(\partial\Omega_r)_{r>0}$ converges to $\partial\Omega_0$ locally in the Hausdorff sense.

2. as $u_1 \in W^{1,\infty}(\Omega)$, up to a subsequence $(u_r)_{r>0}$ converges locally uniformly to a function u_0 defined and Lipschitz on $\mathbb{R}^d$. Moreover, as for $r > 0$, one has $-\Delta u_r(x) = rf(rx) - c\mathcal{H}^{d-1}_{|\partial\Omega_r}$ in the sense of distribution in $\mathbb{R}^d$, we have at the limit (using the previous point to justify the convergence):
$$\Delta u_0(x) = c\mathcal{H}^{d-1}_{|\partial\Omega_0}.$$
As Ω_0 is a cone, this implies that u_0 is 1-homogeneous: indeed, for $\lambda \in (0,\infty)$, consider $u_0^\lambda : x \mapsto \frac{1}{\lambda}u_0(\lambda x)$. It is easy to see that u_0^λ has the same Laplacian as u_0 (in the sense of distribution in $\mathbb{R}^d$), so $v := u_0 - u_0^\lambda$ is harmonic in $\mathbb{R}^d$. As ∇v is bounded, from Liouville Theorem we deduce that v is affine, but as $v(0) = 0$ and $\nabla v(0) = 0$, we deduce that $v = 0$, which means u_0 is 1-homogeneous.
3. as φ is smooth, $(\varphi_r)_{r>0}$ converges locally uniformly to an affine function $\varphi_0(x)$ that is such that, up to a choice of coordinates,
$$\forall x \in \mathbb{R}^d, \quad \varphi_0(x) := Ax_d$$
where $A = |\nabla\varphi(x_0)|$.
4. (a) Assume now $u_1 \geq \varphi_+$. Then $u_0(x) \geq \varphi_0(x) = Ax_d$ in $\mathbb{R}^d$. If $A = 0$ then $A \leq c$. Otherwise, we get $\{u_0 > 0\} \supset \{x_d > 0\}$. From convexity of Ω_0 we obtain equality of these two domains. Then as u_0 and $x \mapsto cx_d$ both satisfy the same Cauchy problem with conditions on $\partial\{x_d > 0\}$, we deduce that $u_0(x) = c(x_d)_+$, and then clearly $u_0 \geq \varphi_0$ implies $c \geq A$.
   (b) Assume finally that $u_1 \leq \varphi_+$. We reproduce here a proof similar to [161, Lemma 5.31]. Using that u_0 is 1-homogeneous and nonnegative, we get that the trace of u_0 on $^{d-1}$ is a first eigenfunction of the Laplace-Beltrami operator on $\Omega_0 \cap ^{d-1}$ with Dirichlet boundary condition on $\partial\Omega_0 \cap ^{d-1}$ corresponding to the eigenvalue $d-1$. As $\Omega_0 \cap ^{d-1} \subset_+^{d-1} :=^{d-1} \cap \{x_d > 0\}$ and the Laplace-Beltrami of $\mathcal{S}_+^{d-1}$ is also $d-1$ we obtain that $\Omega_0 = \{x_d > 0\}$ and as in the previous case $u_0(x) = c(x_d)_+$ and $c \leq A$.

   We have therefore shown that $|\nabla u_1| = c$ is satisfied in the sense of viscosity, which as mentioned above, concludes the proof.

□

Theorem 12 allows us to prove the equivalence between 4 optimization problems.

Corollary 3. *Let $p > P(B)$. The following problems are equivalent:*

(I) $\min\{\lambda_1(\Omega) \mid \Omega \in \mathcal{K}_1^2 \text{ and } P(\Omega) = p\}$ *(III)* $\max\{P(\Omega) \mid \Omega \in \mathcal{K}_1^2 \text{ and } \lambda_1(\Omega) = f(p)\}$

(II) $\min\{\lambda_1(\Omega) \mid \Omega \in \mathcal{K}_1^2 \text{ and } P(\Omega) \geq p\}$ *(IV)* $\max\{P(\Omega) \mid \Omega \in \mathcal{K}_1^2 \text{ and } \lambda_1(\Omega) \leq f(p)\}$.

in the sense that any solution to one of the problem also solves the other ones. Moreover, any solution to these problems is a polygon.

Similarly the following problems are equivalent :

(I') $\max\{\lambda_1(\Omega) \mid \Omega \in \mathcal{K}_1^2 \text{ et } P(\Omega) = p\}$ *(III')* $\min\{P(\Omega) \mid \Omega \in \mathcal{K}_1^2 \text{ et } \lambda_1(\Omega) = g(p)\}$

(II') $\max\{\lambda_1(\Omega) \mid \Omega \in \mathcal{K}_1^2 \text{ et } P(\Omega) \leq p\}$ *(IV')* $\min\{P(\Omega) \mid \Omega \in \mathcal{K}_1^2 \text{ et } \lambda_1(\Omega) \geq g(p)\}$.

and any solution is $C^{1,1}$.

Proof. Let us prove the equivalence between the first four problems.

- We first show that any solution of (I) solves (II): let Ω_p be a solution to (I). Then for every $\Omega \in \mathcal{K}_1^2$ such that $P(\Omega) \geq p$, one has:

$$\lambda_1(\Omega) \geq f\big(P(\Omega)\big) \geq f(p) = \lambda_1(\Omega_p),$$

  where we used the monotonicity of f given by Theorem 12: therefore Ω_p solves (II).

- Reciprocally, let now Ω^p be a solution of (II): we want to show that Ω^p must be of perimeter p. We notice that

$$f(p) \geq \lambda_1(\Omega^p) \geq f\big(P(\Omega^p)\big) \geq f(p),$$

  where the first inequality follows as problem (II) allows more candidates than in the definition of f, and the last inequality uses again the monotonicity of f. Therefore $f(p) = f\big(P(\Omega^p)\big)$, and since f is strictly increasing, we obtain $P(\Omega^p) = p$, which implies that Ω^p solves (I).

We proved the equivalence between problems (I) and (II); equivalence between problems (III) and (IV) is shown by similar manipulations.

It remains to prove the equivalence between (I) and (III).

- Let Ω_p be a solution of (I), which means that $\Omega_p \in \mathcal{K}_1^2, P(\Omega_p) = p$ and $\lambda_1(\Omega_p) = f(p)$. Then for every $\Omega \in \mathcal{K}_1^2$ such that $\lambda_1(\Omega) = f(p)$ we have:

$$f(p) = \lambda_1(\Omega) \geq f\big(P(\Omega)\big),$$

  thus, since f is increasing, we get $p = P(\Omega_p) \geq P(\Omega)$, which means Ω_p solves (III).

- Let now Ω'_p be a solution of (III), then we have:

$$f(p) = \lambda_1(\Omega'_p) \geq f\big(P(\Omega'_p)\big),$$

  thus, by monotonicity of f we get $p \geq P(\Omega'_p)$. On the other hand, since Ω'_p solves (III) and that there exists Ω_p solution to (I), we have $P(\Omega'_p) \geq p$ which finally gives $P(\Omega'_p) = p$ and shows that Ω'_p solves (I).

The same approach can be applied to prove the equivalence between the second four problems. It remains finally to show the geometrical properties of optimal shapes:

- Let Ω be a solution of one of the first four problems. Thanks to the previous equivalence, it is necessarily a solution to (III), which enters the category of "reverse isoperimetric problems". We want to apply [134, Theorem 4] (see also [134, Example 8] for a similar problem, even though here λ_1 appears in the constraint of the problem): to that end one needs to see that the constraints in (III), that is to say $m(\Omega) = (\lambda_1(\Omega), |\Omega|) = (f(p), 1)$ have a first order derivative which is onto. As in the end of the proof of Theorem 12, this follows from Lemma 8. We deduce that [134, Theorem 4] applies and therefore Ω is a polygon.

- Let Ω be a solution of one of the last four problems: thanks to the equivalence, it is necessarily a solution of (III') so again as in the end of the proof of Theorem 12 we apply [134, Theorem 2, Corollary 2] (as in [134, Example 8], we also use [134, Propositions 5-6]) which shows that Ω is $C^{1,1}$.

□

Simple-connectedness of the diagram

In order to complete the proof of Theorem 11, we now need the following result:

Theorem 13. *We have:*

$$\mathcal{D}_{\mathcal{K}^2} = \Big\{(x,y) \in \mathbb{R}^2, \;\; x \geq P(B) \text{ and } f(x) \leq y \leq g(x)\Big\},$$

thus, $\mathcal{D}_{\mathcal{K}^2}$ is simply connected.

Proof. We consider a coordinate system $(O, \vec{\imath}, \vec{\jmath})$. Since the involved functionals are invariant by rotations and translations, we preliminarily remark that one may assume if needed that every domain contains the origin O and that its diameter is colinear to the axis $(O, \vec{\imath})$.

For a given convex body K, we denote by $\mathrm{diam}(K)$ its diameter and by h_K and ρ_K respectively the support and radial functions of K defined by

$$\forall \theta \in \mathcal{S}^1, \;\; h_K(\theta) = \sup\{\langle x, \theta\rangle, x \in K\}, \qquad \rho_K(\theta) = \sup\{\lambda \geq 0, \; \lambda\theta \in K\}. \tag{3.20}$$

Step 1: Minkowski sum and continuous paths:

Let $K_0, K_1 \in \mathcal{K}_1^2$ such that $P(K_0) = P(K_1) = p$. Define:

$$\forall t \in [0,1], \qquad K_t := \frac{(1-t)K_0 + tK_1}{\sqrt{|(1-t)K_0 + tK_1|}}. \tag{3.21}$$

- Since $t \in [0,1] \longmapsto (1-t)K_0 + tK_1 \in (\mathcal{K}^2, d^H)$ and the functionals $(|\cdot|, P, \lambda_1)$ are continuous for the Hausdorff distance, we have by composition that $t \in [0,1] \longmapsto \big(P(K_t), \lambda_1(K_t)\big) \in \mathbb{R}^2$ is also continuous.
- We also notice that thanks to the linearity of the perimeter for the Minkowski sum, as well as the Brunn-Minkowski inequality (see for example [164, Theorem 7.1.1]), one has:

$$\forall t \in [0,1], \; P\big((1-t)K_0 + tK_1\big) = (1-t)P(K_0) + tP(K_1) = p,$$
$$\text{and} \quad |(1-t)K_0 + tK_1|^{\frac{1}{2}} \geq (1-t)|K_0|^{\frac{1}{2}} + t|K_1|^{\frac{1}{2}} = 1,$$

  which implies

$$\forall t \in [0,1], \qquad P\big(K_t\big) \leq p. \tag{3.22}$$

This shows that given two convex domains with same perimeter, (3.21) defines a continuous path linking them, which "stays on the left" as we can see on Figure 3.6.

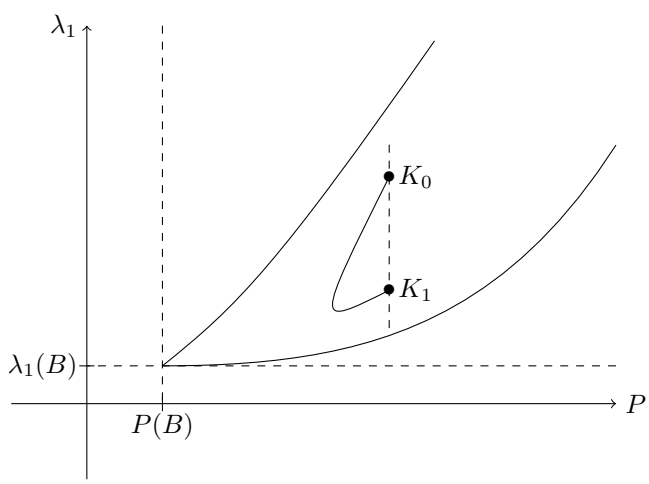

Figure 3.6: The path goes on the left

For $p \geq P(B)$ and for each $K_0, K_1 \in \mathcal{K}^2_{1,p}$, we therefore denote Γ_{K_0,K_1} the following closed path:

$$\begin{array}{rcccl} \Gamma_{K_0,K_1} & : & [0,1] & \longrightarrow & \mathbb{R}^2 \\ & & t & \longmapsto & \begin{cases} \big(P(K_{2t}), \lambda_1(K_{2t})\big) & \text{if } t \in [0, \frac{1}{2}], \\ \big(P(K_0),\ (2-2t)\lambda_1(K_1) + (2t-1)\lambda_1(K_0)\big) & \text{if } t \in [\frac{1}{2}, 1]. \end{cases} \end{array}$$

We note that as defined above, the path Γ_{K_0,K_1} contains two components:

- the first one corresponding to $t \in \big[0, \frac{1}{2}\big]$, which is included in the diagram $\mathcal{D}_{\mathcal{K}^2}$,
- and the second one corresponding to $t \in \big[\frac{1}{2}, 1\big]$, which is just "fictional" (not necessarily included in $\mathcal{D}_{\mathcal{K}^2}$) and is introduced in order to obtain a closed path so as we can use the index theory.

Step 2: Continuity of the paths Γ_{K_0,K_1} with respect to (K_0, K_1):

Let $p_0 > P(B)$. Take $K_0, K_1 \in \mathcal{K}^2_{1,p_0}$ and (K_0^n) and (K_1^n) two sequences of $\mathcal{K}^2_1$ converging respectively to K_0 and K_1 for the Hausdorff distance and such that $P(K_0^n) = P(K_1^n)$ for all $n \in \mathbb{N}^*$. Let $\varepsilon > 0$: we will prove that:

$$\exists N_\varepsilon, \forall n \geq N_\varepsilon, \forall t \in [0,1], \quad \big\| \ \Gamma_{K_0,K_1}(t) - \Gamma_{K_0^n,K_1^n}(t) \ \big\| < \varepsilon.$$

We have for every $t \in [\frac{1}{2}, 1]$:

$$\begin{aligned} \big\| \ \Gamma_{K_0,K_1}(t) - \Gamma_{K_0^n,K_1^n}(t) \ \big\| &\leq |P(K_0) - P(K_0^n)| + (2-2t)|\lambda_1(K_1) - \lambda_1(K_1^n)| + (2t-1)|\lambda_1(K_0) - \lambda_1(K_0^n)| \\ &\leq |P(K_0) - P(K_0^n)| + |\lambda_1(K_1) - \lambda_1(K_1^n)|, \end{aligned}$$

so the estimate is easy to obtain thanks to the convergence of $(K_0^n), (K_1^n)$ and the continuity of λ_1 and P.

For every $t \in [0, \frac{1}{2}]$, we have

$$\big\| \ \Gamma_{K_0,K_1}(t) - \Gamma_{K_0^n,K_1^n}(t) \ \big\| \leq \big|P(K_{2t}) - P(K_{2t}^n)\big| + \big|\lambda_1(K_{2t}) - \lambda_1(K_{2t}^n)\big|. \tag{3.23}$$

We want to control $\big|P(K_{2t}) - P(K_{2t}^n)\big|$ and $\big|\lambda_1(K_{2t}) - \lambda_1(K_{2t}^n)\big|$ independently of t. For the perimeter this will easily follow from the behavior of perimeter and volume with respect to Minkowski sums; for the eigenvalue the situation is more involved and we will use a quantitative version of its continuity with respect to the Hausdorff distance:

- We first notice that for all $t \in [0, 1/2]$ and $n \in \mathbb{N}$:

  $$|(1-2t)K_0 + 2tK_1| \geq 1, \qquad |(1-2t)K_0^n + 2tK_1^n| \geq 1 \qquad \text{and} \qquad P(K_{2t}), P(K_{2t}^n) \geq P(B).$$

  Therefore using Proposition 5

  $$\begin{aligned} \big|P(K_{2t}) - P(K_{2t}^n)\big| &= \frac{|P^2(K_{2t}) - P^2(K_{2t}^n)|}{P(K_{2t}) + P(K_{2t}^n)} \\ &\leq \frac{1}{2P(B)}\Big|\frac{P(K_0)^2}{|(1-2t)K_0 + 2tK_1|} - \frac{P(K_0^n)^2}{|(1-2t)K_0^n + 2tK_1^n|}\Big| \\ &\leq \big|P(K_0)^2\big((1-2t)^2 W_0(K_0^n, K_1^n) + 4t(1-2t)W_1(K_0^n, K_1^n) + 4t^2 W_2(K_0^n, K_1^n)\big) \\ &\quad -P(K_0^n)^2\big((1-2t)^2 W_0(K_0, K_1) + 4t(1-2t)W_1(K_0, K_1) + 4t^2 W_2(K_0, K_1)\big)\big| \\ &\leq \underbrace{\sum_{k=0}^{2}\Big(P(K_0)^2|W_k(K_0^n, K_1^n) - W_k(K_0, K_1)| \\ &\qquad + |W_k(K_0, K_1)| \times |P(K_0^n)^2 - P(K_0)^2|\Big)}_{H^n_{K_0,K_1}}. \end{aligned} \tag{3.24}$$

By continuity of the perimeter, P, W_0,W_1 and W_2 for the Hausdorff distance, we have $\lim_{n\to+\infty} H^n_{K_0,K_1} = 0$ while $H^n_{K_0,K_1}$ does not depend on t.

- The result [59, Lemma 2.1] states that if Ω_1 and Ω_2 are starlike planar domains with radial functions ρ_{Ω_1} and ρ_{Ω_2} for which there exists $r_0 > 0$ such that $\rho_{\Omega_1}, \rho_{\Omega_2} \geq r_0$ and $\|\rho_{\Omega_1} - \rho_{\Omega_2}\|_\infty \leq r_0$, then:

$$\left|\lambda_1(\Omega_1) - \lambda_1(\Omega_2)\right| \leq \frac{3}{r_0^3}\lambda_1(B_1)\|\rho_{\Omega_1} - \rho_{\Omega_2}\|_\infty. \tag{3.25}$$

We want to apply this result to (K_{2t}, K^n_{2t}) for $t \in [0, \frac{1}{2}]$ and n large enough. We therefore seek for a suitable r_0 such that the conditions of [59, Lemma 2.1] are satisfied.

Let $t \in \left[0, \frac{1}{2}\right]$ and $n \in \mathbb{N}^*$ sufficiently large so that $P(K^n_0), P(K^n_1) \leq p_0 + 1$. This implies by (3.22) that $P(K^n_{2t}) \leq p_0 + 1$ for every $t \in \left[0, \frac{1}{2}\right]$. We now use the classical inequality (see for example [35]) that asserts that for any convex body $\Omega \in \mathcal{K}^d$, one has $r(\Omega) \geq \frac{|\Omega|}{P(\Omega)}$, where $r(\Omega)$ denotes the inradius of Ω. In particular if $\Omega \in \mathcal{K}^2_1$ and $P(\Omega) \leq p_0 + 1$, we have:

$$r(\Omega) \geq r_0 := \frac{1}{p_0 + 1} > 0. \tag{3.26}$$

One can apply this result to K_{2t} and K^n_{2t}, and this implies that one can assume without loss of generality that K_{2t} and K^n_{2t} contain the ball of center O and radius r_0, and this gives $\rho_{K_{2t}} \geq r_0$ and $\rho_{K^n_{2t}} \geq r_0$. We moreover have:

$$\begin{aligned}
\left\|\rho_{K_{2t}} - \rho_{K^n_{2t}}\right\|_\infty &\leq \frac{\|\rho_{K_{2t}}\|_\infty \|\rho_{K^n_{2t}}\|_\infty}{r_0^2} d^H(K_{2t}, K^n_{2t}) \qquad \text{(see [37, Proposition 2])} \\
&\leq \frac{(p_0+1)^2}{r_0^2} d^H(K_{2t}, K^n_{2t}) \qquad \text{(we used } \|\rho_\Omega\|_\infty \leq diam(\Omega) \leq P(\Omega) \leq p_0 + 1).
\end{aligned}$$

On the other hand, we have:

$$\begin{aligned}
d^H(K_{2t}, K^n_{2t}) &= \left\|h_{K_{2t}} - h_{K^n_{2t}}\right\|_\infty \\
&= \left\| \frac{(1-2t)h_{K_0} + 2th_{K_1}}{\sqrt{|(1-2t)K_0 + 2tK_1|}} - \frac{(1-2t)h_{K^n_0} + 2th_{K^n_1}}{\sqrt{|(1-2t)K^n_0 + 2tK^n_1|}} \right\|_\infty \\
&\leq (1-2t) \left\| \frac{h_{K_0}}{\sqrt{|(1-2t)K_0 + 2tK_1|}} - \frac{h_{K^n_0}}{\sqrt{|(1-2t)K^n_0 + 2tK^n_1|}} \right\|_\infty \\
&\quad + 2t \left\| \frac{h_{K_1}}{\sqrt{|(1-2t)K_0 + 2tK_1|}} - \frac{h_{K^n_1}}{\sqrt{|(1-2t)K^n_0 + 2tK^n_1|}} \right\|_\infty \\
&\leq \frac{1}{\sqrt{|(1-2t)K^n_0 + 2tK^n_1|}} \left(\left\|h_{K_0} - h_{K^n_0}\right\|_\infty + \left\|h_{K_1} - h_{K^n_1}\right\|_\infty \right) \\
&\quad + (\|h_{K_0}\|_\infty + \|h_{K_1}\|_\infty) \left| \frac{1}{\sqrt{|(1-2t)K^n_0 + 2tK^n_1|}} - \frac{1}{\sqrt{|(1-2t)K_0 + 2tK_1|}} \right| \\
&\leq \left(d^H(K_0, K^n_0) + d^H(K_1, K^n_1)\right) \\
&\quad + (\|h_{K_0}\|_\infty + \|h_{K_1}\|_\infty) \times \Big| \, |(1-2t)K^n_0 + 2tK^n_1| - |(1-2t)K_0 + 2tK_1| \, \Big| \\
&\leq \underbrace{\left(d^H(K_0, K^n_0) + d^H(K_1, K^n_1)\right) + (\|h_{K_0}\|_\infty + \|h_{K_1}\|_\infty) \times \sum_{k=0}^{2} |W_k(K^n_0, K^n_1) - W_k(K_0, K_1)|}_{G^n_{K_0,K_1}}.
\end{aligned}$$

We then obtain the following estimate:

$$\forall t \in \left[0, \frac{1}{2}\right], \quad \left\|\rho_{K_{2t}} - \rho_{K^n_{2t}}\right\|_\infty \leq \frac{(p_0+1)^2}{r_0^2} \times G^n_{K_0,K_1}. \tag{3.27}$$

As for $H^n_{K_0,K_1}$, by continuity argument we have $\lim_{n\to+\infty} G^n_{K_0,K_1} = 0$. Then, we for n sufficiently large (independently on t), we have $\left\|\rho_{K_{2t}} - \rho_{K^n_{2t}}\right\|_\infty \leq r_0$.

We are finally able to apply (3.25) on K_{2t} and K^n_{2t}. We get that for n sufficiently large, we have

$$\forall t \in \left[0, \frac{1}{2}\right], \quad \left|\lambda_1(K_{2t}) - \lambda_1(K^n_{2t})\right| \leq \frac{3}{r_0^3}\lambda_1(B_1)\|\rho_{K^n_{2t}} - \rho_{K_{2t}}\|_\infty \leq \frac{3\lambda_1(B_1)}{r_0^5}(p_0+1)^2 G^n_{K_0,K_1}. \tag{3.28}$$

By (3.23), (3.24), (3.28) and the fact that $\lim_{n\to+\infty} G^n_{K_0,K_1} = \lim_{n\to+\infty} H^n_{K_0,K_1} = 0$, we conclude that there exists $N_\varepsilon \in \mathbb{N}^*$ such that:

$$\forall n \geq N_\varepsilon, \quad \sup_{t\in[0,1]} \left\| \Gamma_{K_0,K_1}(t) - \Gamma_{K^n_0,K^n_1}(t) \right\| < \varepsilon.$$

Step 3: The arcs go infinitely to the right when the perimeter increases:

Let $p \geq P(B)$ and (K_0, K_1) two elements of $\mathcal{K}^2_{1,p}$; taking advantage of the invariance with translation and rotation, we choose to align the diameters of K_0 and K_1 with the same axe (say $(O, \vec{i})$). We prove here that this implies:

$$\forall t \in [0,1] \quad P\big(K_t\big) \geq \frac{p}{2},$$

where $(K_t)_{t\in[0,1]}$ is defined in (3.21).

As mentioned in the beginning of the proof, we can assume that the diameter of every involved convex $K \in \mathcal{K}^2_1$ is aligned with $(O, \vec{i})$, thus the diameter of K is given by

$$\mathrm{diam}(K) = h_K(0) + h_K(\pi),$$

where h_K is the support functional of K, defined in (3.20). On the other hand we denote ε_K the width in the direction orthogonal to $(O, \vec{i})$:

$$\varepsilon_K := h_K(\pi/2) + h_K(-\pi/2).$$

We easily get the following estimates from Figure 3.7:

$$2 \times \mathrm{diam}(K) \leq P(K) \leq 4 \times \mathrm{diam}(K) \quad \text{and} \quad |K| \leq \varepsilon_K \times \mathrm{diam}(K) \leq 2|K|,$$

In particular if $K \in \mathcal{K}^2_{1,p}$, then

$$\mathrm{diam}(K) \leq \frac{p}{2} \qquad \text{and} \qquad \varepsilon_K \leq \frac{2}{\mathrm{diam}(K)} \leq \frac{8}{p}.$$

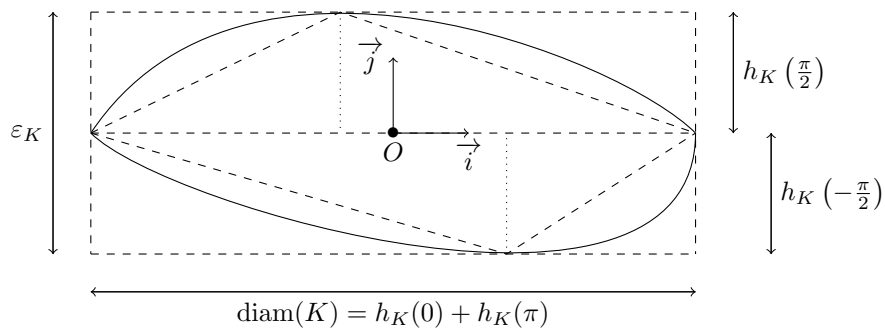

Figure 3.7: The convex contains a quadrilateral and is contained in a rectangle

We denote by d_t and ε_t the diameter and width in the direction orthogonal to $(O, \vec{i})$ of $(1-t)K_0 + tK_1$, where $t \in [0,1]$. We have:

$$\begin{aligned}
d_t &:= \max_{\theta\in[0,2\pi]} \big(h_{(1-t)K_0+tK_1}(\theta) + h_{(1-t)K_0+tK_1}(\pi+\theta)\big) \\
&= \max_{\theta\in[0,2\pi]} \big((1-t)\times(h_{K_0}(\theta)+h_{K_0}(\pi+\theta)) + t\times(h_{K_1}(\theta)+h_{K_1}(\pi+\theta))\big) \\
&\leq (1-t)\times \max_{\theta\in[0,2\pi]}(h_{K_0}(\theta)+h_{K_0}(\pi+\theta)) + t\times \max_{\theta\in[0,2\pi]}(h_{K_1}(\theta)+h_{K_1}(\pi+\theta)) \\
&= (1-t)\times\big(\underbrace{h_{K_0}(0)+h_{K_0}(\pi)}_{d_0=\mathrm{diam}(K_0)}\big) + t\times\big(\underbrace{h_{K_1}(0)+h_{K_1}(\pi)}_{d_1=d(K_1)}\big) \quad \text{(the diameters of } K_0 \text{ and } K_1 \text{ are colinear to } (O,\vec{i})\text{)} \\
&= h_{(1-t)K_0+tK_1}(0) + h_{(1-t)K_0+tK_1}(\pi) \\
&\leq \max_{\theta\in[0,2\pi]} \big(h_{(1-t)K_0+tK_1}(\theta) + h_{(1-t)K_0+tK_1}(\pi+\theta)\big) = d_t.
\end{aligned}$$

Thus, we have the equalities:

$$\begin{cases} d_t &= h_{(1-t)K_0+tK_1}(0) + h_{(1-t)K_0+tK_1}(\pi) = (1-t)d_0 + td_1. \\ \varepsilon_t &= h_{(1-t)K_0+tK_1}(\pi/2) + h_{(1-t)K_0+tK_1}(-\pi/2) = (1-t)\varepsilon_0 + t\varepsilon_1. \end{cases}$$

This implies:

$$\begin{aligned}
\forall t\in[0,1], \quad |(1-t)K_0+tK_1| &\leq d_t\times\varepsilon_t = \big((1-t)d_0+td_1\big)\times\big((1-t)\varepsilon_0+t\varepsilon_1\big) \\
&\leq \left((1-t)\frac{p}{2}+t\frac{p}{2}\right)\times\left((1-t)\frac{8}{p}+t\frac{8}{p}\right) = 4
\end{aligned}$$

Finally, we get:

$$\forall t\in[0,1], \quad P(K_t) = P\Big(\frac{(1-t)K_0+tK_1}{\sqrt{|(1-t)K_0+tK_1|}}\Big) = \frac{(1-t)P(K_0)+tP(K_1)}{\sqrt{|(1-t)K_0+tK_1|}} \geq \frac{p}{2}.$$

Step 4: Relevant paths and conclusion

We denote $\mathcal{E} := \Big\{(x,y) \in \mathbb{R}^2 \mid x \geq P(B) \text{ and } f(x) \leq y \leq g(x)\Big\}$. We already noticed that $\mathcal{D}_{\mathcal{K}^2} \subset \mathcal{E}$. Assume by contradiction that there exists $A(x_A, y_A) \in \mathcal{E} \setminus \mathcal{D}_{\mathcal{K}^2}$. From Proposition 4, there exists $r > 0$ such that $B(A,r) \subset \mathcal{E} \setminus \mathcal{D}_{\mathcal{K}^2}$. We are interested in analyzing if A is inside a judiciously chosen closed curve: to that end, let us introduce the set:

$$I = \Big\{ \; p \geq x_A + \frac{r}{2} \quad / \; \exists K_1, K_2 \in \mathcal{K}^2_{1,p} \text{ such that } A \text{ is in the interior of } \Gamma_{K_1,K_2} \Big\}.$$

We note that for every $p \geq x_A + \frac{r}{2}$ and $K_1, K_2 \in \mathcal{K}^2_{1,p}$, the path Γ_{K_1,K_2} does not cross the point A. Indeed:

- $A \notin \{\Gamma_{K_1,K_2}(t) \mid t \in \big[0, \frac{1}{2}\big]\}$, because $\{\Gamma_{K_1,K_2}(t) \mid t \in \big[0, \frac{1}{2}\big]\}$ is contained in $\mathcal{D}_{\mathcal{K}^2}$, which is not the case for the point A as assumed above.
- $A \notin \{\Gamma_{K_1,K_2}(t) \mid t \in \big[\frac{1}{2}, 1\big]\} = \{(P(K_1), (2-2t)\lambda_1(K_2) + (2t-1)\lambda_1(K_1)) \mid t \in \big[\frac{1}{2}, 1\big]\}$, because $P(K_1) = P(K_2) = p \geq x_A + \frac{r}{2} > x_A$.

Moreover, as we do not know whether Γ_{K_1,K_2} is a simple closed curve, we define the interior of Γ_{K_1,K_2} as the set of points A such that the index (also called winding number) of A with respect to the closed curve Γ_{K_1,K_2} is not zero, that is to say $\text{ind}(\Gamma_{K_1,K_2}, A) \neq 0$. We will also say that A is exterior to Γ_{K_1,K_2} if this index is zero.

Using the first step, we note that $x_A + r/2 \in I$: indeed using Corollary 1 we know that there exist K_1 and K_2 respectively solutions of the problems

$$\min \Big\{\lambda_1(\Omega), \quad \Omega \in \mathcal{K}^2_{1,x_A+r/2}\Big\} \quad \text{ and } \quad \max \Big\{\lambda_1(\Omega), \quad \Omega \in \mathcal{K}^2_{1,x_A+r/2}\Big\},$$

and as the path Γ_{K_1,K_2} stays on the left of $x_A + r/2$ and its vertical arc is on the right of A, using that $B(A,r) \cap \mathcal{D}_{\mathcal{K}^2} = \emptyset$ we deduce that A is in the interior of Γ_{K_1,K_2}, thus $x_A + r/2 \in I$ and in particular I is not empty. It is also bounded from above, as using Step 3, when the perimeter of two domains K_1, K_2 is sufficiently large, A cannot be in the interior of Γ_{K_1,K_2}. As a consequence, we can define $p_0 = \sup I \in [x_A + r/2, +\infty)$. We analyze the two following cases:

- **<u>Case 1</u>: $p_0 \notin I$, i.e. for every $K_1, K_2 \in \mathcal{K}^2_{1,p_0}$, A is in the exterior of Γ_{K_1,K_2}.**

  As p_0 is defined as the supremum of I, there exists $(p_n)_{n\geq 1}$ converging to p_0 and $(K_1^n, K_2^n)_{n\geq 1}$ two sequences of elements of $\mathcal{K}^2_{1,p_n}$ such that A is in the interior of $\Gamma_{K_1^n,K_2^n}$.

  By Blaschke selection Theorem, there exist $(K_1^{p_0}, K_2^{p_0})$ such that up to a subsequence (that we do not denote) $K_1^n \underset{n\to\infty}{\longrightarrow} K_1^{p_0}$ and $K_2^n \underset{n\to\infty}{\longrightarrow} K_2^{p_0}$ for the Hausdorff distance. Using the result of Step 2 we get that:

  $$\forall \varepsilon > 0, \exists n_\varepsilon \in \mathbb{N}^*, \forall t \in [0,1], \quad \Big\| \, \Gamma_{K_1^{p_0},K_2^{p_0}}(t) - \Gamma_{K_1^{n_\varepsilon},K_2^{n_\varepsilon}}(t) \Big\| < \varepsilon,$$

  so for a sufficiently small value of $\varepsilon > 0$, by continuity of the index under this uniform estimate, we have:

  $$\text{ind}\big(\Gamma_{K_1^{p_0},K_2^{p_0}}, A\big) = \text{ind}\big(\Gamma_{K_1^{n_\varepsilon},K_2^{n_\varepsilon}}, A\big).$$

  This is a contradiction (see Figure 3.8) since A is in the interior of $\Gamma_{K_1^{p_{n_\varepsilon}},K_2^{p_{n_\varepsilon}}}$ (ie. $\text{ind}\big(\Gamma_{K_1^{p_{n_\varepsilon}},K_2^{p_{n_\varepsilon}}}, A\big) \neq 0$) while as $K_1^{p_0}, K_2^{p_0} \in \mathcal{K}^2_{1,p_0}$, it must also be in the exterior of $\Gamma_{K_1^{p_0},K_2^{p_0}}$ (ie. $\text{ind}\big(\Gamma_{K_1^{p_0},K_2^{p_0}}, A\big) = 0$).

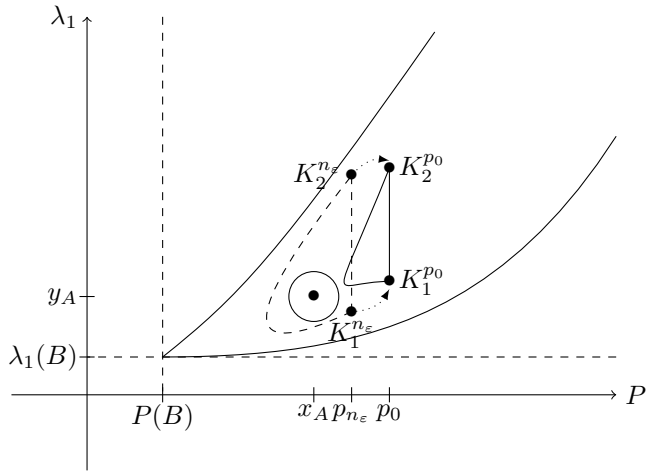

Figure 3.8: Using compactness to find sets $K_1^{p_0}$ and $K_2^{p_0}$

- **<u>Case 2</u>: $p_0 \in I$, i.e. there exist $K_1^{p_0}, K_2^{p_0} \in \mathcal{K}^2_{1,p_0}$ such that A is in the interior of Γ_{K_1,K_2}.**
  Consider $p_n = p_0 + 1/n$ for $n \geq 1$. By Corollary 2, there exist (K_1^n, K_2^n) two sequences in $\mathcal{K}^2_{1,p_n}$ such that $K_1^n \underset{n\to\infty}{\longrightarrow} K_1^{p_0}$ and $K_2^n \underset{n\to\infty}{\longrightarrow} K_2^{p_0}$ for the Hausdorff distance, see Figure 3.9.

  Similarly to the first case, using Step 3 and the continuity of the index (with respect to the curve) we have for n large enough

  $$\operatorname{ind}\big(\Gamma_{K_1^{p_0},K_2^{p_0}}, A\big) = \operatorname{ind}\big(\Gamma_{K_1^n,K_2^n}, A\big).$$

  This is also a contradiction since A is in the interior of $\Gamma_{K_1^{p_0},K_2^{p_0}}$ while as $p_n > \sup I$, it must be in the exterior of $\Gamma_{K_1^n,K_2^n}$.

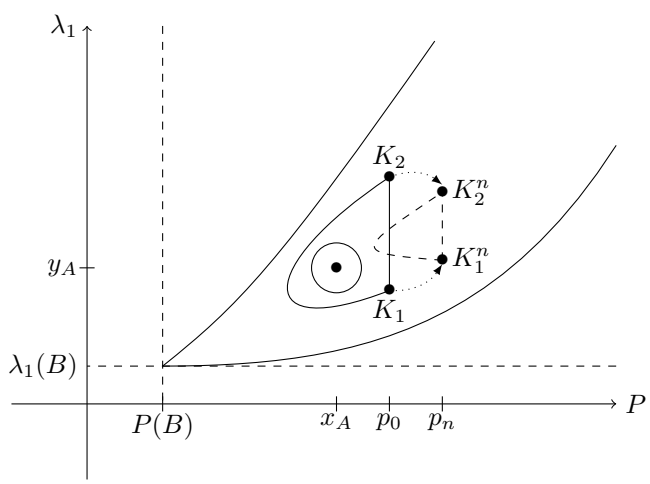

Figure 3.9: Using Corollary 2 to increase the perimeter

We obtained a contradiction in both cases, which proves that $\mathcal{D}_{\mathcal{K}^2} = \mathcal{E}$. Thus $\mathcal{D}_{\mathcal{K}^2} \subset \mathbb{R}^2$ does not contain any hole and so is simply connected. This concludes the proof. $\square$

The following result is a direct consequence of Theorem 13.

Corollary 4. *The diagram $\mathcal{D}_{\mathcal{K}^2}$ is vertically and horizontally convex.*

3.3.3 Asymptotics of the diagram

Upper behavior: It has been proven in [145] and [64, Proposition 5.5] that

Proposition 7. *Let B_1 be a ball of radius 1 in $\mathbb{R}^d$ with $d \geq 2$, and $p > d$.*

1. *If $\gamma < \dfrac{d(d+1)P(B_1)}{4\lambda_1(B_1)(\lambda_1(B_1)-d)}$, then B_1 is a local minimizer of $P - \gamma\lambda_1$ in a $W^{2,p}$-neighborhood with volume constraint, in the sense that there exists $\eta = \eta(\gamma) > 0$ such that*
$$P(B_1^\varphi) - P(B_1) \geq \gamma\left[\lambda_1(B_1^\varphi) - \lambda_1(B_1)\right]$$
for every B_1^φ such that $|B_1^\varphi| = |B_1|$ and being nearly spherical in the sense that
$$B_1^\varphi := \Big\{ tx(1+\varphi(x)), t \in [0,1[, x \in^{d-1} \Big\} \quad \text{with } \varphi :^{d-1} \to \mathbb{R} \text{ satisfying } \|\varphi\|_{W^{2,p}(^{d-1})} \leq \eta.$$

2. *If $\gamma > \dfrac{d(d+1)P(B_1)}{4\lambda_1(B_1)(\lambda_1(B_1)-d)}$, then B_1 is not a local minimizer $P - \gamma\lambda_1$ among domains with given volume; more precisely, for $\eta > 0$, there exists $\varphi :^{d-1} \to \mathbb{R}$ such that*
$$|B_1^\varphi| = |B_1|, \qquad \|\varphi\|_{W^{2,p}(^{d-1})} \leq \eta, \qquad \text{and} \quad P(B_1^\varphi) - P(B_1) < \gamma\left[\lambda_1(B_1^\varphi) - \lambda_1(B_1)\right].$$

Corollary 5. *Let $d \geq 2$, $x_0 = \frac{P(B_1)}{|B_1|^{\frac{d-1}{d}}}$ and g the function defined in Section 3.3.2. Then*
$$\limsup_{x \to x_0} \frac{g(x) - g(x_0)}{x - x_0} \geq \frac{4|B_1|^{\frac{d+1}{d}}\lambda_1(B_1)\big(\lambda_1(B_1) - d\big)}{d(d+1)P(B_1)}. \tag{3.29}$$

Remark 9. *When $d = 2$, inequality (3.29) becomes*
$$\limsup_{x \to x_0} \frac{g(x) - g(x_0)}{x - x_0} \geq \frac{\sqrt{\pi}}{3}\lambda_1(B_1) \times \big(\lambda_1(B_1) - 2\big) \geq 12.9264,$$
where the numerical lower bound is obtained by using a lower numerical value of $\lambda_1(B_1) = j_{0,1}^2$ (where $j_{0,1}$ denotes the first zero of the Bessel function J_0).

Proof. Given $\gamma > \dfrac{d(d+1)P(B_1)}{4\lambda_1(B_1)(\lambda_1(B_1)-d)}$ and $n \in \mathbb{N}^*$, from Proposition 7, there exists $\varphi_n :^{d-1} \to \mathbb{R}$ such that
$$|B_1| = |B_1^{\varphi_n}|, \qquad \|\varphi_n\|_{W^{2,p}(^{d-1})} \leq \frac{1}{n}, \qquad \text{and} \quad P(B_1^{\varphi_n}) - P(B_1) < \gamma\left[\lambda_1(B_1^{\varphi_n}) - \lambda_1(B_1)\right].$$
Defining $\Omega_n = \frac{B_1^{\varphi_n}}{|B_1^{\varphi_n}|^{1/d}}$ and $B = \frac{B_1}{|B_1|^{1/d}}$ having unit area, we get
$$P(\Omega_n) - P(B) = \frac{P(B_1^{\varphi_n}) - P(B_1)}{|B_1|^{\frac{d-1}{d}}} < \frac{\gamma}{|B_1|^{\frac{d-1}{d}}}\left[\lambda_1(B_1^{\varphi_n}) - \lambda_1(B_1)\right] = \frac{\gamma}{|B_1|^{\frac{d+1}{d}}}\left[\lambda_1(\Omega_n) - \lambda_1(B)\right].$$
Defining $x_n = P(\Omega_n)$, we get, as g is defined as a maximum:
$$x_n - x_0 < \frac{\gamma}{|B_1|^{\frac{d+1}{d}}}(g(x_n) - g(x_0)).$$
When n diverges to $+\infty$, x_n goes to x_0, and therefore
$$\limsup_{x \to x_0} \frac{g(x) - g(x_0)}{x - x_0} \geq \lim_{n \to +\infty} \frac{g(x_n) - g(x_0)}{x_n - x_0} \geq \frac{|B_1|^{\frac{d+1}{d}}}{\gamma},$$
where γ is arbitrary chosen in $\left(\dfrac{d(d+1)P(B_1)}{4\lambda_1(B_1)(\lambda_1(B_1)-d)}, +\infty\right)$.

This ends the proof. □

Lower behavior: In the next result, we study the stability of the ball for the minimality of $\lambda_1 - c[P - P(B)]^\alpha$ in order to have information about the behavior of the lower part of the diagram near the ball:

Theorem 14. *Let B_1 be the ball of radius 1 in $\mathbb{R}^d$ with $d \geq 2$, and $p > d$.*

1. *Then there exists $c > 0$ and $\eta > 0$ such that*

$$\lambda_1(B_1^\varphi) - \lambda_1(B_1) \geq c\Big[P(B_1^\varphi) - P(B_1)\Big]^{3/2}$$

for every B_1^φ such that $|B_1^\varphi| = |B_1|$ and being nearly spherical with $\|\varphi\|_{W^{2,p}(^{d-1})} \leq \eta$.

2. *If however $\alpha \in (0, 3/2)$, then for any $c > 0$ and $\eta > 0$, there exists $\varphi :^{d-1}\to \mathbb{R}$ such that*

$$|B_1^\varphi| = |B_1|, \quad \|\varphi\|_{W^{2,p}(^{d-1})} \leq \eta, \quad \text{and} \quad \lambda_1(B_1^\varphi) - \lambda_1(B_1) < c\Big[P(B_1^\varphi) - P(B_1)\Big]^\alpha.$$

Such nearly spherical sets were considered by Fuglede in [93] where he was studying the stability of the ball for the usual isoperimetric problem. See also [42] where the authors use nearly spherical sets when studying the quantitative Faber-Krahn inequality, and [64] for a more general approach about stability among smooth deformations of a given set.

Proof. 1. Let $\varphi :^{d-1}\to \mathbb{R}$ such that $|B_1^\varphi| = |B_1|$ and the barycenter of B_1^φ is 0. From [93], there exists $\eta_1 > 0$ and $C_1 > 0$ such that

$$P(B_1^\varphi) - P(B_1) \leq C_1\|\varphi\|^2_{H^1(^{d-1})} \quad \text{if } \|\varphi\|_{W^{1,\infty}(^{d-1})} \leq \eta_1.$$

Moreover, using [64, Theorem 1.3 and Section 5.2] (see also [42, Theorem 3.3] in the context of $C^{2,\alpha}$-perturbations), there exists $\eta_2 > 0$ and $c_2 > 0$ such that

$$\lambda_1(B_1^\varphi) - \lambda_1(B_1) \geq c_2\|\varphi\|^2_{H^{1/2}(^{d-1})} \quad \text{if } \|\varphi\|_{W^{2,p}(^{d-1})} \leq \eta_2.$$

Therefore, setting $\eta = \min\{\eta_1, \eta_2\}$ and assuming $\|\varphi\|_{W^{2,p}(^{d-1})} \leq \eta$, we get for $c > 0$:

$$\lambda_1(B_1^\varphi) - \lambda_1(B_1) - c\Big[P(B_1^\varphi) - P(B_1)\Big]^{3/2} \geq c_2\|\varphi\|^2_{H^{1/2}(^{d-1})} - cC_1^{3/2}\|\varphi\|^3_{H^1(^{d-1})},$$

but from a Gagliardo-Nirenberg type inequality (see for example [45]), we have that there exists $C_3, C_4 > 0$ such that

$$\|\varphi\|_{H^1(^{d-1})} \leq C_3\|\varphi\|^{2/3}_{H^{1/2}(^{d-1})}\|\varphi\|^{1/3}_{H^2(^{d-1})} \leq C_4\|\varphi\|^{2/3}_{H^{1/2}(^{d-1})}\|\varphi\|^{1/3}_{W^{2,p}(^{d-1})},$$

(we used $p > d \geq 2$) therefore

$$\lambda_1(B_1^\varphi) - \lambda_1(B_1) - c\Big[P(B_1^\varphi) - P(B_1)\Big]^{3/2} \geq \|\varphi\|^2_{H^{1/2}(^{d-1})}\Big[c_2 - cC_1^{3/2}C_4^3\|\varphi\|_{W^{2,p}(^{d-1})}\Big],$$

which is positive if $\|\varphi\|_{W^{2,p}(^{d-1})} \leq \eta$ is small enough.

2. Assume to the contrary that for every $\varphi :^{d-1}\to \mathbb{R}$ such that $|B_1^\varphi| = |B_1|$ and $\|\varphi\|_{W^{2,p}(^{d-1})} \leq \eta$, we have

$$\lambda_1(B_1^\varphi) - \lambda_1(B_1) \geq c\Big[P(B_1^\varphi) - P(B_1)\Big]^\alpha,$$

where $\alpha \in [0, 3/2)$ and $c > 0$. We choose the origin as the center of B_1 so that $\mathrm{Bar}(B_1) = 0$ where Bar denotes the barycenter of a given shape. We also denote $\mathrm{Vol} : \Omega \mapsto |\Omega|$.

We now use the framework from [64], and in particular, if J denotes a shape functional, then $J'(B_1), J''(B_1)$ denote respectively the first and second order derivatives of $\varphi \mapsto J(B_1^\varphi)$. From

[64, Proposition 4.5] the perimeter functional satisfies $\mathbf{(IT}_{H^1,W^{1,\infty}}\mathbf{)}$ which means there exists ω_1 a modulus of continuity such that

$$P(B_1^\varphi) - P(B_1) = P'(B_1).\varphi + \frac{1}{2}P''(B_1).(\varphi,\varphi) + \omega_1(\|\varphi\|_{W^{1,\infty}({}^{d-1})})\|\varphi\|^2_{H^1({}^{d-1})}.$$

Moreover, B_1 is a stable critical shape of P under volume constraint and up to translations (see [64, Section 5.1]), which means that there exists $\mu \in \mathbb{R}$ a Lagrange multiplier such that

$$P'(B_1).\varphi = \mu \mathrm{Vol}'(B_1).\varphi, \quad \forall \varphi \in W^{1,\infty}({}^{d-1})$$

and there exists $c_1 > 0$ such that

$$(P-\mu\mathrm{Vol})''(B_1).(\varphi,\varphi) \geq c_1\|\varphi\|^2_{H^1({}^{d-1})}, \qquad \forall \varphi \in W^{1,\infty}({}^{d-1}) \text{ such that } \mathrm{Vol}'(B_1).\varphi = 0 \text{ and } \mathrm{Bar}'(B_1).\varphi = 0.$$

Therefore, one gets that there exists $\eta_1 > 0$ such that for any $\varphi \in W^{1,\infty}({}^{d-1})$ satisfying

$$\mathrm{Vol}'(B_1).\varphi = 0, \qquad \mathrm{Bar}'(B_1).\varphi = 0 \qquad \text{and} \qquad \|\varphi\|_{W^{1,\infty}({}^{d-1})} \leq \eta_1,$$

one has

$$\begin{aligned} P(B_1^\varphi) - P(B_1) &\geq \frac{1}{2}(P-\mu\mathrm{Vol})''(B_1).(\varphi,\varphi) + \frac{\mu}{2}\mathrm{Vol}''(B_1).(\varphi,\varphi) - \frac{c_1}{4}\|\varphi\|^2_{H^1({}^{d-1})} \\ &\geq \frac{c_1}{2}\|\varphi\|^2_{H^1({}^{d-1})} - C_1\|\varphi\|^2_{L^2({}^{d-1})}, \end{aligned}$$

for some $C_1 \in \mathbb{R}$ (coming from the fact that $\mathrm{Vol}''(B)$ is a continuous quadratic form on $L^2({}^{d-1})$, see [64, Section 2.2]).

Similarly, from [64, Theorem 1.4] λ_1 satisfies $\mathbf{(IT}_{H^{1/2},W^{2,p}}\mathbf{)}$ and moreover B_1 is a critical point of λ_1 under volume constraint, and $\lambda_1''(B_1)$ is a continuous quadratic form on $H^{1/2}({}^{d-1})$, so there exists $\eta_2 > 0$ such that for any $\varphi \in W^{2,p}({}^{d-1})$ satisfying

$$\mathrm{Vol}'(B_1).\varphi = 0, \qquad \mathrm{Bar}'(B_1).\varphi = 0 \qquad \text{and} \qquad \|\varphi\|_{W^{2,p}({}^{d-1})} \leq \eta_2,$$

one has

$$\lambda_1(B_1^\varphi) - \lambda_1(B_1) \leq C_2\|\varphi\|^2_{H^{1/2}({}^{d-1})}.$$

Therefore we get as above, setting $\eta = \min\{\eta_1, \eta_2\}$:

$$\begin{aligned} &\forall \varphi \text{ such that } \|\varphi\|_{W^{2,p}({}^{d-1})} \leq \eta, \quad \mathrm{Vol}'(B_1).\varphi = 0, \quad \text{and} \quad \mathrm{Bar}'(B_1).\varphi = 0, \\ &\qquad\qquad \|\varphi\|^2_{H^1({}^{d-1})} \leq C\|\varphi\|^{2/\alpha}_{H^{1/2}({}^{d-1})} + \widetilde{C}\|\varphi\|^2_{L^2({}^{d-1})}, \end{aligned}$$

for some $(C, \widetilde{C}) \in \mathbb{R}^2_+$. Using scaling, and looking at the expressions of $\mathrm{Vol}'(B_1), \mathrm{Bar}'(B_1)$, we finally obtain:

$$\begin{aligned} &\forall \varphi \text{ such that } \int_{{}^{d-1}} \varphi = 0, \quad \text{and} \quad \forall i \in [\![1,d]\!], \int_{{}^{d-1}} x_i\varphi(x) = 0, \\ &\qquad\qquad \|\varphi\|^2_{H^1({}^{d-1})} \leq C\eta^{2/\alpha-2}\|\varphi\|^{2-2/\alpha}_{W^{2,p}({}^{d-1})}\|\varphi\|^{2/\alpha}_{H^{1/2}({}^{d-1})} + \widetilde{C}\|\varphi\|^2_{L^2({}^{d-1})}. \end{aligned} \tag{3.30}$$

We want to get a contradiction by testing such interpolation inequality for an oscillating function φ. To that end (see [168, pages 139-141] for more details), we denote $\mathcal{H}_k$ the space of spherical harmonics of degree $k \in \mathbb{N}$ (that is, the restriction to ${}^{d-1}$ of homogeneous polynomials in $\mathbb{R}^d$, of degree k) and $(Y^{k,l})_{1\leq l\leq d_k}$ an orthonormal basis of $\mathcal{H}_k$ with respect to the $L^2({}^{d-1})$ scalar

product. The family $(Y^{k,l})_{k\in\mathbb{N},1\le l\le d_k}$ is a Hilbert basis of $L^2({}^{d-1})$, so any function φ in $L^2({}^{d-1})$ can be decomposed:

$$\varphi(x)=\sum_{k=0}^{\infty}\sum_{l=1}^{d_k}\alpha_{k,l}(\varphi)Y^{k,l}(x),\quad \text{for } x\in{}^{d-1},\quad \text{with}\quad \alpha_{k,l}(\varphi)=\int_{{}^{d-1}}\overline{Y_{k,l}}\varphi.$$

Moreover, for $s\in\mathbb{R}_+$, $\|\varphi\|_{H^s({}^{d-1})}$ is equivalent to $\left(\sum_{k\in\mathbb{N}}(1+k)^{2s}\sum_l|\alpha_{k,l}|^2\right)^{1/2}$.
We therefore choose $\varphi_k=Y_{k,1}$ for $k\ge 2$. As $\mathcal{H}_0$ is made of constant functions and $\mathcal{H}_1=\operatorname{span}(x_i)_{i\in[\![1,d]\!]}$, we have

$$\forall k\ge 2,\quad \int_{{}^{d-1}}\varphi_k=0\qquad\text{and}\qquad \forall i\in[\![1,d]\!],\ \int_{{}^{d-1}}x_i\varphi_k(x)=0$$

so that $(\varphi_k)_{k\ge 2}$ are admissible for (3.30). Moreover

$$\forall s\ge 0,\ \ \|\varphi_k\|_{H^s({}^{d-1})}\underset{k\to\infty}{\sim}k^s,\quad\text{and}\quad \|\varphi_k\|_{W^{2,p}({}^{d-1})}\ge\|\varphi_k\|_{H^2({}^{d-1})}$$

so that (3.30) gives $k^2=O(k^{4-4/\alpha}k^{1/\alpha}+1)$ which contradicts the assumption $\alpha<3/2$ and concludes the proof.

□

Corollary 6. *Take $\alpha\in(0,3/2)$, $d\ge 2$ and $x_0=\frac{P(B_1)}{|B_1|^{\frac{d-1}{d}}}$, we have*

$$\liminf_{x\to x_0}\frac{f(x)-f(x_0)}{(x-x_0)^\alpha}=0.$$

Proof. Take $c>0$. By the second assertion of Theorem 14, for every $n\in\mathbb{N}^*$ there exists $\varphi_n:{}^{d-1}\to\mathbb{R}$ such that

$$|B_1^{\varphi_n}|=|B_1|,\quad \|\varphi_n\|_{W^{2,p}({}^{d-1})}\le\frac{1}{n},\quad\text{and}\quad 0\le\lambda_1(B_1^{\varphi_n})-\lambda_1(B_1)<c\times\left[P(B_1^{\varphi_n})-P(B_1)\right]^\alpha.$$

The last inequality is equivalent to

$$0\le|B_1^{\varphi_n}|^{\frac{2}{d}}\lambda_1(B_1^{\varphi_n})-|B_1|^{\frac{2}{d}}\lambda_1(B_1)<c\times|B_1|^{\frac{d+1}{d}}\left(\frac{P(B_1^{\varphi_n})}{|B_1^{\varphi_n}|^{\frac{d-1}{d}}}-\frac{P(B_1)}{|B_1|^{\frac{d-1}{d}}}\right)^\alpha,$$

so, we get

$$0\le f(x_n)-f(x_0)\le c\times|B_1|^{1+\frac{1}{d}}(x_n-x_0)^\alpha,$$

where $x_n:=P(B_1^{\varphi_n})/|B_1^{\varphi_n}|^{\frac{d-1}{d}}\underset{n\to+\infty}{\longrightarrow}P(B_1)/|B_1|^{\frac{d-1}{d}}=x_0$, because $\|\varphi_n\|_{W^{2,p}({}^{d-1})}\le\frac{1}{n}\underset{n\to+\infty}{\longrightarrow}0$.

Thus, we can write

$$\forall c>0,\qquad 0\le\liminf_{x\to x_0}\frac{f(x)-f(x_0)}{(x-x_0)^\alpha}\le\liminf_{n\to+\infty}\frac{f(x_n)-f(x_0)}{(x_n-x_0)^\alpha}\le c|B_1|^{1+\frac{1}{d}}.$$

Finally, we get the result $\liminf_{x\to x_0}\frac{f(x)-f(x_0)}{(x-x_0)^\alpha}=0$.

□

The most interesting part of Theorem 14 and Corollary 6 is that the exponent 3/2 was apparently unknown and seems to be optimal (see Section 3.4); in the planar case $d=2$, we actually improve the result of Corollary 6 and retrieve the same exponent in a completely different (and independent) way, by studying the asymptotics of λ_1 and P for regular polygons:

Proposition 8. *Let $d = 2$ and for $n \geq 3$, denote S_n the regular $n-$gon with unit area (and again B denotes the disk of unit area). We have:*

$$\big(\lambda_1(S_n) - \lambda_1(B)\big) \underset{n\to\infty}{\sim} \beta_0 \times \big(P(S_n) - P(B)\big)^{3/2},$$

with

$$\beta_0 := \frac{4 \times 3^{\frac{3}{2}} \zeta(3) \lambda_1(B)}{\pi^{\frac{15}{4}}},$$

where $\zeta : x \in (1, +\infty) \longmapsto \sum_{n=1}^{\infty} \frac{1}{n^x}$ is the Riemann zeta function.

Proof. We take the asymptotic expansion of the fundamental frequency of regular polygons found in [144] :

$$\lambda_1(S_n) - \lambda_1(B) = \frac{4\zeta(3)\lambda_1(B)}{n^3} + o\left(\frac{1}{n^3}\right) \tag{3.31}$$

and

$$P(S_n) - P(B) = 2\sqrt{n}\sqrt{\tan\frac{\pi}{n}} - 2\sqrt{\pi} = \frac{\pi^{\frac{5}{2}}}{3} \times \frac{1}{n^2} + o\left(\frac{1}{n^3}\right). \tag{3.32}$$

Then we can write:

$$\frac{\lambda_1(S_n) - \lambda_1(B)}{\big(P(S_n) - P(B)\big)^{3/2}} \underset{n\to+\infty}{\sim} \frac{4 \times 3^{\frac{3}{2}} \zeta(3) \lambda_1(B)}{\pi^{\frac{15}{4}}} = \beta_0.$$

□

This Proposition allows us to get the following asymptotic property on f.

Corollary 7. *Let $d = 2$, x_0 and f defined in Section 3.3.2. Then*

1. $\forall \alpha \in (0, 3/2), \qquad f(x) - f(x_0) = o\big((x - x_0)^\alpha\big),$
   in particular by taking $\alpha = 1$, we get that f is differentiable at x_0 and $f'(x_0) = 0$.
2. $0 \leq \liminf_{x\to x_0} \frac{f(x)-f(x_0)}{(x-x_0)^{3/2}} \leq \limsup_{x\to x_0} \frac{f(x)-f(x_0)}{(x-x_0)^{3/2}} \leq \beta_0.$

Remark 10. *Enlightened with the results of Theorem 14 and Corollary 6, which are stated for arbitrary dimensions, we believe that the first assertion holds for $d \geq 2$. Unfortunately, we did not manage to prove it because of the lack of information on the asymptotic behaviour of $x_n := P(B_1^{\varphi_n})/|B_1^{\varphi_n}|^{\frac{d-1}{d}}$ introduced in the proof of Corollary 6.*

Proof. Take $\alpha \in (0, 3/2]$, we introduce the integer valued function which associates to $x \in \big(x_0, P(S_3)\big)$ the integer $n_x := \max\{n \geq 3, \ \ P(S_n) \geq x\}$, note that $\lim_{x\to x_0} n_x = +\infty$.

We have:

$$\begin{aligned}
0 \quad \leq \quad \frac{f(x) - f(x_0)}{(x - x_0)^\alpha} \quad &\leq \quad \frac{f\big(P(S_{n_x})\big) - f\big(P(B)\big)}{\big(P(S_{n_x+1}) - P(B)\big)^\alpha} \qquad \text{(because } x \geq P(S_{n_x+1}) \text{ and } f(x) \leq f\big(P(S_{n_x})\big)\text{)} \\
&\leq \quad \frac{\lambda_1(S_{n_x}) - \lambda_1(B)}{(P(S_{n_x+1}) - P(B))^\alpha} \qquad \text{(by the definition of } f\text{)} \\
&= \quad \frac{\lambda_1(S_{n_x}) - \lambda_1(B)}{\big(P(S_{n_x}) - P(B)\big)^\alpha} \times \left(\frac{P(S_{n_x}) - P(B)}{P(S_{n_x+1}) - P(B)}\right)^\alpha \\
&\underset{x\to x_0}{\sim} \quad \frac{\frac{4\zeta(3)\lambda_1(B)}{n_x^3}}{\left(\frac{\pi^{\frac{5}{2}}}{3} \times \frac{1}{n_x^2}\right)^\alpha} \times \left(\frac{\frac{\pi^{\frac{5}{2}}}{3} \times \frac{1}{n_x^2}}{\frac{\pi^{\frac{5}{2}}}{3} \times \frac{1}{(n_x+1)^2}}\right)^\alpha \qquad \text{(by (3.31) and (3.32))} \\
&\underset{x\to x_0}{\sim} \quad \beta_0 \times \left(\frac{\pi^{5/2}}{3}\frac{1}{n_x^2}\right)^{3/2-\alpha} \qquad \text{(because } n_x \underset{x\to x_0}{\longrightarrow} +\infty\text{)},
\end{aligned}$$

thus, if $\alpha \in (0, 3/2)$, we have $\lim_{x \to x_0} \frac{f(x)-f(x_0)}{(x-x_0)^\alpha} = 0$, which is equivalent to the first assertion. On the other hand if $\alpha = 3/2$, we get the proof of the second assertion.

□

3.4 Further remarks and Conjectures

3.4.1 About $\mathcal{D}_{\mathcal{K}^2}$

Our theoretical and numerical studies highlight some remaining open problems about $\mathcal{D}_{\mathcal{K}^2}$:

1. is it true that f and g defined in (3.14) and (3.15) are convex?
2. is it true that

$$g'(x_0) = \frac{\sqrt{\pi}}{3}\lambda_1(B_1) \times \big(\lambda_1(B_1) - 2\big) \qquad \text{and} \qquad f(x) - f(x_0) \underset{x \to x_0}{\sim} c(x - x_0)^{3/2}$$

for some $c > 0$? These questions are closely related to the following: for $\gamma > \frac{\sqrt{\pi}}{3}\lambda_1(B_1) \times \big(\lambda_1(B_1) - 2\big)$, can we find $c > 0$ and $\mathcal{V}$ a neighborhood of B in $\mathcal{K}_1^2$ (for the Hausdorff distance) such that

$$\forall \Omega \in \mathcal{V}, \quad c(P(\Omega) - P(B))^{3/2} \leq \lambda_1(\Omega) - \lambda_1(B) \leq \gamma(P(\Omega) - P(B)) \quad ?$$

Proposition 7 and Theorem 14 shows that such inequalities are valid in a smooth neighborhood of B, but it is well-known that achieving a similar result in a non-smooth neighborhood requires more work (see for example [1, 94] and [64, Section 6]). We note that numerical evidence that will appear in [89] suggests that the optimal value of the constant c is given by the β_0 introduced in Proposition 8. It also supports that the inequality may in fact be global, which means we conjecture the following inequality:

$$\forall \Omega \in \mathcal{K}_1^2, \qquad \lambda_1(\Omega) - \lambda_1(B) \geq \beta_0 \times \big(P(\Omega) - P(B)\big)^{3/2}.$$

Remark 11. *It is interesting to note that if we combine the conjectured inequality*

$$\lambda_1(\Omega) - \lambda_1(B) \geq c\big(P(\Omega) - P(B)\big)^{3/2}, \tag{3.33}$$

with the famous quantitative isoperimetric inequality of [95], which affirms the existence of a constant α_d , depending only on the dimension d, such that for every Borel set $\Omega \subset \mathbb{R}^d$, one has

$$P(\Omega) - P(B) \geq \alpha_d \times \mathcal{A}(\Omega)^2,$$

where $\mathcal{A}(\Omega)$ is the so called Fraenkel asymmetry of the set Ω, we get that for every $\Omega \in \mathcal{K}_1^2$

$$\lambda_1(\Omega) - \lambda_1(B) \geq c\alpha_d^{3/2} \times \mathcal{A}(\Omega)^3.$$

The exponent 3 is not optimal, it is higher than the optimal one given in [42], where the authors prove that there exists a dimensional constant σ_d such that for every open set $\Omega \subset \mathbb{R}^d$ with unit measure, one has

$$\lambda_1(\Omega) - \lambda_1(B) \geq \sigma_d \times \mathcal{A}(\Omega)^2. \tag{3.34}$$

Nevertheless, we note that inequality (3.33) is stronger in some cases than (3.34). Indeed, if we take the regular polygons (S_n) introduced in Proposition 8, we have by straightforward computations:

$$P(S_n) - P(B) \underset{n \to \infty}{\sim} \mu_2 \times \mathcal{A}(S_n),$$

where μ_2 is a positive constant. Thus, for sufficiently large values of n, we have

$$\lambda_1(\Omega) - \lambda_1(B) \geq c\big(P(S_n) - P(B)\big)^{3/2} \geq c' \times \mathcal{A}(S_n)^{3/2},$$

where c' is a positive constant. This shows that (3.34) *is (in this case) weaker than the conjecture* (3.33)*.*

One could also wonder if we can improve our understanding of the shapes realizing the boundary of the diagram, that is to say solutions of the optimization problems in Corollary 3. For example, one can state:

Conjecture 4. *The regular polygons are on the lower part of $\partial\mathcal{D}_{\mathcal{K}^2}$.*

This result seems to be verified numerically. Using Theorem 12, we will observe however (see the proof below) that this statement (regular polygons are on the lower boundary) is actually a stronger statement than Polya's conjecture in the restricted class of convex sets. Recall that this conjecture states that among polygons of fixed measure and whose number of sides is bounded by N, the regular N-gon has the lowest first Dirichlet eigenvalue. This conjecture is expected to be valid for any polygon, but even in the class of convex polygons, the result is not known (for $N \geq 5$) and already expected to be very challenging.

Indeed, let us take $N \geq 3$ and denote Ω_N^* the regular polygon of unit measure and N sides. By the isoperimetric inequality for polygons (see [147, Theorem 5.1]), we have $P(\Omega) \geq P(\Omega_N^*)$, for every convex polygon Ω of unit measure and at most N sides. Now, if we assume that the regular polygon Ω_N^* is on the lower boundary of the diagram, that is to say $\lambda_1(\Omega_N^*) = f\big(P(\Omega_N^*)\big)$, then by monotonicity of f, we conclude that: $\lambda_1(\Omega_N^*) = f\big(P(\Omega_N^*)\big) \leq f\big(P(\Omega)\big) \leq \lambda_1(\Omega)$, with equality if and only if Ω is equal to Ω_N^* up to rigid motions.

3.4.2 About $\mathcal{D}_{\mathcal{K}^d}$ for $d \geq 3$

As stated in the introduction, a major part of our results for convex sets are restricted to the planar case mainly because some of the assertions of Lemma 7 are only given in dimension 2 and seem to be rather challenging to extend to higher dimensions, see Remark 3.3.2. Nevertheless, we believe that once a similar result is proven for $d \geq 3$, it would be possible to apply the same strategy developed in the present paper to prove the following conjecture:

Conjecture 5. *We denote $x_0 = P(B)$ where B is a ball of unit volume.*

1. *the diagram $\mathcal{D}_{\mathcal{K}^d}$ is made of all points in $\mathbb{R}^2$ lying between the graphs of f and g, more precisely:*

$$\mathcal{D}_{\mathcal{K}^d} = \Big\{(x,y) \in \mathbb{R}^2,\ x \geq x_0 \quad \text{and} \quad f(x) \leq y \leq g(x)\Big\}, \tag{3.35}$$

   where f and g are defined in (3.14) *and* (3.15)*.*

2. *functions f and g are continuous and strictly increasing.*

3.4.3 About $\mathcal{D}_{\mathcal{S}^d}$ where $\mathcal{S}^d$ is the class of simply connected domains

We decided to focus on two classes of domains, $\mathcal{O}$ the class of open domains in $\mathbb{R}^d$, and $\mathcal{K}^d$ the class of convex domains in $\mathbb{R}^d$. But one could also focus on an intermediate class which is

$$\mathcal{S}^d = \{\Omega \subset \mathbb{R}^d,\ \ \Omega \text{ is open, bounded and simply-connected}\}.$$

We give here some thoughts about the Blaschke-Santaló diagram of $(\lambda_1, P, |\cdot|)$ in this class, denoted $\mathcal{D}_{\mathcal{S}^d}$: note first that as for the class of open domains, there is uncertainty about the definition of the perimeter P. But since we are not giving any specific statement here, we consider part of the investigation to decide in which way a change in the definition of P may affect the shape of $\mathcal{D}_{\mathcal{S}^d}$.

1. Assume first that $d = 2$: since inequalities (3.8) and (3.11) also hold for the class of planar simply connected domains, the diagram $\mathcal{D}_{\mathcal{S}^2}$ is bounded from above by a continuous function, and therefore different from the diagram of open sets $\mathcal{D}_{\mathcal{O}}$ described in Theorem 10. However, we expect that the lower boundary of the diagram is simply given by the horizontal half line $[P(B), +\infty) \times \{\lambda_1(B)\}$. More precisely we formulate:

   Conjecture 6. *There exists h a continuous and increasing function such that*

   $$\mathcal{D}_{\mathcal{S}^2} = \{\big(P(B), \lambda_1(B)\big)\} \cup \{(x, y) \mid x > P(B), \quad \lambda_1(B) < y \leq h(x)\}.$$

   This is supported by the fact that we can find shapes with a high perimeter but whose first Dirichlet-eigenvalue is close to the one of the ball, for example by adding a thin tail to a ball (see for example [68] for results on tailed domains).

   Finally, notice that we do not know whether we should expect h and g to be equal or not. This is probably also a challenging question.

2. If we now assume $d \geq 3$, the class of simply connected domains behave very differently. Actually, we can introduce an even more restrictive class of domains, namely

   $$\widetilde{\mathcal{S}}^d = \{\Omega \subset \mathbb{R}^d, \ \ \Omega \text{ is open and homeomorphic to a ball}\}.$$

   We believe that in this case we have

   $$\mathcal{D}_{\mathcal{S}^d} = \mathcal{D}_{\widetilde{\mathcal{S}}^d} = \mathcal{D}_{\mathcal{O}}.$$

   To support this conjecture, we refer to the construction described in [64, Remark 6.2] and inspired by [82].

3. It would also be interesting to study the diagram in the class of sharshaped domains. In dimension 2, it is not clear whether we expect the diagram to be the same as the diagram for simply connected sets or not. In dimension higher than 3 however, it would be more natural to expect that the diagram differs from the one of simply connected sets, but we did not investigate this question yet.

Chapter 4

On the Cheeger inequality for convex sets

This chapter is a reprint of the submitted paper: ***"On the Cheeger inequality for convex sets"*** *[90].*

Abstract

In this paper, we prove new sharp bounds for the Cheeger constant of planar convex sets that we use to study the relations between the Cheeger constant and the first eigenvalue of the Laplace operator with Dirichlet boundary conditions. This problem is closely related to the study of the so-called Cheeger inequality for which we provide an improvement in the class of planar convex sets. We then provide an existence theorem that highlights the tight relation between improving the Cheeger inequality and proving the existence of a minimizer of a the functional $J_n := \lambda_1/h^2$ in any dimension n. We finally, provide some new sharp bounds for the first Dirichlet eigenvalue of planar convex sets and a new sharp upper bound for triangles which is better than the conjecture stated in [167] in the case of thin triangles.

4.1 Introduction and main results

A celebrated inequality due to Jeff Cheeger states that for every open bounded set $\Omega \in \mathbb{R}^n$ (where $n \geq 2$) one has:

$$\lambda_1(\Omega) \geq \frac{1}{4} h(\Omega)^2,$$

where $\lambda_1(\Omega)$ is the first Dirichlet eigenvalue and $h(\Omega)$ is the Cheeger constant of Ω, which is defined as follows:

$$h(\Omega) := \inf \left\{ \frac{P(E)}{|E|} \;\middle|\; E \text{ measurable and } E \subset \Omega \right\}, \tag{4.1}$$

where $P(E)$ is the perimeter of De-Giorgi of E measured with respect to $\mathbb{R}^n$ (see for example [151] for definitions) and $|E|$ is the n-dimensional Lebesgue measure of E. Any set $C_\Omega \subset \Omega$ for which the infimum is attained is called (when it exists) a *Cheeger set of* Ω. We refer to [151] for an introduction to the Cheeger problem.

In the present paper, d and r respectively correspond to the diameter and the inradius functionals.

Recently, E. Parini [152] remarked that the constant $\frac{1}{4}$ can be improved for the class $\mathcal{K}^2$ (for every $n \in \mathbb{N}^*$, we denote $\mathcal{K}^n$ the class of bounded convex subsets of $\mathbb{R}^n$). He proved the following inequality:

$$\forall \Omega \in \mathcal{K}^2, \quad \lambda_1(\Omega) \geq \frac{\pi^2}{16} h(\Omega)^2, \tag{4.2}$$

and noted that the constant $\frac{\pi^2}{16}$ is also not optimal. He then took a shape optimization point of view by introducing the functional $J_2 : \Omega \in \mathcal{K}^2 \longmapsto J_2(\Omega) := \frac{\lambda_1(\Omega)}{h(\Omega)^2}$ for which he proves the existence of a minimizer in $\mathcal{K}^2$ and conjectures that it is the square; in which case the optimal lower bound would be given by:

$$\min_{\Omega \in \mathcal{K}^2} J_2(\Omega) = J_2\big((0,1)\big) = \frac{2\pi^2}{(2+\sqrt{\pi})^2} \approx 1.387...$$

Nevertheless, as far as we know, as mentioned in [152, Section 6] the existence of an optimal shape in higher dimensions ($n \geq 3$) remains open.

Moreover, in the same paper [152], the author proved the following reverse Cheeger's inequality:

$$\forall \Omega \in \mathcal{K}^2, \quad \lambda_1(\Omega) < \frac{\pi^2}{4} h(\Omega)^2, \tag{4.3}$$

which is sharp as it is asymptotically attained by any sequence $(\Omega_k)_{k\in\mathbb{N}}$ of planar convex sets such that $|\Omega_k| = V$ (where $V > 0$) and $d(\Omega_k) \underset{k\to+\infty}{\longrightarrow} +\infty$, see [152, Proposition 4.1]. It was then remarked by L. Brasco [40, Remark 1] that the main argument used by Parini, which is Polya's inequality $\lambda_1(\Omega) < \frac{\pi^2}{4}\left(\frac{P(\Omega)}{|\Omega|}\right)^2$ holds in higher dimensions (see [119]). Thus, the reverse Cheeger inequality also holds for higher dimensions and is sharp as any sequence $\big(\omega \times (0,1/k)\big)_k$, where $\omega \in \mathcal{K}^{n-1}$, provides asymptotic equality when k tends to $+\infty$.

For the lower bound, one can combine the inequality $h(\Omega) \leq \frac{n}{r(\Omega)}$ (which is obtained by taking the inscribed ball $B_{r(\Omega)}$ as a test set in the definition of the Cheeger constant $h(\Omega)$) and Protter's inequality [158]:

$$\forall \Omega \in \mathcal{K}^n, \quad \lambda_1(\Omega) \geq \frac{\pi^2}{4}\left(\frac{1}{r(\Omega)^2} + \frac{n-1}{d(\Omega)^2}\right), \tag{4.4}$$

which generalises Hersch's inequality [115] (used by Parini for the planar case) to higher dimensions. We then obtain the following lower bound:

$$\forall n \geq 2, \forall \Omega \in \mathcal{K}^n, \quad J_n(\Omega) := \frac{\lambda_1(\Omega)}{h(\Omega)^2} > \frac{\pi^2}{4n^2},$$

which improves the original constant $\frac{1}{4}$ given by J. Cheeger only for $n \in \{2,3\}$. In which cases, we have:

$$\forall \Omega \in \mathcal{K}^2, \quad J_2(\Omega) > \frac{\pi^2}{16} \approx 0.616... \quad \text{and} \quad \forall \Omega \in \mathcal{K}^3, \quad J_3(\Omega) > \frac{\pi^2}{36} \approx 0.274...$$

In the present paper, we improve the Cheeger-Parini's inequality (4.2). Our result in this direction is stated as follows:

Theorem 15. *We have:*

$$\forall \Omega \in \mathcal{K}^2, \quad J_2(\Omega) = \frac{\lambda_1(\Omega)}{h(\Omega)^2} \geq \left(\frac{\pi j_{01}}{2j_{01}+\pi}\right)^2 \approx 0.902...$$

where j_{01} denotes the first zero of the first Bessel function.

This result relies on the combination of Protter's inequality (4.4) and a diametrical Faber-Krahn type inequality (see [33, Theorem 2.1] or [79, Theorem 3.3]) in order to bound $\lambda_1(\Omega)$ from below.

The study of complete systems of inequalities relating some given functionals is an interesting subject for its own. It is closely related to the so called *Blaschke-Santaló* diagrams, we refer to the

original works of Blaschke [28] and Santaló [163] and to the more recent works [36, 71, 111, 112, 113] for some interesting examples involving geometric functionals.

In the present paper we provide a complete system of inequalities relating the Cheeger constant h, the inradius r and the area $|\cdot|$ of planar convex sets, which corresponds to a complete description of the related Blaschke-Santaló diagram introduced in the following Theorem:

Theorem 16. *We have:*

$$\forall \Omega \in \mathcal{K}^2, \qquad \frac{1}{r(\Omega)} + \frac{\pi r(\Omega)}{|\Omega|} \leq h(\Omega) \leq \frac{1}{r(\Omega)} + \sqrt{\frac{\pi}{|\Omega|}}, \tag{4.5}$$

These inequalities are sharp as equalities are obtained for stadiums in the lower estimate and for domains that are homothetic to their form bodies[1] *in the upper one.*

Moreover, we have the following explicit description of the Blaschke-Santaló diagram:

$$\left\{ \left(\frac{1}{r(\Omega)}, h(\Omega) \right) \mid \Omega \in \mathcal{K}^2 \text{ and } |\Omega| = 1 \right\} = \left\{ (x,y) \;\middle|\; x \geq \frac{1}{r(B)} = \sqrt{\pi} \text{ and } x + \frac{\pi}{x} \leq y \leq x + \sqrt{\pi} \right\},$$

where $B \subset \mathbb{R}^2$ is a ball of unit area.

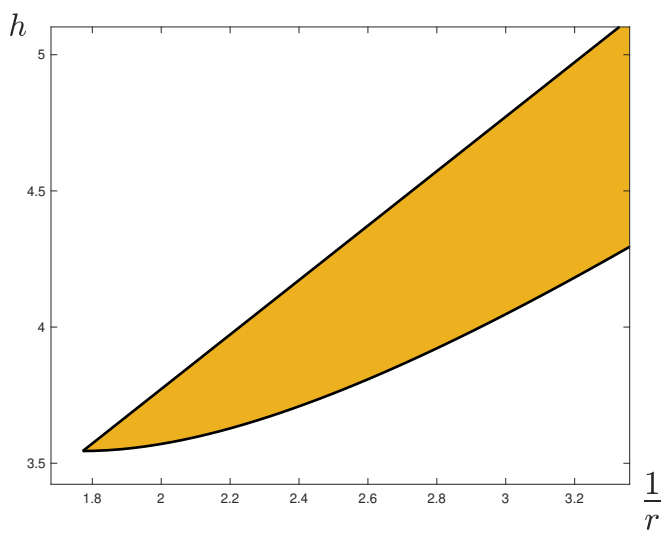

Figure 4.1: The diagram of the triplet $(r, h, |\cdot|)$.

At last, we are interested by the question of the existence of an minimizer of J_n for higher dimensions $n \geq 3$. We prove the following Theorem:

Theorem 17. *Let us define the real sequence $(\beta_n)_n$ as follows:*

$$\forall n \in \mathbb{N}^*, \qquad \beta_n := \inf_{\Omega \in \mathcal{K}^n} J_n(\Omega).$$

We have:

1. *$(\beta_n)_n$ is a decreasing sequence.*
2. $\lim_{n \to +\infty} \beta_n = \frac{1}{4}$.

[1] We refer to [136, Section 1.1] for the definition of form bodies and to [164] for more details.

3. *For $n \geq 2$, if the* <u>*strict*</u> *inequality $\beta_n < \beta_{n-1}$ holds, we have the following existence result:*

$$\exists \Omega_n^* \in \mathcal{K}^n, \quad J_n(\Omega_n^*) = \inf_{\Omega \in \mathcal{K}^n} J_n(\Omega).$$

Let us give a few interesting comments on Theorem 17:

- The convergence result $\lim_{n \to +\infty} \beta_n = \frac{1}{4}$ of shows that the constant $\frac{1}{4}$ given in the original Cheeger inequality [55] is optimal in the sense that there exists no constant $C > \frac{1}{4}$ such that:

$$\forall n \geq 1, \forall \Omega \in \mathcal{K}^n, \quad \frac{\lambda_1(\Omega)}{h(\Omega)^2} \geq C.$$

- We believe that the assertion $\beta_n < \beta_{n-1}$ is true for any $n \geq 2$. This conjecture is motivated by the discussion of Section 4.4.2. In particular, when $n = 2$, we have:

$$\inf_{\Omega \in \mathcal{K}^2} J_2(\Omega) < \frac{\pi^2}{4} = \inf_{\omega \in \mathcal{K}^1} J_1(\omega).$$

  Thus, we retrieve Parini's result of existence in the class of planar sets without using the explicit formulae of Cheeger constants of planar convex sets.

The present paper is organized as follows: in Section 4.2, we provide the proof of the sharp estimates of the Cheeger constant given in Theorem 16. Section 4.3 is devoted to the improvement of the Cheeger-Parini's inequality for planar convex sets (4.2), we also give improved results for some special shapes (triangles, rhombii and stadiums), see Proposition 9. We then prove the existence result of Theorem 17 in Section 4.4. We finally discuss some new sharp inequalities involving the first Dirichlet eigenvalue, the Cheeger constant, the inradius and the area of planar convex sets in Appendix 4.5.

4.2 Sharp estimates for the Cheeger constant: Proof of Theorem 16

The proof of Theorem 16 is presented in 3 parts:

<u>The upper bound:</u>

Let $\Omega \in \mathcal{K}^2$. We have by [142, Theorem 2]:

$$\forall t \in \big(0, r(\Omega)\big), \qquad |\Omega_{-t}| \geq |\Omega| \left(1 - \frac{t}{r(\Omega)}\right)^2, \tag{4.6}$$

with equality if and only if Ω is homothetic to its form body.

If Ω is homothetic to its form body, we have by solving the equation $|\Omega_{-t}| = |\Omega| \left(1 - \frac{t}{r(\Omega)}\right)^2 = \pi t^2$:

$$h(\Omega) = \frac{1}{r(\Omega)} + \sqrt{\frac{\pi}{|\Omega|}}.$$

From now on, we assume that Ω is not homothetic to its form body. Let us introduce the functions:

- $f : t \in \big(0, r(\Omega)\big) \longmapsto |\Omega| \left(1 - \frac{t}{r(\Omega)}\right)^2 - \pi t^2 = |\Omega| - \frac{2|\Omega|}{r(\Omega)} t + \left(\frac{|\Omega|}{r(\Omega)^2} - \pi\right) t^2,$
- $g : t \in \big(0, r(\Omega)\big) \longmapsto |\Omega_{-t}| - \pi t^2.$

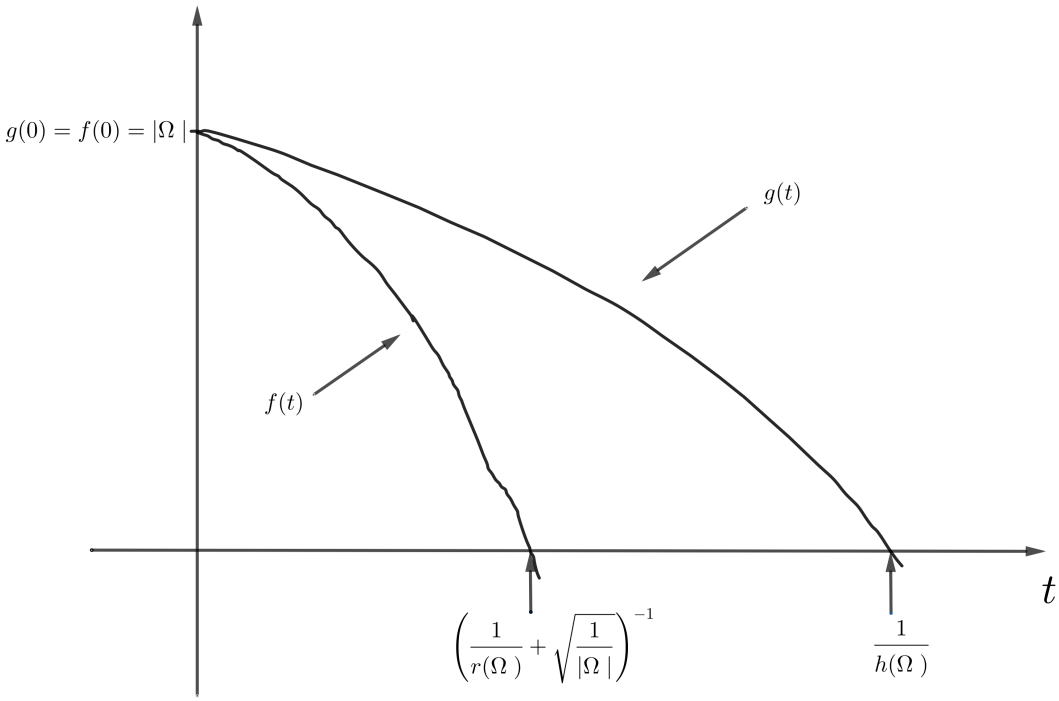

Figure 4.2: Idea of proof of the upper bound.

By (4.6), we have:

$$\begin{cases} g(0) = f(0), \\ \forall t \in \big(0, r(\Omega)\big), \qquad g(t) > f(t), \end{cases}$$

This implies that $1/h(\Omega)$, the first zero of g on $[0, r(\Omega)]$, is strictly larger than the first zero of f given by $\left(\frac{1}{r(\Omega)} + \sqrt{\frac{\pi}{|\Omega|}}\right)^{-1}$ (see Figure 4.2) , which proves the inequality.

<u>The lower bound:</u>

Let $\Omega \in \mathcal{K}^2$, we denote $C_\Omega \in \mathcal{K}^2$ its (unique) Cheeger set. Let us show that:

$$r(\Omega) = r(C_\Omega).$$

By the characterization of the Cheeger set of planar convex sets of [122], we have $C_\Omega = \Omega_{-\frac{1}{h(\Omega)}} + \frac{1}{h(\Omega)} B_1$, where B_1 is the ball of unit radius centred at the origin. We then have:

$$r(C_\Omega) = r\left(\Omega_{-\frac{1}{h(\Omega)}} + \frac{1}{h(\Omega)} B_1\right) = r\left(\Omega_{-\frac{1}{h(\Omega)}}\right) + r\left(\frac{1}{h(\Omega)} B_1\right) = r(\Omega) - \frac{1}{h(\Omega)} + \frac{1}{h(\Omega)} r(B_1) = r(\Omega).$$

Since, the Cheeger set C_Ω is convex, we can use the following Bonnesen's inequality [35]:

$$P(C_\Omega) \geq \pi r(C_\Omega) + \frac{|C_\Omega|}{r(C_\Omega)},$$

with equality if and only if C_Ω is a stadium (note that does not mean that Ω is a stadium). Thus:

$$h(\Omega) = \frac{P(C_\Omega)}{|C_\Omega|} \geq \frac{\pi r(C_\Omega) + \frac{|C_\Omega|}{r(C_\Omega)}}{|C_\Omega|} = \frac{\pi r(\Omega)}{|C_\Omega|} + \frac{1}{r(\Omega)} \geq \frac{\pi r(\Omega)}{|\Omega|} + \frac{1}{r(\Omega)},$$

where the last inequality is a consequence of the inclusion $C_\Omega \subset \Omega$ and thus is an equality if and only if $\Omega = C_\Omega$. Finally, we proved the lower bound and the equality holds if and only if Ω is a stadium.

The diagram:

The demonstration is exactly similar to the case of the diagram relating the Cheeger constant, the area and the perimeter studied in detail in [88], one just has to replace the perimeter by the inradius and reproduce the same steps of the proof of [88, Theorem 1].

4.3 Improving the Cheeger inequality for planar convex sets

In this section, we provide the proof of Theorem 15 and prove some improved bounds for J_2 in some special sub-classes of $\mathcal{K}^2$, namely: triangles, rhombii and stadiums.

4.3.1 Proof of Theorem 15

Let $\Omega \in \mathcal{K}^2$. We have by Hersch inequality [115] and Faber-krahn inequaliy [78, 126]:

$$|\Omega|\lambda_1(\Omega) \geq \max\left(\pi j_{01}^2, \frac{\pi^2|\Omega|}{4r(\Omega)^2}\right).$$

On the other hand, we recall the upper estimate of Theorem 16:

$$\sqrt{|\Omega|}h(\Omega) \leq \frac{\sqrt{|\Omega|}}{r(\Omega)} + \sqrt{\pi}.$$

Thus, we have:

$$J(\Omega) = \frac{\lambda_1(\Omega)}{h(\Omega)^2} \geq \frac{\max\left(\pi j_{01}^2, \frac{\pi^2|\Omega|}{4r(\Omega)^2}\right)}{\left(\frac{\sqrt{|\Omega|}}{r(\Omega)} + \sqrt{\pi}\right)^2} \geq \min_{x\geq\sqrt{\pi}} \frac{\max\left(\pi j_{01}^2, \frac{\pi^2 x^2}{4}\right)}{(x+\sqrt{\pi})^2} = \left(\frac{\pi j_{01}}{2j_{01}+\pi}\right)^2 \approx 0.902...$$

The minimum is taken over $[\sqrt{\pi}, +\infty)$ because $\frac{\sqrt{|\Omega|}}{r(\Omega)} \geq \sqrt{\pi}$ for every $\Omega \in \mathcal{K}^2$. Moreover, it is attained for $x = \frac{\pi j_{01}}{\sqrt{\pi}}$, see Figure 4.3.

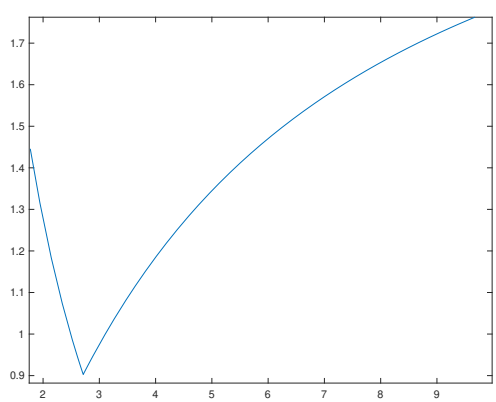

Figure 4.3: Curve of the function $x \longmapsto \frac{\max\left(\pi j_{01}^2, \frac{\pi^2 x^2}{4}\right)}{(x+\sqrt{\pi})^2}$.

4.3.2 A slight improvement of the result of Theorem 15

We note that one can combine the following Protter's inequality [158]:

$$\forall \Omega \in \mathcal{K}^2, \quad \lambda_1(\Omega) \geq \frac{\pi^2}{4}\left(\frac{1}{r(\Omega)^2} + \frac{1}{d(\Omega)^2}\right),$$

which is an improvement of Hersch's inequality [115, Section 8] with the optimal inequality (7) of [113]:

$$\forall \Omega \in \mathcal{K}^2, \qquad \frac{|\Omega|}{r(\Omega)^2} \geq \sqrt{1 + \left(\frac{d(\Omega)}{r(\Omega)}\right)^2} + 2\arcsin\left(\frac{2r(\Omega)}{d(\Omega)}\right) := \varphi\left(\frac{d(\Omega)}{r(\Omega)}\right), \tag{4.7}$$

to provide a slight improvement of the lower bound of Theorem 15.

Indeed, the function φ is continuous and strictly increasing on $[2, +\infty)$ (we note that $d(\Omega)/r(\Omega) \in [2, +\infty)$, thus by considering the inverse function denoted φ^{-1}, inequality 4.7 becomes:

$$\forall \Omega \in \mathcal{K}^2, \qquad \frac{d(\Omega)}{r(\Omega)} \leq \varphi^{-1}\left(\frac{|\Omega|}{r(\Omega)^2}\right)$$

. We then write:

$$\begin{aligned}
\frac{\lambda_1(\Omega)}{h(\Omega)^2} &\geq \frac{\max\left(\frac{\pi^2}{4r(\Omega)^2} \times \left(1 + \left(\frac{1}{\varphi^{-1}\left(\frac{|\Omega|}{r(\Omega)^2}\right)}\right)\right)^2, \frac{\pi j_{01}^2}{|\Omega|}\right)}{\left(\frac{1}{r(\Omega)} + \sqrt{\frac{\pi}{|\Omega|}}\right)^2} \\
&= \frac{\max\left(\frac{\pi^2}{4} \times \frac{|\Omega|}{r(\Omega)^2} \times \left(1 + \left(\frac{1}{\varphi^{-1}\left(\frac{|\Omega|}{r(\Omega)^2}\right)}\right)^2\right), \pi j_{01}^2\right)}{\left(\left(\frac{|\Omega|}{r(\Omega)^2}\right)^{1/2} + \sqrt{\pi}\right)^2} \\
&\geq \min_{x \in [\pi, +\infty)} \frac{\max\left(\frac{\pi^2}{4} x \left(1 + \frac{1}{\varphi^{-1}(x)^2}, \pi j_{01}^2\right)\right)}{(\sqrt{x} + \sqrt{\pi})} \qquad \left(\text{because } \frac{|\Omega|}{r(\Omega)^2} \geq \frac{\pi r(\Omega)^2}{r(\Omega)^2} = \pi\right).
\end{aligned}$$

Numerical computations show that the latter minimum is approximately equal to 0.914..., which slightly improves the lower bound of Theorem 15.

4.3.3 Improvements for special classes of shapes

We state and prove the following Proposition:

Proposition 9. *Let $\Omega \in \mathcal{K}^2$.*

1. *If Ω is a triangle, then $J_2(\Omega) > 1.2076$.*
2. *If Ω is a rhombus, then $J_2(\Omega) \geq 1.3819$.*
3. *If Ω is a stadium (i.e. the convex hull of two identical balls), then $J_2(\Omega) \geq 1.3673$.*

Proof. Let $\Omega \in \mathcal{K}^2$, since J_2 is invariant by homothety (due to scaling properties of λ_1 and h), we may assume without loss of generality that $|\Omega| = 1$.

1. Let us assume Ω to be a triangle and denote d its diameter and L its perimeter. To bound $\lambda_1(\Omega)$ from below, we make use of two inequalities:

- The first one is the polygonal Faber-Krahn inequality for triangles, which states that between triangles of the same area, the regular one minimizes the first Dirichlet eigenvalue:

$$\lambda_1(\Omega) \geq \lambda_1(T_{\text{eq}}) = \frac{4\pi^2}{\sqrt{3}},$$

where T_{eq} is the equilateral triangle of unit area (whose diameter is $d_{eq} = \frac{2}{3^{1/4}}$).

- The second (more recent) is due to P. Freitas and B. Siudeja [84, Corollary 4.1]:

$$\lambda_1(\Omega) \geq \frac{\pi^2}{4|\Omega|^2}\Big(d(\Omega) + \frac{2|\Omega|}{d(\Omega)}\Big)^2.$$

We then have on the one hand:

$$\lambda_1(\Omega) \geq \max\left(\frac{4\pi^2}{\sqrt{3}}, \frac{\pi^2}{4}\Big(d + \frac{2}{d}\Big)^2\right),$$

and on the other hand, the Cheeger constant of the triangle Ω is given by:

$$h(\Omega) = \frac{P(\Omega) + \sqrt{4\pi|\Omega|}}{2|\Omega|} = \frac{L + \sqrt{4\pi}}{2} \leq \frac{L_{iso} + \sqrt{4\pi}}{2},$$

where L_{iso} is the perimeter of the isoceles triangle whose diameter is equal to d and area equal to 1. By using Pythagoras' theorem, we have:

$$L_{iso} = 2d + \sqrt{\left(d - \sqrt{d^2 - \frac{4}{d^2}}\right)^2 + \frac{4}{d^2}}.$$

Finally, we obtain the following inequality:

$$J_2(\Omega) \geq \phi_1(d) := \frac{\max\left(\frac{4\pi^2}{\sqrt{3}}, \frac{\pi^2}{4}\Big(d + \frac{2}{d}\Big)^2\right)}{\left(\frac{2d + \sqrt{\left(d - \sqrt{d^2 - \frac{4}{d^2}}\right)^2 + \frac{4}{d^2}} + \sqrt{4\pi}}{2}\right)^2}.$$

We note that $d \geq d_{eq}$. Indeed, by the isoperimetric inequality of triangles:

$$3d_{eq} = L_{eq} \leq L \leq 3d.$$

Numerically, we obtain $\min\limits_{d \geq d_{eq}} \phi_1(d) \approx 1.2076...$

2. Let us assume Ω to be the rhombus of unit area whose vertices are given by $(-d/2, 0)$, $(0, -1/d)$, $(d/2, 0)$ and $(0, 1/d)$.

   We bound $\lambda_1(\Omega)$ from below by using the following Hooker and Protter's estimate for for rhombi [118]:

$$\lambda_1(\Omega) \geq \pi^2\left(\frac{d}{2} + \frac{1}{d}\right)^2.$$

   As for the Cheeger constant, since Ω is a circumscribed polygon, we have:

$$h(\Omega) = \frac{P(\Omega) + \sqrt{4\pi|\Omega|}}{2|\Omega|} = 2\sqrt{\frac{1}{d^2} + \frac{d^2}{4}} + \sqrt{\pi}$$

we use its explicit value in term of d.

$$J_2(\Omega) \geq \phi_2(d) = \frac{\pi^2 \left(\frac{d}{2} + \frac{1}{d}\right)^2}{\left(2\sqrt{\frac{1}{d^2} + \frac{d^2}{4}} + \sqrt{\pi}\right)^2}.$$

Numerically, we obtain $\min_{d \geq \sqrt{2}} \phi_2(d) \approx 1.3819...$

3. Let us assume Ω to be a stadium of unit area whose diameter is given by $a + 2r$, where $r > 0$ is the radius of the ball of its extremity and $a > 0$. The condition $|\Omega| = 1$ implies that $\pi r^2 + 2ar = 1$, which is equivalent to $a = \frac{1-\pi r^2}{2r}$. We use the monotonicity of λ_1 for inclusion (for $\Omega \subset (-r, r) \times (0, a + 2r)$) and Faber-Krahn inequality to write:

$$\lambda_1(\Omega) \geq \max\left(\lambda_1(B), \pi^2\left(\frac{1}{4r^2} + \frac{1}{(a+2r)^2}\right)\right) = \max\left(\lambda_1(B), \pi^2\left(\frac{4r^2}{(1+(4-\pi)r^2)^2} + \frac{1}{4r^2}\right)\right).$$

It is classical that the stadiums are Cheeger of themselves, see [122], we then have:

$$h(\Omega) = \frac{P(\Omega)}{|\Omega|} = 2a + 2\pi r = \frac{1 + \pi r^2}{r}.$$

Then:

$$J_2(\Omega) \geq \phi_3(r) := \frac{\max\left(\lambda_1(B), \pi^2\left(\frac{4r^2}{(1+(4-\pi)r^2)^2} + \frac{1}{4r^2}\right)\right)}{\left(\frac{1+\pi r^2}{r}\right)^2}$$

Numerically, we obtain $\min_{r \in \left(0, \frac{1}{\sqrt{\pi}}\right]} \phi_3(r) \approx 1.3673...$

□

4.4 On the existence of a minimizer in higher dimensions

4.4.1 Proof of Theorem 17

1. Let $n \geq 2$, let us first prove that:

$$\beta_n := \inf_{\Omega \in \mathcal{K}^n} J_n(\Omega) \leq \inf_{\omega \in \mathcal{K}^{n-1}} J_{n-1}(\omega) =: \beta_{n-1}.$$

The idea is to prove that for any $\omega \in \mathcal{K}^{n-1}$, there exists a family $(\Omega_d)_{d>0}$ of elements of $\mathcal{K}^n$ such that:

$$J_{n-1}(\omega) = \lim_{d \to +\infty} J_n(\Omega_d).$$

As the proof is quite involved, we decompose it in 3 steps.

Step 1: Lower estimates for λ_1 and h

Let us take $\Omega \in \mathcal{K}^n$ and assume without loss of generality that $\inf\{t \in \mathbb{R} \mid \Omega \cap \{x = t\} \neq \varnothing\} = 0$ and denote $d := \sup\{t \in \mathbb{R} \mid \Omega \cap \{x = t\} \neq \varnothing\}$. In the proof of [41, Lemma 6.11], the authors prove that:

$$\exists t_\lambda \in [0, d], \quad \lambda_1(\Omega) \geq \lambda_1(\Omega \cap \{x = t_\lambda\}).$$

We adapt there method to Cheeger's constant and state that:

$$\exists t_h \in [0, d], \quad h(\Omega) \geq h(\Omega \cap \{x = t_h\}).$$

For sake of completeness, we present the proofs of both cases.

Let $t_\lambda, t_h \in (0,d)$ such that:

$$\lambda_1(\Omega \cap \{x = t_\lambda\}) = \inf_{t\in\mathbb{R}} \lambda_1(\Omega \cap \{x = t\}) \quad \text{and} \quad h(\Omega \cap \{x = t_h\}) = \inf_{t\in\mathbb{R}} h(\Omega \cap \{x = t\}),$$

and we denote: $\omega_\lambda = \Omega \cap \{x = t_\lambda\}$ and $\omega_h = \Omega \cap \{x = t_h\}$.

Let $u \in H_0^1(\Omega)$ a positive eigenfunction corresponding to $\lambda_1(\Omega)$ such that $\|u\|_2 = 1$. We have:

$$\begin{aligned}
\lambda_1(\Omega) &= \int_\Omega |\nabla u|^2 dx \\
&\geq \int_0^d \Big(\int_{\Omega\cap\{x=t\}} |\nabla' u|^2 dx' \Big) dt \\
&\geq \int_0^d \Big(\lambda_1(\Omega \cap \{x = t\}) \int_{\Omega\cap\{x=t\}} u^2 dx' \Big) dt \\
&\geq \lambda_1(\omega_\lambda) \int_0^d \Big(\int_{\Omega\cap\{x=t\}} u^2 dx' \Big) dt \\
&= \lambda_1(\omega_\lambda)
\end{aligned}$$

As for Cheeger's constant, we have $\chi_{C_\Omega} \in BV(\Omega)$ (where $BV(\Omega)$ stands for the set of functions of bounded variations on Ω, we refer to [7] for definitions and more details), thus there exists a sequence (f_p) of functions of $BV(\Omega)\cap C^\infty(\Omega)$ such as: $f_k \to \chi_{C_\Omega}$ in $L^1(\Omega)$ and $\lim\limits_{k\to+\infty} |Df_k|(\mathbb{R}^n) = |D\chi_{C_\Omega}|(\mathbb{R}^n) = P(C_\Omega)$.

We have:

$$\begin{aligned}
h(\Omega) = \frac{P(C_\Omega)}{|C_\Omega|} = \frac{|D\chi_{C_\Omega}|(\mathbb{R}^n)}{\int_\Omega |\chi_{C_\Omega}|} &= \lim_{k\to+\infty} \frac{\int_\Omega |\nabla f_k|}{\int_\Omega |f_k|} \\
&\geq \lim_{k\to+\infty} \frac{\int_0^d \int_{\Omega\cap\{x=t\}} |\nabla' f_k| dx' dt}{\int_\Omega |f_k|} \\
&\geq \lim_{k\to+\infty} \frac{\int_0^d \Big(h(\Omega \cap \{x = t\}) \int_{\Omega\cap\{x=t\}} |f_k| dx' \Big) dt}{\int_\Omega |f_k|} \\
&\geq \lim_{k\to+\infty} h(\Omega \cap \{x = t_h\}) \frac{\int_0^d \Big(\int_{\Omega\cap\{x=t\}} |f_k| dx' \Big) dt}{\int_\Omega |f_k|} \\
&= h(\Omega \cap \{x = t_h\})
\end{aligned}$$

Step 2: Study of sets with increasing diameters and fixed volume

Let (Ω_k) a sequence of elements $\mathcal{K}^n$ of the same volumes 1, such that $d_k := d(\Omega_k) \to +\infty$. Let us prove that:

$$\liminf_{k\to+\infty} J_n(\Omega_k) \geq \inf_{\omega\in\mathcal{K}^{n-1}} J_{n-1}(\omega).$$

For every $k \in \mathbb{N}$, we consider A_k and A'_k two diametrical points of Ω_k (ie. such as $|A_k A'_k| = d_k$). Since J_n is invariant by rigid motions we can assume without loss of generality that $A_k = (0, ..., 0)$ and $A'_k = (d_k, 0, ..., 0)$.

By Step 1, we have for all $k \in \mathbb{N}$:

$$\lambda_1(\Omega_k) \geq \lambda_1(\omega_k)$$

where $\omega_k := \Omega_k \cap \{x = t_k\}$.

We can assume without loss of generality that $t_k \geq d_k/2$. Let $\mathcal{T}_k$ be the cone obtained by taking the convex hull of $\{A_k\} \cup C_k$, where C_k is the Cheeger set of the convex section ω_k.

Let $\alpha \in]0,1[$, we introduce the tube $U_k^\alpha := \alpha C_k \times (0,(1-\alpha)t_k)$. By convexity, we have the following inclusions:

$$U_n^\alpha \subset \mathcal{T}_k \subset \Omega_k$$

By definition of the Cheeger constant, we have:

$$h(\Omega_k) \leq \frac{P(U_k^\alpha)}{|U_k^\alpha|} = \frac{2\alpha^{n-1}|C_k| + \alpha^{n-2}(1-\alpha)P(C_k)t_k}{\alpha^{n-1}(1-\alpha)|C_k|t_k} = \frac{2}{(1-\alpha)t_k} + \frac{h(\omega_k)}{\alpha} \underset{k\to+\infty}{\sim} \frac{h(\omega_k)}{\alpha}.$$

Indeed: $\frac{1}{t_k} = \underset{k\infty}{o}\left(\frac{P(C_k)}{|C_k|}\right)$, because:

$$\frac{|C_k|}{P(C_k)} = \frac{|C_k|}{P\left(|C_k|^{\frac{1}{n}} \times \frac{C_k}{|C_k|^{\frac{1}{n}}}\right)} = \frac{|C_k|}{|C_k|^{\frac{n-1}{n}} P\left(\frac{C_k}{|C_k|^{\frac{1}{n}}}\right)} = \frac{|C_k|^{\frac{1}{n}}}{P\left(\frac{C_k}{|C_k|^{\frac{1}{n}}}\right)} \leq \frac{|C_k|^{\frac{1}{n}}}{P(B_{n-1})} \leq \frac{|\Omega_k|^{\frac{1}{n}} n^{\frac{1}{n}}}{P(B_{n-1})} \times \frac{1}{t_k^{1/n}} = \underset{k\infty}{o}(t_k),$$

where $B_{n-1} \subset \mathbb{R}^{n-1}$ is a ball of volume 1.

We deduce that:

$$\forall \alpha \in (0,1), \quad J_n(\Omega_k) \geq \frac{\lambda_1(\omega_k)}{\left(\frac{2}{(1-\alpha)t_k} + \frac{h(\omega_k)}{\alpha}\right)^2} \underset{k\to+\infty}{\sim} \alpha^2 J_{n-1}(\omega_k)$$

Thus:

$$\forall \alpha \in (0,1), \quad \liminf_{k\to+\infty} J_n(\Omega_k) \geq \alpha^2 \liminf_{k\to+\infty} J_{n-1}(\omega_k) \geq \alpha^2 \inf_{\omega \in \mathcal{K}^{n-1}} J_{n-1}(\omega)$$

By letting $\alpha \to 1$, we obtain:

$$\liminf_{k\to+\infty} J_n(\Omega_k) \geq \inf_{\omega \in \mathcal{K}^{n-1}} J_{n-1}(\omega)$$

Step 3: Study of long tubes

In this step, we show that when the height of a tube goes to infinity, the value of J_n of this tube converges to the value corresponding to the $(n-1)$-dimensional section given by its basis. More precisely, if we take $\omega \in \mathcal{K}^{n-1}$, we prove that

$$\lim_{d\to+\infty} J_n\big((0,d)\times\omega\big) = J_{n-1}(\omega).$$

We have by Step 2:

$$\liminf_{k\to+\infty} J_n(\Omega_k) \geq J_{n-1}(\omega)$$

We recall that $\lambda_1\big((0,d)\times\omega\big) = \left(\frac{\pi}{d}\right)^2 + \lambda_1(\omega)$ and use the second assertion of Step 1 to bound $J_n\big((0,d)\times\omega\big)$ from above:

$$J_n\big((0,d)\times\omega\big) = \frac{\lambda_1\big((0,d)\times\omega\big)}{h\big((0,d)\times\omega\big)^2} \leq \frac{\left(\frac{\pi}{d}\right)^2 + \lambda_1(\omega)}{h(\omega)^2}.$$

By passing to superior limit:

$$\limsup_{d\to+\infty} J_n\big((0,d)\times\omega\big) \le J_{n-1}(\omega).$$

Then:

$$\lim_{d\to+\infty} J_n\big((0,d)\times\omega\big) = J_{n-1}(\omega).$$

At last, we write:

$$\beta_{n-1} = \inf_{\omega\in\mathcal{K}^{n-1}} J_{n-1}(\omega) = \inf_{\omega\in\mathcal{K}^{n-1}} \Big(\lim_{d\to+\infty} \underbrace{J_n\big((0,d)\times\omega\big)}_{\ge \inf_{\Omega\in\mathcal{K}^n} J_n(\Omega)}\Big) \ge \inf_{\Omega\in\mathcal{K}^n} J_n(\Omega) = \beta_n.$$

2. For every $n\ge 2$, we take a ball $B_n\subset\mathbb{R}^n$ of unit radius, we have:

$$\frac{1}{4} \le \inf_{\Omega\in\mathcal{K}^n} J_n(\Omega) \le J_n(B_n) = \frac{\lambda_1(B_n)}{h(B_n)^2} = \frac{j^2_{\frac{n}{2}-1,1}}{n^2} \underset{n\to+\infty}{\sim} \frac{\left(\frac{n}{2}\right)^2}{n^2} = \frac{1}{4},$$

where $j_{\frac{n}{2}-1,1}$ is the first root of the nth Bessel function of first kind. We refer to [170] for the equivalence $j_{\frac{n}{2}-1,1} \underset{n\to+\infty}{\sim} \frac{n}{2}$.

3. **<u>The existence result</u>**:

Now, we assume that: $\inf_{\Omega\in\mathcal{K}^n} J_n(\Omega) < \inf_{\omega\in\mathcal{K}^{n-1}} J_{n-1}(\omega)$. Let us prove the existence of a minimizer of J_n on $\mathcal{K}^n$.

Let (Ω_k) be a minimizing sequence of $\mathcal{K}^n$ (ie. such as $\lim_{k\to+\infty} J_n(\Omega_k) = \inf_{\Omega\in\mathcal{K}^n} J_n(\Omega)$). Since J_n is scaling invariant we can assume without loss of generality that $|\Omega_k| = 1$ for all $n\in\mathbb{N}$.

If $\big(d(\Omega_k)\big)$ is not bounded, we can extract a subsequence $(\Omega_{\varphi(k)})$ such as

$$\lim_{k\to+\infty} d(\Omega_{\varphi(k)}) = +\infty.$$

Thus, by Step 2:

$$\inf_{\Omega\in\mathcal{K}^n} J_n(\Omega) = \lim_{k\to+\infty} J(\Omega_k) \ge \inf_{\omega\in\mathcal{K}^{n-1}} J_{n-1}(\omega).$$

which contradicts hypothesis $\beta_{n-1} > \beta_n$.

We deduce that the sequence of diameters $\big(d(\Omega_k)\big)$ is bounded, then by compactness, there exists $\Omega^*\in\mathcal{K}^n$ and a strictly increasing map $\sigma:\mathbb{N}\longrightarrow\mathbb{N}$ such that $\Omega_{\sigma(k)} \underset{k\infty}{\longrightarrow} \Omega^*$ for Hausdorff distance. We then have by continuity of J_n for the same metric (see [152, Proposition 3.2]):

$$J_n(\Omega^*) = \lim_{k\to+\infty} J(\Omega_k) = \inf_{\Omega\in\mathcal{K}^n} J_n(\Omega).$$

4.4.2 Discussion of the hypothesis $\beta_n < \beta_{n-1}$

We believe that hypothesis $\beta_n < \beta_{n-1}$ is true for any dimension n and that one can use convex cylinders (i.e. those of the form $\omega\times(0,d)$, where $\omega\in\mathcal{K}^{n-1}$ and $d>0$) to show it.

Let us analyse what happens when $n=2$. In this case convex cylinders are rectangles. We consider the family of cylinders $\Omega_d = (0,1)\times(0,d)$ (where $d>0$) and denote

$$\Psi_{(0,1)} : d>0 \longmapsto J_2(\Omega_d) = \frac{\lambda_1(\Omega_d)}{h(\Omega_d)^2} = \frac{\pi^2\left(1+\frac{1}{d^2}\right)}{\left(\frac{4-\pi}{1+d-\sqrt{(d-1)^2+\pi d}}\right)^2}.$$

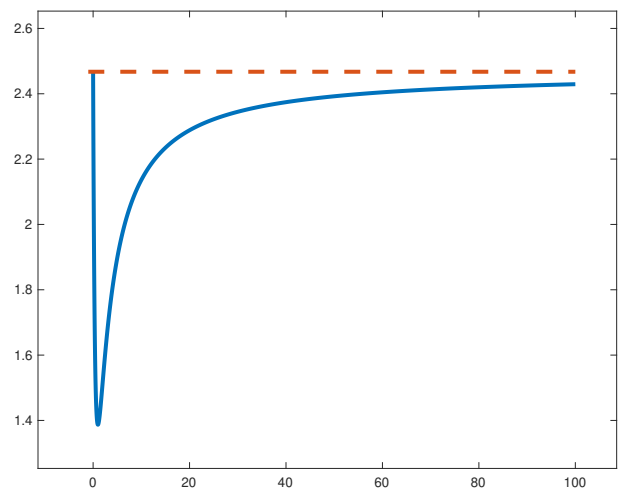

Figure 4.4: The curve of $\Psi_{(0,1)}$.

We plot the curve of $\Psi_{(0,1)}$ in Figure 4.4.

We remark that when d goes to infinity, $\Psi_{(0,1)} = J_2(\Omega_d)$ tends to $J_1\big((0,1)\big) = \frac{\pi^2}{4}$ from below, in the sense that there exists an order from which the function $\Psi_{(0,1)}$ should be strictly increasing and thus cannot have values above the limit $J_1\big((0,1)\big)$. We believe that the same property should hold in higher dimensions: let $n \geq 2$, $\Omega_d := \omega \times (0,d)$ where $d > 0$ and $\omega \in \mathcal{K}^{n-1}$, as before we denote $\Psi_\omega : d > 0 \longmapsto J_n(\Omega_d)$. We have already proved above that:

$$\lim_{d\to+\infty} \Psi_\omega(d) = \lim_{d\to+\infty} J_n(\Omega_d) = J_{n-1}(\omega).$$

It remains to prove that for large values of d one has:

$$\Psi_\omega(d) = J_n(\Omega_d) < J_{n-1}(\omega).$$

To do so, we propose to show that function Ψ_ω is strictly increasing for large values of d by studying the derivative $\Psi'_\omega(d)$.

Let us take $d > 0$, we have for $t > 0$ sufficiently small:

$$\lambda_1(\Omega_{d+t}) = \lambda_1(\omega) + \frac{\pi^2}{(d+t)^2} = \lambda_1(\omega) + \frac{\pi^2}{d^2} - \frac{2\pi^2}{d^3}t + \underset{t\to 0}{o}(t),$$

and

$$h(\Omega_{d+t}) = h(\Omega_d) + h'(\Omega_d, V_d) \times t + \underset{t\to 0}{o}(t),$$

where $V_d : \mathbb{R}^n \to \mathbb{R}^n$ is the smooth dilatation field such that $V_d(x_1, \cdots, x_n) = \big(0, \cdots, 0, \frac{x_n}{d}\big)$. As proved in [153], we have:

$$h'(\Omega_d, V_d) = \frac{1}{|C_{\Omega_d}|} \int_{\partial\Omega_d \cap \partial C_{\Omega_d}} \big(\kappa - h(\Omega_d)\big)\langle V_d, n\rangle d\sigma,$$

where κ is the mean curvature and C_{Ω_d} is the Cheeger set of Ω_d. Since $\langle V_d, n\rangle = 0$ on all $\partial\Omega_d \cap \partial C_{\Omega_d}$ except on the upper basis $\partial\Omega_d \cap \partial C_{\Omega_d} \cap \{x_n = d\}$ where κ is null, we have the following formula for the shape derivative:

$$h'(\Omega_d, V_d) = -\frac{|\partial C_{\Omega_d} \cap \{x_n = d\}|}{|C_d|} h(\Omega_d).$$

By straightforward computations we obtain:

$$\begin{aligned}\Psi'_\omega(d) &= \frac{1}{h(\Omega_d)^2}\left(-\frac{2\pi^2}{d^3} + 2\left(\lambda_1(\omega) + \frac{\pi^2}{d^2}\right)\frac{|\partial C_{\Omega_d} \cap \{x_n = d\}|}{|C_d|}\right)\\ &> \frac{2\pi^2}{h(\Omega_d)^2}\left(-\frac{1}{d^3} + \lambda_1(\omega)\frac{|\partial C_{\Omega_d} \cap \{x_n = d\}|}{|C_d|}\right)\\ &\geq \frac{2\pi^2}{d \times h(\Omega_d)^2}\left(\frac{\lambda_1(\omega)}{|\omega|}|\partial C_{\Omega_d} \cap \{x_n = d\}| - \frac{1}{d^2}\right) \qquad \text{(because } C_{\Omega_d} \subset \Omega_d\text{, thus } |C_{\Omega_d}| \leq |\Omega_d| = |\omega| \times d\text{).}\end{aligned}$$

Finally, it remains to prove that for sufficiently large values of d one can prove estimate of the type:

$$|\partial C_{\Omega_d} \cap \{x_n = d\}| > \frac{1}{d^2}.$$

One can check that this assertion is correct when $n = 2$. Indeed, if we consider the cylinder $\Omega_d = (0,1) \times (0,d)$, we can easily check that

$$|\partial C_{\Omega_d} \cap \{x_n = d\}| \underset{d\to+\infty}{\sim} M_2 \times \frac{1}{d} > \frac{1}{d^2},$$

where M_2 is some dimensional constant.

At last, let us mention the very recent work of E. Parini and V. Bobkov [29] where they manage to explicitly describe the Cheeger sets of rationally invariant sets in any dimension and thus compute their Cheeger values. By applying these results to cylinders of the form $B_{n-1} \times (0,d)$, where $B_{n-1} \subset \mathbb{R}^{n-1}$ is a ball, we remark as expected that $\Psi_{B_{n-1}}$ is strictly increasing for higher values of d and thus converges to $J_{n-1}(B_{n-1})$ from below, which supports our strategy.

4.5 Appendix: Some applications

In this Appendix, we apply the sharp estimates given in (4.5) to obtain some new bounds for the first Dirichlet eigenvalue in the case of planar convex sets.

4.5.1 Some sharp upper bounds for the first Dirichlet eigenvalue

General planar convex sets

Proposition 10. *We have the following sharp inequality:*

$$\forall \Omega \in \mathcal{K}^2, \qquad \lambda_1(\Omega) < \frac{\pi^2}{4}\left(\frac{1}{r(\Omega)} + \sqrt{\frac{\pi}{|\Omega|}}\right)^2, \tag{4.8}$$

where equality is asymptotically attained by any family of convex sets $(\Omega_k)_{k\in\mathbb{N}}$ such as $|\Omega_k| = V_0$ for any $k \in \mathbb{N}$ (where V_0 is a positive constant) and $d(\Omega_k) \underset{k\to+\infty}{\longrightarrow} +\infty$.

Proof. We have for every $\Omega \in \mathcal{K}^2$:

$$\lambda_1(\Omega) < \frac{\pi^2}{4}h(\Omega)^2 \leq \frac{\pi^2}{4}\left(\frac{1}{r(\Omega)} + \sqrt{\frac{\pi}{|\Omega|}}\right)^2,$$

where the first inequality is the reverse Cheeger inequality proved by E. Parini in [152, Proposition 4.1] and the second inequality corresponds to the upper bound given in (4.5).

Let us now prove the sharpness inequality (4.8). Let $V_0 > 0$ and $(\Omega_k)_{k\in\mathbb{N}}$ a family of convex sets such as $|\Omega_k| = V_0$ for any $k \in \mathbb{N}$ and $d(\Omega_k) \underset{k\to+\infty}{\longrightarrow} +\infty$. We have on the one hand:

$$\forall k \in \mathbb{N}^*, \qquad \frac{\pi^2}{4r(\Omega_k)^2} < \lambda_1(\Omega_k) < \frac{\pi^2}{4}\left(\frac{1}{r(\Omega_k)} + \sqrt{\frac{\pi}{|\Omega_k|}}\right)^2 = \frac{\pi^2}{4}\left(\frac{1}{r(\Omega_k)} + \sqrt{\frac{\pi}{V_0}}\right)^2,$$

on the other hand, we have:

$$\frac{1}{r(\Omega_k)} \geq \frac{P(\Omega_k)}{2|\Omega_k|} \geq \frac{d(\Omega_k)}{V_0} \underset{k\to+\infty}{\longrightarrow} +\infty,$$

thus:

$$\lambda_1(\Omega_k) \underset{k\to+\infty}{\sim} \frac{\pi^2}{4r(\Omega_k)^2}, \tag{4.9}$$

which proofs the sharpness of inequality (4.8). □

Remark 12. *We note that one can use inequalities* (4.5)*, to provide a similar equivalence as* (4.9) *for the Cheeger constant. Indeed, let us consider* $V_0 > 0$ *and* $(\Omega_k)_{k\in\mathbb{N}}$ *a family of convex sets such as* $|\Omega_k| = V_0$ *for any* $k \in \mathbb{N}$ *and* $d(\Omega_k) \underset{k\to+\infty}{\longrightarrow} +\infty$*. We have by* (4.5)*:*

$$\forall k \in \mathbb{N}, \qquad \frac{1}{r(\Omega_k)} + \frac{\pi r(\Omega_k)}{V_0} \leq h(\Omega_k) \leq \frac{1}{r(\Omega_k)} + \sqrt{\frac{\pi}{|V_0|}},$$

and since $\frac{1}{r(\Omega_k)} \underset{k\to+\infty}{\longrightarrow} +\infty$*, we have the following equivalence:*

$$h(\Omega_k) \underset{k\to+\infty}{\sim} \frac{1}{r(\Omega_k)}. \tag{4.10}$$

By combining (4.9) *and* (4.10)*, we retrieve (with an alternative method) the asymptotic result of [152, Proposition 4.1]:*

$$\lim_{k\to+\infty} J_2(\Omega_k) = \lim_{k\to+\infty} \frac{\lambda_1(\Omega_k)}{h(\Omega_k)^2} = \frac{\pi^2}{4}.$$

It is interesting to compare inequality (4.8) with other inequalities involving the inradius and the area. One immediate estimate can be obtained by considering the inclusion $B_{r(\Omega)} \subset \Omega$ (where $B_{r(\Omega)}$ is an inscribed ball of Ω (with radius $r(\Omega)$). We have by the monotonicity of λ_1:

$$\lambda_1(\Omega) \leq \lambda_1\big(B_{r(\Omega)}\big) = \frac{j_{01}^2}{r(\Omega)^2}, \tag{4.11}$$

where j_{01} denotes the first zero of the first Bessel function. This inequality was already stated in [152, inequality (3)] and in [43, inequality (1.5)] in higher dimensions and for a more general setting. In Figure 4.5, we plot the curves corresponding to the latter inequalities and an approximation of the Blaschke-Santaló diagram corresponding to the functionals λ_1, the inradius r and the area $|\cdot|$, that is the set of points:

$$\mathcal{D} := \left\{ \left(\frac{1}{r(\Omega)}, \lambda_1(\Omega) \right) \mid \Omega \in \mathcal{K}^2 \text{ and } |\Omega| = 1 \right\}.$$

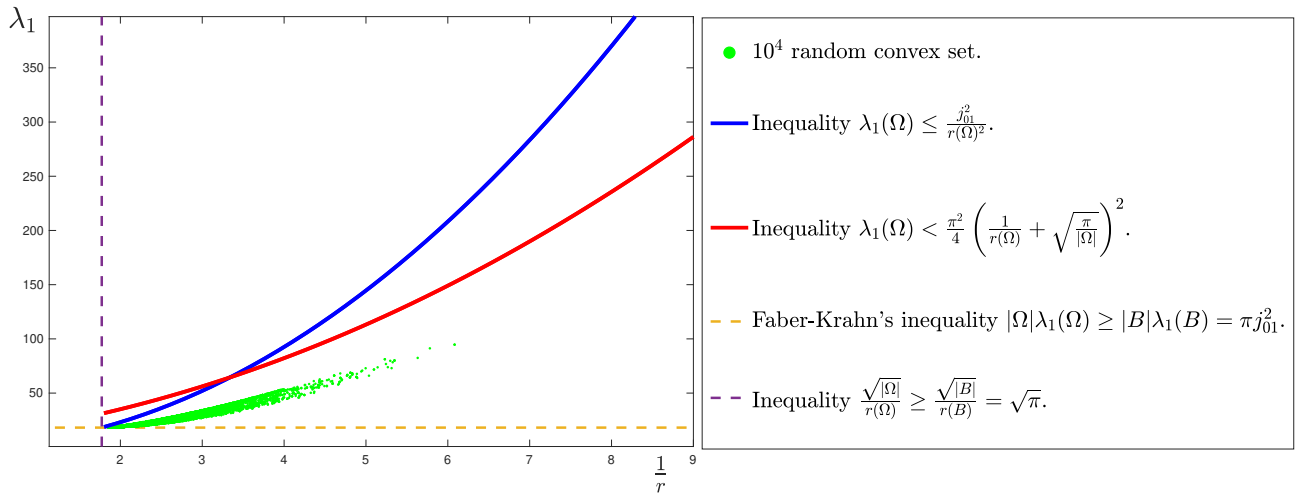

Figure 4.5: Inequality (4.8) improves (4.11) for convex sets with small inradius (ie. large $\frac{1}{r}$).

Sets that are homothetic to their form bodies: in particular "triangles"

We recall that in the case of sets that are homothetic to their form bodies, one has $\frac{1}{2}P(\Omega)r(\Omega) = |\Omega|$ and:

$$h(\Omega) = \frac{P(\Omega) + \sqrt{4\pi|\Omega|}}{2|\Omega|} = \frac{1}{r(\Omega)} + \sqrt{\frac{\pi}{|\Omega|}}.$$

Thus one can write the following result, which is an immediate Corollary of the reverse Cheeger's inequality of [152, Proposition 4.1]:

Corollary 8. *For every set $\Omega \in \mathcal{K}^2$, that is homothetic to its form body (in particular triangles), we have the following inequality:*

$$\lambda_1(\Omega) < \frac{\pi^2}{4} \times \left(\frac{1}{r(\Omega)} + \sqrt{\frac{\pi}{|\Omega|}}\right)^2 = \frac{\pi^2}{16} \times \left(\frac{P(\Omega)}{|\Omega|} + 2\sqrt{\frac{\pi}{|\Omega|}}\right)^2. \tag{4.12}$$

The inequality is sharp as it is asymptotically attained by any sequence of convex sets (Ω_k) of unit area that are homothetic to their form bodies such that $d(\Omega_k) \underset{k\to+\infty}{\longrightarrow} +\infty$.

The most important thing about this upper bound is that in the case of triangles, inequality (4.12) is better than the following bound obtained by B. Siudeja in [167, Theorem 1.1] for "thin" triangles:

$$\lambda_1(T) \leq \frac{\pi^2}{9} \times \left(\frac{P(T)}{|T|}\right)^2. \tag{4.13}$$

It is also interesting to note that inequality (4.12) is even better (also for thin triangles) than the following upper bound stated in [167, Conjecture 1.2]:

Conjecture 7. *For every triangle T, one has:*

$$\lambda_1(T) \leq \frac{\pi^2}{12} \times \left(\frac{P(T)}{|T|}\right)^2 + \frac{\sqrt{3}\pi^2}{3|T|}. \tag{4.14}$$

Here also, let us compare the different estimates in a Blaschke-Santaló diagram: we consider the one involving the perimeter, the area and λ_1 in the class of triangles, that is the set of points:

$$\mathcal{T} := \big\{\big(P(T), \lambda_1(T)\big) \mid T \text{ is a triangle such that } |T| = 1\big\}.$$

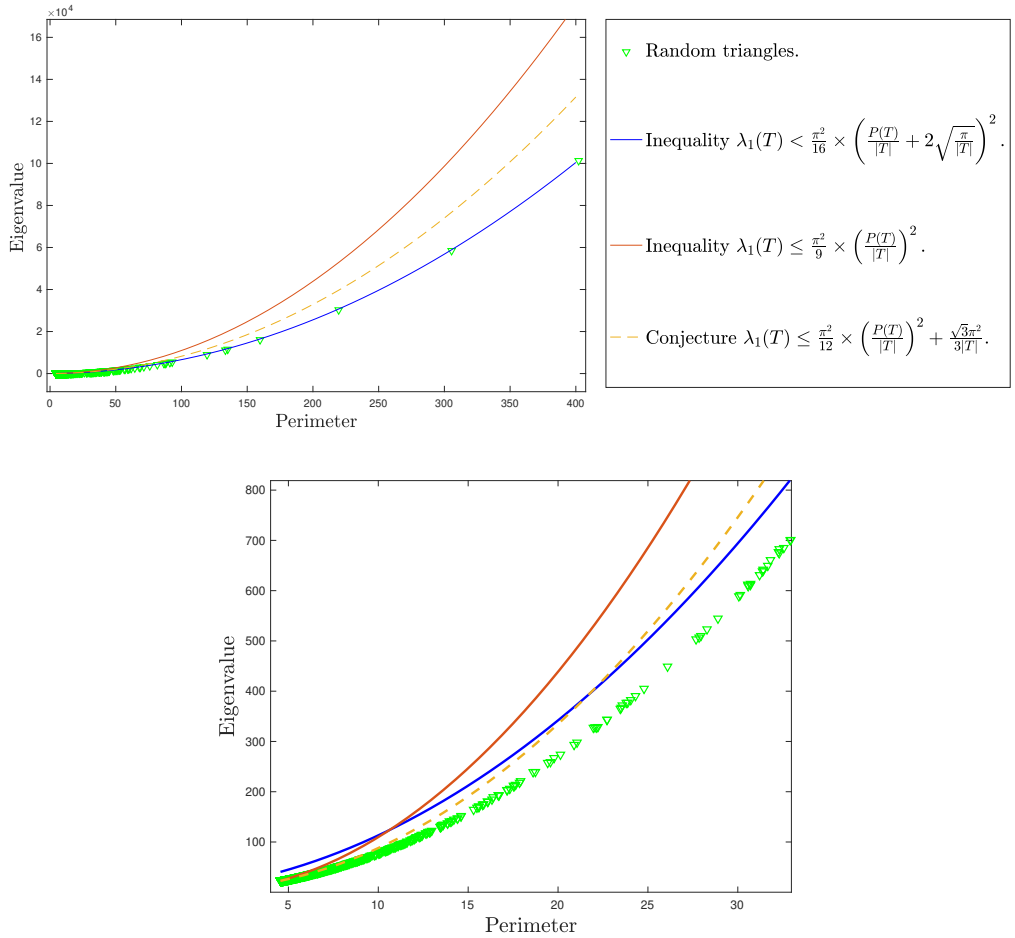

Figure 4.6: Comparison between inequalities (4.12) and (4.13) and Conjecture (4.14) with a zoom on smaller values of the perimeter.

4.5.2 A sharp Cheeger-type inequality

Proposition 11. *We have the following sharp Cheeger-type inequality:*

$$\forall \Omega \in \mathcal{K}^2, \qquad \lambda_1(\Omega) > \frac{\pi^2}{4}\left(h(\Omega) - \sqrt{\frac{\pi}{|\Omega|}}\right)^2, \tag{4.15}$$

where equality is asymptotically attained by any family of convex sets $(\Omega_k)_{k\in\mathbb{N}}$ such as $|\Omega_k| = V_0$ for any $k \in \mathbb{N}$ (where V_0 is a positive constant) and $d(\Omega_k) \underset{k\to+\infty}{\longrightarrow} +\infty$.

Proof. Let $\Omega \in \mathcal{K}^2$, we have:

$$\lambda_1(\Omega) > \frac{\pi^2}{4} \times \frac{1}{r(\Omega)^2} \geq \frac{\pi^2}{4}\left(h(\Omega) - \sqrt{\frac{\pi}{|\Omega|}}\right)^2,$$

where the first inequality is the classical Hersch's inequality [115] and the second follows from is the upper estimate of (4.5).

As for the equality case, let (Ω_k) a family of convex sets $(\Omega_k)_{k\in\mathbb{N}}$ such as $|\Omega_k| = V_0$ for any $k \in \mathbb{N}$ and $d(\Omega_k) \underset{k\to+\infty}{\longrightarrow} +\infty$. By [152, Proposition 4.1], we have: $\lambda_1(\Omega_k) \underset{k\to+\infty}{\sim} \frac{\pi^2}{4} h(\Omega_k)^2$ and by the equivalence

(4.10) and $\lim_{k\longrightarrow+\infty} \frac{1}{r(\Omega_k)} = +\infty$ (see the proof of Proposition 10), we have $\lim_{k\longrightarrow+\infty} h(\Omega_k) = +\infty$ which implies the equivalence: $\lambda_1(\Omega) \underset{k\to+\infty}{\sim} \frac{\pi^2}{4}\left(h(\Omega) - \sqrt{\frac{\pi}{|\Omega|}}\right)^2$. $\square$

We note that inequality (4.15) is better than the improved Cheeger inequality of Theorem 15 (and even the conjecture $J_2(\Omega) \geq J_2((0,1)^2)$) for thin planar convex domains, see Figure 4.7, where we provide an approximation of the following Blaschke-Santaló diagram relating λ_1, the Cheeger constant and the area:

$$\mathcal{C} := \left\{ \left(h(\Omega), \lambda_1(\Omega)\right) \mid \Omega \in \mathcal{K}^2 \ \text{ and } \ |\Omega| = 1 \right\}.$$

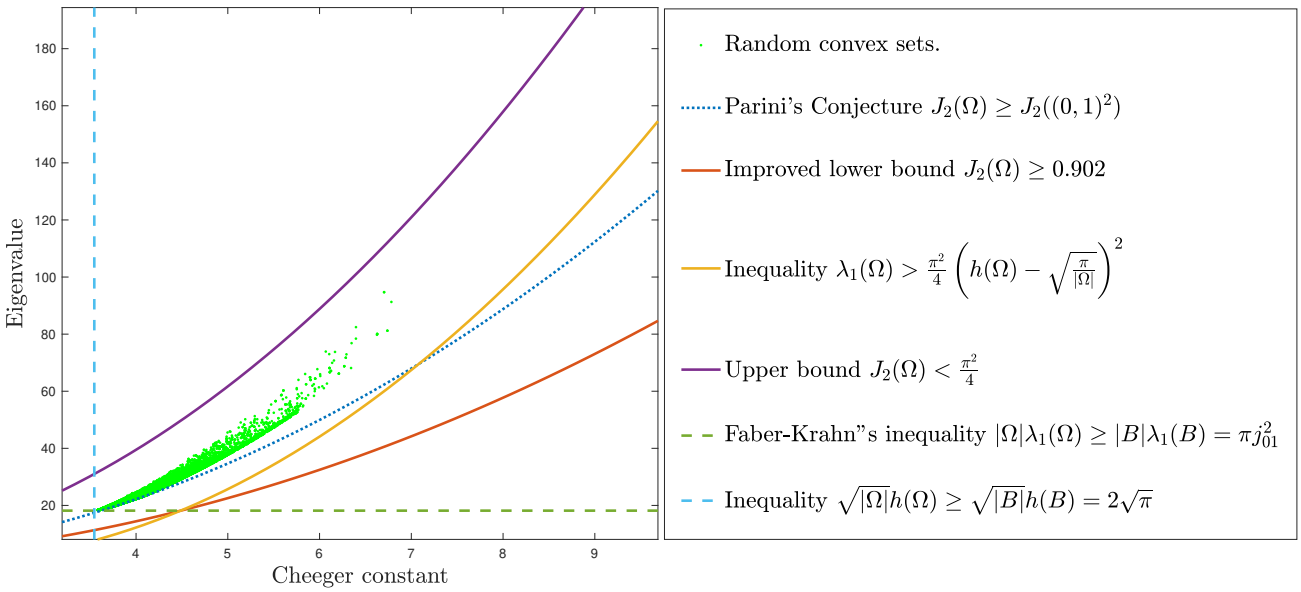

Figure 4.7: Approximation of the Blaschke-Santaló diagram $\mathcal{C}$ and relevant inequalities.

Chapter 5

Numerical study of convexity constraint and application to Blaschke-Santaló diagrams

This chapter is devoted to the numerical study of convexity constraint in shape optimization in the plane. It contains some results of the work in progress [89].

The convexity constraint allows in general to prove the existence of shape optimization problems. The optimal shape may be smooth or singular (polygonal for example), see for example [19, 131, 134]. This makes these kind of problems very interesting from a numerical point of view as one has to adapt the method for each one in function of the expected regularity of the solution. We present various (classical and more original) methods of parametrization that allow to handle convexity constraint (and other ones related to the involved functionals). We apply these techniques for Blaschke-Santaló diagrams involving the area $|\cdot|$, the perimeter P, the diameter d and the first Dirichlet eigenvalue λ_1. We are then able to obtain approximations of the extremal sets (those corresponding to points on the boundary) of these diagrams. This, combined with theoretical upcoming vertical convexity results stated in this chapter (see Theorem 18 and also Corollary 4 of Chapter 3) give an improved description of the studied Blaschke-Santaló diagrams.

We consider 4 different parametrizations of the convex sets:

1. by the support function introduced in Section 5.1.1,
2. by the gauge function introduced in Section 5.1.2,
3. by the radial function introduced in Section 5.1.3
4. and by the vertices of a polygonal approximation introduced in Section 5.1.4.

In the present chapter, we perform some qualitative comparisons between each method by testing them on different shape optimization problems (for which the solutions vary from regular shapes to irregular ones like polygons).

5.1 Parametrization of convex sets and numerical setting

Before describing the parametrizations used in the present thesis, let us recall the definition of (directional) first order shape derivative that is very important in numerical shape optimization.

Definition 3. *let us take a shape depending functional $J : \Omega \subset \mathbb{R}^n \longrightarrow \mathbb{R}$, where $n \geq 2$, and let $V : \mathbb{R}^n \to \mathbb{R}^n$ a perturbation vector field. Let $\Omega \subset \mathbb{R}^n$, we denote $\Omega_t := (I+tV)(\Omega)$ where $I : x \in \mathbb{R}^n \longmapsto x$ is the identity map and t a sufficiently small positive number. We say that the functional J admits a directional shape derivative at Ω in the direction V if the following limit $\lim\limits_{t\to 0^+} \frac{J(\Omega_t)-J(\Omega)}{t}$ exists. In this case we denote:*

$$J'(\Omega, V) := \lim_{t\to 0^+} \frac{J(\Omega_t) - J(\Omega)}{t}.$$

Now, let us present the 4 parametrizations considered in this thesis and show how convexity and other constraints are implemented.

5.1.1 Support function parametrization

Definitions and main properties

The support function is a useful tool to parametrize a convex set by a function defined on the unit sphere, it allows to turn geometrical problem into analytical problems and thus use tools from calculus of variations to solve geometrical problems, we refer for example to [104] for an analytical proof of the classical Blaschke-Lebesgue Theorem which states that among all planar convex domains of given constant width the Reuleaux triangle has minimal area and to [25, 103] for more examples.

Let us now recall the definition of the support function:

Definition 4. *Let $\Omega \in \mathcal{K}^n$ be a convex body (where $n \geq 2$). The support function h_Ω is defined on $\mathbb{R}^n$ by:*

$$\forall x \in \mathbb{R}^n, \quad h_\Omega(x) := \sup_{y\in\Omega} \langle x, y\rangle.$$

The support function is positively 1-homogeneous, so one can equivalently consider the restriction of h_Ω to the unit sphere $\mathbb{S}^{n-1}$.

The support function has various interesting properties as linearity for Minkowski sums, characterizing a convex set and quite practical formulations of different geometrical quantities as the perimeter, diameter, area and width. There are many other properties that enhance the popularity of this parametrization, we refer to [164, Section 1.7.1] for a complete survey and detailed proofs.

Let us state the main properties of the support function used in the present thesis.

Proposition 12. *Let $\Omega_1, \Omega_2 \in \mathcal{K}^n$ and $h_{\Omega_1}, h_{\Omega_2}$ the corresponding support functions, we have the following properties:*

1. $\Omega_1 = \Omega_2 \iff h_{\Omega_1} = h_{\Omega_2}$.
2. *If $\Omega_1 \subset \Omega_2$, then $h_{\Omega_1} \leq h_{\Omega_2}$.*
3. $h_{\Omega_1\cap\Omega_2} = \min(h_{\Omega_1}, h_{\Omega_2})$.
4. $h_{\lambda_1\Omega_1+\lambda_2\Omega_2} = \lambda_1 h_{\Omega_1} + \lambda_2 h_{\Omega_2}$, *where $\lambda_1, \lambda_2 > 0$.*
5. $d^H(\Omega_1, \Omega_2) = \|h_{\Omega_1} - h_{\Omega_2}\|_\infty := \sup\limits_{u\in\mathbb{S}^{n-1}} |h_{\Omega_1}(u) - h_{\Omega_2}(u)|$.

Since we are interested in the case of planar convex sets, from now on the support function of a set $\Omega \in \mathcal{K}^2$ is defined by:

$$\forall \theta \in \mathbb{R}, \quad h_\Omega(\theta) = \sup_{x\in\Omega} \left\langle x, \begin{pmatrix}\cos\theta \\ \sin\theta\end{pmatrix}\right\rangle = \sup_{(x_1,x_2)\in\Omega} (x_1\cos\theta + x_2\sin\theta).$$

It is now natural to wonder how can the support function describe a convex shape (or more precisely its boundary). The following Proposition provides an efficient parametrization of strictly convex planar domains, which are considered in numerical simulations to approach the optimal shapes.

Proposition 13. *Let $\Omega \in \mathcal{K}^2$. The support function h_Ω of the convex Ω is of class C^1 on $\mathbb{R}$ if and only if Ω is strictly convex, in which case its boundary $\partial\Omega$ will be parametrized as follows:*

$$\begin{cases} x_\theta = h_\Omega(\theta)\cos\theta - h'_\Omega(\theta)\sin\theta, \\ y_\theta = h_\Omega(\theta)\sin\theta + h'_\Omega(\theta)\cos\theta, \end{cases}$$

where $\theta \in [0, 2\pi]$.

Now that we know that for any convex set one can associate a support function, it is natural to seek for conditions that a function should satisfy in order to be the support function of a convex set. The answer is tightly related to the fact that the convexity of a set is equivalent to the positivity of the radius of curvature at any point of its boundary.

Proposition 14. *Let Ω a strictly convex planar set, we assume that its support function h_Ω is $C^{1,1}$, then the geometric radius of curvature of $\partial\Omega$ is given by $R_\Omega = h''_\Omega + h_\Omega$ and we have:*

$$\forall\theta \in [0, 2\pi], \qquad R_\Omega(\theta) = h''_\Omega(\theta) + h_\Omega(\theta) \geq 0. \tag{5.1}$$

Reciprocally, if h is a $C^{1,1}$, 2π periodic function satisfying 5.1, then there exists a convex set $\Omega \in \mathcal{K}^2$ such that $h = h_\Omega$.

Remark 13. *The results above are stated for strictly convex sets with smooth support functions (which is enough for the numerical simulations, see 5.1.1). Nevertheless, let us give some remarks on the singular cases:*

- *When h is just C^1, the condition $R := h'' + h \geq 0$ can be understood in the sense of distributions that is to say that $R := h'' + h$ is a positive Radon measure (i.e. for all C^∞ positive function ϕ of compact support in $[0, 2\pi]$, one has: $\int_0^{2\pi} R\phi \geq 0$).*
- *When Ω is not strictly convex, the support function h_Ω is not C^1 and the measure corresponding to the radius of curvature R_Ω may involve Dirac measures. This is for example the case for polygons where R_Ω will be given by a finite sum of Dirac measures, see [164] for example.*

In addition to providing a quite simple description to the convexity constraint (see (5.1)), the support function provides elegant expressions for some relevant geometric functionals.

Proposition 15. *Let $\Omega \in \mathcal{K}^2$ and h_Ω its support function, we have the following formulae:*

1. *for the perimeter*
$$P(\Omega) = \int_0^{2\pi} h_\Omega(\theta)d\theta,$$
2. *for the minimal width*
$$w(\Omega) = \min_{\theta\in[0,2\pi)} \big(h_\Omega(\theta) + h_\Omega(\pi + \theta)\big),$$
3. *for the diameter*
$$d(\Omega) = \max_{\theta\in[0,2\pi)} \big(h_\Omega(\theta) + h_\Omega(\pi + \theta)\big),$$
4. *for the area*
$$|\Omega| = \frac{1}{2}\int_0^{2\pi} \big(h_\Omega^2(\theta) - h_\Omega'^2(\theta)\big)d\theta.$$

Numerical setting

Let us take $\Omega \in \mathcal{K}^2$. Since h_Ω is an H^1, 2π-periodic function, it admits a decomposition in Fourier series:

$$h_\Omega(\theta) = a_0 + \sum_{n=1}^{\infty}(a_n \cos n\theta + b_n \sin n\theta),$$

where $(a_n)_n$ and $(b_n)_n$ denote the Fourier coefficients defined by:

$$a_0 = \frac{1}{2\pi}\int_0^{2\pi} h_\Omega(\theta)d\theta$$

and

$$\forall n \in \mathbb{N}^*, \quad a_n = \frac{1}{\pi}\int_0^{2\pi} h_\Omega(\theta)\cos(n\theta)d\theta, \quad b_n = \frac{1}{\pi}\int_0^{2\pi} h_\Omega(\theta)\sin(n\theta)d\theta.$$

We can then express the area and perimeter via the latter coefficient as follows:

$$P(\Omega) = 2\pi a_0 \quad \text{and} \quad |\Omega| = \pi a_0^2 + \frac{\pi}{2}\sum_{k=1}^{\infty}(1-k^2)(a_k^2 + b_k^2).$$

To retrieve a finite dimensional setting, the idea is to parametrize sets via Fourier coefficients of their support functions truncated at a certain order $N \geq 1$. Thus, we will look for solutions in the set:

$$\mathcal{H}_N := \left\{ \theta \longmapsto a_0 + \sum_{k=1}^{N}\left(a_k \cos(k\theta) + b_k \sin(k\theta)\right) \;\middle|\; a_0, \cdots, a_N, b_1, \cdots, b_N \in \mathbb{R} \right\}.$$

This approach is justified by the following approximation proposition:

Proposition 16. *([164, Section 3.4])*
Let $\Omega \in \mathcal{K}^2$ and $\varepsilon > 0$. Then there exists N_ε and Ω_ε with support function $h_{\Omega_\varepsilon} \in \mathcal{H}_{N_\varepsilon}$ such that $d^H(\Omega, \Omega_\varepsilon) < \varepsilon$.

For more convergence results and application of this method for different problems, we refer to [15].

Let $N \geq 1$, we summarize the parametrizations of functionals and constraints:

- The set Ω is parametrized via $a_0, \ldots, a_N, b_1, \ldots, b_N$.
- The convexity constraint is given by the condition $h''_\Omega + h_\Omega \geq 0$ on $[0, 2\pi)$. In [20] the authors provide an exact characterization of this condition in terms of the Fourier coefficients, involving concepts from semidefinite programming. In [14] the author provides a discrete alternative of the convexity inequality which has the advantage of being linear in terms of the Fourier coefficients. We choose $\theta_m = 2\pi m/M$ where $m \in [\![1, M]\!]$ for some positive integer M and we impose the inequalities $h''_\Omega(\theta_m) + h_\Omega(\theta_m) \geq 0$ for $m \in [\![1, M]\!]$. As already shown in [14] we obtain the following system of linear inequalities:

$$\begin{pmatrix} 1 & \alpha_{1,1} & \cdots & \alpha_{1,N} & \cdots & \beta_{1,1} & \cdots & \beta_{1,N} \\ \vdots & \vdots & \ddots & \vdots & \cdots & \vdots & \ddots & \vdots \\ 1 & \alpha_{N,1} & \cdots & \alpha_{N,N} & \cdots & \beta_{N,1} & \cdots & \beta_{N,N} \end{pmatrix} \begin{pmatrix} a_0 \\ a_1 \\ \vdots \\ a_N \\ b_1 \\ \vdots \\ b_N \end{pmatrix} \geq \begin{pmatrix} 0 \\ \vdots \\ 0 \end{pmatrix}$$

where $\alpha_{m,k} = (1-k^2)\cos(k\theta_m)$ and $\beta_{m,k} = (1-k^2)\sin(k\theta_m)$ for $(m,k) \in [\![1, M]\!] \times [\![1, N]\!]$.

- The perimeter constraint $P(\Omega) = p_0$ is given by

$$2\pi a_0 = p_0.$$

- The area constraint $|\Omega| = A_0$ is given by

$$\pi a_0^2 + \frac{\pi}{2}\sum_{n=1}^{N}(1-k^2)(a_k^2+b_k^2) = A_0.$$

- The diameter constraint $d(\Omega) = d_0$ is equivalent to

$$\begin{cases} \forall\theta \in [0,2\pi), & h_\Omega(\theta) + h_\Omega(\pi+\theta) \leq d_0, \\ \exists\theta_0 \in [0,2\pi), & h_\Omega(\theta_0) + h_\Omega(\pi+\theta_0) = d_0, \end{cases}$$

  again as for the convexity We choose $\theta_m = 2\pi m/M$ where $m \in [\![1, M']\!]$ for some positive integer M' and we impose the inequalities $h_\Omega(\theta_m) + h_\Omega(\pi+\theta_m) \leq d_0$ for $m \in [\![1, M']\!]$, we also assume without loss of generality that $h_\Omega(0) + h_\Omega(\pi) = d_0$ (because all functionals are invariant by rotations). All theses conditions can be written in terms of (a_k) and (b_k) as the following linear constraints:

$$\begin{cases} \forall m \in [\![1, M']\!], \quad 2a_0 + \sum\limits_{k=1}^{N}\big((1+(-1)^k)\cos(k\theta_m)\times a_k + (1+(-1)^k)\sin(k\theta_m)\times b_k\big) \leq d_0, \\ \quad 2a_0 + \sum\limits_{k=1}^{N}(1+(-1)^k)a_k = d_0. \end{cases}$$

Computation of the gradients

In order to have an efficient optimization algorithm, we compute the derivatives of the eigenvalue and the area in terms of the Fourier coefficients of the support function (while for the convexity, the diameter and the perimeter constraints no gradient computation is needed in this setting since these constraints are linear). To this aim, we first consider two types of perturbations, a cosine term and a sine term, namely two families of deformations (V_{a_k}) and (V_{b_k}) that respectively correspond to the perturbation of the coefficients (a_k) and (b_k) in the Fourier decomposition of the support function. As stated in Proposition 13, when Ω is strictly convex, the support function provides a parametrization of its boundary $\partial\Omega = \{(x_\theta, y_\theta)|\ \theta \in [0,2\pi]\}$; then the perturbation fields (V_{a_k}) and (V_{b_k}) are explicitly given on the boundary of Ω as follows:

$$\begin{cases} V_{a_k}(x_\theta, y_\theta) = \big(\cos(k\theta)\cos\theta + k\sin(k\theta)\sin\theta, \cos(k\theta)\sin\theta - k\sin(k\theta)\cos(\theta)\big), & \text{where } k \in [\![0, N]\!] \\ V_{b_k}(x_\theta, y_\theta) = \big(\sin(k\theta)\cos\theta + k\cos(k\theta)\sin\theta, \sin(k\theta)\sin\theta - k\cos(k\theta)\cos\theta\big), & \text{where } k \in [\![1, N]\!] \end{cases}$$

If we denote $\mathcal{A} : \Omega \longmapsto |\Omega|$ the area functional, we have the following formulae for the shape derivatives of the functional $\mathcal{A}$ in the directions (V_{a_k}) and (V_{b_k}):

$$\begin{cases} \mathcal{A}'(\Omega, V_{a_0}) = 2\pi a_0 \\ \mathcal{A}'(\Omega, V_{a_k}) = \pi(1-k^2)a_k, & \text{where } k \in [\![1, N]\!] \\ \mathcal{A}'(\Omega, V_{b_k}) = \pi(1-k^2)b_k, & \text{where } k \in [\![1, N]\!] \end{cases}$$

As for the Dirichlet eigenvalue, we recall that when Ω is convex (or sufficiently smooth), the shape derivative of λ_1 in a direction $V : \mathbb{R}^2 \longrightarrow \mathbb{R}^2$ is given by the following formula:

$$\lambda_1'(\Omega, V) = -\int_{\partial\Omega} |\nabla u_1|^2(x_\theta, y_\theta)\big\langle V(x_\theta, y_\theta), n(x_\theta, y_\theta)\big\rangle d\sigma,$$

where $n(x_\theta, y_\theta) = (\cos\theta, \sin\theta)$ stands for the exterior unit normal vector to $\partial\Omega$, $u_1 \in H_0^1(\Omega)$ corresponds to a normalized eigenfunction (i.e. $\|u_1\|_2 = 1$) corresponding to the first eigenvalue $\lambda_1(\Omega)$ and $d\sigma = (h''_\Omega + h_\Omega)(\theta)d\theta$, we refer to [106, Section 2.5] for more details on shape derivatives of eigenvalues. It is then possible by a change of variables to write the directional shape derivatives of λ_1 as an integral on $[0, 2\pi]$ as follows:

$$\begin{cases} \lambda_1'(\Omega, V_{a_k}) = -\int_0^{2\pi} |\nabla u|^2(x_\theta, y_\theta)\cos(k\theta)\big(h''_\Omega(\theta) + h_\Omega(\theta)\big)d\theta, & \text{where } k \in [\![0, N]\!], \\ \lambda_1'(\Omega, V_{b_k}) = -\int_0^{2\pi} |\nabla u|^2(x_\theta, y_\theta)\sin(k\theta)\big(h''_\Omega(\theta) + h_\Omega(\theta)\big)d\theta, & \text{where } k \in [\![1, N]\!]. \end{cases}$$

The computation of the integrals is done by using an order 1 trapezoidal quadrature.

5.1.2 Gauge function parametrization

Definition and main properties

A classical way to parametrize starshaped open sets (in particular convex ones) is by using the so-called *gauge function*.

Definition 5. *Let Ω a bounded, open subset of $\mathbb{R}^n$ (with $n \geq 2$) starshaped with respect to the origin. The gauge function u_Ω is defined on $\mathbb{R}^n$ by:*

$$\forall x \in \mathbb{R}^n, \quad u_\Omega(x) = \inf\{t > 0 \mid tx \in \Omega\}.$$

The gauge function is positively 1-homogeneous, so one can equivalently consider the restriction of u_Ω to the unit sphere $\mathbb{S}^{n-1}$.

In the planar case ($n = 2$), we use polar coordinates representation (r, θ) for the domains, we then define the gauge function on $\mathbb{R}$ as follows:

$$\forall \theta \in \mathbb{R}, \quad u_\Omega(\theta) = \inf\left\{t > 0 \mid t\begin{pmatrix}\cos\theta \\ \sin\theta\end{pmatrix} \in \Omega\right\}.$$

The open set Ω is then given by:

$$\Omega = \left\{(r, \theta) \in [0, +\infty) \times \mathbb{R} \mid r < \frac{1}{u_\Omega(\theta)}\right\}.$$

The curvature of the boundary of Ω is given by:

$$\kappa_\Omega = \frac{u''_\Omega + u_\Omega}{\left(1 + \left(\frac{u'_\Omega}{u_\Omega}\right)^2\right)^{\frac{3}{2}}},$$

where the second order derivative is to be understood in the sense of distributions. Thus, as for the support function, the starshaped set $\Omega \subset \mathbb{R}^2$ is convex if and only if:

$$u''_\Omega + u_\Omega \geq 0.$$

Moreover, straight lines in $\partial\Omega$ are parameterized by the set $\{u''_\Omega + u_\Omega = 0\}$, and corners in the boundary are seen as Dirac masses in the measure $u''_\Omega + u_\Omega$. For example, the gauge function of a polygon will be given by a finite sum of Dirac masses at angles parametrizing the corners.

Both the perimeter and area can be expressed via gauge function. Unfortunately, this is not the case for the diameter.

Proposition 17. *Let Ω a planar set star-shaped with respect to the origin. We have the following formulae:*

1. *for the perimeter*

$$P(\Omega) = \int_0^{2\pi} \frac{\sqrt{u_\Omega^2 + u_\Omega'^2}}{u_\Omega^2} d\theta.$$

2. *for the area*

$$|\Omega| = \frac{1}{2} \int_0^{2\pi} \frac{d\theta}{u_\Omega^2}.$$

Numerical setting

Similarly to the case of support function, in the planar case, we can decompose its gauge function as a Fourier series:

$$u_\Omega(\theta) = a_0 + \sum_{k=1}^{\infty} (a_k \cos k\theta + b_k \sin k\theta),$$

where $(a_n)_n$ and $(b_n)_n$ denote the Fourier coefficients defined by:

$$a_0 = \frac{1}{2\pi} \int_0^{2\pi} u_\Omega(\theta) d\theta$$

and

$$\forall k \in \mathbb{N}^*, \quad a_k = \frac{1}{\pi} \int_0^{2\pi} u_\Omega(\theta) \cos(k\theta) d\theta, \quad b_k = \frac{1}{\pi} \int_0^{2\pi} u_\Omega(\theta) \sin(k\theta) d\theta.$$

Here also, we look for solutions among truncated functions given in the following space:

$$\mathcal{H}_N := \left\{ \theta \longmapsto a_0 + \sum_{k=1}^{N} \left(a_k \cos(k\theta) + b_k \sin(k\theta) \right) \mid a_0, \cdots, a_N, b_1, \cdots, b_N \in \mathbb{R} \right\}.$$

In practice, the computation of the perimeter and the area is done by considering a uniform discretization $\left\{ \theta_k := \frac{2k\pi}{M} \mid k \in [\![0, M-1]\!] \right\}$ of the interval $[0, 2\pi)$, with M a positive integer (we take it equal to 200 for the applications). We then approach the domain Ω by the polygon Ω_M of vertices $A_k \left(\frac{\cos\theta_k}{u_\Omega(\theta_k)}, \frac{\sin\theta_k}{u_\Omega(\theta_k)} \right)$, where $k \in [\![0, M-1]\!]$. The functionals perimeter and area (given as integrals in Proposition 17) are then computed in terms of (a_k) and (b_k) by using an order 1 trapezoidal quadrature:

$$\begin{cases} P(\Omega) \approx \frac{1}{M} \sum_{k=0}^{M-1} \frac{\sqrt{u_\Omega^2(\theta_k) + u_\Omega'^2(\theta_k)}}{u_\Omega^2(\theta_k)} = \frac{1}{M} \sum_{k=0}^{M-1} \frac{\sqrt{\left(a_0 + \sum_{p=1}^{N} \left(a_p \cos(p\theta_k) + b_p \sin(p\theta_k) \right) \right)^2 + \left(\sum_{p=1}^{N} \left(-p a_p \sin(p\theta_k) + p b_p \cos(p\theta_k) \right) \right)^2}}{\left(a_0 + \sum_{p=1}^{N} \left(a_p \cos(p\theta_k) + b_p \sin(p\theta_k) \right) \right)^2}, \\ |\Omega| \approx \frac{1}{M} \sum_{k=0}^{M-1} \frac{1}{u_\Omega^2(\theta_k)} = \frac{1}{M} \sum_{k=0}^{M-1} \frac{1}{\left(a_0 + \sum_{p=1}^{N} \left(a_p \cos(p\theta_k) + b_p \sin(p\theta_k) \right) \right)^2}. \end{cases}$$

Here also the convexity is parametrized as in the last section by linear inequalities involving the coefficients (a_k) and (b_k).

Computation of the gradients

The shape gradients of the area and the perimeter are computed by differentiating the explicit formulae above with respect to the Fourier coefficients. As for the Dirichlet eigenvalue, one has to use the Hadamard formula:

$$\lambda_1'(\Omega, V) = -\int_{\partial\Omega} |\nabla u_1|^2 \langle V, n \rangle d\sigma,$$

where $u_1 \in H_0^1(\Omega)$ is a normalized eigenfunction (i.e. $\|u_1\|_2 = 1$) corresponding to $\lambda_1(\Omega)$ and V is a perturbation field corresponding to the perturbation of a Fourier coefficient. Let us investigate the values of such perturbations on the boundary of Ω: let $\phi : \theta \in \mathbb{R} \longmapsto v(\theta)$ a Lipschitz 2π-periodic function, for sufficiently small values of $t > 0$, we write:

$$\frac{1}{u_\Omega + t\phi} = \frac{1}{u_\Omega}\left(1 + t\frac{\phi}{u_\Omega}\right)^{-1} = \frac{1}{u_\Omega}\left(1 - \frac{\phi}{u_\Omega} \times t + \underset{t\to 0}{o}(t)\right) = \frac{1}{u_\Omega} - \frac{\phi}{u_\Omega^2} \times t + \underset{t\to 0}{o}(t).$$

We deduce that perturbating the gauge function in a direction ϕ corresponds to a perturbation field defined on the boundary $\partial\Omega = \left\{\left(\frac{\cos\theta}{u_\Omega(\theta)}, \frac{\sin\theta}{u_\Omega(\theta)}\right) \mid \theta \in [0, 2\pi]\right\}$ by:

$$\left(\frac{\cos\theta}{u_\Omega(\theta)}, \frac{\sin\theta}{u_\Omega(\theta)}\right) \in \partial\Omega \longmapsto -\frac{\phi(\theta)}{u_\Omega^3(\theta)}\begin{pmatrix}\cos(\theta)\\ \sin(\theta)\end{pmatrix} \in \mathbb{R}^2.$$

We then deduce that the perturbation fields corresponding to the perturbations of the coefficients (a_k) and (b_k) are given by:

$$\begin{cases} V_{a_k}\left(\frac{\cos\theta}{u_\Omega(\theta)}, \frac{\sin\theta}{u_\Omega(\theta)}\right) = -\frac{\cos(k\theta)}{u_\Omega^3(\theta)}\binom{\cos(\theta)}{\sin(\theta)}, & \text{where } k \in [\![0, N]\!], \\ V_{b_k}\left(\frac{\cos\theta}{u_\Omega(\theta)}, \frac{\sin\theta}{u_\Omega(\theta)}\right) = -\frac{\sin(k\theta)}{u_\Omega^3(\theta)}\binom{\cos(\theta)}{\sin(\theta)}, & \text{where } k \in [\![1, N]\!], \end{cases}$$

where $\theta \in [0, 2\pi]$.

Once the perturbation fields are known, we use the polygonal approximation Ω_M (introduced above in Paragraph 5.1.2) of the domain Ω to provide a numerical approximation of the shape gradient as follows:

$$\lambda_1'(\Omega, V) \approx -\sum_{k=0}^{M-1} |\nabla u_1|^2(x_{I_k}, y_{I_k})\langle V(x_{I_k}, y_{I_k}), n_k\rangle d\sigma_k,$$

with the convention $A_M := A_0$ and:

- $d\sigma_k = \sqrt{(x_{A_k} - x_{A_{k+1}})^2 + (y_{A_k} - y_{A_{k+1}})^2}$,
- I_k is the middle of the segment $[A_k A_{k+1}]$.
- $n_k := \frac{1}{d\sigma_k}\binom{-(y_{A_k} - y_{A_{k+1}})}{x_{A_k} - x_{A_{k+1}}}$ is the exterior unit vector normal to the segment $[A_k A_{k+1}]$.

5.1.3 Radial function parametrization

Definition and main properties

It is common to parametrize star-shaped domains via their *radial function*. In this section, we present this parametrization

Definition 6. *Let $n \geq 2$ and $\Omega \subset \mathbb{R}^n$ a domain star-shaped with respect to the origin. The radial function ρ_Ω is defined on $\mathbb{R}^n$ by:*

$$\forall x \in \mathbb{R}^n, \quad \rho_\Omega(x) = \sup\{t > 0 \mid tx \in \Omega\}.$$

The radial function is positively 1-homogeneous, so one can equivalently consider the restriction of ρ_Ω to the unit sphere $\mathbb{S}^{n-1}$.

In the planar case we can define the radial function on $\mathbb{R}$ as follows:

$$\forall \theta \in \mathbb{R}, \quad \rho_\Omega(\theta) = \sup\left\{ t > 0 \mid t\begin{pmatrix}\cos\theta \\ \sin\theta\end{pmatrix} \in \Omega \right\}.$$

If $\Omega \subset \mathbb{R}^2$ is open, it can be given in polar coordinates as follows:

$$\Omega = \{(r,\theta) \in [0;+\infty) \times \mathbb{R} \mid r < \rho_\Omega(\theta)\}.$$

We remark that the radial function is simply the inverse of the gauge function introduced before.

Numerical setting

Unfortunately, in contrary to the previous cases, convexity cannot be given by linear constraints on the Fourier coefficients of the periodic function ρ_Ω. We propose to approximate a set via polygons of vertices $\rho_\Omega(\theta_k)\binom{\cos\frac{2k\pi}{M}}{\sin\frac{2k\pi}{M}} \in \mathbb{R}^2$, where $k \in [\![0, M-1]\!]$ and M a sufficiently large integer (in practice we take $M = 200$).

Thus, a star-shaped set Ω will be parametrized via M positive distances $(\rho_k)_{k\in[\![1,M]\!]}$ that describe a polygonal approximation of Ω given by vertices $A_k = \rho_k\binom{\cos\frac{2k\pi}{M}}{\sin\frac{2k\pi}{M}}$. We always consider the convention $A_M := A_0$ and $A_{-1} := A_{M-1}$ (in particular $\rho_M := \rho_0$ and $\rho_{-1} := \rho_{M-1}$).

This setting allows to give good approximations of the involved geometrical functionals (perimeter, area and diameter). we have:

1. for the area:
$$|\Omega| = \frac{1}{2}\sin\frac{2\pi}{M} \times \sum_{k=0}^{M-1} \rho_k\rho_{k+1},$$

2. for the perimeter:
$$P(\Omega) = \sum_{k=0}^{M-1} \sqrt{\rho_k^2 + \rho_{k+1}^2 - 2\rho_k\rho_{k+1}\cos\left(\frac{2k\pi}{M}\right)},$$

3. and the diameter:
$$d(\Omega) = \max_{i\neq j} \sqrt{\left[\rho_i\cos\frac{2i\pi}{M} - \rho_j\cos\frac{2j\pi}{M}\right]^2 + \left[\rho_i\sin\frac{2i\pi}{M} - \rho_j\sin\frac{2j\pi}{M}\right]^2},$$

   this formula provides the diameter in $\mathcal{O}(M^2)$ complexity. When the polygon is convex we use a faster method of computation (with complexity $\mathcal{O}(M)$), which consists of finding all antipodal pairs of points and looking for the diametrical between them. This is classically known as Shamos algorithm [157].

It remains to describe the convexity constraint via the parameters $(\rho_k)_{k\in[\![0,M-1]\!]}$: we remark that the polygon (which contains the origin O) whose vertices are given by $A_k := \left(\rho_k\cos\frac{2k\pi}{M}, \rho_k\sin\frac{2k\pi}{M}\right)$ is convex if and only if the sum of the areas of the triangles OA_kA_{k+1} and OA_kA_{k-1} is less or equal than the area of $OA_{k-1}A_{k+1}$, see Figure 5.1.

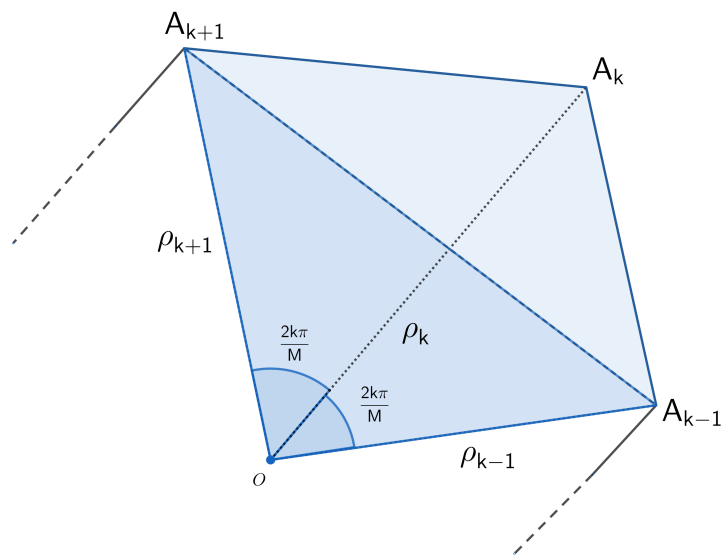

Figure 5.1: Convexity constraint via areas of the triangles.

We have:

$$\begin{cases} \mathcal{S}_{OA_{k-1}A_k} = \frac{1}{2}\rho_{k-1}\rho_k \sin\frac{2k\pi}{M} \\ \mathcal{S}_{OA_kA_{k+1}} = \frac{1}{2}\rho_k\rho_{k+1} \sin\frac{2k\pi}{M} \\ \mathcal{S}_{OA_{k-1}A_{k+1}} = \frac{1}{2}\rho_{k-1}\rho_{k+1} \sin\frac{4k\pi}{M} = \rho_{k-1}\rho_{k+1} \sin\frac{2k\pi}{M}\cos\frac{2k\pi}{M}. \end{cases}$$

Thus, the convexity constraint given by $\mathcal{S}_{OA_{k-1}A_k} + \mathcal{S}_{OA_kA_{k+1}} \geq \mathcal{S}_{OA_{k-1}A_{k+1}}$ is equivalent to the following quadratic constraint:

$$C_k := 2\cos\left(\frac{2\pi}{M}\right)\rho_{k-1}\rho_{k+1} - \rho_k(\rho_{k-1} + \rho_{k+1}) \leq 0,$$

where $k \in [\![0, M-1]\!]$.

Computation of the gradients

Now that we brought the shape optimization problem to a finite dimensional optimization one, it remains to compute the gradients of the involved functionals and constraints.

Let us take $\Omega \subset \mathbb{R}^2$ a domain whose starshaped with respect to the origin O, that we assume to be parametrized by $(\rho_k)_{k\in[\![0,M-1]\!]}$. For any $k \in [\![0, M-1]\!]$ we denote V_{ρ_k} the perturbation field corresponding to the perturbation of the variable ρ_k. It is null on the whole boundary except on the sides $[A_{k-1}A_k]$ and $[A_kA_{k+1}]$, see Figure 5.2.

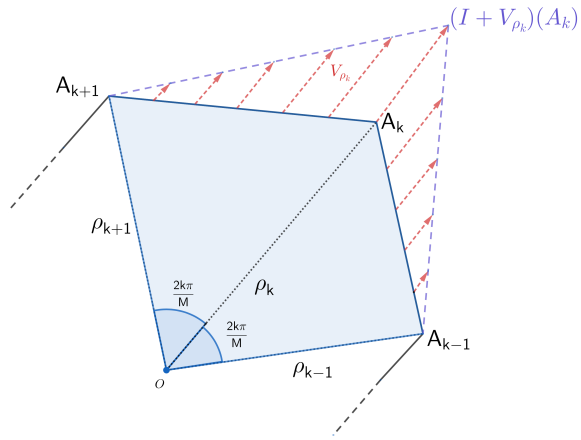

Figure 5.2: Perturbation field V_{ρ_k}.

Since we dispose of explicit formulae for the perimeter and the area, we can directly compute the corresponding shape gradients. We have for every $k \in [\![0, M-1]\!]$:

$$\mathcal{A}'(\Omega, V_{\rho_k}) = \frac{\sin\left(\frac{2\pi}{M}\right)}{2} \times (\rho_{k-1} + \rho_{k+1}),$$

and

$$P'(\Omega, V_{\rho_k}) = \frac{\rho_k - \rho_{k-1}\cos\left(\frac{2\pi}{M}\right)}{\sqrt{\rho_{k-1}^2 + \rho_k^2 - 2\rho_{k-1}\rho_k\cos\left(\frac{2\pi}{M}\right)}} + \frac{\rho_k - \rho_{k+1}\cos\left(\frac{2\pi}{M}\right)}{\sqrt{\rho_{k+1}^2 + \rho_k^2 - 2\rho_{k+1}\rho_k\cos\left(\frac{2\pi}{M}\right)}}.$$

For the eigenvalue, we use as before the Hadamard formula:

$$\lambda_1'(\Omega, V) = -\int_{\partial\Omega} |\nabla u_1|^2 \langle V, n\rangle d\sigma,$$

where $u_1 \in H_0^1(\Omega)$ is a normalized eigenfunction (i.e. $\|u_1\|_2 = 1$) corresponding to $\lambda_1(\Omega)$ and V is a perturbation field.

For every $k \in [\![0, M-1]\!]$, we discretize the side $[A_k A_{k+1}]$ in ℓ small segments of length $\frac{A_k A_{k+1}}{\ell}$ centred in some points $B_k^i \in [A_k A_{k+1}]$. We then compute approximations of the gradients as follows:

$$\lambda_1'(\Omega, V_{\rho_k}) \approx -\frac{1}{\ell}\sum_{i=1}^{\ell}\left(|\nabla u_1|^2(x_{B_k^i}, y_{B_k^i})\langle V_{\rho_k}(x_{B_k^i}, y_{B_k^i}), n_k\rangle d\sigma_k - |\nabla u_1|^2(x_{B_{k-1}^i}, y_{B_{k-1}^i})\langle V_{\rho_k}(x_{B_{k-1}^i}, y_{B_{k-1}^i}), n_{k-1}\rangle d\sigma_{k-1}\right),$$

with:

- the conventions $A_M := A_0$ and $A_{-1} := A_{M-1}$ (in particular $\rho_M := \rho_0$ and $\rho_{-1} := \rho_{M-1}$),
- the points $(B_k^i)_{i\in[\![1,M]\!]}$
- $d\sigma_k = \sqrt{(x_{A_k} - x_{A_{k+1}})^2 + (y_{A_k} - y_{A_{k+1}})^2}$,
- $\forall i \in [\![1, \ell]\!], \quad B_k^i := \left(1 - \frac{i}{2\ell}\right) A_k + \frac{i}{2\ell} A_{k+1}$,
- $n_k := \frac{1}{d\sigma_k}\binom{-(y_{A_k} - y_{A_{k+1}})}{x_{A_k} - x_{A_{k+1}}}$ is the exterior unit vector normal to the segment $[A_k A_{k+1}]$.

Finally, for the diameter, we use the following shape derivative formula obtained in Theorem 19:

$$d'(\Omega, V) = \max\left\{\left\langle \frac{x-y}{|x-y|}, V(x) - V(y)\right\rangle \;\middle|\; x, y \in \Omega, \text{ such that } |x-y| = d(\Omega)\right\}.$$

5.1.4 Polygonal approximation and parametrization via vertices

In this section, we propose to parametrize a convex set via the coordinates $(x_k, y_k)_{k\in[\![0,M-1]\!]}$ of the vertices A_k of a corresponding polygonal approximation denoted Ω_M (with $M \geq 3$). We assume that the points $(A_k)_{k\in[\![0,M-1]\!]}$ form in this order a simple polygon (that is a polygon that does not intersect itself and has no holes) and recall the conventions $A_M := A_0$ and $A_{-1} := A_{M-1}$.

As for the previous cases, we have formulae for the involved geometrical quantities:

$$\begin{cases} P(\Omega_M) &= \displaystyle\sum_{k=0}^{M-1} \sqrt{(x_{k+1}-x_k)^2 + (y_{k+1}-y_k)^2}, \\ |\Omega_M| &= \frac{1}{2}\left|\displaystyle\sum_{k=0}^{M-1} x_k y_{k+1} - x_{k+1} y_k\right| \\ d(\Omega_M) &= \max_{i,j} \sqrt{(x_i-x_j)^2 + (y_i-y_j)^2} \end{cases}$$

It is easily seen that Ω_M is convex if and only if all the interior angles are less than or equal to π. By using the cross product, this, in turn, is equivalent to the following quadratic constraints:

$$(x_{k-1}-x_k)(y_{k+1}-y_k) - (y_{k-1}-y_k)(x_{k+1}-x_k) \leq 0,$$

for $k \in [\![0, M-1]\!]$, where we used the conventions $x_0 := x_M$, $y_0 := y_M$, $x_{M+1} := x_1$ and $y_{M+1} := y_1$. This characterization of convexity is quite natural and has already been considered in literature, see [19] for example.

The gradients of the perimeter, area and convexity constraints (corresponding to the variables (x_k) and (y_k)) are directly obtained by differentiating the explicit formulae given above. On the other hand, the gradients of the eigenvalue and diameter are computed (as in the last section) by using shape derivative formulae (see [106, Section2.5] for λ_1 and Theorem 19 for the diameter), where, we use the perturbation vector fields (V_{x_k}) and (V_{y_k}) corresponding to the variables (x_k) and (y_k), see Figure 5.3.

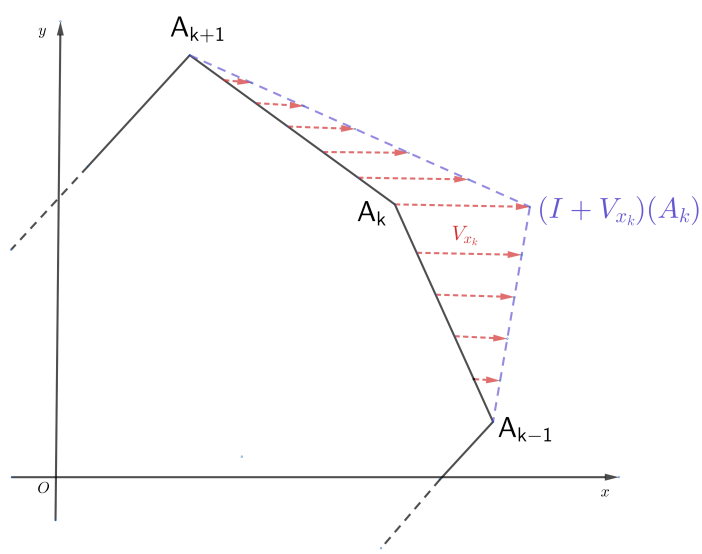

Figure 5.3: Perturbation field V_{x_k} associated to the parameter x_k.

5.1.5 Computations of the functionals and numerical optimization

Let us give few words on the numerical computation of the functionals. In all the parametrizations above we dispose of analytical formulae that provide good approximations of the area and the perimeter. Let us give some elements on the computations of the remaining functionals involved in the present thesis:

- **the first Dirichlet eigenvalue** is computed by the "Partial Differential Equation Toolbox" of Matlab that is based on finite elements methods.
- As explained in the sections above, the computation of **the diameter** depends on the choice of the parametrization: indeed, when parametrizing a convex Ω via its support function h_Ω, it is given by $d(\Omega) = \max_{\theta\in[0,2\pi]} \big(h_\Omega(\theta) + h_\Omega(\pi+\theta)\big)$, meanwhile, when using a polygonal approximation, we compute the diameter of the convex hull via a fast method of computation (with complexity $\mathcal{O}(M)$, where M is the number of vertices), which consists of finding all antipodal pairs of points and looking for the diametrical between them. This is classically known as Shamos algorithm [157].
- **The Cheeger constant** is computed by using a Beniamin Bogosel's code [30] based on the characterization of the Cheeger sets of planar convex sets given in [122] and the toolbox Clipper, a very good implementation of polygon offset computation by Agnus Johnson.
- **The inradius** is also computed by using the tootbox Clipper and the fact that $r(\Omega)$ is the solution of the equation $|\Omega_{-t}| = 0$.

As for the optimization, we used Matlab's `fmincon` function with the `interior-point` and/or `sqp` algorithms.

5.2 Application to Blaschke-Santaló diagrams

In chapters 2 and 3 we gave theoretical results on Blaschke-Santaló diagrams that we combine with the latter optimization methods in order to obtain a quite advanced numerical description of diagrams involving the diameter, area, perimeter and Dirichlet eigenvalue.

If we want to have an idea of the shape of a Blaschke-Santaló diagram, we generate in a first time a large number of convex sets (polygons) for which we compute the values of the involved functionals. This allows to approximate the diagram via a cloud of dots, this was done before in [11] for the case of the triplet $(P, \lambda_1, |\cdot|)$ and [13] for the case of $(\lambda_1, \lambda_2, |\cdot|)$ and in Chapters 2 for the triplet $(P, h, |\cdot|)$ and 3 for the triplet $(P, \lambda_1, |\cdot|)$.

In order to improve the results obtained with this random generation, we propose to use shape optimization methods based on the parametrizations described in Section 5.1 to describe the upper and lower boundaries of the diagrams and use theoretical vertical convexity results on the diagrams to conclude that the sets of points between the latter boundaries is included in the diagrams and thus give a quite advanced description.

5.2.1 Some theoretical results on the diagrams

We recall the following setting: if J_1, J_2 and J_3 are three shape functionals defined on a class $\mathcal{F}$ of subsets of $\mathbb{R}^n$, we call *a Blaschke-Santaló diagram* of the triplet (J_1, J_2, J_3) on the class $\mathcal{F}$, the following set of points:

$$\mathcal{D}_{\mathcal{F}} := \big\{ \big(J_1(\Omega), J_2(\Omega)\big) \mid J_3(\Omega) = 1 \text{ and } \Omega \in \mathcal{F} \big\}.$$

In this section we are interested in the numerical study of some Blaschke-Santaló diagrams involving the first Dirichlet eigenvalue λ_1, the diameter d, the perimeter P and the area $|\cdot|$. Let us state the following theoretical result that will appear in [89]:

Theorem 18. *(to appear in [89])*
The diagrams associated to the triplets $(P, |\cdot|, d)$, $(d, \lambda_1, |\cdot|)$ and $(P, \lambda_1, |\cdot|)$ are closed, simply connected and vertically convex; indeed they are given by sets of points contained between the curves of two continuous functions defined on some corresponding intervals.

This result, combined with the optimization methods described above allow to give quite accurate descriptions of the diagrams which are given by sets of points located between the numerically obtained lower and upper boundaries.

Let us give some hints on the proof of this result:

- As explained in the introduction (Section 1.3.1) when the diagram involves two functionals that are linear for Minkowski sums and dilatations (which is the case for the triplet $(P, |\cdot|, d)$), it is quite easy to prove the vertical (or horizontal) convexity of the diagram, indeed, in this case the paths constructed by Minkowski sums are given by segments (see the example of the diagram of $(r, P, |\cdot|)$ developed in the introduction).

- The result on the diagram of the triplet $(P, \lambda_1, |\cdot|)$ is proved in Chapter 3 and the same method applies for $(d, \lambda_1, |\cdot|)$, the only difference is that we had to prove a perturbation lemma in the spirit of Lemma 7.

5.2.2 The purely geometric diagram $(P, |\cdot|, d)$

Naive approach and classical results

We recall that the diagram of the triplet $(P, |\cdot|, d)$ is given by the set of points:

$$\mathcal{D}_1 := \left\{ \big(P(\Omega), |\Omega|\big) \mid \Omega \in \mathcal{K}^2 \text{ and } d(\Omega) = 1 \right\}.$$

This diagram is (as far as we know) one of the unsolved diagrams introduced by Santaló in [163]: but one has to note that there are quite advanced results on the characterization of its boundary:

- in [148], the authors solve the problem corresponding to the upper boundary, namely they prove that the problem
$$\sup\{|\Omega| \mid \Omega \in \mathcal{K}^2,\ P(\Omega) = p_0 \text{ and } d(\Omega) = 1\},$$
where $p_0 \in (2, \pi]$, is solved by symmetric lenses (that are given by the intersection of two balls with the same radius) of diameter 1 and perimeter p_0.

- In [127], the author manages to describe the lower boundary of the diagram that corresponds to perimeters $p_0 \in (2, 3]$, he shows that the optimal domains are given by *subequilateral triangles* (ie. isosceles triangles whose smaller inner angle is less than $\frac{\pi}{3}$).

- At last, there is the famous Blaschke–Lebesgue's Theorem, named after W. Blaschke and H. Lebesgue, which states that the Reuleaux triangle (see Figure 5.4) has the least area of all domains of given constant width. It is classical that sets of constant width have the same perimeter, thus in the diagram, those sets fill the vertical line $\{\pi\} \times [\frac{1}{2}(\pi - \sqrt{3}), \frac{\pi}{4}]$, see Figure 5.4.

In the following figure, we plot the curves corresponding to the extremal sets described above and a cloud of dots obtained by randomly generating 10^5 polygons whose numbers of sides are in $[\![3, 30]\!]$.

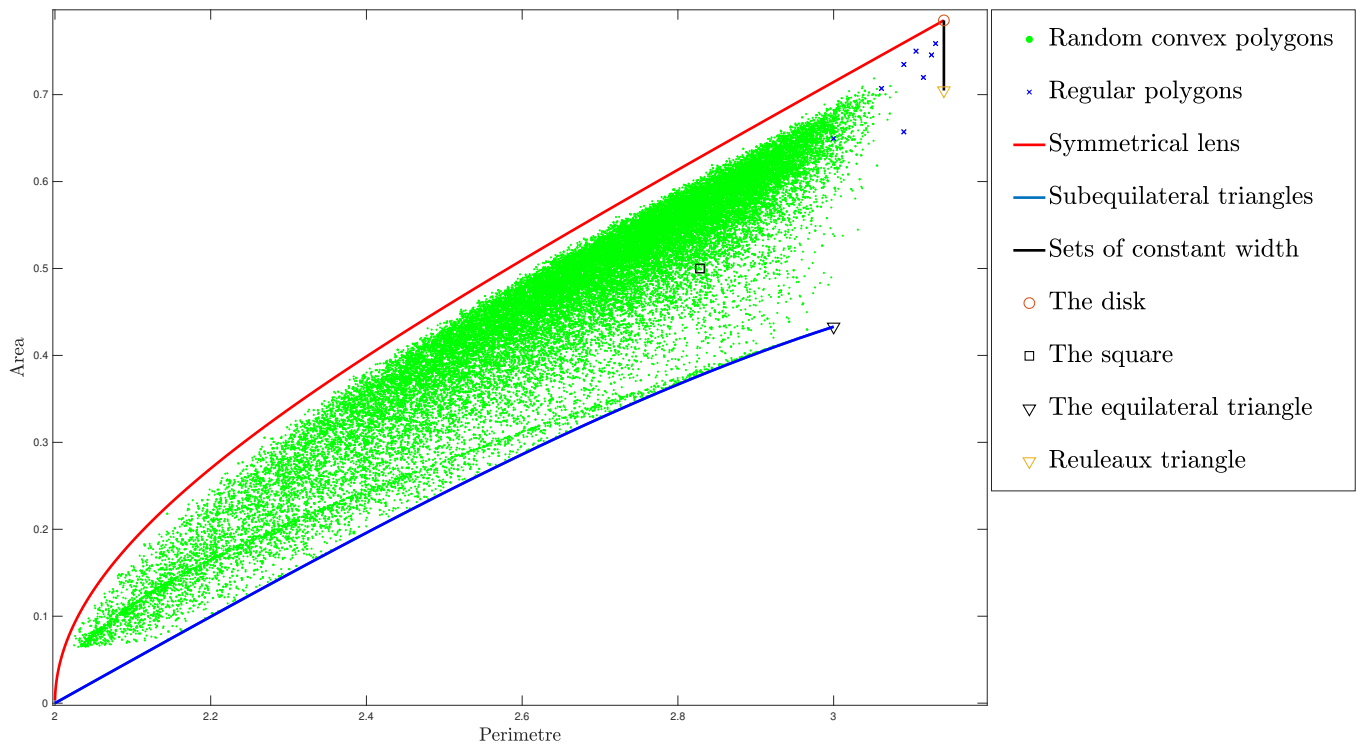

Figure 5.4: Approximation of $(P, |\cdot|, d)$-diagram via random convex sets and some relevant shapes.

Study of the extremal shapes

We use methods of Section 5.1, in order to obtain a numerical approximation of the missing boundary (which should be connecting the equilateral and Reuleaux triangles in Figure 5.4).

We numerically solve the following shape optimization problems:

$$\min \setminus \max\{|\Omega| \mid \Omega \in \mathcal{K}^2,\ P(\Omega) = p_0 \text{ and } d(\Omega) = 1\},$$

where $p_0 \in (3, \pi/4)$.

The parametrization via the Fourier coefficients of the support function (Section 5.1.1) allows to obtain quite satisfying results as we obtain symmetrical lenses (see Figure 5.5) as optimal shapes (which is in concordance with the result proved in [148]).

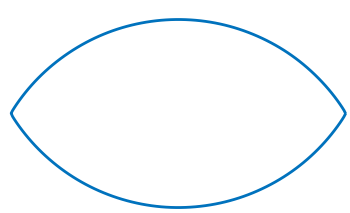

Figure 5.5: Symmetrical lens obtained as a solution of the problem $\max\{|\Omega| \mid \Omega \in \mathcal{K}^2,\ P(\Omega) = 2.4 \text{ and } d(\Omega) = 1\}$.

As for the lower boundary,to obtain good approximations, we combine the two methods of sections 5.1.1 and 5.1.3. We first use the parametrization via Fourier coefficients of the support function truncated at a certain order N to find first approximations of the extremal sets that will be used as initial shapes for the parametrization using radial function. We note that by this process we are able to obtain quite accurate description of the lower boundary, see Figure 5.10.

In a first time, as explained in section 5.1.1, problem 5.2.2 is reduced to the following finite dimensional minimization problem

$$\min_{(a_0,\dots,b_N)\in\mathbb{R}^{2N+1}} \left(\pi a_0^2 + \frac{\pi}{2}\sum_{k=1}^{N}(1-k^2)(a_k^2+b_k^2)\right),$$

with linear constraints on the Fourier coefficients:

- perimeter constraint: $2\pi a_0 = p_0$,
- and convexity constraint:

$$\begin{pmatrix} 1 & \alpha_{1,1} & \cdots & \alpha_{1,N} & \cdots & \beta_{1,1} & \cdots & \beta_{1,N} \\ \vdots & \vdots & \ddots & \vdots & \dots & \vdots & \ddots & \vdots \\ 1 & \alpha_{N,1} & \cdots & \alpha_{N,N} & \cdots & \beta_{N,1} & \cdots & \beta_{N,N} \end{pmatrix} \begin{pmatrix} a_0 \\ a_1 \\ \vdots \\ a_N \\ b_1 \\ \vdots \\ b_N \end{pmatrix} \geq \begin{pmatrix} 0 \\ \vdots \\ 0 \end{pmatrix}$$

  where $\alpha_{m,k} = (1-k^2)\cos k\theta_m$ and $\beta_{m,k} = (1-k^2)\sin k\theta_m$ for $(m,k) \in [\![1,M]\!] \times [\![1,N]\!]$, with M taken to be equal to 1000.

Before showing the obtained results, let us first analyse the accuracy of the present method (based the support function): we solve the latter optimization problem for different values of the parameter N in the case $p_0 = 3$ for which we know that the optimal shape is given by the equilateral triangle.

Here are the optimal shapes obtained for the choices of $N \in \{20, 40, 100, 140\}$:

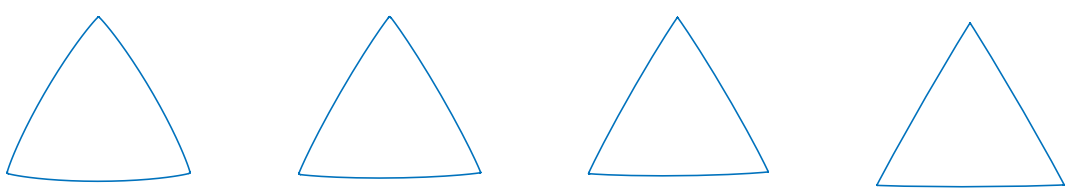

Figure 5.6: Obtained solutions for $p_0 = 3$ and $N \in \{20, 40, 100, 140\}$ (approximation of an equilateral triangle).

In the Figure 5.7, we plot the relative errors in function of the order of truncation N. It shows that the method based on the support function is not very relevant when the optimal shape is polygonal (which is frequent when imposing convexity constraint).

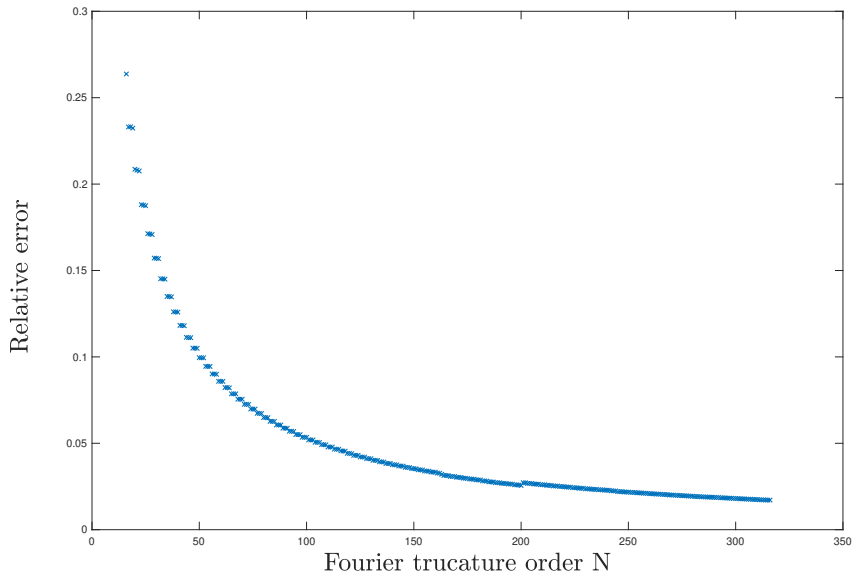

Figure 5.7: Relative errors in function of the truncation order N in the case $p_0 = 3$.

We then obtain (see Figure 5.8) an approximation of the missing lower boundary corresponding to domains obtained by considering 401 Fourier coefficients ($N = 200$).

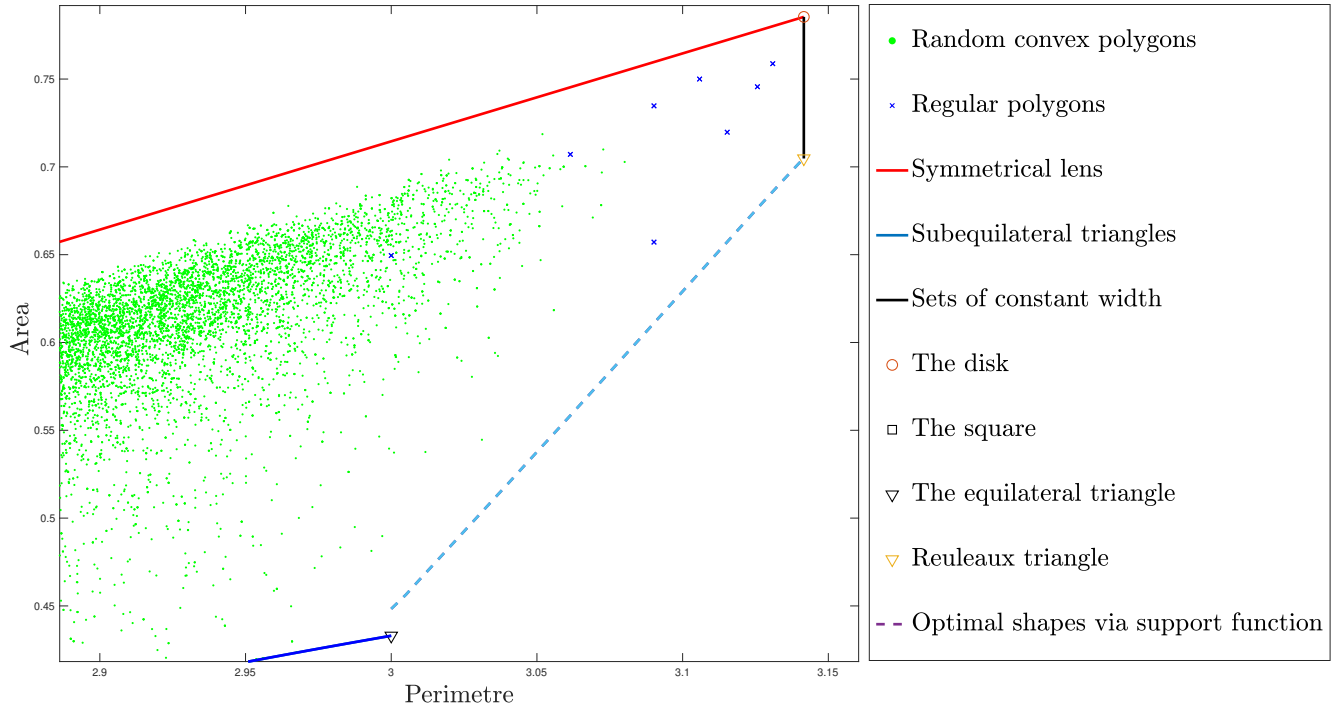

Figure 5.8: Approximation of the missing part of the lower boundary by optimizing the Fourier coefficients of the support function.

Finally, Figures 5.9 and 5.10 show how using the shapes obtained by the method of support function as initial points for the method via the radial function (section 5.1.3) allows to improve the description of the missing lower boundary

Method	Support function	Radial function
Obtained shape for $p_0 = 3.07$	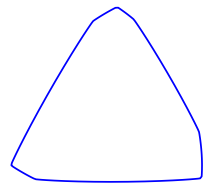	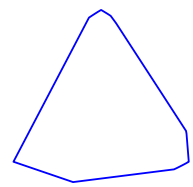
Corresponding area	0.5881	0.5687

Figure 5.9: The radial function parametrization allows to improve the result of the support function method.

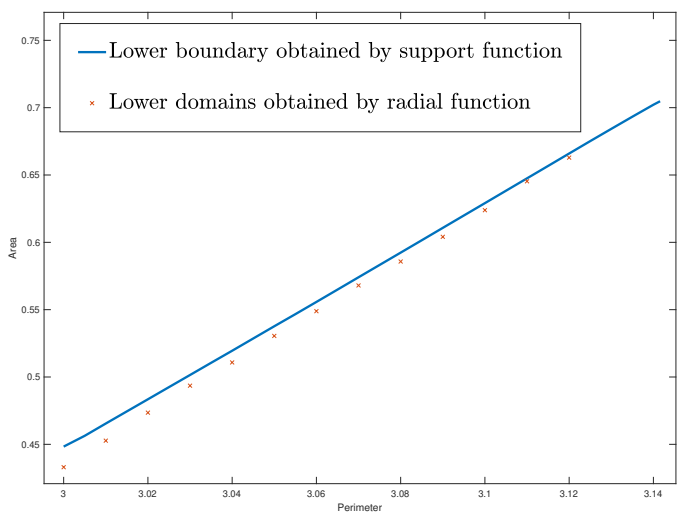

Figure 5.10: Improved description of the lower boundary by combining the two methods.

Extremal shapes and improved description of the diagram

At last, we provide some extremal shapes obtained for relevant values of p_0 in Figure 5.11 and improved description of the diagram $\mathcal{D}_1$ in Figure 5.12.

Problem	$p_0 = \pi$	$p_0 = 3.07$	$p_0 = 3$	$p_0 = 2.4$
Upper boundary	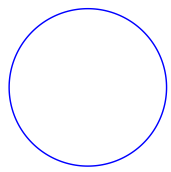	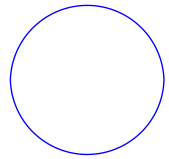	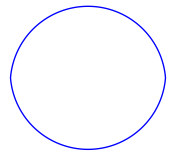	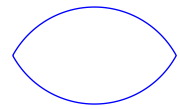
Lower boundary	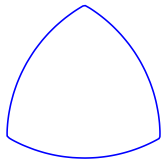	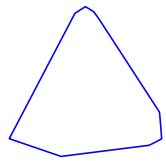	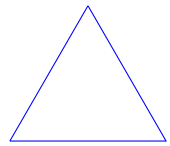	

Figure 5.11: Extremal shapes corresponding to different values of p_0.

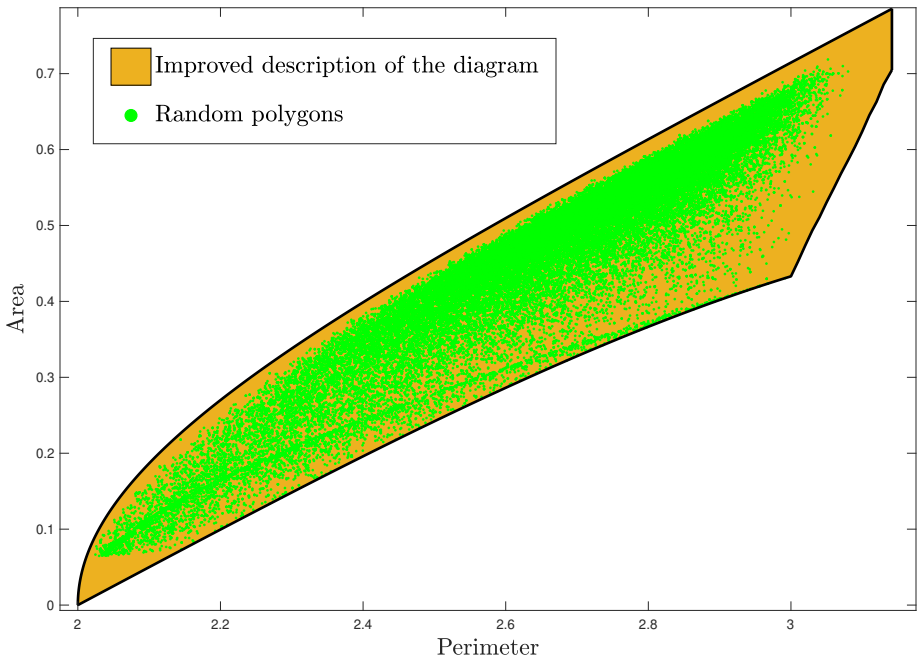

Figure 5.12: Improved description of the diagram of the triplet $(P, |\cdot|, d)$.

5.2.3 Diagram $(P, \lambda_1, |\cdot|)$

The diagram $(P, \lambda_1, |\cdot|)$ is theoretically studied in Chapter 3. We recall that the diagram is given by the set of points:

$$\mathcal{D}_2 := \{\big(P(\Omega), \lambda_1(\Omega)\big) \mid \Omega \in \mathcal{K}^2 \text{ and } |\Omega| = 1\}.$$

In a first time, we give an approximation of the diagram by generating 10^5 random convex polygons (as it was done before in [11]). We obtain the following Figure 5.13:

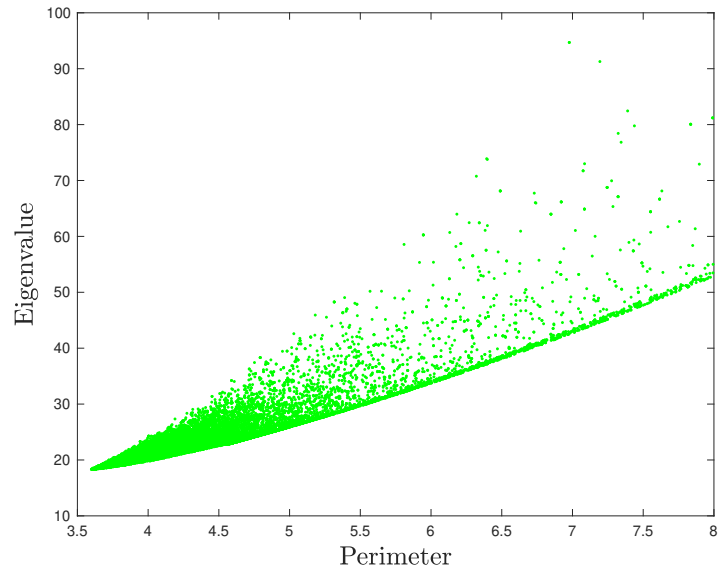

Figure 5.13: Approximation of the diagram via random convex polygons.

In order to give a more satisfying approximation of the diagram, we want to find the upper and lower domains and thus have a more accurate description of the boundary of the diagram. We are then led to (numerically) solve the following shape optimization problems:

$$\max \setminus \min\{\lambda_1(\Omega) \mid \Omega \in \mathcal{K}^2,\ P(\Omega) = p_0 \text{ and } |\Omega| = 1\},$$

It is shown in Theorem 11 of Chapter 3 that apart from the ball the domains that lay on the lower boundary are polygonal meanwhile the ones that lay on the upper boundary are smooth ($C^{1,1}$), we then apply **Method 4** (the one based on the coordinates of the vertices) for the lower boundary and the other methods for the upper one and obtain quite satisfying results. In Figure 5.14, we provide the obtained optimal shapes corresponding to some relevant values of p_0.

Problem	$p_0 = P(B) = 2\sqrt{\pi}$	$p_0 = 3.8$	$p_0 = 4$	$p_0 = 4.2$
Upper boundary	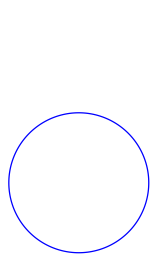	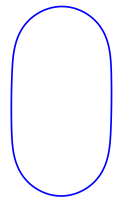	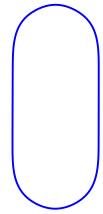	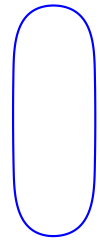
Lower boundary	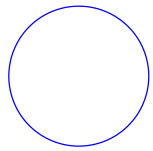	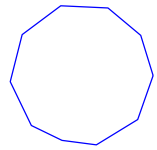	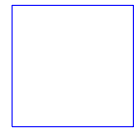	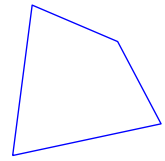

Figure 5.14: Numerically obtained optimal shapes corresponding to different values of p_0.

Finally, once the boundary is known, we use the vertical convexity of the diagram of Theorem 18 to provide an improved and quite optimal numerical description of the diagram, see Figure 5.15.

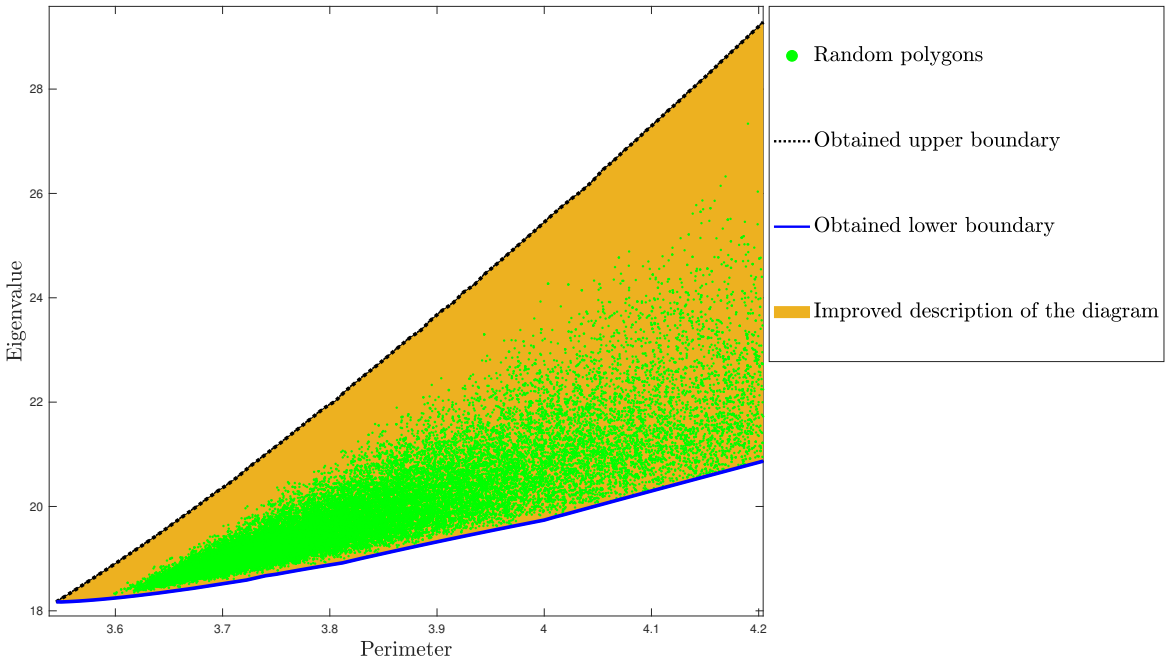

Figure 5.15: Optimal description of the diagram $(P, \lambda_1, |\cdot|)$.

5.2.4 Diagram $(d, \lambda_1, |\cdot|)$

Let us now consider the diagram relating the diameter, the first Dirichlet eigenvalue and the area. We are interested in the following set of points:

$$\mathcal{D}_3 := \{\big(d(\Omega), \lambda_1(\Omega)\big) \mid \Omega \in \mathcal{K}^2 \text{ and } |\Omega| = 1\}.$$

In a first time, let us give an approximation of the diagram by generating 10^5 random convex polygons. We obtain the following Figure 5.16:

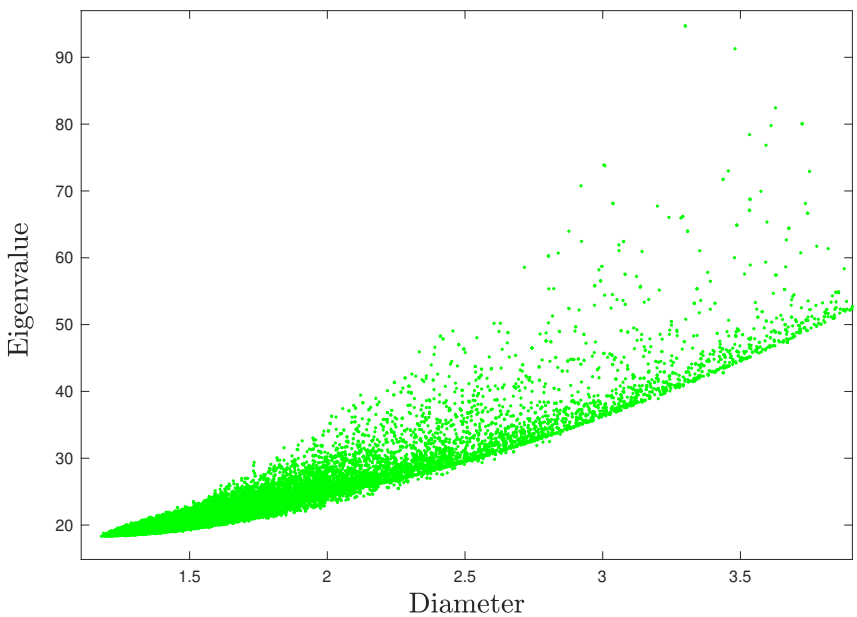

Figure 5.16: Approximation of the $(d, \lambda_1, |\cdot|)$-diagram via 10^5 random convex polygons.

Here also, by the vertical convexity of the diagram given in Theorem 18, to obtain an improved description of the diagram we numerically describe the upper and lower boundaries of the diagram $\mathcal{D}_3$, which means that we solve the following shape optimization problems:

$$\max \setminus \min\{\lambda_1(\Omega) \mid \Omega \in \mathcal{K}^2,\ d(\Omega) = d_0 \text{ and } |\Omega| = 1\},$$

where $d_0 \in [2/\sqrt{\pi}, +\infty)$.

For **the lower boundary**, both the methods of parametrization via the Fourier coefficients of the support function (see Section 5.1.1) and via the discretized radial function (see Section 5.1.3) provide satisfying results and suggest that the optimal sets are symmetrical 2-cap bodies, that are given by the the convex hulls of a ball and two points symmetric with respect its center (see Figure 5.17).

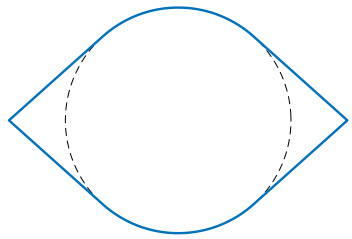

Figure 5.17: Obtained symmetrical 2-cap body.

On the other hand, **the upper domains** are quite surprising, since we (numerically) observe the existence of a threshold d^*, such that the solutions for $d > d^*$ seem to be given by symmetric spherical slices, that are domains defined as the intersection of a disk with a strip of width smaller that the disk's radius and centered at its center, see Figure 5.18, meanwhile, when $d < d^*$, the optimal domains seem to be given by some kind of smoothed regular nonagons, see Figure 5.18.

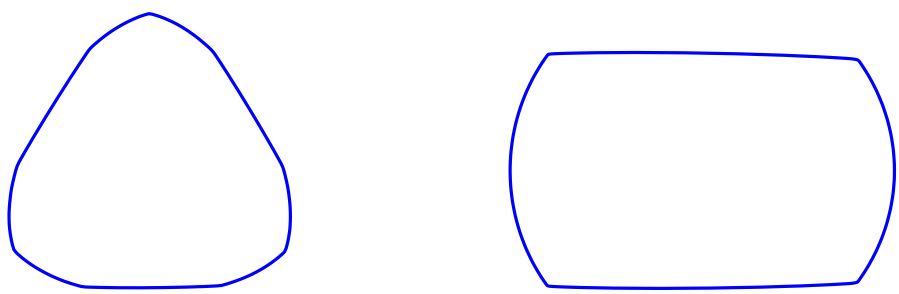

Figure 5.18: Obtained upper shapes corresponding to $d_0 = 1.18$ for the smoothed nonagon and to $d_0 = 1.33$ for the symmetric slice, we used the parametrization via the Fourier coefficients of the support function with 161 coefficient ($N = 80$).

At a first sight, it may be surprising that the optimal shapes do not "continuously" vary in terms of the involved parameters, but, we should note that this phenomena has recently been observed in [71], where the authors provide the complete description of the $(d, r, |\cdot|)$-diagram involving the diameter, the inradius and the area; they prove that the one of the boundaries is given by smoothed nonagos and symmetrical slices meanwhile the other one is given by symmetrical 2-cap bodies. This leads us to investigate these families of shapes that also seem to be extremal shapes for our $(d, \lambda_1, |\cdot|)$-diagram (see Figure 5.19) and also for the $(d, h, |\cdot|)$-diagram discussed in Section 1.5.1 of the introduction. This similarities may be explained by the fact that $1/r$ corresponds to the first eigenvalue of the infinity-Laplacian operator Δ_∞ which may be defined as the limit when $p \to +\infty$ of the pLaplacian operator (see [21] and references therein), meanwhile, λ_1 and h respectively correspond to the first eigenvalues of the 2 and 1 Laplace operators, see [121] for more details.

At last, by the vertical convexity of the diagram stated in Theorem 18, we are able to provide an improved description of the $(d, \lambda_1, |\cdot|)$-diagram.

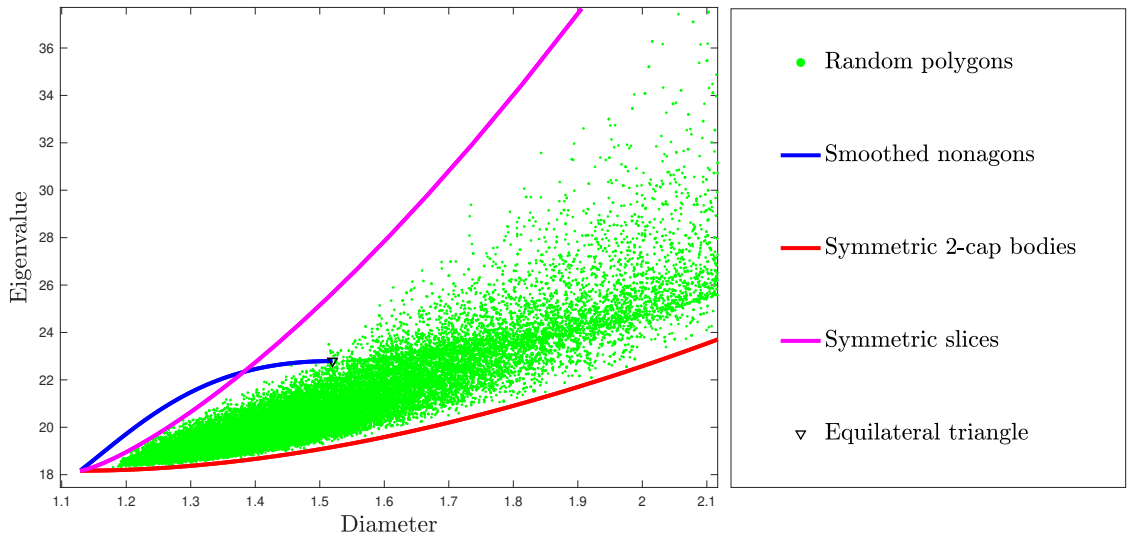

Figure 5.19: The diagram $(d, \lambda_1, |\cdot|)$ with expected extremal sets.

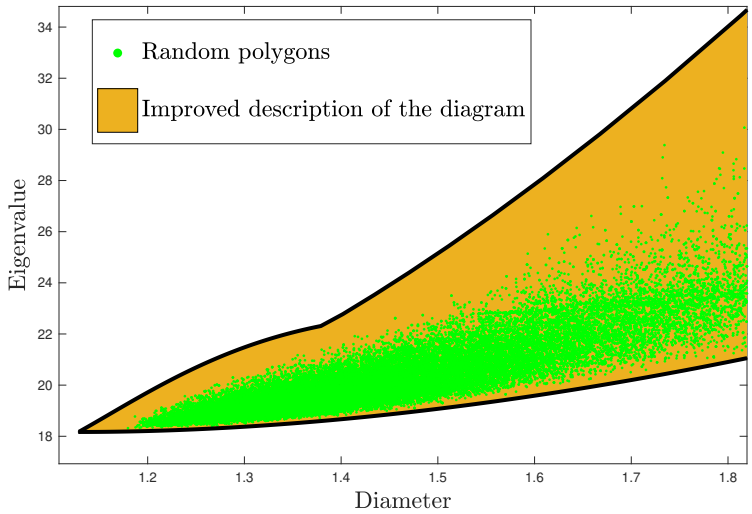

Figure 5.20: An improved description of the diagram $(d, \lambda_1, |\cdot|)$.

5.2.5 Conclusion and comments

In the present chapter, we presented 4 different parametrizations that allow to solve shape optimization problems under convexity constraint. We presented the best shapes we managed to obtain, but it would be very interesting to perform a more deep and quantitative comparison between the methods: this will be the main purpose of the work in progress [89]. At this point, let us summarize the qualitative observations made when testing each method on the several problems presented above.

Situation	Fourier coefficients of the support function	Fourier coefficients of the gauge function	Discretized radial function	Coordinates of the vertices
The optimal shape is a polygon.	We obtain approximations that are not very accurate.	We obtain approximations that are not very accurate.	Provide good approximations in some cases if the initial point is judiciously chosen	Provide very good results when the number of vertices is not very large.
The optimal shape has flat parts but is smooth	Provide acceptable results when the number of Fourier coefficients is large enough.	Provide very good results even when the number of Fourier coefficients is small.	May provide good results, but sometimes the convexity is lost during the optimization process.	We did not succeed to obtain results as the sides always overlap after few iterations.
The optimal shape is strictly convex.	We obtain very good results.	We obtain good results especially when the shape do not have corners.	We obtain good results when the convexity is preserved during the optimization process (but less accurate than the first method).	We did not succeed to obtain results as the sides always overlap after few iterations.
Handling the diameter constraint	This method is very adapted as this constraint corresponds to linear inequalities on the Fourier coefficients.	This method is not very adapted, because in contrast to the support function, there is no immediate formula relating the Fourier coefficients of the gauge function to the diameter.	We obtain good results when convexity is not lost during the optimization process and when the initial shape is judiciously chosen.	We obtain good results when the number of vertices is not very large.

5.3 Appendix 1: Some useful shape derivatives

We consider a smooth vector field $V \in C^1(\mathbb{R}^n, \mathbb{R}^n)$. We compute the first order directional shape derivative of the diameter in Section 5.3.1 and the Cheeger constant in Section 5.3.2 (we provide a slight improved version of [153, Theorem 1.1]).

5.3.1 First order shape derivative of the diameter

In this section, we compute the shape derivative of the diameter functional, which we recall to be defined as follows:

$$d : \Omega \subset \mathbb{R}^n \longmapsto d(\Omega) = \sup_{(x,y)\in\Omega^2} |x-y|,$$

where Ω is a compact subset of $\mathbb{R}^n$.

Theorem 19. *The diameter functional d admits a directional shape derivative in the direction V, we have:*

$$\begin{aligned}
\exists (x_\infty, y_\infty) \in \Omega^2, \quad d'(\Omega, V) &= \lim_{t\to 0^+} \frac{d(\Omega_t) - d(\Omega)}{t} \\
&= \sup\left\{ \left\langle \frac{x-y}{|x-y|}, V(x) - V(y) \right\rangle \;\middle|\; x, y \in \Omega, \text{ such that } |x-y| = d(\Omega) \right\} \\
&= \left\langle \frac{x_\infty - y_\infty}{|x_\infty - y_\infty|}, V(x_\infty) - V(y_\infty) \right\rangle,
\end{aligned}$$

where $\Omega_t := (I + tV)(\Omega)$, where $I : x \in \mathbb{R}^n \longmapsto x \in \mathbb{R}^n$ is the identity map.

Proof. We want to prove the existence and compute the limit $\lim\limits_{t\to 0^+} \frac{d(\Omega_t)-d(\Omega)}{t}$.

For every $t \geq 0$ Ω_t is compact: indeed, it is the image of the compact Ω by the continuous map $I + tV$). Thus since $d : (x, y) \in \mathbb{R}^n \times \mathbb{R}^n \to |x - y|$ is continuous, it is bounded from above and there exists $(x_t, y_t) \in \Omega$ such that $d(\Omega_t) = |(I + tV)(x_t) - (I + tV)(y_t)|$. In what follows, we denote $(x, y) := (x_0, y_0)$.

We use (x_t, y_t) (resp. (x, y)) as test points to majorate (resp. minorate) $d(\Omega_t) - d(\Omega)$:

$$|(I + tV)(x) - (I + tV)(y)| - |x - y| \leq d(\Omega_t) - d(\Omega) \leq |(I + tV)(x_t) - (I + tV)(y_t)| - |x_t - y_t|$$

Let us begin by the lower estimate. We have:

$$\begin{aligned}
d(\Omega_t) - d(\Omega) &\geq |(I + tV)(x) - (I + tV)(y)| - |x - y| \\
&= |x + tV(x) - y - tV(y)| - |x - y| \\
&= \Big|(x - y) + t\Big(V(x) - V(y)\Big)\Big| - |x - y| \\
&= \sqrt{\Big|(x - y) + t\Big(V(x) - V(y)\Big)\Big|^2} - |x - y| \\
&= \sqrt{|x - y|^2 + 2t\,\langle x - y, V(x) - V(y)\rangle + o(t)} - |x - y| \\
&= |x - y|\sqrt{1 + 2t\left\langle \frac{x-y}{|x-y|}, \frac{V(x)-V(y)}{|x-y|} \right\rangle + o(t)} - |x - y| \\
&= |x - y|\left(1 + t\left\langle \frac{x-y}{|x-y|}, \frac{V(x)-V(y)}{|x-y|} \right\rangle + o(t)\right) - |x - y| \\
&= t\left\langle \frac{x-y}{|x-y|}, V(x) - V(y) \right\rangle + o(t).
\end{aligned}$$

Thus:

$$\liminf_{t\to 0^+} \frac{d(\Omega_t)-d(\Omega)}{t} \geq \sup\left\{ \left\langle \frac{x-y}{|x-y|}, V(x)-V(y) \right\rangle \mid x,y\in\Omega \text{ such that } |x-y|=d(\Omega)\right\}.$$

Let us now consider the upper estimate. Let $\Big((x_{t_n},y_{t_n})\Big)_n$ a subsequence of $\Big((x_t,y_t)\Big)_t$ such that $t_n\to 0$ and $\lim\limits_{n\to\infty}\frac{d(\Omega_{t_n})-d(\Omega)}{t_n} = \limsup\limits_{t\to 0^+}\frac{d(\Omega_t)-d(\Omega)}{t}$. By Bolzano-Weirstrass Theorem, we assume without loss of generality that there exists $(x_\infty,y_\infty)\in\Omega^2$ such that the sequence $\Big((x_{t_n},y_{t_n})\Big)_n$ converges to (x_∞,y_∞).

We have $|x_\infty-y_\infty|=d(\Omega)$. Indeed:

$$\forall (v,w)\in\Omega^2,\quad |(I+t_nV)(x_{t_n})-(I+t_nV)(y_{t_n})|\geq |(I+t_nV)(v)-(I+t_nV)(w)|,$$

which is equivalent to

$$\forall (v,w)\in\Omega^2,\quad |x_{t_n}-y_{t_n}+t_n.V(x_{t_n})-t_n.V(y_{t_n})|\geq |v-w+t_n.V(v)-t_n.V(w)|.$$

Finally:

$$\begin{aligned}
d(\Omega_{t_n})-d(\Omega) &\leq |(I+tV)(x_{t_n})-(I+tV)(y_{t_n})|-|x_{t_n}-y_{t_n}| \\
&= |x_{t_n}+t_n.V(x_{t_n})-y_{t_n}-t_nV(y_{t_n})|-|x_{t_n}-y_{t_n}| \\
&= \Big|(x_{t_n}-y_{t_n})+t_n.\Big(V(x_{t_n})-V(y_{t_n})\Big)\Big|-|x_{t_n}-y_{t_n}| \\
&= \sqrt{\Big|(x_{t_n}-y_{t_n})+t_n.\Big(V(x_{t_n})-V(y_{t_n})\Big)\Big|^2}-|x_{t_n}-y_{t_n}| \\
&= \sqrt{\Big|x_{t_n}-y_{t_n}\Big|^2+2t_n\Big\langle x_{t_n}-y_{t_n},V(x_{t_n})-V(y_{t_n})\Big\rangle+o(t_n)}-|x_{t_n}-y_{t_n}| \\
&= |x_{t_n}-y_{t_n}|.\sqrt{1+2t_n\left\langle \frac{x_{t_n}-y_{t_n}}{|x_{t_n}-y_{t_n}|},\frac{V(x_{t_n})-V(y_{t_n})}{|x_{t_n}-y_{t_n}|}\right\rangle+o(t_n)}-|x_{t_n}-y_{t_n}| \\
&= |x_{t_n}-y_{t_n}|.\sqrt{1+2t_n\left(\left\langle \frac{x_\infty-y_\infty}{|x_\infty-y_\infty|},\frac{V(x_\infty)-V(y_\infty)}{|x_\infty-y_\infty|}\right\rangle+o(1)\right)+o(t_n)}-|x_{t_n}-y_{t_n}| \\
&= |x_{t_n}-y_{t_n}|.\sqrt{1+2t_n\left\langle \frac{x_\infty-y_\infty}{|x_\infty-y_\infty|},\frac{V(x_\infty)-V(y_\infty)}{|x_\infty-y_\infty|}\right\rangle+o(t_n)}-|x_{t_n}-y_{t_n}| \\
&= |x_{t_n}-y_{t_n}|.\left(1+t_n\left\langle \frac{x_\infty-y_\infty}{|x_\infty-y_\infty|},\frac{V(x_\infty)-V(y_\infty)}{|x_\infty-y_\infty|}\right\rangle+o(t_n)\right)-|x_{t_n}-y_{t_n}| \\
&= t_n\left\langle \frac{x_\infty-y_\infty}{|x_\infty-y_\infty|},V(x_\infty)-V(y_\infty)\right\rangle+o(t_n)
\end{aligned}$$

Thus:

$$\limsup_{t\to 0^+}\frac{d(\Omega_t)-d(\Omega)}{t}\leq \left\langle \frac{x_\infty-y_\infty}{|x_\infty-y_\infty|},V(x_\infty)-V(y_\infty)\right\rangle$$

By combining the lim inf and lim sup inequalities, we obtain:

$$\begin{aligned}
\liminf_{t\to 0^+} \frac{d(\Omega_t)-d(\Omega)}{t} &\geq \sup\left\{\left\langle \frac{x-y}{|x-y|}, V(x)-V(y)\right\rangle \mid x,y\in\Omega\ ,\ \text{tels que } |x-y|=d(\Omega)\right\}\\
&\geq \left\langle \frac{x_\infty-y_\infty}{|x_\infty-y_\infty|}, V(x_\infty)-V(y_\infty)\right\rangle\\
&\geq \limsup_{t\to 0^+} \frac{d(\Omega_t)-d(\Omega)}{t}\\
&\geq \liminf_{t\to 0^+} \frac{d(\Omega_t)-d(\Omega)}{t}
\end{aligned}$$

Finally, we deduce that the diameter admits a directional shape derivative in the direction V and:

$$\begin{aligned}
\exists (x_\infty,y_\infty)\in\Omega^2,\quad \lim_{t\to 0^+} \frac{d(\Omega_t)-d(\Omega)}{t} &= \sup\left\{\left\langle \frac{x-y}{|x-y|}, V(x)-V(y)\right\rangle \,\Big|\, x,y\in\Omega,\ \text{tel que } |x-y|=d(\Omega)\right\}\\
&= \left\langle \frac{x_\infty-y_\infty}{|x_\infty-y_\infty|}, V(x_\infty)-V(y_\infty)\right\rangle
\end{aligned}$$

□

5.3.2 First order shape derivative of the Cheeger constant

In this section, Ω is a bounded open un ouvert subset of $\mathbb{R}^n$ with Lipschitz boundary. for every $t\geq 0$, we denote $\Omega_t=(I+tV)(\Omega)$ and $h_t:=h(\Omega_t)$ and $g: t\longmapsto h_t$.

We recall that the Cheeger constant of a Lipschitz set Ω can be defined by:

$$h(\Omega):=\inf_{u\in BV(\Omega)\setminus\{0\}} \frac{|Du|(\mathbb{R}^n)}{||u||_1},$$

where $BV(\Omega)$ is the space of functions of bounded variations on Ω and

$$|Du|(\Omega):=\sup\left\{\int_\Omega u\mathrm{div}\varphi \Big| \varphi\in C_c^1(\Omega;\mathbb{R}^n),\ ||\varphi||_\infty\leq 1\right\}$$

is the total variation in Ω of the function $u\in L^1(\Omega)$.

In order to prove the differentiability of g in 0, the authors of [153] assume the uniqueness of the Cheeger set of Ω, they give a counterexample where differentiability fails when the Cheeger set is non-unique (in which case one has $g'(0^+)\neq g'(0^-)$). Nevertheless, they do not study the "directional" differentiability of the function g in 0^+ (or 0^-). In the following Theorem 20, we provide a slightly improved version of [153, Theorem 1.1] where we prove the directional differentiability of g (in 0^+) without assuming the uniqueness of the Cheeger set of Ω.

Theorem 20. *([153, Theorem 1] revisited)*
The shape derivative

$$h'(\Omega,V):=\lim_{t\to 0^+}\frac{h(\Omega_t)-h(\Omega)}{t}$$

exists and there exists $u_0\in X(0):=\{u\in BV(\Omega)\mid \|u\|_1=1\ h(\Omega)=|Du|(\mathbb{R}^n)\}$, *such that:*

$$\begin{aligned}
h'(\Omega,V) &= \int_{\mathbb{R}^n}\Big(divV-\langle\sigma,DV\sigma\rangle\Big)d|Du_0| - h\int_\Omega u_0.divV\\
&= \inf_{u\in X(0)}\left(\int_{\mathbb{R}^n}\Big(divV-\langle\sigma,DV\sigma\rangle\Big)d|Du| - h\int_\Omega u.divV\right)
\end{aligned}$$

Proof. We recall that any measure μ can be decomposed as $\mu = \sigma|\mu|$, where σ is a measurable function such as $|\sigma(x)| = 1$ almost everywhere, this is known as the polar decomposition of the measure μ.

Continuity of g in 0:

Let $u \in BV(\Omega)$ a positive eigenfunction (for the 1-Laplace operator (see [121]) associated to the Cheeger constant $h(\Omega)$ such that $\|u\|_1 := \int_\Omega |u|dx = 1$. We use the function $w_t = u \circ G_t \in BV(\Omega_t)$ as a test function in the variational definition of $h(\Omega_t)$ and use a change of variable formula for functions of bounded variations (see [98, Lemma 10.1]):

$$h_t \leq \frac{|Dw_t|(\mathbb{R}^n)}{\int_{\Omega_t} w_t} = \frac{\int_{\mathbb{R}^n} |DG_t^T((I+tV)(y))\sigma|.|detD(I+tV)(y)|d|Du|}{\int_\Omega u(y)|detD(I+tV)(y)|dy} = (1+o(1))\frac{|Du|(\mathbb{R}^n)}{\int_\Omega u},$$

thus:

$$\limsup_{t\to 0} h_t \leq h.$$

Now, let $u_t \in BV(\Omega)$ a positive function such that $\|u_t\|_1 = 1$ and $|Du_t|(\mathbb{R}^\ltimes) = h_t$. We take $v_t = u_t \circ (I+tV) \in BV(\Omega)$, we have:

$$\begin{aligned}|Dv_t|(\mathbb{R}^n) &= \int_{\mathbb{R}^n} \Big|D(I+tV)^T\Big(G_t(x)\Big)\sigma\Big|.|detDG_t(x)|d|Dv_t| \\ &= h_t + o(1) \\ &\leq h + o(1),\end{aligned}$$

thus:

$$\limsup_{t\to 0} h_t \leq h$$

and

$$\int_\Omega v_t(x)dx = \int_{\Omega_t} u_t|detD(I+tV)^{-1}|dx = 1 + o(1)$$

Le sequence $(v_t)_{t>0}$ is bounded in $BV(\mathbb{R}^n)$ and every v_t is vanishing outside Ω, thus, one can extract a subsequence (v_{t_n}) such that there exists a function $v \in BV(\mathbb{R}^n)$ satisfying $v_{t_n} \underset{n\to+\infty}{\longrightarrow} v$ in $L^1_{loc}(\mathbb{R}^n)$. Up to an extraction, we can assume that $v_{t_n} \underset{n\to+\infty}{\longrightarrow} v$ almost everywhere on $\mathbb{R}^n$.

We have $v = 0$ in $\mathbb{R}^n \backslash \Omega$, moreover:

$$\int_\Omega v(y)dy = \lim_{n\to+\infty} \int_\Omega v_{t_n}(y)dy = 1,$$

thus by semicontinuity:

$$h \leq |Dv|(\mathbb{R}^n) \leq \liminf_{n\to\infty} |Dv_{t_n}|(\mathbb{R}^n) \leq \limsup_{t\to 0} |Dv_t|(\mathbb{R}^n) \leq h$$

On the other hand, we have:

$$\liminf_{t\to 0} |Dv_t|(\mathbb{R}^n) = \liminf_{t\to 0} \frac{|Dv_t|(\mathbb{R}^n)}{\int_\Omega v_t}.\int_\Omega v_t = \liminf_{t\to 0} \frac{|Dv_t|(\mathbb{R}^n)}{\int_\Omega v_t}.(1+o(1)) \geq h$$

thus:

$$\lim_{t\to 0} |Dv_t|(\mathbb{R}^n) = h.$$

(Because: $|Dv_t|(\mathbb{R}^n) = h_t + \underset{t\to 0}{o}(1)$).

We finally conclude that $g : t \longmapsto h_t$ is continuous in 0 and $v \in BV(\Omega)$ is an eigenfunction corresponding to the eigenvalue $h(\Omega)$.

Differentiability of g in 0^+:

Upper estimate:
By taking $w_t = u \circ G_t$ as a test function in the variational characterization of $h(\Omega_t)$, we have:

$$h_t - h \leq \frac{|Dw_t|(\mathbb{R}^n)}{\int_{\Omega_t} w_t} = \frac{\int_{\mathbb{R}^n} |DG_t^T((I+tV)(y))|.|detD(I+tV)(y)|d|Du|}{\int_\Omega u(y)|detD(I+tV)(y)|dy} - h \tag{5.2}$$

We have:

$$|detD(I+tV)(y)| = 1 + t.\mathrm{div}V(y) + o(t) \quad \text{(uniformly in } y\text{)}, \tag{5.3}$$

and:

$$\begin{aligned}
\left|\Big[DG_t\Big((I+tV)(y)\Big)\Big]^T.\sigma(y)\right| &= \left|\Big[DG_t\Big(y+t.V(y)\Big)\Big]^T.\sigma(y)\right| \\
&= \left|\Big[I_n - t.DV\Big(y+t.V(y)\Big)^T + o(t).I_n\Big].\sigma(y)\right| \\
&= \Big|\sigma(y) - t.DV(y)^T.\sigma(y) + o(t)\Big| \\
&= \sqrt{\Big|\sigma(y) - t.DV(y)^T.\sigma(y) + o(t)\Big|^2} \\
&= \sqrt{|\sigma(y)|^2 - 2t\Big\langle \sigma(y), DV(y)\sigma(y)\Big\rangle + o(t)} \\
&= 1 - t\Big\langle \sigma(y), DV(y)\sigma(y)\Big\rangle + o(t) \quad \text{(uniformly in } y\text{)}.
\end{aligned}$$

We then deduce that inequality (5.2) becomes:

$$\begin{aligned}
h_t - h &\leq \frac{h + \int_{\mathbb{R}^n}(\mathrm{div}V - \langle\sigma, DV\sigma\rangle)d|Du| + o(t)}{1 + t\int_\Omega u.\mathrm{div}V + o(t)} - h \\
&= \frac{t\Big(\int_{\mathbb{R}^n}(\mathrm{div}V - \langle\sigma, DV\sigma\rangle)d|Du| - h\int_\Omega u.\mathrm{div}V + o(1)\Big)}{1 + t\int_\Omega u.\mathrm{div}V + o(t)}.
\end{aligned}$$

Since this estimate holds for any $u \in X(0)$, we write:

$$\forall u \in X(0), \quad \frac{h_t - h}{t} \leq \frac{\int_{\mathbb{R}^n}(\mathrm{div}V - \langle\sigma, DV\sigma\rangle)d|Du| - h\int_\Omega u.\mathrm{div}V + o(1)}{1 + t\int_\Omega u.\mathrm{div}V + o(t)}$$

Thus:

$$\forall u \in X(0), \quad \limsup_{t\to 0^+} \frac{h_t - h}{t} \leq \int_{\mathbb{R}^n}[\mathrm{div}V - \langle\sigma, DV\sigma\rangle]d|Du| - h\int_\Omega u.\mathrm{div}V$$

Finally:

$$\limsup_{t\to 0^+} \frac{h_t - h}{t} \leq \inf_{u\in X(0)}\left(\int_{\mathbb{R}^n}[\mathrm{div}V - \langle\sigma, DV\sigma\rangle]d|Du| - h\int_\Omega u.\mathrm{div}V\right) \tag{5.4}$$

We consider a subsequence (t_n) of elements of $\mathbb{R}^+$ which decreases to 0, such as:

$$\lim_{n\to+\infty} \frac{h_{t_n} - h}{t_n} = \liminf_{n\to+\infty} \frac{h_t - h}{t} \in \mathbb{R} \cup \{-\infty\}.$$

Le computations performed above for the continuity show that up to extracting a subsequence, we can assume that (v_{t_n}) converges to $u \in BV(\Omega) \cap X(0)$:

$$\lim_{n\to\infty} |Dv_{t_n}|(\mathbb{R}^n) = |Du|(\mathbb{R}^n)$$

Thus by [7, Proposition 3.13]:

$$\forall \phi \in C_c(\mathbb{R}^n), \qquad \int_{\mathbb{R}^n} \phi.d|Dv_t| = \int_{\mathbb{R}^n} \phi.d|Du| \tag{5.5}$$

<u>Lower estimate:</u>

Now, we use v_{t_n} as a test function for $h(\Omega)$:

$$h_{t_n} - h = \int_{\mathbb{R}^n} d|Du_{t_n}| - h \geq \int_{\mathbb{R}^n} \Big|\Big((DG_{t_n}) \circ (I + t_n V)\Big)^T \sigma_{t_n}\Big|.|\det D(I + t_n V)| d|Dv_{t_n}| - \frac{\int_{\mathbb{R}^n} d|Dv_{t_n}|}{\int_\Omega v_{t_n}}$$

where σ_{t_n} is taken such that: $Du_{t_n} = \sigma_{t_n}|Du_{t_n}|$.

Similarly to the case above, we have:

$$h_{t_n} - h \geq \int_{\mathbb{R}^n} d|Dv_{t_n}| + t_n \int_{\mathbb{R}^n} [\mathrm{div}V - \langle \sigma_{t_n}, DV\sigma\rangle] d|Dv_{t_n}| - \frac{\int_{\mathbb{R}^n} d|Dv_{t_n}|}{\int_\Omega v_{t_n}} + o(t_n).$$

We observe that:

$$\int_\Omega v_{t_n} = 1 - \int_{\mathbb{R}^n} u_{t_n}.\mathrm{div}V + o(t_n) = 1 - t_n \int_{\mathbb{R}^n} u.\mathrm{div}V + o(t),$$

thus, by using the fact that $|Dv_{t_n}|(\mathbb{R}^n) = h + o(1)$, we obtain:

$$\begin{aligned} \frac{\int_{\mathbb{R}^n} d|Dv_{t_n}|}{\int_\Omega v_{t_n}} &= \int_{\mathbb{R}^n} d|Dv_{t_n}| + t_n \Big(\int_{\mathbb{R}^n} d|Dv_{t_n}|\Big)\Big(\int_\Omega u.\mathrm{div}V\Big) + o(t_n) \\ &= \int_{\mathbb{R}^n} d|Dv_{t_n}| + t_n h \int_\Omega u.\mathrm{div}V + o(t_n). \end{aligned}$$

Thus:

$$h_{t_n} - h \geq t_n \Big(\int_{\mathbb{R}^n} (\mathrm{div}V - \langle \sigma_{t_n}, DV\sigma_{t_n}\rangle) d|Dv_{t_n}| - h \int_\Omega u.\mathrm{div}V\Big).$$

By (5.5) (we took $\phi = \mathrm{div}V \in C_c(\mathbb{R}^n)$), we have:

$$\int_{\mathbb{R}^n} \mathrm{div}V \; d|Dv_{t_n}| = \int_{\mathbb{R}^n} \mathrm{div}V \; d|Du| + o(1).$$

By Reshetnyak's Theorem (cf.[7, Théorème 2.39]), we have:

$$\int_{\mathbb{R}^n} \langle \sigma_{t_n}, DV\sigma_{t_n}\rangle) d|Dv_{t_n}| \underset{n\to\infty}{\longrightarrow} \int_{\mathbb{R}^n} \langle \sigma, DV\sigma\rangle) d|Du|.$$

Finally:

$$\begin{aligned} \exists u_0 \in X(0), \quad \liminf_{t\to 0^+} \frac{h_t - h}{t} &= \lim_{n\to\infty} \frac{h_{t_n} - h}{t_n} \\ &\geq \int_{\mathbb{R}^n} \Big(\mathrm{div}V - \langle \sigma, DV\sigma\rangle\Big) d|Du| - h \int_\Omega u.\mathrm{div}V. \end{aligned}$$

Thus:

$$\exists u_0 \in X(0), \quad \liminf_{t\to 0^+} \frac{h_t - h}{t} \geq \inf_{u\in X(0)} \left(\int_{\mathbb{R}^n} \Big(\mathrm{div}V - \langle \sigma, DV\sigma\rangle\Big) d|Du| - h \int_\Omega u.\mathrm{div}V\right) \tag{5.6}$$

At last, by (5.4) and (5.6) we deduce that $g : t \longmapsto h_t$ is differentiable in 0^+ and:

$$\begin{aligned} \exists u_0 \in X(0), \quad h'(0^+) &= \int_{\mathbb{R}^n} \Big(\mathrm{div}V - \langle \sigma, DV\sigma\rangle\Big) d|Du_0| - h \int_\Omega u_0.\mathrm{div}V \\ &= \inf_{u\in X(0)} \left(\int_{\mathbb{R}^n} \Big(\mathrm{div}V - \langle \sigma, DV\sigma\rangle\Big) d|Du| - h \int_\Omega u.\mathrm{div}V\right), \end{aligned}$$

which ends the proof.

□

5.4 Appendix 2: Validation of Parini's conjecture [152]

To validate Parini's conjecture that states that the square minimizes the functional $J_2 : \Omega \longmapsto \frac{\lambda_1(\Omega)}{h(\Omega)^2}$, we randomly generated 10^5 convex polygons (whose numbers of sides are randomly chosen between 3 and 30) and computed their Cheeger constants (by using the code found in [30]) and their first Dirichlet eigenvalues (by Matlab's PDEtool). We did not succeed to find a shape that is better than the square. This can be observed in a Blaschke-Santaló diagram: let us consider the one involving the Cheeger constant, the first Dirichlet eigenvalue and the area:

$$\mathcal{D} := \big\{ \big(h(\Omega), \lambda_1(\Omega) \mid \Omega \in \mathcal{K}^2 \text{ and } |\Omega| = 1\big) \big\}.$$

The conjecture $J_2(\Omega) \geq J_2\big((0,1)^2\big)$ is then equivalent to the inclusion:

$$\mathcal{D} \subset \big\{ (x,y) \mid y \geq J_2\big((0,1)^2\big) \times x^2 \big\},$$

which is observed in Figure 5.21.

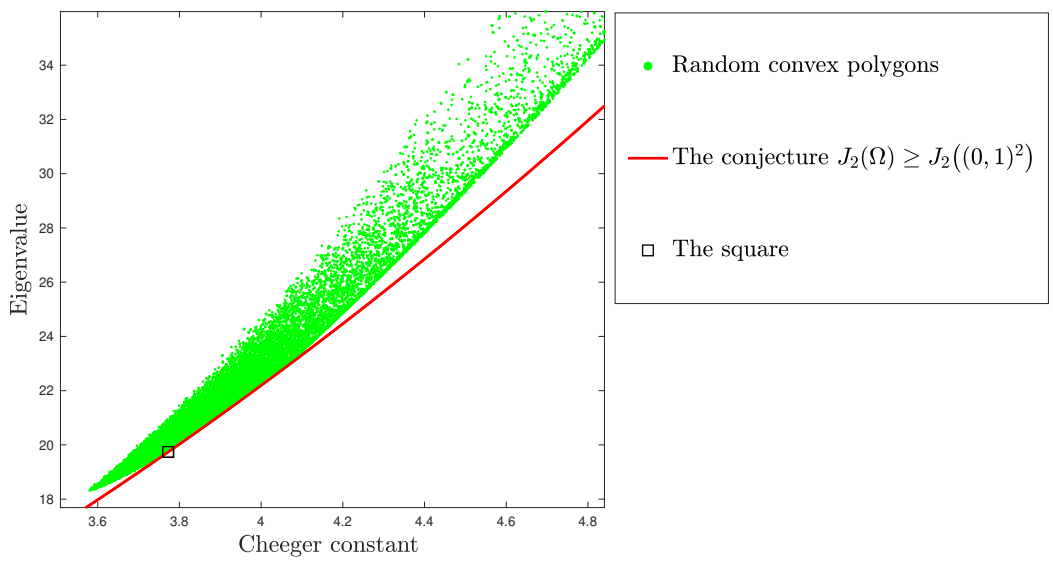

Figure 5.21: Validation of Parini's conjecture.

Part II

Optimal placement of an obstacle

Chapter 6

Where to place a spherical obstacle so as to maximize the first Steklov eigenvalue ?

This chapter is a reprint of the submitted paper ***Where to place a spherical obstacle so as to maximize the first Steklov eigenvalue ?*** *[91].*

Abstract

We prove that among all doubly connected domains of $\mathbb{R}^n$ of the form $B_1 \backslash \overline{B_2}$, where B_1 and B_2 are open balls of fixed radii such that $\overline{B_2} \subset B_1$, the first non-trivial Steklov eigenvalue achieves its maximal value uniquely when the balls are concentric. Furthermore, we show that the ideas of our proof also apply to a mixed boundary conditions eigenvalue problem found in literature.

6.1 Introduction

6.1.1 Optimization of the Steklov eigenvalue

Let $\Omega \subset \mathbb{R}^n$, be a bounded, open set with Lipschitz boundary. In this paper we consider the following Steklov eigenvalue problem for the Laplace operator:

$$\begin{cases} \Delta u = 0 & \text{in } \Omega, \\ \frac{\partial u}{\partial n} = \sigma u & \text{on } \partial\Omega, \end{cases} \tag{6.1}$$

where $\partial u / \partial n$ is the outer normal derivative of u on $\partial\Omega$. It is well-know that the Steklov spectrum is discrete as long as the trace operator $H^1(\Omega) \to L^2(\partial\Omega)$ is compact, which is the case when the domain has Lipschitz boundary; in other words, in our framework the values of σ for which the problem (6.1) admits non-trivial solutions form an increasing sequence of eigenvalues $0 = \sigma_0(\Omega) < \sigma_1(\Omega) \leq \sigma_2(\Omega) \leq \cdots \nearrow +\infty$, known as the Steklov spectrum of Ω.

We are interested in the first non-trivial Steklov eigenvalue, which can be given by a Rayleigh quotient:

$$\sigma_1(\Omega) = \inf \left\{ \frac{\int_\Omega |\nabla u|^2 dx}{\int_{\partial\Omega} u^2 d\sigma} \;\middle|\; u \in H^1(\Omega) \backslash \{0\} \text{ such that } \int_{\partial\Omega} u d\sigma = 0 \right\},$$

where the infimum is attained for the corresponding eigenfunctions.

Among classical questions in spectral geometry, there are the problems of minimizing (or maximizing) the Laplace eigenvalues with various boundary conditions and different geometrical and topological constraints. The constraint of volume has been extensively studied in the last years. For example there is the celebrated Faber-Krahn inequality [78, 126], which states that the ball minimizes the first eigenvalue of the Laplacian with Dirichlet boundary condition among domains of fixed volume. There is a similar result for the maximization of the first non-trivial eigenvalue of the Laplacian with Neumann boundary known as the Szego-Weinberger inequality [169, 174]. For the Steklov problem, Brock proved in [46] that the first non-trivial eigenvalue of a lipschitz domain is less than the eigenvalue of the ball with the same volume.

The perimeter constraint is very interesting to study, especially in the case of Steklov eigenvalues. One early result is due to Weinstock [175], who used conformal mapping techniques to prove the following inequality for simply connected planar sets:

$$P(\Omega)\sigma_1(\Omega) \leq P(B)\sigma_1(B),$$

where $P(\Omega)$ stands for the perimeter of Ω and B a unit ball.

Recently, A. Fraser and R. Schoen proved in [83] that the ball does not maximize the first nonzero Steklov eigenvalue among all contractible domains of fixed boundary measure in $\mathbb{R}^n$ for $n \geq 3$. The proof was inspired from the following formula for the annulus:

$$P(B\backslash\varepsilon B)^{\frac{1}{n-1}}\sigma_1(B\backslash\varepsilon B) = P(B)^{\frac{1}{n-1}}\sigma_1(B) + \frac{1}{n-1}\varepsilon^{n-1} + o(\varepsilon^{n-1}) > P(B)^{\frac{1}{n-1}}\sigma_1(B),$$

where $\varepsilon B = \{\varepsilon x \mid x \in B\}$.

Note that by studying the variations of the function $\varepsilon \in [0,1] \longmapsto P(B\backslash\varepsilon B)^{\frac{1}{n-1}}\sigma_1(B\backslash\varepsilon B)$ one can prove that there exists a unique $\varepsilon_n \in (0,1)$ such that:

$$\forall \varepsilon \in [0,1), \qquad P(B\backslash\varepsilon B)^{\frac{1}{n-1}}\sigma_1(B\backslash\varepsilon B) \leq P(B\backslash\varepsilon_n B)^{\frac{1}{n-1}}\sigma_1(B\backslash\varepsilon_n B)$$

This motivates to look at the problem of maximizing σ_1 among domains with holes and wondering if the spherical shell $B\backslash\varepsilon_n B$ maximizes σ_1 under perimeter constraint among some class of perforated domains, for example the doubly connected ones. Not long ago, L. R. Quinones used shape derivatives to prove that the annulus $B\backslash\varepsilon_2 B$ is a critical shape of the first non-trivial Steklov eigenvalue among planar doubly connected domains with fixed perimeter (see [159]).

At last, we mention that in contrast with the result in [83], it was recently proven in [51] that the Weinstock inequality is true in higher dimensions in the case of convex sets. Namely, the authors show that for every bounded convex set $\Omega \subset \mathbb{R}^n$ one has:

$$P(\Omega)^{\frac{1}{n-1}}\sigma_1(\Omega) \leq P(B)^{\frac{1}{n-1}}\sigma_1(B).$$

A natural question arises: can we remove the topological constraints (convexity or simple connectedness in the plane) as for the Laplacian eigenvalues with other boundary conditions ? Does there exist a domain which maximizes σ_1 under perimeter constraint ? If not can we determine the supremum of σ_1 on Lipschitz open sets ? In fact, all these questions are still open and the techniques used to deal with other eigenvalues problems don't apply for Steklov framework, this pushes to seek new methods and makes the problem very challenging.

6.1.2 Perforated domains: state of the art

The optimization of the placement of obstacles has interested many authors in the last decades. We briefly point out some classical and recent works in the topic.

Some early results, due to Payne and Weinberger [154] on the one hand and Hersch [114] on the other, are that for some extremum eigenvalue problems with mixed boundary conditions a certain

annulus is the optimal set among multi-connected planar domains, i.e. whose boundary admits more than one component (see also [18]). The main ideas consist in constructing judicious test functions by using the notion of web-functions (see [60] for more details on web functions). These ideas were very recently used and adapted for other similar problems (see [10, 150]). A classical family of obstacle problems that attracted a lot of attention was to find the best emplacement of a spherical hole inside a ball that optimizes the value of a given spectral functional (see [16], section (9)). An early result in this direction is that the first Dirichlet eigenvalue is maximal when the spherical obstacle is in the center of the larger ball. The proof is based on shape derivatives (see [106, Theorem 2.5.1]) and on a reflection and domain monotonicity arguments, followed by the use of the boundary maximum principle. These arguments have been applied in greater generality by many authors: in [160] Ramm and Shivakumar proved this result in dimension 2, in [123] Kesavan gave a generalization to higher dimensions and showed a similar result for the Dirichlet energy, then Harrell, Kröger, and Kurata managed in [105] to replace the exterior ball by a convex set which is symetric with respect to a given hyperplane. In the same spirit, El Soufi and Kiwan proved in [75] that the second Dirichlet eigenvalue is also maximal when the balls are concentric. Furthermore, many authors considered mixed boundary conditions problems, for instance in [2], while studying the internal stabilizability for a reaction–diffusion problem modeling a predator–prey system, the authors are led to consider an obstacle shape optimization problem for the first laplacian eigenvalue with mixed Dirichlet-Neumann boundary conditions. Another interesting work in the same direction is due to Bonder, Groisman and Rossi, who studied the so called Sobolev trace inequality (see [27, 76]), thus they were interested in the optimization of the first nontrivial eigenvalue of an elliptic operator with mixed Steklov-Dirichlet boundary conditions among perforated domains: the existence and regularity of an optimal hole are proved in [80, 81], and by using shape derivatives it is shown that annulus is a critical but not an optimum shape (see [80]). At last, we point out the recent paper [172], where the author considers the first eigenvalue of the Laplace operator with mixed Steklov-Dirichlet boundary conditions.

Many examples stated in the last paragraph deal with linear operators eigenvalues in the special case of doubly connected domains with spherical outer and inner boundaries. The question we are treating in this paper belongs to this family of problems. Yet, it is also natural to seek for generalizations and the literature is quite rich of works treating more general cases: for results on linear operators with more general shapes of the domain and the obstacle in the euclidean case we refer to [73, 74, 96, 109, 125], on the other hand, many results for manifolds were obtained by Anisa and Aithal [8] in the setting of space-forms (complete simply connected Riemannian manifolds of constant sectional curvature), by Anisa and Vemuri [57] in the setting of rank 1 symmetric spaces of non-compact type and by Aithal and Raut [3] in the case of punctured regular polygons in two dimensional space forms. As for the case of non-linear operators we refer to the interesting progress made for the p-Laplace operator (see [9, 56]).

6.1.3 Results of the paper

In this paper, we are interested in finding the optimal placement of a spherical obstacle in a given ball so that the first non-trivial Steklov eigenvalue is maximal.

Our main result is stated as follows:

Theorem 21. *Among all doubly connected domains of $\mathbb{R}^n$ $(n \geq 2)$ of the form $B_1 \backslash \overline{B_2}$, where B_1 and B_2 are open balls of fixed radii such that $\overline{B_2} \subset B_1$, the first non-trivial Steklov eigenvalue achieves its maximal value uniquely when the balls are concentric.*

In [172], the authors consider a mixed Steklov-Dirichlet eigenvalue problem. They prove that the first non-trivial eigenvalue is maximal when the balls are concentric in dimensions larger or equal than 3 (cf. Theorem 1 [172]) and remark that the planar case remains open (cf. Remark 2). We show that the ideas developed in this paper allow us to give an alternative and simpler proof of Theorem 1 [172]. Then we extend this result to the planar case.

Theorem 22. *Among all doubly connected domains of $\mathbb{R}^n$ $(n \geq 2)$ of the form $B_1 \backslash \overline{B_2}$, where B_1 and B_2 are open balls of fixed radii such that $\overline{B_2} \subset B_1$, the first non-trivial eigenvalue of the problem*

$$\begin{cases} \Delta u = 0 & \text{in } B_1 \backslash \overline{B_2}, \\ u = 0 & \text{on } \partial B_2, \\ \frac{\partial u}{\partial n} = \tau u & \text{on } \partial B_1, \end{cases}$$

achieves its maximal value uniquely when the balls are concentric.

This paper is organized in 3 parts. First, we give the proof of Theorem 21. Then we use the ideas developed in section 6.2 to give a new proof of [172, Theorem 1] and tackle the planar case which was up to our knowledge still open. Finally, the Appendix is devoted to the computation of the Steklov eigenvalues and eigenfunctions of the spherical shell and the determination of the first non-trivial Steklov eigenvalue (Theorem 23) via a monotonicity result (Lemma 11).

6.2 Proof of Theorem 21

By invariance with respect to rotations and translations and scaling properties of σ_1, we can reformulate the problem as follows:

We assume that the obstacle B_2 is the open ball of radius $a \in (0,1)$ centred at the origin 0 and $B_1 = y_d + B$, where B is the unit ball centred in 0, $y_d := (0, ..., 0, d) \in \mathbb{R}^n$ and $d \in [0, 1-a)$. What is the value of d such that $\sigma_1(B_1 \backslash \overline{B_2})$ is maximal ?

For every $d \in [0, 1-a)$, we denote $\Omega_d := (y_d + B) \backslash aB$ (see Figure 6.1).

It is sufficient to prove that:

$$\forall d \in (0, 1-a), \qquad \sigma_1(\Omega_0) > \sigma_1(\Omega_d).$$

The proof is based on the following Proposition:

Proposition 18. *There exists a function $f_n \in H^1(\mathbb{R}^n \backslash \overline{B_2})$ satisfying:*

1. *f_n is an eigenfunction associated to $\sigma_1(\Omega_0)$ and can be used as a test function in the variational definition of $\sigma_1(\Omega_d)$.*

2. *$\int_{\Omega_d} |\nabla f_n|^2 dx \leq \int_{\Omega_0} |\nabla f_n|^2 dx$, with equality if and only if $d = 0$.*

3. *$\int_{\partial\Omega_d} f_n^2 d\sigma \geq \int_{\partial\Omega_0} f_n^2 d\sigma$, with equality if and only if $d = 0$.*

Using Proposition 18, we conclude as follows:

$$\forall d \in (0, 1-d), \qquad \sigma_1(\Omega_d) \leq \frac{\int_{\Omega_d} |\nabla f_n|^2 dx}{\int_{\partial\Omega_d} f_n^2 d\sigma} < \frac{\int_{\Omega_0} |\nabla f_n|^2 dx}{\int_{\partial\Omega_0} f_n^2 d\sigma} = \sigma_1(\Omega_0).$$

This proves Theorem 21.

6.2.1 Proof of the first assertion of Proposition 18

The first eigenvalue of the spherical shell Ω_0 is computed in Theorem 23. It is also proven that its multiplicity is equal to n and the corresponding eigenfunctions are:

$$\begin{array}{rccc} u_n^i & : & \mathbb{R}^n & \longrightarrow & \mathbb{R} \\ & & x = (x_1, \cdots, x_n) & \longmapsto & x_i \left(1 + \frac{\mu_{\sigma,n}}{|x|^n}\right) \end{array}$$

Where $i \in [\![1, n]\!]$ and $\mu_{\sigma,n} = \frac{1-\sigma_1(\Omega_0)}{n+\sigma_1(\Omega_0)-1}$.

Take $i \in [\![1, n-1]\!]$. Since Ω_d is symmetrical to the hyperplane $\{x_i = 0\}$, we have:

$$\begin{aligned}
\int_{\partial\Omega_d} u_n^i d\sigma &= \int_{\partial\Omega_d \cap \{x_i \geq 0\}} u_n^i d\sigma + \int_{\partial\Omega_d \cap \{x_i \leq 0\}} u_n^i d\sigma, \\
&= \int_{\partial\Omega_d \cap \{x_i \geq 0\}} u_n^i d\sigma - \int_{\partial\Omega_d \cap \{x_i \geq 0\}} u_n^i d\sigma \qquad (\text{because } u_n^i(x_1, \cdots, -x_i, \cdots, x_n) = -u_n^i(x_1, \cdots, x_i, \cdots, x_n)) \\
&= 0.
\end{aligned}$$

Thus, every eigenfunction u_n^i (where $i \in [\![1, n-1]\!]$) can be taken as a test function in the variational definition of $\sigma_1(\Omega_d)$ (note that this is not the case for u_n^n). This proves the first assertion of Proposition 18.

6.2.2 Spherical coordinates and preliminary computations

Since the shapes considered are described by spheres, it is more convenient to work with the spherical coordinates instead of the Cartesian ones.

We set:

$$\begin{cases}
x_1 = r \sin\theta_1 \sin\theta_1 \ldots \sin\theta_{n-2} \sin\theta_{n-1} \\
x_2 = r \sin\theta_1 \sin\theta_1 \ldots \sin\theta_{n-2} \cos\theta_{n-1} \\
\qquad \vdots \\
x_{n-1} = r \sin\theta_1 \cos\theta_2 \\
x_n = r \cos\theta_1
\end{cases}$$

where $(r, \theta_1, \cdots, \theta_{n-1}) \in \mathbb{R}^+ \times [0, \pi] \times ... \times [0, \pi] \times [0, 2\pi]$.

Since, every eigenfunction u_n^i (where $i \in [\![1, n-1]\!]$) can be used as a test function in the variational definition of $\sigma_1(\Omega_d)$, we chose to take $f_n = u_n^{n-1}$ (see Remark 14).

Using spherical coordinates, we write:

$$\begin{array}{rcccc}
f_2 & : & \mathbb{R}_+ \times [0, 2\pi] & \longrightarrow & \mathbb{R} \\
 & & (r, \theta_1) & \longmapsto & \sin\theta_1 \left(r + \frac{\mu_{\sigma,n}}{r}\right),
\end{array}$$

and for $n \geq 3$:

$$\begin{array}{rcccc}
f_n & : & \mathbb{R}_+ \times [0, \pi] \times \cdots \times [0, \pi] \times [0, 2\pi] & \longrightarrow & \mathbb{R} \\
 & & (r, \theta_1, \cdots, \theta_{n-1}) & \longmapsto & \sin\theta_1 \cos\theta_2 \left(r + \frac{\mu_{\sigma,n}}{r^{n-1}}\right)
\end{array}$$

Remark 14. *The choice of the test function $f_n = u_n^{n-1}$ between all u_n^i ($i \in [\![1, n-1]\!]$) is motivated by the will to have less variables to deal with while computing the gradient (see section 6.2.3). Nevertheless, one should note that all these functions satisfy the three assertions of Proposition 18.*

The following Figure 6.2.2 shows the perforated domains Ω_0 and Ω_d, the angle θ_1 and the radius $R_d(\theta_1)$ which plays an important role in the upcoming computations.

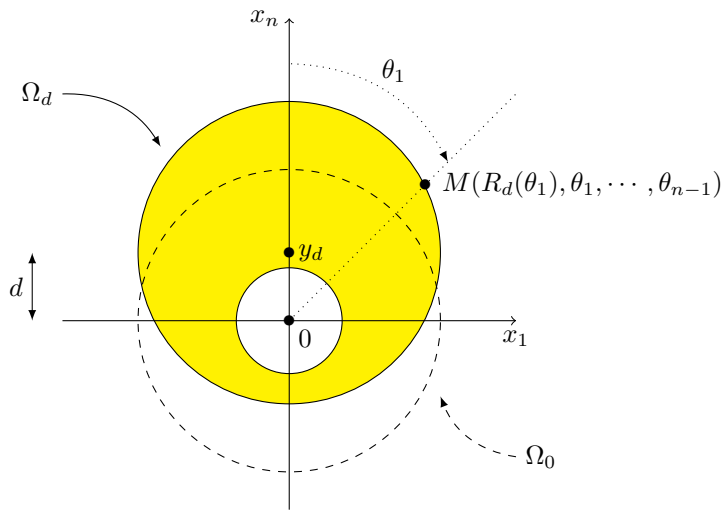

Figure 6.1: The domains Ω_d and Ω_0

Let $M \in \partial(y_d + B)$, by using Al-Kashi's formula on the triangle $0y_dM$, we have:

$$1^2 = d^2 + R_d^2(\theta_1) - 2dR_d(\theta_1)\cos\theta_1$$

By solving the equation of second degree satisfied by $R_d(\theta_1)$ we get two roots $d\cos\theta_1 \pm \sqrt{1 - d^2\sin^2\theta_1}$. The lower one being negative due to the fact that $d \in [0, 1)$, we deduce that:

$$R_d(\theta_1) = d\cos\theta_1 + \sqrt{1 - d^2\sin^2\theta_1}.$$

We compute the first derivative of R_d, which appears in the area element when integrating on $\partial\Omega_d$ (more precisely on $\partial(y_d + B)$).

$$R_d'(\theta_1) = -d\sin\theta_1 - \frac{d^2\sin\theta_1\cos\theta_1}{\sqrt{1 - d^2\sin^2\theta_1}} = -\frac{d\sin\theta_1}{\sqrt{1 - d^2\sin^2\theta_1}} \times \left(d\cos\theta_1 + \sqrt{1 - d^2\sin^2\theta_1}\right).$$

With straightforward computations, we get the important equalities:

$$\sqrt{R_d^2(\theta_1) + {R_d'}^2(\theta_1)} = 1 + \frac{d\ddot{o}\cos\theta_1}{\sqrt{1 - d^2\sin^2\theta_1}} = \frac{R_d(\theta_1)}{\sqrt{1 - d^2\sin^2\theta_1}}. \tag{6.2}$$

6.2.3 Proof of the second assertion of Proposition 18

We compute the gradient of f_n in the spherical coordinates and calculate the L^2-norm of its gradient on Ω_d.

For $n = 2$, we have:

$$\nabla f_2(r, \theta_1) = \begin{bmatrix} \frac{\partial f}{\partial r} \\ \frac{1}{r}\frac{\partial f}{\partial \theta_1} \end{bmatrix} = \begin{bmatrix} \sin\theta_1\left(1 - \frac{\mu_{\sigma,n}}{r^2}\right) \\ \cos\theta_1\left(1 + \frac{\mu_{\sigma,n}}{r^2}\right) \end{bmatrix}$$

then:

$$\begin{aligned}
\int_{\Omega_d} |\nabla f_2|^2 dx &= \int_{\theta_1=0}^{2\pi} \int_{r=a}^{R_d(\theta_1)} \left[\sin^2\theta_1 \left(1 - \frac{\mu_{\sigma,2}}{r^2}\right)^2 + \sin^2\theta_1 \left(1 - \frac{\mu_{\sigma,2}}{r^2}\right)^2 \right] r dr d\theta_1, \\
&= \int_{\theta_1=0}^{2\pi} \int_{r=a}^{R_d(\theta_1)} \left[r + 2\mu_{\sigma,2} \left(\cos^2\theta_1 - \sin^2\theta_1\right) \frac{1}{r} + \frac{\mu_{\sigma,2}}{r^3} \right] dr d\theta_1, \\
&= \int_{\theta_1=0}^{2\pi} \left(\frac{R_d^2(\theta_1) - a^2}{2} - 2\mu_{\sigma,2} \left(\cos^2\theta_1 - \sin^2\theta_1\right) \ln R_d(\theta_1) - \frac{\mu_{\sigma,2}^2}{2} \times \left(\frac{1}{R_d^2(\theta_1)} - \frac{1}{a^2} \right) \right) d\theta_1
\end{aligned}$$

In the same spirit, for $n \geq 3$, we have:

$$\nabla f_n(r, \theta_1, ..., \theta_{n-1}) = \begin{bmatrix} \frac{\partial f}{\partial r} \\ \frac{1}{r} \frac{\partial f}{\partial \theta_1} \\ \frac{1}{r \sin\theta_1} \frac{\partial f}{\partial \theta_2} \\ \frac{1}{r \sin\theta_1 \sin\theta_2} \frac{\partial f}{\partial \theta_3} \\ \vdots \\ \frac{1}{r \sin\theta_1 ... \sin\theta_{n-2}} \frac{\partial f}{\partial \theta_{n-1}} \end{bmatrix} = \begin{bmatrix} \sin\theta_1 \cos\theta_2 \left(1 - \frac{(n-1)\mu_{\sigma,n}}{r^n}\right) \\ \cos\theta_1 \cos\theta_2 \left(1 + \frac{\mu_{\sigma,n}}{r^n}\right) \\ -\sin\theta_2 \left(1 + \frac{\mu_{\sigma,n}}{r^n}\right) \\ 0 \\ \vdots \\ 0 \end{bmatrix}$$

For $p \in \mathbb{N}$, we introduce $I_p := \int_0^\pi \sin^p t dt$, which is the double of the classical Wallis integral. These integrals satisfy the essential recursive property:

$$\forall p \in \mathbb{N}, \qquad I_{p+2} = \frac{p+1}{p+2} I_p. \tag{6.3}$$

We compute:

$$\begin{aligned}
A_1^n(d) &= \int_{\partial B_d} [\nabla f_n]_1^2 dx \\
&= 2 \int_{\theta_1=0}^{\pi} ... \int_{\theta_{n-1}=0}^{\pi} \int_{r=a}^{R_d(\theta_1)} \sin^2\theta_1 \cos^2\theta_2 \left(1 - \frac{(n-1)\mu_{\sigma,n}}{r^n}\right)^2 r^{n-1} \times \prod_{i=1}^{n-2} \sin^{n-1-i}\theta_i dr d\theta_1 ... d\theta_{n-1} \\
&= 2 \left(\prod_{k=0}^{n-4} I_k \right) \int_{\theta_2=0}^{\pi} \cos^2\theta_2 \sin^{n-3}\theta_2 d\theta_2 \int_{\theta_1=0}^{\pi} \sin^n\theta_1 \int_{r=a}^{R_d(\theta_1)} \left(r^{n-1} - \frac{2(n-1)\mu_{\sigma,n}}{r} + \frac{(n-1)^2\mu_{\sigma,n}^2}{r^{n+1}} \right) dr d\theta_1 \\
&= 2 \left(\prod_{k=0}^{n-4} I_k \right) (I_{n-3} - I_{n-1}) \times \\
&\int_{\theta_1=0}^{\pi} \sin^n\theta_1 \left(\frac{R_d^n(\theta_1) - a^n}{n} - 2(n-1)\mu_{\sigma,n} \ln\left(\frac{R_d(\theta_1)}{a}\right) - \frac{(n-1)^2\mu_{\sigma,n}^2}{n} \times \left(\frac{1}{R_d^n(\theta_1)} - \frac{1}{a^n} \right) \right) d\theta_1 \\
&= \frac{2}{n-1} \left(\prod_{k=0}^{n-3} I_k \right) \times \\
&\int_{\theta_1=0}^{\pi} \sin^n\theta_1 \left(\frac{R_d^n(\theta_1) - a^n}{n} - 2(n-1)\mu_{\sigma,n} \ln\left(\frac{R_d(\theta_1)}{a}\right) - \frac{(n-1)^2\mu_{\sigma,n}^2}{n} \times \left(\frac{1}{R_d^n(\theta_1)} - \frac{1}{a^n} \right) \right) d\theta_1,
\end{aligned}$$

where we used (6.3) for the last equality.

$$
\begin{aligned}
A_2^n(d) &= \int_{\partial B_d} [\nabla f_n]_2^2 dx, \\
&= 2\left(\prod_{k=0}^{n-4} I_k\right)(I_{n-3} - I_{n-1})\times \\
&\int_{\theta_1=0}^{\pi} \cos^2\theta_1 \sin^{n-2}\theta_1 \left(\frac{R_d^n(\theta_1) - a^n}{n} + 2\mu_{\sigma,n}\ln\left(\frac{R_d(\theta_1)}{a}\right) - \frac{\mu_{\sigma,n}^2}{n}\times\left(\frac{1}{R_d^n(\theta_1)} - \frac{1}{a^n}\right)\right) d\theta_1, \\
&= \frac{2}{n-1}\left(\prod_{k=0}^{n-3} I_k\right)\times \\
&\int_{\theta_1=0}^{\pi} (\sin^{n-2}\theta_1 - \sin^n\theta_1)\left(\frac{R_d^n(\theta_1) - a^n}{n} + 2\mu_{\sigma,n}\ln\left(\frac{R_d(\theta_1)}{a}\right) - \frac{\mu_{\sigma,n}^2}{n}\times\left(\frac{1}{R_d^n(\theta_1)} - \frac{1}{a^n}\right)\right) d\theta_1,
\end{aligned}
$$

then:

$$
\begin{aligned}
A_3^n(d) &= \int_{\partial B_d} [\nabla f_n]_3^2 dx \\
&= 2\left(\prod_{k=0}^{n-4} I_k\right) I_{n-1}\times \\
&\int_{\theta_1=0}^{\pi} \sin^{n-2}\theta_1 \left(\frac{R_d^n(\theta_1) - a^n}{n} + 2\mu_{\sigma,n}\ln\left(\frac{R_d(\theta_1)}{a}\right) - \frac{\mu_{\sigma,n}^2}{n}\times\left(\frac{1}{R_d^n(\theta_1)} - \frac{1}{a^n}\right)\right) d\theta_1, \\
&= \frac{2(n-2)}{n-1}\left(\prod_{k=0}^{n-3} I_k\right)\times \\
&\int_{\theta_1=0}^{\pi} \sin^{n-2}\theta_1 \left(\frac{R_d^n(\theta_1) - a^n}{n} + 2\mu_{\sigma,n}\ln\left(\frac{R_d(\theta_1)}{a}\right) - \frac{\mu_{\sigma,n}^2}{n}\times\left(\frac{1}{R_d^n(\theta_1)} - \frac{1}{a^n}\right)\right) d\theta_1.
\end{aligned}
$$

We decompose the integral in three parts:

$$
\int_{\Omega_d} |\nabla f|^2 dx = A_1^n(d) + A_2^n(d) + A_3^n(d) = \frac{2}{n-1}\left(\prod_{k=0}^{n-3} I_k\right)\left((n-1)W_1^n(d) + 2\mu_{\sigma,n}W_2^n(d) - \frac{\mu_{\sigma,n}^2}{n}W_3^n(d)\right), \tag{6.4}
$$

where:

$$
\begin{cases}
W_1^n(d) = \int_0^\pi \sin^{n-2}\theta_1 \big(R_d^n(\theta_1) - a^n\big) d\theta_1 \\
W_2^n(d) = \int_0^\pi \phi_n(\theta_1)\ln\left(\frac{R_d(\theta_1)}{a}\right) d\theta_1, \qquad \text{with: } \phi_n(\theta_1) = -n\sin^n\theta_1 + (n-1)\sin^{n-2}\theta_1 \\
W_3^n(d) = \int_0^\pi \psi_n(\theta_1)\left(\frac{1}{R_d^n(\theta_1)} - \frac{1}{a^n}\right) d\theta_1, \quad \text{with: } \psi_n(\theta_1) = n(n-2)\sin^n\theta_1 + (n-1)\sin^{n-2}\theta_1 \geq 0
\end{cases}
$$

Note that the equality (6.4) applies also for the planar case. From now on, we take $n \geq 2$.

In the following Lemma, we study $W_k^n(d)$ for each $k \in \{1,2,3\}$.

Lemma 9. *For every $n \geq 2$ and every $d \in [0, 1-a]$:*

1. $W_1^n(d) = W_1^n(0)$.
2. $W_2^n(d) = 0$.
3. $W_3^n(d) \geq W_3^n(0)$, *with equality if and only of* $d = 0$.

Proof. 1. The idea is to see that the quantities $W_1^n(0)$ and $W_1^n(d)$ can be interpreted (up to a multiplicative constant) as volumes of the unit balls B and $y_d + B$ in $\mathbb{R}^n$. Then, since the measure is invariant by translations, we get the equality.

We have:

$$\begin{aligned}
W_1^n(d) &= \int_0^\pi \sin^{n-2}\theta_1 \big(R_d^n(\theta_1) - a^n\big) d\theta_1 \\
&= \frac{n}{\prod_{k=0}^{n-3} I_k} \times 2 \int_{\theta_1=0}^{\pi} \dots \int_{\theta_{n-1}=0}^{\pi} \int_{r=a}^{R_d(\theta_1)} 1 \times r^{n-1} \prod_{i=1}^{n-2} \sin^{n-1-i}\theta_i dr d\theta_1 \dots d\theta_{n-1} \\
&= \frac{n}{\prod_{k=0}^{n-3} I_k} \times |\Omega_d| = \frac{n}{\prod_{k=0}^{n-3} I_k} \times (|y_d + B| - |aB|) = \frac{n}{\prod_{k=0}^{n-3} I_k} \times (|B| - |aB|) \\
&= \frac{n}{\prod_{k=0}^{n-3} I_k} \times 2 \int_{\theta_1=0}^{\pi} \dots \int_{\theta_{n-1}=0}^{\pi} \int_{r=a}^{1} 1 \times r^{n-1} \prod_{i=1}^{n-2} \sin^{n-1-i}\theta_i dr d\theta_1 \dots d\theta_{n-1} \\
&= W_1^n(0).
\end{aligned}$$

2. We remark that for every $\theta_1 \in (0,\pi)$ one has $\phi_n(\pi - \theta_1) = \phi_n(\theta_1)$, thus:

$$\begin{aligned}
W_2(d) &= \int_0^{\frac{\pi}{2}} \phi_n(\theta_1) \ln\left(\frac{R_d(\theta_1)}{a}\right) d\theta_1 + \int_{\frac{\pi}{2}}^{\pi} \phi_n(\theta_1) \ln\left(\frac{R_d(\theta_1)}{a}\right) d\theta_1 \\
&= \int_0^{\frac{\pi}{2}} \phi_n(\theta_1) \ln\left(\frac{d\cos\theta_1 + \sqrt{1 - d^2\sin^2\theta_1}}{a}\right) d\theta_1 + \int_0^{\frac{\pi}{2}} \phi_n(\theta_1) \ln\left(\frac{-d\cos\theta_1 + \sqrt{1 - d^2\sin^2\theta_1}}{a}\right) d\theta_1 \\
&= \int_0^{\frac{\pi}{2}} \phi_n(\theta_1) \ln\left(\frac{\big(\, d\cos\theta_1 + \sqrt{1 - d^2\sin^2\theta_1}\,\big) \times \big(\, -d\cos\theta_1 + \sqrt{1 - d^2\sin^2\theta_1}\,\big)}{a^2}\right) d\theta_1 \\
&= \ln\left(\frac{1-d^2}{a^2}\right) \times \int_0^{\frac{\pi}{2}} \phi_n(\theta_1) d\theta_1 \quad = \quad \ln\left(\frac{1-d^2}{a^2}\right) \times \int_0^{\frac{\pi}{2}} (-n\sin^n\theta_1 + (n-1)\sin^{n-2}\theta_1) d\theta_1 \\
&= \frac{1}{2}\ln\left(\frac{1-d^2}{a^2}\right) \times \Big(-nI_n + (n-1)I_{n-2}\Big) = 0 \qquad \text{(by (6.3))}
\end{aligned}$$

3. We have:

$$\begin{aligned}
W_3(d) &= \int_{\theta_1=0}^{\pi} \psi_n(\theta_1) \left(\frac{1}{\big(\, d\cos\theta_1 + \sqrt{1 - d^2\sin^2\theta_1}\,\big)^n} - \frac{1}{a^n}\right) d\theta_1 \\
&\geq \int_{\theta_1=0}^{\pi} \psi_n(\theta_1) \left(\frac{1}{\big(d\cos\theta_1 + 1\big)^n} - \frac{1}{a^n}\right) d\theta_1 =: G(d) \geq G(0) = W_3(0)
\end{aligned}$$

Inequality $G(d) \geq G(0)$ is a consequence of the monotonicity of the function G and equality occurs if and only if $d = 0$. Indeed for every $d \in (0, 1-a)$:

$$\begin{aligned}
G'(d) &= \int_0^{\pi} -n\psi_n(\theta_1)\frac{\cos\theta_1}{\big(d\cos\theta_1+1\big)^{n+1}}d\theta_1 \\
&= \int_0^{\frac{\pi}{2}} -n\psi_n(\theta_1)\frac{\cos\theta_1}{\big(d\cos\theta_1+1\big)^{n+1}}d\theta_1 + \int_{\theta_1=\frac{\pi}{2}}^{\pi} -n\psi_n(\theta_1)\frac{\cos\theta_1}{\big(d\cos\theta_1+1\big)^{n+1}}d\theta_1 \\
&= n\int_0^{\frac{\pi}{2}} \psi_n(\theta_1)\cos\theta_1\left(\frac{1}{(1-d\cos\theta_1)^{n+1}} - \frac{1}{(1+d\cos\theta_1)^{n+1}}\right)d\theta_1 \\
&> 0 \qquad (\text{because } \forall\theta_1 \in (0,\pi/2), \quad \psi_n(\theta_1)\cos\theta_1 > 0 \quad \text{and} \quad (1+d\cos\theta_1)^{n+1} > (1-d\cos\theta_1)^{n+1})
\end{aligned}$$

□

Using the results of Lemma 9, we get:

$$\begin{aligned}
\int_{\Omega_d} |\nabla f|^2 dx &= \frac{2}{n-1}\left(\prod_{k=0}^{n-3} I_k\right)\left((n-1)W_1^n(d) + 2\mu_{\sigma,n}W_2^n(d) - \frac{\mu_{\sigma,n}^2}{n}W_3^n(d)\right) \\
&\leq \frac{2}{n-1}\left(\prod_{k=0}^{n-3} I_k\right)\left((n-1)W_1^n(0) + 2\mu_{\sigma,n}W_2^n(0) - \frac{\mu_{\sigma,n}^2}{n}W_3^n(0)\right) = \int_{\Omega_0} |\nabla f|^2 dx,
\end{aligned}$$

with equality if and only if $d = 0$. This proves the second assertion of Proposition 18.

6.2.4 Proof of the third assertion of Proposition 18

Take $n \geq 2$, we have:

$$\begin{aligned}
\int_{\partial(y_d+B)} f_n^2 d\sigma &= 2\int_{\theta_1=0}^{\pi} ... \int_{\theta_{n-2}=0}^{\pi}\int_{\theta_{n-1}=0}^{\pi} f_n^2(r,\theta_1,...,\theta_{n-1}) \times R_d^{n-2}(\theta_1)\prod_{i=1}^{n-2}\sin^{n-1-i}\theta_i \times \sqrt{R_d^2(\theta_1) + {R'_d}^2(\theta_1)}\; d\theta_1...d\theta_{n-} \\
&= \left(2\prod_{k=2}^{n-1} I_k\right)\int_0^{\pi}\left(R_d(\theta_1) + \frac{\mu_{\sigma,n}}{R_d^{n-1}(\theta_1)}\right)^2 \times R_d^{n-2}(\theta_1)\sin^n\theta_1 \times \sqrt{R_d^2(\theta_1) + {R'_d}^2(\theta_1)}d\theta_1 \\
&= \left(2\prod_{k=2}^{n-1} I_k\right)\int_0^{\pi}\left(R_d^n(\theta_1) + 2\mu_{\sigma,n} + \frac{\mu_{\sigma,n}^2}{R_d^n(\theta_1)}\right)\sin^n\theta_1 \times \sqrt{R_d^2(\theta_1) + {R'_d}^2(\theta_1)}\; d\theta_1 \\
&= \left(2\prod_{k=2}^{n-1} I_k\right) \times \big(V_1^n(d) + 2\mu_{\sigma,n}(I_n + V_2^n(d)) + \mu_{\sigma,n}^2 V_3^n(d)\big)
\end{aligned}$$

where:

$$\begin{cases}
V_1^n(d) = \int_0^{\pi}\sin^n\theta_1 R_d^n(\theta_1)\sqrt{R_d^2(\theta_1) + {R'_d}^2(\theta_1)}d\theta_1 \\
V_2^n(d) = \int_0^{\pi}\sin^n\theta_1 \frac{d\cos\theta_1}{\sqrt{1-d^2\sin^2\theta_1}}d\theta_1 \qquad (\text{by using (6.2)}) \\
V_3^n(d) = \int_0^{\pi}\frac{\sin^n\theta_1}{R_d^{n-1}(\theta_1)\sqrt{1-d^2\sin^2\theta_1}}d\theta_1 \qquad (\text{by using (6.2)})
\end{cases}$$

Let us prove the following Lemma:

Lemma 10. *For every $n \geq 1$ and every $d \in [0, 1-a]$:*

1. $V_1^n(d) = V_1^n(0)$.
2. $V_2^n(d) = 0$.
3. $V_3^n(d) \geq V_3^n(0)$, *with equality if and only of* $d = 0$.

Proof. 1. Take B the unit ball of $\mathbb{R}^{n+2}$ centred in 0 and $y_d = (0, \cdots, 0, d) \in \mathbb{R}^{n+2}$.

In the same spirit of the proof of the assertion 1 of Lemma 9, the idea is to see that the quantities $V_1^n(0)$ and $V_1^n(d)$ can be interpreted (up to a multiplicative constant) as perimeters of B and $y_d + B$. Then, since the perimeter is invariant by translations we get the equality.

We have:

$$\begin{aligned}
V_1^n(d) &= \int_0^\pi \sin^n \theta_1 R_d^n(\theta_1) \sqrt{R_d^2(\theta_1) + {R'_d}^2(\theta_1)} d\theta_1 \\
&= \frac{1}{2\prod_{k=0}^{n-1} I_k} \times 2 \int_{\theta_1=0}^{\pi} \dots \int_{\theta_{n+1}=0}^{\pi} 1 \times R_d^n(\theta_1) \sqrt{R_d^2(\theta_1) + {R'_d}^2(\theta_1)} \prod_{i=1}^{n} \sin^{n+1-i} \theta_i d\theta_1 \dots d\theta_{n+1} \\
&= \frac{1}{2\prod_{k=0}^{n-1} I_k} \times P(y_d + B) \;=\; \frac{1}{2\prod_{k=0}^{n-1} I_k} \times P(B) \;=\; V_1^n(0)
\end{aligned}$$

2. We compute:

$$\begin{aligned}
V_2^n(d) &= \int_0^{\frac{\pi}{2}} \sin^n \theta_1 \frac{d\cos\theta_1}{\sqrt{1 - d^2 \sin^2 \theta_1}} d\theta_1 + \int_{\frac{\pi}{2}}^{\pi} \sin^n \theta_1 \frac{d\cos\theta_1}{\sqrt{1 - d^2 \sin^2 \theta_1}} d\theta_1 \\
&= \int_0^{\frac{\pi}{2}} \sin^n \theta_1 \frac{d\cos\theta_1}{\sqrt{1 - d^2 \sin^2 \theta_1}} d\theta_1 - \int_0^{\frac{\pi}{2}} \sin^n t \frac{d\cos t}{\sqrt{1 - d^2 \sin^2 t}} dt \\
&= 0
\end{aligned}$$

3. We have:

$$\begin{aligned}
V_3^n(d) &= \int_0^\pi \frac{\sin^n \theta_1}{\left(d\cos\theta_1 + \sqrt{1 - d^2 \sin^2 \theta_1}\right)^{n-1} \sqrt{1 - d^2 \sin^2 \theta_1}} d\theta_1 \\
&\geq \int_0^\pi \frac{\sin^n \theta_1}{\left(d\cos\theta_1 + 1\right)^{n-1}} d\theta_1 =: H(d) \geq H(0) = V_3^n(0).
\end{aligned}$$

Inequality $H(d) \geq H(0)$ follows from the monotonicity of H and is an equality if and only if $d = 0$. This can be proven with the same method used for G in the previous section.

□

Using the results of Lemma 10, we get:

$$\begin{aligned}
\int_{\partial\Omega_d} f^2 d\sigma &= \left(2 \prod_{k=2}^{n-1} I_k\right) \times \left(V_1^n(d) + 2\mu_{\sigma,n}(I_n + V_2^n(d)) + \mu_{\sigma,n}^2 V_3^n(d)\right) + \int_{\partial(aB)} f^2 d\sigma \\
&\geq \left(2 \prod_{k=2}^{n-1} I_k\right) \times \left(V_1^n(0) + 2\mu_{\sigma,n}(I_n + V_2^n(0)) + \mu_{\sigma,n}^2 V_3^n(0)\right) + \int_{\partial(aB)} f^2 d\sigma \\
&= \int_{\partial\Omega_0} f^2 d\sigma.
\end{aligned}$$

which proofs the third assertion of Proposition 18.

6.3 The Dirichlet-Steklov problem

In this section, we show that the ideas of our proof in section 6.2 also apply to the problem considered in [172]. Thus, we give an alternative proof of Theorem 1 [172] which deals with $n \geq 3$ and tackle the planar case which was to our knowledge still open (Remark 2 [172]).

Let $n \geq 2$ and B_1 be an open ball in $\mathbb{R}^n$ and B_2 be an open ball contained in B_1. We are interested in the eigenvalue problem

$$\begin{cases} \Delta u = 0 & \text{in } B_1 \backslash \overline{B_2}, \\ u = 0 & \text{on } \partial B_2, \\ \frac{\partial u}{\partial n} = \tau u & \text{on } \partial B_1, \end{cases}$$

The first eigenvalue of $B_1 \backslash \overline{B_2}$ is given by the following Rayleigh quotient:

$$\tau_1 \left(B_1 \backslash \overline{B_2} \right) = \inf \left\{ \frac{\int_{B_1 \backslash \overline{B_2}} |\nabla u|^2 dx}{\int_{\partial B_1} u^2 d\sigma} \;\middle|\; u \in H^1(\Omega) \backslash \{0\} \text{ such that } u = 0 \text{ on } \partial B_2 \right\}$$

As stated in Theorem 22, the eigenvalue τ_1 is maximal when the balls are concentric. As for the case of pure Steklov boundary condition, we can assume without loss of generality that the obstacle B_2 is the open ball of radius $a \in (0,1)$ centred at the origin 0 and $B_1 = y_d + B$, where B is the unit ball centred in 0. We use the notations introduced in section 6.2.

Using separation of variables S. Verma and G. Santhanam proved that the first eigenfunction g_n of the spherical shell Ω_0 is given by:

$$g_n(r, \theta_1, ..., \theta_{n-1}) = \begin{cases} \ln r - \ln a & \text{if n=2} \\ \left(\frac{1}{a^{n-2}} - \frac{1}{r^{n-2}} \right) & \text{if } n \geq 3 \end{cases}$$

6.3.1 A key Proposition

Here also, Theorem 22 is an immediate consequence of the following Proposition:

Proposition 19. *Let $n \geq 2$, we have:*

1. *g_n can be used as a test function in the variational definition of $\tau_1(\Omega_d)$.*
2. *$\int_{\Omega_d} |\nabla g_n|^2 dx \leq \int_{\Omega_0} |\nabla g_n|^2 dx$.*
3. *$\int_{\partial(y_d+B)} g_n^2 d\sigma \geq \int_{\partial B} g_n^2 d\sigma$, with equality if and only if $d = 0$.*

Proof. This Proposition has been proved in [172] for the case $n \geq 3$.

The first assertion is obvious since $g_n(a, \theta_1, \cdots, \theta_{n-1}) = 0$.

As for the second, it has been remarked in [172] page 13, the inequality $\int_{\Omega_d} |\nabla g_n|^2 dx \leq \int_{\Omega_0} |\nabla g_n|^2 dx$ is a straightforward consequence of the monotonicity of $r \longmapsto \frac{\partial g_n}{\partial r}$. Unfortunately, this is not the case for the inequality on the boundary (assertion 3) for which the author needs more computations (see [172] section 2.2).

First, we show that Lemma 10 allows us to give an alternative and simpler proof of the last inequality in the case $n \geq 3$, then we prove it in the planar case $n = 2$.

If $n \geq 3$, we have:

$$\begin{aligned}
\int_{\partial(y_d+B)} g_n^2 d\sigma &= \left(2\prod_{j=2}^{n-3} I_j\right)\int_0^\pi \left(\frac{1}{a^{n-2}} - \frac{1}{R_d^{n-2}(\theta_1)}\right)^2 R_d^{n-2}(\theta_1)\sin^{n-2}\theta_1\sqrt{R_d^2(\theta_1)+{R_d'}^2(\theta_1)}d\theta_1 \\
&= \left(2\prod_{j=2}^{n-3} I_j\right)\left(\frac{1}{a^{2n-4}}V_1^{n-2}(d) - \frac{2}{a^{n-2}}\left(I_{n-2}+V_2^{n-2}(d)\right)+V_3^{n-2}(d)\right) \\
&\geq \left(2\prod_{j=2}^{n-3} I_j\right)\left(\frac{1}{a^{2n-4}}V_1^{n-2}(0) - \frac{2}{a^{n-2}}\left(I_{n-2}+V_2^{n-2}(0)\right)+V_3^{n-2}(0)\right) = \int_{\partial B} g_n^2 d\sigma
\end{aligned}$$

Now take $n = 2$. We use the following parameterization of the shifted sphere:

$$y_d + \partial B = \{M(t) = (\sin t, d + \cos t) \mid t \in [0, 2\pi)\}.$$

Note that: $|M(t)| = 1 + d^2 + 2d\cos t$. We have:

$$\begin{aligned}
\int_{\partial(y_d+B)} g_2^2 d\sigma &= \int_0^{2\pi} \left(\ln\left(1+d^2+2d\cos t\right) - \ln a\right)^2 dt \\
&= \int_0^{2\pi} \ln^2\left(1+d^2+2d\cos t\right)dt - 2\ln a\int_0^{2\pi}\ln\left(1+d^2+2d\cos t\right)dt + 2\pi\ln^2 a \\
&\geq 2\pi\ln^2 a = \int_{\partial B} g_2^2 d\sigma,
\end{aligned}$$

because:

$$\int_0^{2\pi} \ln^2\left(1+d^2+2d\cos t\right)dt \geq 0 \quad \text{and} \quad \int_0^{2\pi}\ln\left(1+d^2+2d\cos t\right)dt = 0.$$

Indeed, on the one hand the inequality is obvious and is an equality if and only if $d = 0$, on the other hand the second assertion is a special case of a classical Lemma in complex analysis used in the proof of the so called Jensen formula (see for example 4.3.1. [176]).

This ends the proof of the third assertion and the demonstration of Proposition 19.

□

6.3.2 Proof of Theorem 22

Finally, we conclude as before:

$$\tau_1(\Omega_d) \leq \frac{\int_{\Omega_d}|\nabla g_n|^2 dx}{\int_{\partial(y_d+B)} g_n^2 d\sigma} \leq \frac{\int_{\Omega_0}|\nabla g_n|^2 dx}{\int_{\partial B} g_n^2 d\sigma} = \tau_1(\Omega_0),$$

with equality if and only if $d = 0$. This ends the proof of Theorem 22.

6.4 Appendix

In this appendix we compute the Steklov eigenvalues of the spherical shell $\Omega_0 = B\backslash aB \subset \mathbb{R}^n$, where $a \in (0,1)$. We then prove a monotonicity result on these eigenvalues, which allows us to give the exact value of $\sigma_1(\Omega_0)$ and its corresponding eigenfunctions.

Theorem 23. *Let $n \geq 2$. The first non-trivial Steklov eigenvalue of the spherical shell $\Omega_0 = B\backslash aB \subset \mathbb{R}^n$ is:*

$$\sigma_1(\Omega_0) = \frac{(n+1)a^{n+1}+a^n+a+n-1-\sqrt{\left((n+1)a^{n+1}+a^n+a+n-1\right)^2-4(n-1)a\left(1-a^n\right)^2}}{2a\left(1-a^n\right)}.$$

It is of multiplicity n and the corresponding eigenfunctions are:

$$\begin{array}{rccc} u_n^i & : & \mathbb{R}^n & \longrightarrow & \mathbb{R} \\ & & x=(x_1,\cdots,x_n) & \longmapsto & x_i\left(1+\frac{\mu_{\sigma,n}}{|x|^n}\right), \end{array}$$

where $i \in [\![1,n]\!]$ and $\mu_{\sigma,n} = \frac{1-\sigma_1(\Omega_0)}{n+\sigma_1(\Omega_0)-1}$.

Remark 15. *Theorem 23 has already been proved for the planar case by B. Dittmar [72] (see also [101]). For higher dimensions, A. Fraser and R. Schoen [83] gave asymptotic formula for the lowest eigenvalues of spherical shells when the hole is vanishing. In this case, it is easy to identify the first eigenvalues (in particular the first one). Unfortunately, this is no longer the case when the hole is not vanishing as explained in sections 6.4.1 and 6.4.2.*

6.4.1 Computation of the eigenvalues via classical separation of variables technique

Finding the eigenvalues and eigenfunctions of the Laplacian on special domains (balls, rectangles, annulus...) is a classical problem (see for example [99] Section 3). The standard method is to look for eigenfunctions via separation of variables and then prove that they form a complete basis of a convenient function space, this combined with orthogonality properties of the eigenfunctions shows that we didn't miss any.

Take $k \in \mathbb{N}$, let us search harmonic functions h_k of the form

$$\begin{array}{rccc} h_k & : & \mathbb{R}_+ \times [0,\pi] \times \cdots \times [0,\pi] \times [0,2\pi] & \longrightarrow & \mathbb{R} \\ & & (r,\theta_1,\cdots,\theta_{n-1}) & \longmapsto & \alpha_k(r)\beta_k(\theta_1,\cdots,\theta_{n-1}) \end{array}$$

where $\beta_k \in H_k^n$ is a spherical harmonic of order k and H_k^n is the set of restrictions of homogeneous harmonic polynomial of degree k with n variables on the unit sphere ∂B (for an introduction to harmonic polynomials we refer to [17] Chapter 5). It is well-known that the set H_k^n corresponds to the eigenspace of the Laplace-Beltrami operator $-\Delta_{\partial B}$ associated to the eigenvalue $k(k+n-1)$.

We have:

$$\Delta h_k = \left(\frac{\partial^2}{\partial r^2} + \frac{n-1}{r}\frac{\partial}{\partial r} + r^{-2}\Delta_{\partial B}\right) h_k = \left(\alpha_k''(r) + \frac{n-1}{r}\alpha_k'(r) - \frac{k(k+n-1)}{r^2}\alpha_k(r)\right)\beta_k(\theta_1,\cdots,\theta_{n-1}).$$

The condition $\Delta h_k = 0$ implies that α_k must satisfy the differential equation:

$$\alpha_k''(r) + \frac{n-1}{r}\alpha_k'(r) - \frac{k(k+n-1)}{r^2}\alpha_k(r) = 0.$$

By standard methods of solving ODEs, the solutions of the last equation are given by:

$$\alpha_0(r) = \begin{cases} p_{0,2} + q_{0,2}\ln r & \text{if } n=2 \\ p_{0,n} + \frac{q_{0,n}}{r^{n-2}} & \text{if } n \geq 3, \end{cases}$$

and for $k \geq 1$:

$$\alpha_k(r) = p_{k,n} r^k + \frac{q_{k,n}}{r^{k+n-2}},$$

where $p_{k,n}$ and $q_{k,n}$ are constants.

It remains to look for all possible values δ_k such that: $\frac{\partial h_k}{\partial n} = \delta_k h_k$ on $\partial\Omega_0$. This equality is equivalent to

$$\begin{cases} \alpha_k'(1) = \delta_k \alpha_k(1), \\ \alpha_k'(a) = \delta_k \alpha_k(a). \end{cases}$$

As explained in the proof of Proposition 3 of [83], those equalities imply that the possible eigenvalues δ_k are solutions of equations of second order.

When $k = 0$, we find two eigenvalues: 0 that corresponds to constant eigenfunctions and δ_0 that corresponds to a (non-constant) radial one.

$$\delta_0 = \begin{cases} \frac{1+a}{a \ln 1/a} & \text{if } n = 2 \\ \frac{(n-2)(1+a^{n-1})}{a(1-a^{n-2})} & \text{if } n \geq 3. \end{cases}$$

The corresponding (radial) eigenfunction is given by:

$$h_0(r, \theta_1, \cdots, \theta_{n-1}) = \begin{cases} 1 + \delta_0 \ln r & \text{if } n = 2 \\ (2 - n - \delta_0) + \frac{\delta_0}{r^{n-2}} & \text{if } n \geq 3. \end{cases}$$

On the other hand, as mentioned in [83], when $k \geq 1$, one finds two eigenvalues $\delta_k^{(1)} < \delta_k^{(2)}$ corresponding to the solutions of the following equation:

$$A_k \delta^2 + B_k \delta + C_k = 0, \tag{6.5}$$

where:

$$\begin{cases} A_k = a - a^{2k+n-1}, \\ B_k = -\big((k+n-2)a^{2k+n-1} + ka^{2k+n-2} + ka + k + n - 2\big), \\ C_k = (k+n-2)k(1 - a^{2k+n-2}). \end{cases}$$

We compute the determinant Δ_k, and use the fact that $a \in (0, 1)$ to check that $\Delta_k > 0$:

$$\begin{aligned} \Delta_k &= B_k^2 - 4A_k \times C_k \\ &= \Big[(k+n-2)a^{2k+n-1} + ka^{2k+n-2} + ka + k + n - 2\Big]^2 - (k+n-2)ka(1 - a^{2k+n-2})^2 \\ &\geq (k+n-2)^2 - (k+n-2)ka\big(1 - a^{2k+n-2}\big)^2 \qquad (\text{because } a \geq 0) \\ &\geq (k+n-2)\big[(k+n-2) - k\big] \qquad (\text{because } 0 \leq a\big(1 - a^{2k+n-2}\big)^2 \leq 1) \\ &= (k+n-2)(n-2) > 0. \end{aligned}$$

Then, the equation (6.5) admits two different positive solutions

$$\delta_k^{(1)} := \frac{-B_k - \sqrt{\Delta_k}}{2A_k} < \frac{-B_k + \sqrt{\Delta_k}}{2A_k} =: \delta_k^{(2)}.$$

By straightforward computations, the corresponding eigenfunctions are given by:

$$h_k^{(i)}(r, \theta_1, \cdots, \theta_{n-1}) = \left(r^k + \frac{k - \delta_k^{(i)}}{n + \delta_k^{(i)} + k - 2} \times \frac{1}{r^{k+n-2}} \right) Y_{k,j}(\theta_1, \cdots, \theta_{n-1}), \tag{6.6}$$

where $Y_{k,j} \in H_k^n$ denotes the j-th ($j \in [\![1, \dim H_k^n]\!]$) spherical harmonic of order k and $i \in \{1, 2\}$.

Thus, the multiplicity of $\delta_k^{(i)}$ is equal to

$$\dim H_k^n = \binom{n+k-1}{n-1} - \binom{n+k-3}{n-1}.$$

At last, by using expansions results for harmonic functions on annuli (see 9.17 [17] for $n = 2$ and 10.1 [17] for $n \geq 3$), we deduce that the eigenfunctions we found form a complete basis of the space of harmonic functions on the annulus Ω_0.

It remains to determine the lowest eigenvalue between δ_0 and the $\delta_k^{(i)}$ for $k \in \mathbb{N}^*$ and $i \in \{1, 2\}$.

6.4.2 A monotonicity result

We state and prove the following key lemma, which combined with results of section 6.4.1 gives an immediate proof of Theorem 23.

Lemma 11. *We have:*

1. *The sequence* $\left(\delta_k^{(1)}\right)_{k\geq 1}$ *is strictly increasing.*
2. $\sigma_1(\Omega_0) < \delta_0$.

Proof. The case $n = 2$ had been considered in [72, 101]. Let $n \geq 3$.

1. We have:

$$\delta_k^{(1)} = \frac{2C_k}{-B_k + \sqrt{B_k^2 - 4A_k \times C_k}} = \frac{2(k+n-2)k(1-a^{2k+n-2})}{-B_k + \sqrt{B_k^2 - 4(k+n-2)ka(1-a^{2k+n-2})^2}}.$$

The idea of proof is to write $\delta_k^{(1)} = P_k/Q_k$, where $(P_k)_k$ (resp. $(Q_k)_k$) is a positive increasing (resp. decreasing) sequence. Indeed, we can write:

$$\delta_k^{(1)} = \frac{2\sqrt{(k+n-2)k}(1-a^{2k+n-2})}{-\frac{B_k}{\sqrt{(k+n-2)k}} + \sqrt{\left(-\frac{B_k}{\sqrt{(k+n-2)k}}\right)^2 - 4a(1-a^{2k+n-2})^2}}$$

The sequences $\left(2\sqrt{(k+n-2)k}(1-a^{2k+n-2})\right)_k$ and $\left(a(1-a^{2k+n-2})\right)_k$ are strictly increasing. It remains to prove that the (positive) sequence $\left(-\frac{B_k}{\sqrt{(k+n-2)k}}\right)_{k\geq 1}$ is strictly decreasing.

We have:

$$\begin{aligned}
-\frac{B_k}{\sqrt{(k+n-2)k}} &= \frac{(k+n-2)a^{2k+n-1} + ka^{2k+n-2} + ka + k + n - 2}{\sqrt{k}\sqrt{k+n-2}} \\
&= \frac{(k+n-2)\left(a^{2k+n-1}+1\right) + ka\left(a^{2k+n-3}+1\right)}{\sqrt{k}\sqrt{k+n-2}} \\
&= \sqrt{\frac{k+n-2}{k}}\left(a^{2k+n-1}+1\right) + a\sqrt{\frac{k}{k+n-2}}\left(a^{2k+n-3}+1\right).
\end{aligned}$$

Let us introduce the function:

$$\begin{array}{rcccl}
h_{a,n} & : & [1,+\infty[& \longrightarrow & \mathbb{R} \\
 & & t & \longmapsto & \sqrt{\frac{t+n-2}{t}} \times \left(a^{2t+n-1}+1\right) + a\sqrt{\frac{t}{t+n-2}} \times \left(a^{2t+n-3}+1\right).
\end{array}$$

we prove that $h_{a,n}$ is strictly decreasing. To do so, we compute the derivative $h'_{a,n}$ and prove that it is negative on $[1,+\infty[$.

We have for every $t \geq 1$:

$$\begin{aligned}
h'_{a,n}(t) &= \frac{-\frac{n-2}{t^2}\left(a^{n+2t-1}+1\right)}{2\sqrt{\frac{n+t-2}{t}}} + \frac{\frac{n-2}{(n+t-2)^2}a\left(a^{n+2t-3}+1\right)}{2\sqrt{\frac{t}{n+t-2}}} \\
&+ 2\ln(a)\sqrt{\frac{t}{n+t-2}}a^{n+2t-2} + 2\ln(a)\sqrt{\frac{n+t-2}{t}}a^{n+2t-1} \\
&< \frac{-\frac{n-2}{t^2}\left(a^{n+2t-1}+1\right)}{2\sqrt{\frac{n+t-2}{t}}} + \frac{\frac{n-2}{(n+t-2)^2}a\left(a^{n+2t-3}+1\right)}{2\sqrt{\frac{t}{n+t-2}}} \qquad \text{(because } \ln(a) < 0\text{)}. \\
&= \frac{2(n-2)}{t(n+t-2)(a^{n+2t-1}+1)}\sqrt{\frac{t}{n+t-2}} \times \left(a \times \frac{a^{n+2t-3}+1}{a^{n+2t-1}+1} - 1 - \frac{n-2}{t}\right) \\
&< \frac{2(n-2)}{t(n+t-2)(a^{n+2t-1}+1)}\sqrt{\frac{t}{n+t-2}} \times \left(\frac{a^{n+2t-3}+1}{a^{n+2t-1}+1} - \frac{t+n-2}{t}\right) \qquad \text{(because } a \in (0,1)\text{)}.
\end{aligned}$$

We have:

$$\frac{a^{n+2t-3}+1}{a^{n+2t-1}+1} - \frac{t+n-2}{t} < 0 \quad \Leftrightarrow \quad \frac{t+n-2}{t} \times a^{n+2t-1} - a^{n+2t-3} + \frac{n-2}{t} > 0$$

Now, let $t \geq 1$ and $n \geq 3$. Consider the function:

$$\begin{array}{rccc}
g_{t,n} & : & (0,1) & \longrightarrow & \mathbb{R} \\
 & & a & \longmapsto & \frac{n+t-2}{t} \times a^{n+2t-1} - a^{n+2t-3} + \frac{n-2}{t}
\end{array}$$

We compute the derivative of $g_{t,n}$, for every $a \in (0,1)$:

$$g'_{t,n}(a) = \frac{n+t-2}{t} \times (n+2t-1) \times a^{n+2t-4} \times \left(a^2 - \frac{t}{n+t-2} \times \frac{n+2t-3}{n+2t-1}\right).$$

We deduce that $g_{t,n}$ is decreasing on $(0, a_{t,n})$ and increasing on $(a_{t,n}, 1)$, which implies that it attains its minimum in $a_{t,n}$, where:

$$a_{t,n} = \sqrt{\frac{t}{n+t-2} \times \frac{n+2t-3}{n+2t-1}}.$$

We have:

$$\begin{aligned}
g_{t,n}(a) &\geq g_{t,n}(a_{t,n}) \\
&= \frac{n+t-2}{t} \times \left(\frac{t}{n+t-2}\right)^{\frac{n+2t-1}{2}} \left(\frac{n+2t-3}{n+2t-1}\right)^{\frac{n+2t-1}{2}} - \left(\frac{t}{n+t-2}\right)^{\frac{n+2t-3}{2}} \left(\frac{n+2t-3}{n+2t-1}\right)^{\frac{n+2t-3}{2}} + \frac{n-2}{t} \\
&= -\left(\frac{t}{n+t-2}\right)^{\frac{n+2t-3}{2}} \left(\frac{n+2t-3}{n+2t-1}\right)^{\frac{n+2t-3}{2}} \times \frac{2}{n+2t-1} + \frac{n-2}{t} \\
&\geq -\frac{1}{t+\frac{n-1}{2}} + \frac{n-2}{t} > 0 \qquad \text{(because: } n-2 \geq 1 \text{ and } t + \frac{n-1}{2} > t\text{)}.
\end{aligned}$$

We deduce that for all $t \geq 1$: $h'_{a,n}(t) < 0$, which implies that $h_{a,n}$ is strictly decreasing on $[1, +\infty[$. In particular, the sequence $\left(-\frac{B_k}{\sqrt{(k+n-2)k}}\right)_{k\geq 1}$ is strictly decreasing and so is

$$\left(-\frac{B_k}{\sqrt{(k+n-2)k}} + \sqrt{\left(-\frac{B_k}{\sqrt{(k+n-2)k}}\right)^2 - 4a(1-a^{2k+n-2})^2}\right)_{k\geq 1}.$$

2. Take $\gamma : x \in \mathbb{R}^n \longmapsto x_1$ an eigenfunction corresponding to the first nontrivial Steklov eigenvalue of the unit ball B centred in 0. This function can be used as a test function in the variational definition of $\sigma_1(B\backslash aB)$.

   We write:

$$\begin{aligned}
\sigma_1(B\backslash aB) &= \inf\left\{ \frac{\int_{B\backslash aB} |\nabla u|^2 dx}{\int_{\partial(B\backslash aB)} u^2 d\sigma} \;\middle|\; u \in H^1(\Omega)\backslash\{0\} \text{ such that } \int_{\partial\Omega} u d\sigma = 0 \right\} \\
&\leq \frac{\int_{B\backslash aB} |\nabla\gamma|^2 dx}{\int_{\partial B\cup\partial(aB)} \gamma^2 d\sigma} \leq \frac{\int_B |\nabla\gamma|^2 dx}{\int_{\partial B} \gamma^2 d\sigma} = \sigma_1(B) = 1 \quad \text{(see [97] Example 1.3.2 for the last equality)} \\
&< (n-2)\frac{1+a^{n-1}}{a(1-a^{n-2})} = \delta_0.
\end{aligned}$$

□

6.4.3 Proof of Theorem 23

We have $\delta_1^{(1)} < \delta_1^{(2)}$ and by Lemma 11:

$$\begin{cases} \forall k \geq 2, \qquad \delta_1^{(1)} < \delta_k^{(1)} < \delta_k^{(2)}, \\ \qquad\qquad\qquad \sigma_1(\Omega_0) < \delta_0. \end{cases}$$

This implies that $\delta_1^{(1)}$ is the lowest non-trivial Steklov eigenvalue of Ω_0, which writes $\sigma_1(\Omega_0) = \delta_1^{(1)}$. It is of multiplicity n and the corresponding eigenfunctions are given by (6.6) as follows:

$$\begin{array}{rcccl} u_n^i & : & \mathbb{R}^n & \longrightarrow & \mathbb{R} \\ & & x = (x_1, \cdots, x_n) & \longmapsto & \left(|x| + \frac{\mu_{\sigma,n}}{|x|^{n-1}}\right)\frac{x_i}{|x|} = x_i\left(1 + \frac{\mu_{\sigma,n}}{|x|^n}\right) \end{array}$$

where $i \in [\![1, n]\!]$ and $\mu_{\sigma,n} = \frac{1-\sigma_1(\Omega_0)}{n+\sigma_1(\Omega_0)-1}$.

Bibliography

[1] E. Acerbi, N. Fusco, and M. Morini. "Minimality via second variation for a nonlocal isoperimetric problem". In: *Comm. Math. Phys.* 322.2 (2013), pp. 515–557. ISSN: 0010-3616. DOI: 10.1007/s00220-013-1733-y. URL: http://dx.doi.org/10.1007/s00220-013-1733-y.

[2] B. Ainseba and S. Aniţa. "Internal stabilizability for a reaction-diffusion problem modeling a predator-prey system". In: *Nonlinear Anal.* 61.4 (2005), pp. 491–501. ISSN: 0362-546X. DOI: 10.1016/j.na.2004.09.055. URL: https://doi.org/10.1016/j.na.2004.09.055.

[3] A. R. Aithal and R. Raut. "On the extrema of Dirichlet's first eigenvalue of a family of punctured regular polygons in two dimensional space forms". In: *Proc. Indian Acad. Sci. Math. Sci.* 122.2 (2012), pp. 257–281. ISSN: 0253-4142. DOI: 10.1007/s12044-012-0068-5. URL: https://doi.org/10.1007/s12044-012-0068-5.

[4] G. Allaire. *Conception optimale de structures.* Vol. 58. Mathématiques & Applications (Berlin) [Mathematics & Applications]. With the collaboration of Marc Schoenauer (INRIA) in the writing of Chapter 8. Springer-Verlag, Berlin, 2007, pp. xii+278. ISBN: 978-3-540-36710-9; 3-540-36710-1.

[5] G. Allaire, M. Bihr, and B. Bogosel. "Support optimization in additive manufacturing for geometric and thermo-mechanical constraints". In: *Struct. Multidiscip. Optim.* 61.6 (2020), pp. 2377–2399. ISSN: 1615-147X. DOI: 10.1007/s00158-020-02551-1. URL: https://doi.org/10.1007/s00158-020-02551-1.

[6] F. Alter and V. Caselles. "Uniqueness of the Cheeger set of a convex body". In: *Nonlinear Anal.* 70.1 (2009), pp. 32–44. ISSN: 0362-546X. DOI: 10.1016/j.na.2007.11.032. URL: https://doi.org/10.1016/j.na.2007.11.032.

[7] L. Ambrosio, N. Fusco, and D. Pallara. *Functions of bounded variation and free discontinuity problems.* Oxford Mathematical Monographs. The Clarendon Press, Oxford University Press, New York, 2000, pp. xviii+434. ISBN: 0-19-850245-1.

[8] M. H. C. Anisa and A. R. Aithal. "On two functionals connected to the Laplacian in a class of doubly connected domains in space-forms". In: *Proc. Indian Acad. Sci. Math. Sci.* 115.1 (2005), pp. 93–102. ISSN: 0253-4142. DOI: 10.1007/BF02829842. URL: https://doi.org/10.1007/BF02829842.

[9] T. V. Anoop, V. Bobkov, and S. Sasi. "On the strict monotonicity of the first eigenvalue of the p-Laplacian on annuli". In: *Trans. Amer. Math. Soc.* 370.10 (2018), pp. 7181–7199. ISSN: 0002-9947. DOI: 10.1090/tran/7241. URL: https://doi.org/10.1090/tran/7241.

[10] T.V. Anoop and K. Ashok Kumar. "On reverse Faber-Krahn inequalities". In: *Journal of Mathematical Analysis and Applications* 485.1 (2020), p. 123766. ISSN: 0022-247X. DOI: https://doi.org/10.1016/j.jmaa.2019.123766. URL: http://www.sciencedirect.com/science/article/pii/S0022247X19310340.

[11] P. Antunes and P. Freitas. "New Bounds for the Principal Dirichlet Eigenvalue of Planar Regions". In: *Experimental Mathematics* 15.3 (Mar. 2006), pp. 333–342.

[12] P. Antunes and P. Freitas. "New Bounds for the Principal Dirichlet Eigenvalue of Planar Regions". In: *Experimental Mathematics* 15.3 (Mar. 2006), pp. 333–342.

[13] P. Antunes and A. Henrot. "On the range of the first two Dirichlet and Neumann eigenvalues of the Laplacian". In: *Proceedings of the Royal Society of London* 467.2 (2011), pp. 1577–1603.

[14] P. R. S. Antunes. "Maximal and minimal norm of Laplacian eigenfunctions in a given subdomain". In: *Inverse Problems* 32.11 (2016), pp. 115003, 18. ISSN: 0266-5611. DOI: 10.1088/0266-5611/32/11/115003. URL: https://doi.org/10.1088/0266-5611/32/11/115003.

[15] P. R. S. Antunes and B. Bogosel. *Parametric Shape Optimization using the Support Function.* 2019. arXiv: 1809.00254 [math.OC].

[16] M. S. Ashbaugh and R. D. Benguria. "Isoperimetric inequalities for eigenvalues of the Laplacian". In: *Spectral theory and mathematical physics: a Festschrift in honor of Barry Simon's 60th birthday.* Vol. 76. Proc. Sympos. Pure Math. Amer. Math. Soc., Providence, RI, 2007, pp. 105–139. DOI: 10.1090/pspum/076.1/2310200. URL: https://doi.org/10.1090/pspum/076.1/2310200.

[17] S. Axler, P. Bourdon, and W. Ramey. *Harmonic function theory.* Second. Vol. 137. Graduate Texts in Mathematics. Springer-Verlag, New York, 2001, pp. xii+259. ISBN: 0-387-95218-7. DOI: 10.1007/978-1-4757-8137-3. URL: https://doi.org/10.1007/978-1-4757-8137-3.

[18] C. Bandle. *Isoperimetric inequalities and applications.* Vol. 7. Monographs and Studies in Mathematics. Pitman (Advanced Publishing Program), Boston, Mass.-London, 1980, pp. x+228. ISBN: 0-273-08423-2.

[19] S. Bartels and G. Wachsmuth. "Numerical approximation of optimal convex shapes". In: *SIAM J. Sci. Comput.* 42.2 (2020), A1226–A1244. ISSN: 1064-8275. DOI: 10.1137/19M1256853. URL: https://doi.org/10.1137/19M1256853.

[20] T. Bayen and D. Henrion. "Semidefinite programming for optimizing convex bodies under width constraints". In: *Optim. Methods Softw.* 27.6 (2012), pp. 1073–1099. ISSN: 1055-6788. DOI: 10.1080/10556788.2010.547580. URL: https://doi.org/10.1080/10556788.2010.547580.

[21] M. Belloni and E. Oudet. "The minimal gap between $\Lambda_2(\Omega)$ and $\Lambda_\infty(\Omega)$ in a class of convex domains". In: *J. Convex Anal.* 15.3 (2008), pp. 507–521. ISSN: 0944-6532.

[22] M. van den Berg and G. Buttazzo. "On capacity and torsional rigidity". In: *Bull. Lond. Math. Soc., (to appear), preprint available at* http://cvgmt.sns.it *and at* http://www.arxiv.org ().

[23] M. van den Berg and G. Buttazzo. "Some inequalities involving perimeter and torsional rigidity". In: *Appl. Math. Optim., (to appear), preprint available at* http://cvgmt.sns.it *and at* http://www.arxiv.org ().

[24] M. van den Berg, G. Buttazzo, and A. Pratelli. "On the relations between principal eigenvalue and torsional rigidity". In: *Commun. Contemp. Math. (to appear)* (2020).

[25] C. Bianchini and A. Henrot. "Optimal sets for a class of minimization problems with convex constraints". In: *J. Convex Anal.* 19.3 (2012), pp. 725–758. ISSN: 0944-6532.

[26] C. Bianchini, A. Henrot, and T. Takahashi. "Elastic energy of a convex body". In: *Mathematische Nachrichten* 289.5 (2016), pp. 546–574.

[27] R. J. Biezuner. "Best constants in Sobolev trace inequalities". In: *Nonlinear Anal.* 54.3 (2003), pp. 575–589. ISSN: 0362-546X. DOI: 10.1016/S0362-546X(03)00114-7. URL: https://doi.org/10.1016/S0362-546X(03)00114-7.

[28] W. Blaschke. "Konvexe Bereiche gegebener konstanter Breite und kleinsten Inhalts". In: *Math. Ann.* 76.4 (1915), pp. 504–513. ISSN: 0025-5831. DOI: 10.1007/BF01458221. URL: https://doi.org/10.1007/BF01458221.

[29] V. Bobkov and E. Parini. *On the Cheeger problem for rotationally invariant domains*. 2019. arXiv: 1907.10474 [math.OC].

[30] B. Bogosel. https://github.com/bbogo/Cheeger_patch.

[31] B. Bogosel. "Efficient algorithm for optimizing spectral partitions". In: *Appl. Math. Comput.* 333 (2018), pp. 61–75. ISSN: 0096-3003. DOI: 10.1016/j.amc.2018.03.087. URL: https://doi.org/10.1016/j.amc.2018.03.087.

[32] B. Bogosel, D. Bucur, and A. Giacomini. "Optimal shapes maximizing the Steklov eigenvalues". In: *SIAM J. Math. Anal.* 49.2 (2017), pp. 1645–1680. ISSN: 0036-1410. DOI: 10.1137/16M1075260. URL: https://doi.org/10.1137/16M1075260.

[33] B. Bogosel, A. Henrot, and I. Lucardesi. "Minimization of the eigenvalues of the Dirichlet-Laplacian with a diameter constraint". In: *SIAM J. Math. Anal.* 50.5 (2018), pp. 5337–5361. ISSN: 0036-1410. DOI: 10.1137/17M1162147. URL: https://doi.org/10.1137/17M1162147.

[34] B. Bogosel and É. Oudet. "Partitions of minimal length on manifolds". In: *Exp. Math.* 26.4 (2017), pp. 496–508. ISSN: 1058-6458. DOI: 10.1080/10586458.2016.1223570. URL: https://doi.org/10.1080/10586458.2016.1223570.

[35] T. Bonnesen and W. Fenchel. *Theory of convex bodies*. Translated from the German and edited by L. Boron, C. Christenson and B. Smith. BCS Associates, Moscow, ID, 1987, pp. x+172. ISBN: 0-914351-02-8.

[36] K. Böröczky Jr., M. A. Hernández Cifre, and G. Salinas. "Optimizing area and perimeter of convex sets for fixed circumradius and inradius". In: *Monatsh. Math.* 138.2 (2003), pp. 95–110. ISSN: 0026-9255. DOI: 10.1007/s00605-002-0486-z. URL: https://doi.org/10.1007/s00605-002-0486-z.

[37] A. Boulkhemair. "On a shape derivative formula in the Brunn-Minkowski theory". In: *SIAM J. Control Optim.* 55.1 (2017), pp. 156–171. ISSN: 0363-0129. DOI: 10.1137/15M1015844. URL: https://doi.org/10.1137/15M1015844.

[38] B. Brandolini, C. Nitsch, and C. Trombetti. "An upper bound for nonlinear eigenvalues on convex domains by means of the isoperimetric deficit". In: *Arch. Math. (Basel)* 94.4 (2010), pp. 391–400. ISSN: 0003-889X. DOI: 10.1007/s00013-010-0102-8. URL: https://doi.org/10.1007/s00013-010-0102-8.

[39] L. Brasco. "On principal frequencies and inradius in convex sets". In: *Bruno Pini Math. Anal. Semin.* (2018), p. 20.

[40] L. Brasco. "On principal frequencies and isoperimetric ratios in convex sets". In: *Ann. Fac. Sci. Toulouse Math.* (2019), p. 25.

[41] L. Brasco and G. De Philippis. "Spectral inequalities in quantitative form". In: *Shape optimization and spectral theory*. De Gruyter Open, Warsaw, 2017, pp. 201–281. DOI: 10.1515/9783110550887-007. URL: https://doi.org/10.1515/9783110550887-007.

[42] L. Brasco, G. De Philippis, and B. Velichkov. "Faber-Krahn inequalities in sharp quantitative form". In: *Duke Math. J.* 164.9 (2015), pp. 1777–1831. ISSN: 0012-7094. DOI: 10.1215/00127094-3120167. URL: http://dx.doi.org/10.1215/00127094-3120167.

[43] L. Brasco and D. Mazzoleni. "On principal frequencies, volume and inradius in convex sets". In: *NoDEA Nonlinear Differential Equations Appl.* 27.2 (2020), Paper No. 12, 26. ISSN: 1021-9722. DOI: 10.1007/s00030-019-0614-2. URL: https://doi.org/10.1007/s00030-019-0614-2.

[44] L. Brasco, C. Nitsch, and A. Pratelli. "On the boundary of the attainable set of the Dirichlet spectrum". In: *Z. Angew. Math. Phys.* 64.3 (2013), pp. 591–597. ISSN: 0044-2275. DOI: 10.1007/s00033-012-0250-8. URL: https://doi.org/10.1007/s00033-012-0250-8.

[45] H. Brezis and P. Mironescu. "Gagliardo-Nirenberg inequalities and non-inequalities: The full story". In: *Annales de l'Institut Henri Poincaré C, Analyse non linéaire* 35.5 (2018), pp. 1355–1376. ISSN: 0294-1449. DOI: https://doi.org/10.1016/j.anihpc.2017.11.007. URL: http://www.sciencedirect.com/science/article/pii/S0294144917301397.

[46] F. Brock. "An isoperimetric inequality for eigenvalues of the Stekloff problem". In: *ZAMM Z. Angew. Math. Mech.* 81.1 (2001), pp. 69–71. ISSN: 0044-2267. DOI: 10.1002/1521-4001(200101)81:1<69::AID-ZAMM69>3.0.CO;2-#. URL: https://doi.org/10.1002/1521-4001(200101)81:1%3C69::AID-ZAMM69%3E3.0.CO;2-#.

[47] F. Brock. "Continuous Steiner-symmetrization". In: *Math. Nachr.* 172 (1995), pp. 25–48. ISSN: 0025-584X. DOI: 10.1002/mana.19951720104. URL: https://doi.org/10.1002/mana.19951720104.

[48] R. Brooks and P. Waksman. "The first eigenvalue of a scalene triangle". In: *Proc. Amer. Math. Soc.* 100.1 (1987), pp. 175–182. ISSN: 0002-9939. DOI: 10.2307/2046142. URL: https://doi.org/10.2307/2046142.

[49] D. Bucur, G. Buttazzo, and I. Figueiredo. "On the attainable eigenvalues of the Laplace operator". In: *SIAM J. Math. Ana.* 30 (1999), pp. 527–536.

[50] D. Bucur and I. Fragalà. "A Faber-Krahn inequality for the Cheeger constant of N-gons". In: *J. Geom. Anal.* 26.1 (2016), pp. 88–117. ISSN: 1050-6926. DOI: 10.1007/s12220-014-9539-5. URL: https://doi.org/10.1007/s12220-014-9539-5.

[51] V. Bucur D. Ferone, C. Nitsch, and C. Trombetti. "Weinstock inequality in higher dimensions". In: *Journal of Differential equations* (2019).

[52] M. Caroccia and F. Maggi. "A sharp quantitative version of Hales' isoperimetric honeycomb Theorem". In: *J. Math. Pures Appl. (9)* 106.5 (2016), pp. 935–956. ISSN: 0021-7824. DOI: 10.1016/j.matpur.2016.03.017. URL: https://doi.org/10.1016/j.matpur.2016.03.017.

[53] M. Caroccia and R. Neumayer. "A note on the stability of the Cheeger constant of N-gons". In: *J. Convex Anal.* 22.4 (2015), pp. 1207–1213. ISSN: 0944-6532.

[54] T. Chatelain and A. Henrot. "Some results about Schiffer's conjectures". In: *Inverse Problems* 15 (Mar. 1999), pp. 647–658.

[55] J. Cheeger. "A lower bound for the smallest eigenvalue of the Laplacian". In: *Problems in analysis (Papers dedicated to Salomon Bochner, 1969)*. 1970, pp. 195–199.

[56] A. M. H. Chorwadwala and R. Mahadevan. "An eigenvalue optimization problem for the p-Laplacian". In: *Proc. Roy. Soc. Edinburgh Sect. A* 145.6 (2015), pp. 1145–1151. ISSN: 0308-2105. DOI: 10.1017/S0308210515000232. URL: https://doi.org/10.1017/S0308210515000232.

[57] A. M. H. Chorwadwala and M. K. Vemuri. "Two functionals connected to the Laplacian in a class of doubly connected domains on rank one symmetric spaces of non-compact type". In: *Geom. Dedicata* 167 (2013), pp. 11–21. ISSN: 0046-5755. DOI: 10.1007/s10711-012-9800-7. URL: https://doi.org/10.1007/s10711-012-9800-7.

[58] D. Cioranescu and F. Murat. "A strange term coming from nowhere". In: *Topics in the mathematical modelling of composite materials*. Vol. 31. Progr. Nonlinear Differential Equations Appl. Birkhäuser Boston, Boston, MA, 1997, pp. 45–93.

[59] S. J. Cox and M. Ross. "Extremal eigenvalue problems for starlike planar domains". In: *J. Differential Equations* 120.1 (1995), pp. 174–197. ISSN: 0022-0396. DOI: 10.1006/jdeq.1995.1109. URL: https://doi.org/10.1006/jdeq.1995.1109.

[60] G. Crasta, I. Fragalà, and F. Gazzola. "A sharp upper bound for the torsional rigidity of rods by means of web functions". In: *Arch. Ration. Mech. Anal.* 164.3 (2002), pp. 189–211. ISSN: 0003-9527. DOI: 10.1007/s002050200205. URL: https://doi.org/10.1007/s002050200205.

[61] G. Crasta, I. Fragalà, and F. Gazzola. "A sharp upper bound for the torsional rigidity of rods by means of web functions". In: *Arch. Ration. Mech. Anal.* 164.3 (2002), pp. 189–211. ISSN: 0003-9527. DOI: 10.1007/s002050200205. URL: https://doi.org/10.1007/s002050200205.

[62] M. Crouzeix. "Une famille d'inégalités pour les ensembles convexes du plan". In: *Ann. Math. Blaise Pascal* 12.2 (2005), pp. 223–230. ISSN: 1259-1734. URL: http://ambp.cedram.org/item?id=AMBP_2005__12_2_223_0.

[63] M. Dambrine and J. Lamboley. "Stability in shape optimization with second variation". In: *J. Differential Equations* 267.5 (2019), pp. 3009–3045. ISSN: 0022-0396. DOI: 10.1016/j.jde.2019.03.033. URL: https://doi.org/10.1016/j.jde.2019.03.033.

[64] M. Dambrine and J. Lamboley. "Stability in shape optimization with second variation". In: *Journal of Differential Equations* 267.5 (2019), pp. 3009–3045.

[65] J. M. Danskin. "The theory of max − min, with applications". In: *SIAM J. Appl. Math.* 14 (1966), pp. 641–664. ISSN: 0036-1399. DOI: 10.1137/0114053. URL: https://doi.org/10.1137/0114053.

[66] D. De Silva. "Free boundary regularity for a problem with right hand side". In: *Interfaces Free Bound.* 13.2 (2011), pp. 223–238. ISSN: 1463-9963. DOI: 10.4171/IFB/255. URL: https://doi.org/10.4171/IFB/255.

[67] M. C. Delfour and J. P. Zolesio. *Shapes and Geometries: Metrics, Analysis, Differential Calculus, and Optimization.* 2th. Advances in Design and control SIAM, 2001.

[68] A. L. Delitsyn, B. T. Nguyen, and D. S. Grebenkov. "Exponential decay of Laplacian eigenfunctions in domains with branches of variable cross-sectional profiles". In: *European Physical Journal B* 85.11, 371 (Nov. 2012), p. 371. DOI: 10.1140/epjb/e2012-30286-8. arXiv: 1109.3408 [math-ph].

[69] F. Della Pietra and N. Gavitone. "Sharp bounds for the first eigenvalue and the torsional rigidity related to some anisotropic operators". In: *Math. Nachr.* 287.2-3 (2014), pp. 194–209. ISSN: 0025-584X. DOI: 10.1002/mana.201200296. URL: https://doi.org/10.1002/mana.201200296.

[70] A. Delyon, A. Henrot, and Y. Privat. "Non-dispersal and density properties of infinite packings". In: *SIAM Journal on Control and Optimization* 57.2 (2019), pp. 1467–1492. DOI: 10.1137/18M1181183. URL: https://hal.archives-ouvertes.fr/hal-01753911.

[71] A. Delyon, A. Henrot, and Y. Privat. "The missing (A, d, r) diagram". In: *Submitted - https://hal.archives-ouvertes.fr/hal-02334941* (2020).

[72] B. Dittmar. "Zu einem Stekloffschen Eigenwertproblem in Ringgebieten". In: *Mitt. Math. Sem. Giessen* 228 (1996), pp. 1–7. ISSN: 0373-8221.

[73] A. El Soufi and E. M. Harrell II. "On the placement of an obstacle so as to optimize the Dirichlet heat trace". In: *SIAM J. Math. Anal.* 48.2 (2016), pp. 884–894. ISSN: 0036-1410. DOI: 10.1137/140957275. URL: https://doi.org/10.1137/140957275.

[74] A. El Soufi and R. Kiwan. "Extremal first Dirichlet eigenvalue of doubly connected plane domains and dihedral symmetry". In: *SIAM J. Math. Anal.* 39.4 (2007/08), pp. 1112–1119. ISSN: 0036-1410. DOI: 10.1137/060670250. URL: https://doi.org/10.1137/060670250.

[75] A. El Soufi and R. Kiwan. "Where to place a spherical obstacle so as to maximize the second Dirichlet eigenvalue". In: *Commun. Pure Appl. Anal.* 7.5 (2008), pp. 1193–1201. ISSN: 1534-0392. DOI: 10.3934/cpaa.2008.7.1193. URL: https://doi.org/10.3934/cpaa.2008.7.1193.

[76] J. F. Escobar. "Sharp constant in a Sobolev trace inequality". In: *Indiana Univ. Math. J.* 37.3 (1988), pp. 687–698. ISSN: 0022-2518. DOI: 10.1512/iumj.1988.37.37033. URL: https://doi.org/10.1512/iumj.1988.37.37033.

[77] L. Esposito, N. Fusco, and C. Trombetti. "A quantitative version of the isoperimetric inequality: the anisotropic case". In: *Ann. Sc. Norm. Super. Pisa Cl. Sci. (5)* 4.4 (2005), pp. 619–651. ISSN: 0391-173X.

[78] G. Faber. “dass unter allen homogenen Membranen von gleicher Fl ache undgleicher Spannung die kreisf örmige den tiefsten Grundton gibt”. In: *Sitzungsberichte der mathematisch-physikalischen Klasse der Bauerischen Akademie der Wissenschaften zu München Jahrgang* (1923), pp. 169–172.

[79] Z. Fattah and M. Berrada. “Eigenvalues of Dirichlet Laplacian within the class of open sets with constant diameter”. In: *Rend. Circ. Mat. Palermo (2)* 69.1 (2020), pp. 71–113. ISSN: 0009-725X. DOI: 10.1007/s12215-018-0389-z. URL: https://doi.org/10.1007/s12215-018-0389-z.

[80] J. Fernández Bonder, R. Orive, and J. D. Rossi. “The best Sobolev trace constant in domains with holes for critical or subcritical exponents”. In: *ANZIAM J.* 49.2 (2007), pp. 213–230. ISSN: 1446-1811. DOI: 10.1017/S1446181100012797. URL: https://doi.org/10.1017/S1446181100012797.

[81] J. Fernández Bonder, J. D. Rossi, and N. Wolanski. “Regularity of the free boundary in an optimization problem related to the best Sobolev trace constant”. In: *SIAM J. Control Optim.* 44.5 (2005), pp. 1614–1635. ISSN: 0363-0129. DOI: 10.1137/040613615. URL: https://doi.org/10.1137/040613615.

[82] A. Fraser and R. Schoen. “Shape optimization for the Steklov problem in higher dimensions”. In: *Adv. Math.* 348 (2019), pp. 146–162. ISSN: 0001-8708. DOI: 10.1016/j.aim.2019.03.011. URL: https://doi.org/10.1016/j.aim.2019.03.011.

[83] A. Fraser and R. Schoen. “Shape optimization for the Steklov problem in higher dimensions”. In: *Adv. Math.* 348 (2019), pp. 146–162. ISSN: 0001-8708. DOI: 10.1016/j.aim.2019.03.011. URL: https://doi.org/10.1016/j.aim.2019.03.011.

[84] P. Freitas and B. Siudeja. “Bounds for the first Dirichlet eigenvalue of triangles and quadrilaterals”. In: *ESAIM Control Optim. Calc. Var.* 16.3 (2010), pp. 648–676. ISSN: 1292-8119. DOI: 10.1051/cocv/2009018. URL: https://doi.org/10.1051/cocv/2009018.

[85] G. Fremiot. “Eulerian semiderivatives of the eigenvalues for Laplacian in domains with cracks”. In: *Adv. Math. Sci. Appl.* 12.1 (2002), pp. 115–134. ISSN: 1343-4373.

[86] G. Fremiot and J. Sokolowski. “Hadamard formula in nonsmooth domains and applications”. In: *Partial differential equations on multistructures (Luminy, 1999)*. Vol. 219. Lecture Notes in Pure and Appl. Math. Dekker, New York, 2001, pp. 99–120.

[87] G. Fremiot and J. Sokolowski. “Shape sensitivity analysis of problems with singularities”. In: *Shape optimization and optimal design (Cambridge, 1999)*. Vol. 216. Lecture Notes in Pure and Appl. Math. Dekker, New York, 2001, pp. 255–276.

[88] I. Ftouhi. “Complete systems of inequalities relating the perimeter, the area and the Cheeger constant of planar domains”. working paper or preprint. 2020.

[89] I. Ftouhi. “Numerical study of convexity constraint and application to Blaschke-Santaló diagrams”. (in preparation).

[90] I. Ftouhi. “On the Cheeger inequality for convex sets”. working paper or preprint. 2020.

[91] I. Ftouhi. “Where to place a spherical obstacle so as to maximize the first Steklov eigenvalue”. working paper or preprint. 2020. URL: https://hal.archives-ouvertes.fr/hal-02334941.

[92] I. Ftouhi and J. Lamboley. “Blaschke-Santaló diagram for volume, perimeter and first Dirichlet eigenvalue”. In: *SIAM Journal on Mathematical Analysis* (2020).

[93] B. Fuglede. “Stability in the isoperimetric problem for convex or nearly spherical domains in $\mathbf{R}^n$”. In: *Trans. Amer. Math. Soc.* 314.2 (1989), pp. 619–638. ISSN: 0002-9947. DOI: 10.2307/2001401. URL: http://dx.doi.org/10.2307/2001401.

[94] N. Fusco, M. S. Gelli, and G. Pisante. “On a Bonnesen type inequality involving the spherical deviation”. In: *Journal de Mathématiques Pures et Appliquées* 98.6 (2012), pp. 616–632. ISSN: 0021-7824. DOI: https://doi.org/10.1016/j.matpur.2012.05.006. URL: http://www.sciencedirect.com/science/article/pii/S0021782412000608.

[95] N. Fusco, F. Maggi, and A. Pratelli. "The sharp quantitative isoperimetric inequality". In: *Ann. of Math. (2)* 168.3 (2008), pp. 941–980. ISSN: 0003-486X. DOI: 10.4007/annals.2008.168.941. URL: https://doi.org/10.4007/annals.2008.168.941.

[96] B. Georgiev and M. Mukherjee. "On maximizing the fundamental frequency of the complement of an obstacle". In: *C. R. Math. Acad. Sci. Paris* 356.4 (2018), pp. 406–411. ISSN: 1631-073X. DOI: 10.1016/j.crma.2018.01.018. URL: https://doi.org/10.1016/j.crma.2018.01.018.

[97] I. Girouard A.and Polterovich. "Spectral geometry of the Steklov problem (survey article)". In: *J. Spectr. Theory* 7.2 (2017), pp. 321–359. ISSN: 1664-039X. DOI: 10.4171/JST/164. URL: https://doi.org/10.4171/JST/164.

[98] E. Giusti. *Minimal surfaces and functions of bounded variation.* Vol. 80. Monographs in Mathematics. Birkhäuser Verlag, Basel, 1984, pp. xii+240. ISBN: 0-8176-3153-4. DOI: 10.1007/978-1-4684-9486-0. URL: https://doi.org/10.1007/978-1-4684-9486-0.

[99] D. S. Grebenkov and B.-T. Nguyen. "Geometrical structure of Laplacian eigenfunctions". In: *SIAM Rev.* 55.4 (2013), pp. 601–667. ISSN: 0036-1445. DOI: 10.1137/120880173. URL: https://doi.org/10.1137/120880173.

[100] P. Grisvard. *Elliptic problems in nonsmooth domains.* Vol. 24. Monographs and Studies in Mathematics. Boston, MA: Pitman (Advanced Publishing Program), 1985, pp. xiv+410. ISBN: 0-273-08647-2.

[101] M. Haar. "Summen reziproker Eigenwerte". PhD thesis. Mathematisch-Naturwissenschaftlich-Technischen Fakulta t der Martin-Luther-Universita t Hall, Wittenberg, 2006.

[102] W. Hansen and N. Nadirashvili. "Isoperimetric inequalities in potential theory [MR1266215 (95c:31003)]". In: *ICPT '91 (Amersfoort, 1991).* Kluwer Acad. Publ., Dordrecht, 1994, pp. 1–14.

[103] E. M. Harrell, A. Henrot, and J. Lamboley. "On the local minimizers of the Mahler volume". In: *J. Convex Anal.* 22.3 (2015), pp. 809–825. ISSN: 0944-6532.

[104] E. M. Harrell II. "A direct proof of a theorem of Blaschke and Lebesgue". In: *J. Geom. Anal.* 12.1 (2002), pp. 81–88. ISSN: 1050-6926. DOI: 10.1007/BF02930861. URL: https://doi.org/10.1007/BF02930861.

[105] E. M. Harrell II, P. Kröger, and K. Kurata. "On the placement of an obstacle or a well so as to optimize the fundamental eigenvalue". In: *SIAM J. Math. Anal.* 33.1 (2001), pp. 240–259. ISSN: 0036-1410. DOI: 10.1137/S0036141099357574. URL: https://doi.org/10.1137/S0036141099357574.

[106] A. Henrot. *Extremum problems for eigenvalues of elliptic operators.* Frontiers in Mathematics. Birkhäuser Verlag, Basel, 2006, pp. x+202. ISBN: 978-3-7643-7705-2; 3-7643-7705-4.

[107] A. Henrot and E. Oudet. "Minimizing the second eigenvalue of the Laplace operator with Dirichlet boundary conditions". In: *Arch. Ration. Mech. Anal.* 169.1 (2003), pp. 73–87. ISSN: 0003-9527. DOI: 10.1007/s00205-003-0259-4. URL: https://doi.org/10.1007/s00205-003-0259-4.

[108] A. Henrot and M. Pierre. *Shape variation and optimization.* Vol. 28. EMS Tracts in Mathematics. European Mathematical Society (EMS), Zürich, 2018, pp. xi+365. ISBN: 978-3-03719-178-1. DOI: 10.4171/178. URL: https://doi.org/10.4171/178.

[109] A. Henrot and D. Zucco. "Optimizing the first Dirichlet eigenvalue of the Laplacian with an obstacle". In: *Annali della Scuola Normale Superiore di Pisa* (2018).

[110] M.A. Hernandez Cifre, G. Salinas, and S.S Gomis. "Complete systems of inequalities". In: *Journal of inequalities in pure and applied mathematics* 2.1 (Mar. 2001).

[111] M. A. Hernández Cifre. "Is there a planar convex set with given width, diameter, and inradius?" In: *Amer. Math. Monthly* 107.10 (2000), pp. 893–900. ISSN: 0002-9890. DOI: 10.2307/2695582. URL: https://doi.org/10.2307/2695582.

[112] M. A. Hernández Cifre. "Optimizing the perimeter and the area of convex sets with fixed diameter and circumradius". In: *Arch. Math. (Basel)* 79.2 (2002), pp. 147–157. ISSN: 0003-889X. DOI: 10.1007/s00013-002-8297-y. URL: https://doi.org/10.1007/s00013-002-8297-y.

[113] M. A. Hernández Cifre and G. Salinas. "Some optimization problems for planar convex figures". In: 70, part I. IV International Conference in "Stochastic Geometry, Convex Bodies, Empirical Measures & Applications to Engineering Science", Vol. I (Tropea, 2001). 2002, pp. 395–405.

[114] J. Hersch. "Contribution to the method of interior parallels applied to vibrating membranes". In: *Studies in mathematical analysis and related topics*. Stanford Univ. Press, Stanford, Calif., 1962, pp. 132–139.

[115] J. Hersch. "Sur la fréquence fondamentale d'une membrane vibrante: évaluations par défaut et principe de maximum". In: *Z. Angew. Math. Phys.* 11 (1960), pp. 387–413. ISSN: 0044-2275. DOI: 10.1007/BF01604498. URL: https://doi.org/10.1007/BF01604498.

[116] J. Hersch and L. E. Payne. "Extremal principles and isoperimetric inequalities for some mixed problems of Stekloff's type". In: *Z. Angew. Math. Phys.* 19 (1968), pp. 802–817. ISSN: 0044-2275. DOI: 10.1007/BF01591011. URL: https://doi.org/10.1007/BF01591011.

[117] I. Hong. "On an inequality concerning the eigenvalue problem of membrane". In: *Kodai Math. Sem. Rep.* 6 (1954). {Volume numbers not printed on issues until Vol. **7** (1955)}, pp. 113–114. ISSN: 0023-2599. URL: http://projecteuclid.org/euclid.kmj/1138843535.

[118] W. Hooker and M. H. Protter. "Bounds for the first eigenvalue of a rhombic membrane". In: *J. Math. and Phys.* 39 (1960/61), pp. 18–34. ISSN: 0097-1421.

[119] I. Joó and L. L. Stachó. "Generalization of an inequality of G. Pólya concerning the eigenfrequences of vibrating bodies". In: *Publ. Inst. Math. (Beograd) (N.S.)* 31(45) (1982), pp. 65–72. ISSN: 0350-1302.

[120] B. Kawohl. *Rearrangements and convexity of level sets in PDE*. Vol. 1150. Lecture Notes in Mathematics. Springer-Verlag, Berlin, 1985, pp. iv+136. ISBN: 3-540-15693-3. DOI: 10.1007/BFb0075060. URL: https://doi.org/10.1007/BFb0075060.

[121] B. Kawohl and V. Fridman. "Isoperimetric estimates for the first eigenvalue of the p-Laplace operator and the Cheeger constant". In: *Comment. Math. Univ. Carolin.* 44.4 (2003), pp. 659–667. ISSN: 0010-2628.

[122] B. Kawohl and T. Lachand-Robert. "Characterization of Cheeger sets for convex subsets of the plane". In: *Pacific J. Math.* 225.1 (2006), pp. 103–118. ISSN: 0030-8730. DOI: 10.2140/pjm.2006.225.103. URL: https://doi.org/10.2140/pjm.2006.225.103.

[123] S. Kesavan. "On two functionals connected to the Laplacian in a class of doubly connected domains". In: *Proc. Roy. Soc. Edinburgh Sect. A* 133.3 (2003), pp. 617–624. ISSN: 0308-2105. DOI: 10.1017/S0308210500002560. URL: https://doi.org/10.1017/S0308210500002560.

[124] D. Kinderlehrer and L. Nirenberg. "Regularity in free boundary problems". In: *Ann. Scuola Norm. Sup. Pisa Cl. Sci. (4)* 4.2 (1977), pp. 373–391.

[125] R. Kiwan. "On the Nodal set of a second Dirichlet eigenfunction in a doubly connected domain". en. In: *Annales de la Faculté des sciences de Toulouse : Mathématiques* Ser. 6, 27.4 (2018), pp. 863–873. DOI: 10.5802/afst.1585. URL: https://afst.centre-mersenne.org/item/AFST_2018_6_27_4_863_0.

[126] E. Krahn. "Über eine von Rayleigh formulierte Minimaleigenschaft des Kreises". In: *Math. Ann.* 94 (1925).

[127] T. Kubota. "Eine Ungleichheit für die Eilinien". In: *Math. Z.* 20.1 (1924), pp. 264–266. ISSN: 0025-5874. DOI: 10.1007/BF01188088. URL: https://doi.org/10.1007/BF01188088.

[128] T. Lachand-Robert and É. Oudet. "Bodies of constant width in arbitrary dimension". In: *Math. Nachr.* 280.7 (2007), pp. 740–750. ISSN: 0025-584X. DOI: 10.1002/mana.200510512. URL: https://doi.org/10.1002/mana.200510512.

[129] T. Lachand-Robert and M. A. Peletier. "Newton's problem of the body of minimal resistance in the class of convex developable functions". In: *Math. Nachr.* 226 (2001), pp. 153–176. ISSN: 0025-584X. DOI: 10.1002/1522-2616(200106)226:1<153::AID-MANA153>3.3.CO;2-U. URL: https://doi.org/10.1002/1522-2616(200106)226:1%3C153::AID-MANA153%3E3.3.CO;2-U.

[130] J. Lamboley and A. Novruzi. *Maximizers of Dirichlet eigenvalue among convex domains are polygons.* (in preparation).

[131] J. Lamboley and A. Novruzi. "Polygons As Optimal Shapes With Convexity Constraint". In: *SIAM Control and Optimization* 48.5 (2009), pp. 3003–3025.

[132] J. Lamboley and A. Novruzi. "Polygons as optimal shapes with convexity constraint". In: *SIAM J. Control Optim.* 48.5 (2009/10), pp. 3003–3025. ISSN: 0363-0129. DOI: 10.1137/080738581. URL: https://doi.org/10.1137/080738581.

[133] J. Lamboley, A. Novruzi, and M. Pierre. "Estimates of First and Second Order Shape Derivatives in Nonsmooth Multidimensional Domains and Applications". In: *Journal of Functional Analysis* 270.7 (2016), pp. 2616–2652.

[134] J. Lamboley, A. Novruzi, and M. Pierre. "Regularity and singularities of optimal convex shapes in the plane". In: *Arch. Ration. Mech. Anal.* 205.1 (2012), pp. 311–343. ISSN: 0003-9527. DOI: 10.1007/s00205-012-0514-7. URL: https://doi.org/10.1007/s00205-012-0514-7.

[135] J. Lamboley and M. Pierre. "Structure of shape derivatives around irregular domains and applications". In: *J. Convex Anal.* 14.4 (2007), pp. 807–822. ISSN: 0944-6532.

[136] S. Larson. "A bound for the perimeter of inner parallel bodies". In: *J. Funct. Anal.* 271.3 (2016), pp. 610–619. ISSN: 0022-1236. DOI: 10.1016/j.jfa.2016.02.022. URL: https://doi.org/10.1016/j.jfa.2016.02.022.

[137] J. L. Lewis and A. Vogel. "On Some Almost Everywhere Symmetry Theorems". In: *Nonlinear Diffusion Equations and Their Equilibrium States, 3: Proceedings from a Conference held August 20–29, 1989 in Gregynog, Wales.* Boston, MA: Birkhäuser Boston, 1992, pp. 347–374.

[138] I. Lucardesi and D. Zucco. "On Blaschke-Santaló diagrams for the torsional rigidity and the first Dirichlet eigenvalue". In: *Submitted - http://cvgmt.sns.it/paper/4490/* (2019).

[139] I. Ly. "The first eigenvalue for the p-Laplacian operator". In: *JIPAM. J. Inequal. Pure Appl. Math.* 6.3 (2005), Article 91, 12. ISSN: 1443-5756.

[140] F. Maggi. *Sets of finite perimeter and geometric variational problems.* Vol. 135. Cambridge Studies in Advanced Mathematics. An introduction to geometric measure theory. Cambridge University Press, Cambridge, 2012, pp. xx+454. ISBN: 978-1-107-02103-7. DOI: 10.1017/CBO9781139108133. URL: https://doi.org/10.1017/CBO9781139108133.

[141] E. Makai. "On the principal frequency of a membrane and the torsional rigidity of a beam". In: *Studies in mathematical analysis and related topics.* Stanford Univ. Press, Stanford, Calif., 1962, pp. 227–231.

[142] G. Matheron. "La formule de Steiner pour les érosions". In: *J. Appl. Probability* 15.1 (1978), pp. 126–135. ISSN: 0021-9002. DOI: 10.2307/3213242. URL: https://doi.org/10.2307/3213242.

[143] I. Mazari. "Quantitative inequality for the eigenvalue of a Schrödinger operator in the ball". In: *J. Differential Equations* 269.11 (2020), pp. 10181–10238. ISSN: 0022-0396. DOI: 10.1016/j.jde.2020.06.057. URL: https://doi.org/10.1016/j.jde.2020.06.057.

[144] L. Molinari. "On the ground state of regular polygonal billiards". In: *J. Phys. A* 30.18 (1997), pp. 6517–6524. ISSN: 0305-4470. DOI: 10.1088/0305-4470/30/18/025. URL: https://doi.org/10.1088/0305-4470/30/18/025.

[145] C. Nitsch. "An isoperimetric result for the fundamental frequency via domain derivative". In: *Calc. Var. Partial Differential Equations* 49.1-2 (2014), pp. 323–335. ISSN: 0944-2669. DOI: 10.1007/s00526-012-0584-2. URL: http://dx.doi.org/10.1007/s00526-012-0584-2.

[146] A. Novruzi and M. Pierre. "Structure of shape derivatives". In: *J. Evol. Equ.* 2.3 (2002), pp. 365–382. ISSN: 1424-3199. DOI: 10.1007/s00028-002-8093-y. URL: https://doi.org/10.1007/s00028-002-8093-y.

[147] R. Osserman. "The isoperimetric inequality". In: *Bull. Amer. Math. Soc.* 84.6 (Nov. 1978), pp. 1182–1238. URL: https://projecteuclid.org:443/euclid.bams/1183541466.

[148] S. Pan, X. Sun, and Y. Wang. "A variant of the isoperimetric problem. I". In: *Sci. China Ser. A* 51.6 (2008), pp. 1119–1126. ISSN: 1006-9283. DOI: 10.1007/s11425-008-0043-x. URL: https://doi.org/10.1007/s11425-008-0043-x.

[149] G. Paoli, G. Piscitelli, and R. Sannipoli. *A stability result for the Steklov Laplacian Eigenvalue Problem with a spherical obstacle*. 2020. arXiv: 2005.04449 [math.AP].

[150] G. De Paoli, G. Piscitelli, and L. Trani. "Sharp estimates for the first Laplacian eigenvalue and for the torsional rigidity on convex sets with holes." In: *Preprint* (2019).

[151] E. Parini. "An introduction to the Cheeger problem". In: *Surv. Math. Appl.* 6 (2011), pp. 9–21. ISSN: 1843-7265.

[152] E. Parini. "Reverse Cheeger inequality for planar convex sets". In: *J. Convex Anal.* 24.1 (2017), pp. 107–122. ISSN: 0944-6532.

[153] E. Parini and N. Saintier. "Shape derivative of the Cheeger constant". In: *ESAIM Control, Optimisation and Calculus of Variations* 21 (2015), pp. 348–358.

[154] L. E. Payne and H. F. Weinberger. "Some isoperimetric inequalities for membrane frequencies and torsional rigidity". In: *J. Math. Anal. Appl.* 2 (1961), pp. 210–216. ISSN: 0022-247X. DOI: 10.1016/0022-247X(61)90031-2. URL: https://doi.org/10.1016/0022-247X(61)90031-2.

[155] G. Pólya. "On the characteristic frequencies of a symmetric membrane". In: *Math. Z.* 63 (1955), pp. 331–337. ISSN: 0025-5874. DOI: 10.1007/BF01187944. URL: https://doi.org/10.1007/BF01187944.

[156] G. Pólya. "Two more inequalities between physical and geometrical quantities". In: *J. Indian Math. Soc. (N.S.)* 24 (1960), 413–419 (1961). ISSN: 0019-5839.

[157] F. P. Preparata and M. I. Shamos. *Computational geometry*. Texts and Monographs in Computer Science. An introduction. Springer-Verlag, New York, 1985, pp. xii+390. ISBN: 0-387-96131-3. DOI: 10.1007/978-1-4612-1098-6. URL: https://doi.org/10.1007/978-1-4612-1098-6.

[158] M.H. Protter. "A Lower bound for the fundamental frequency of a convex region". In: *American mathematical society* 81.1 (1981), pp. 65–70.

[159] L. R. Quinones. "A Critical Domain For the First Normalized Nontrivial Steklov Eigenvalue Among Planar Annular Domains". In: *Preprint* (2019).

[160] A. G. Ramm and P. N. Shivakumar. "Inequalities for the minimal eigenvalue of the Laplacian in an annulus". In: *Math. Inequal. Appl.* 1.4 (1998), pp. 559–563. ISSN: 1331-4343. DOI: 10.7153/mia-01-54. URL: https://doi.org/10.7153/mia-01-54.

[161] E. Russ, B. Trey, and B. Velichkov. "Existence and Regularity of optimal shapes for elliptic operators with drift". In: *To appear in Calc. Var. PDE* (2020).

[162] V. Sander. http://cglab.ca/~sander/misc/ConvexGeneration/convex.html.

[163] L. Santaló. "Sobre los sistemas completos de desigualdades entre treselementos de una figura convexa plana". In: *Math. Notae* 17 (1961), pp. 82–104.

[164] R. Schneider. *Convex Bodies: The Brunn-Minkowski Theory*. 2nd expanded edition. Cambridge University Press, 2013.

[165] D. H. Seo. *A shape optimization problem for the first mixed Steklov-Dirichlet eigenvalue*. 2019. arXiv: 1909.06579 [math.SP].

[166] J. Serrin. "A symmetry problem in potential theory". In: *Arch. Rational Mech. Anal.* 43 (1971), pp. 304–318. ISSN: 0003-9527.

[167] B. Siudeja. "Sharp bounds for eigenvalues of triangles". In: *Michigan Math. J.* 55.2 (2007), pp. 243–254. ISSN: 0026-2285. DOI: 10.1307/mmj/1187646992. URL: https://doi.org/10.1307/mmj/1187646992.

[168] E. M. Stein and G. Weiss. *Introduction to Fourier analysis on Euclidean spaces.* Princeton Mathematical Series, No. 32. Princeton University Press, Princeton, N.J., 1971, pp. x+297.

[169] G. Szegö. "Inequalities for certain eigenvalues of a membrane of given area". In: *J. Rational Mech. Anal.* 3 (1954), pp. 343–356. ISSN: 1943-5282. DOI: 10.1512/iumj.1954.3.53017. URL: https://doi.org/10.1512/iumj.1954.3.53017.

[170] F. Tricomi. "Sulle funzioni di Bellel di ordine e argomento pressochè uguali". In: *Atti Accad. Sci. Torino Cl. Sci. Fis. Mat. Natur.* 83 (1949), pp. 3–20. ISSN: 0001-4419.

[171] P. Valtr. "Probability that n random points are in convex position". In: *Discrete Comput. Geom.* 13.3-4 (1995), pp. 637–643. ISSN: 0179-5376. DOI: 10.1007/BF02574070. URL: https://doi.org/10.1007/BF02574070.

[172] S. Verma and G. Santhanam. "On eigenvalue problems related to the laplacian in a class of doubly connected domains". In: *Monatsh. Math.* 193.4 (2020), pp. 879–899. ISSN: 0026-9255. DOI: 10.1007/s00605-020-01466-9. URL: https://doi.org/10.1007/s00605-020-01466-9.

[173] H. F. Weinberger. "An effectless cutting of a vibrating membrane". In: *Pacific J. Math.* 13 (1963), pp. 1239–1240. ISSN: 0030-8730. URL: http://projecteuclid.org/euclid.pjm/1103034559.

[174] H. F. Weinberger. "An isoperimetric inequality for the N-dimensional free membrane problem". In: *J. Rational Mech. Anal.* 5 (1956), pp. 633–636. ISSN: 1943-5282. DOI: 10.1512/iumj.1956.5.55021. URL: https://doi.org/10.1512/iumj.1956.5.55021.

[175] R. Weinstock. "Inequalities for a classical eigenvalue problem". In: *J. Rational Mech. Anal.* 3 (1954), pp. 745–753. ISSN: 1943-5282. DOI: 10.1512/iumj.1954.3.53036. URL: https://doi.org/10.1512/iumj.1954.3.53036.

[176] A. Yger. *Analyse Complexe.* URL: https://www.math.u-bordeaux.fr/~ayger/coursAC-2011.pdf.

Résumé

La présente thèse est une contribution au domaine des calculs de variations et plus précisément la discipline d'optimisation de forme. Nous nous intéressons dans la majeure partie de ce travail à l'étude d'inégalités optimales reliant différentes quantités géométriques et spectrales sur plusieurs classes d'ensembles, ceci passe par l'étude de diagrammes dits de Blaschke-Santaló qui permettent de visualiser les inégalités possibles reliant 3 fonctionnelles de forme données. Nous développons différentes techniques qui permettent de démontrer des résultats qualitatifs sur ces diagrammes et proposons une approche numérique pour en fournir une approximation optimale. Nous nous intéressons aussi à l'étude de l'inégalité de Cheeger, qui est une inégalité classique reliant la première valeur propre du Laplacien avec condition Dirichlet au bord et la constante de Cheeger, pour les domaines convexes. Enfin, nous nous penchons sur le problème de trouver l'emplacement optimal d'un obstacle sphérique contenu dans une boule qui permet de maximiser la première valeur propre du Laplacien avec conditions aux bord de type Steklov.

Mots-clés: Optimisation de forme, Analyse convexe, Diagrammes de Blaschke-Santaló, Analyse numérique, Placement optimal d'un obstacle, Théorie spectrale.

Abstract

The present thesis is a contribution to the field of calculus of variations and more precisely the discipline of shape optimization. We are interested in the major part of this work in the study of sharp inequalities relating different geometric and spectral quantities for various classes of sets, this is tightly related to the study of the so called Blaschke-Santaló diagrams that allow to visualise the possible inqualities relating 3 given shape functionals. We develop different techniques that allow to prove qualitative results on these diagrams and propose a numerical approach in order to provide optimal approximations of them. We are also interested by the study of the Cheeger inequality, that relates the Cheeger constant and the first eigenvalue of the Laplace operator with Dirichlet boundary condition, for convex domains. At last, we focus on the problem of finding the optimal placement of a spherical obstacle so as to maximize the first Laplace eigenvalue with Steklov boundary conditions.

Keywords: Shape optimization, Convex analysis, Blaschke-Santaló diagrams, Numerical analysis, Optimal placement of an obstacle, Spectral theory.